Investigation of the antibacterial activity and the biosynthesis gene cluster of the peptide antibiotic feglymycin

vorgelegt von
Diplom-Biochemikerin
Saskia Rausch
aus Berlin

Von der Fakultät II – Mathematik und Naturwissenschaften
der Technischen Universität Berlin
zur Erlangung des akademischen Grades

Doktor der Naturwissenschaften
- Dr. rer. nat. –

genehmigte Dissertation

Promotionsausschuss:

Vorsitzende: Prof. Dr. Marga Lensen
1. Berichter/Gutachter: Prof. Dr. Roderich Süssmuth
2. Berichter/Gutachter: Prof. Dr. Dirk Schwarzer

Tag der wissenschaftlichen Aussprache: 09.12.2011

Berlin 2012
D 83

Zusammenfassung:

Untersuchung zur antibakteriellen Wirkung und zum Biosynthese-Genclusters des Peptidantibiotikum Feglymycin

Feglymycin ist ein aus *Streptomyces sp*. DSM 11171 isoliertes, lineares 13mer-Peptid, das zu einem hohen Anteil aus den nicht-proteinogenen Aminosäuren Hpg (4-Hydroxyphenylglycine) und Dpg (3,5-Dihydroxyphenylglycine) besteht. Zudem besitzt es eine interessante, alternierende Abfolge von D- und L- Aminosäuren und strukturelle Ähnlichkeiten mit den Glycopeptiden der Vancomycin-Gruppe von Antibiotika und den Glycodepsipeptid-Antibiotika Ramoplanin und Enduracidin. Außerdem besitzt Feglymycin eine interessante Bioaktivität. Es wirkt *in vivo* antibakteriell gegen MRSA-Stämme (multi-resistente *Staphylococcus aureus* Stämme) und inhibitiert *in vitro* die Replikation von HIV-Viren im Zellkulturtest. Aufgrund seiner molekularen Masse und strukturellen Ähnlichkeit mit bekannten Zellwandbiosynthese-Inhibitoren wie z.B. Vancomycin und Ramoplanin, wurde auch Feglymycin als Zellwandbiosynthese-Inhibitor getestet. In diesen Tests zeigte Feglymycin keinen Effekt auf die membran-gebundenen zweite und die dritte Stufe der Peptidoglycanbiosynthese. Jedoch deuteten die Experimente auf eine Inhibition der früheren Biosyntheseschritte hin.

Ziel dieser Arbeit war es, die antibakterielle Wirkung von Feglymycin auf die bakterielle Zellwandbiosynthese im Detail zu untersuchen und das biologische Target zu identifizieren. Zusätzlich wurde das Feglymycin Biosynthese-Gencluster untersucht. In LC-MS „*one-pot assays*“ wurde die Wirkung von Feglymycin auf die isolierten *E. coli*-Enzyme MurA-F getestet. Hierbei konnte reproduzierbar gezeigt werden, das Feglymycin die Enzyme MurA (Enopyruvyl-UDP-GlcNAc Synthase) und MurC (UDP-*N*-Acetyl-muramyl-L-alanin Ligase) inhibiert. In spektrophotometischen Assays mit den *E. coli*-Enzymen MurA und MurC konnte ein K_i-Wert von 0.33 +/- 0.04 µM für das MurC Enzym und ein K_i-Wert von 3.4 +/- 1.1 µM für das MurA Enzym bestimmt werden. Weitere Untersuchungen zeigten, dass Feglmycin auch die MurA (IC_{50} = 3.5 +/- 1.3 µM) und MurC (IC_{50} = 1.0 +/- 0.6 µM) Enzyme des gram-positiven Bakteriums *Staphylococcus aureus* inhibiert. Feglymycin zeigte dabei eine nicht-kompetitive Inhibition gegenüber der Bindung der Substrate des MurA Enzyms PEP (Phosphoenolpyruvat) und UDP-GlcNAc (UDP-*N*-Acetylglucosamin) und der Substrate des MurC Enzyms UDP-MurNAc (UDP-*N*-Acetylmuramat), ATP (Adenosintriphosphat) and L-Alanin. Feglmycin ist daher der erste Naturstoff der das MurC Enzym inhibiert. Zudem zeigt Feglymycin einen nicht-kompetitive Inhibitionstyp. Circulardichromismus (CD) Experimente mit den isolierten *E. coli*-Enzymen MurA und MurC und Feglymycin deuten einen möglichen allosterischen Effekt des Inhibitors auf die Enzyme an.

Zusätzlich wurde die Feglmycinproduktion durch den Stamm *Streptomyces sp*. DSM 11171 und die Feglymycin-Detektion mittels LC-MS optimiert. Durch die Sequezierung des Genoms von *Streptomyces sp*. DSM 11171 konnte das Feglymycin Biosynthese-Gencluster identifiziert werden. Bei der Annotation des Genclusters zeigte sich, dass es sich bei Feglymycin um ein nicht-ribosomal synthetisiertes Peptid (NRPS) handelt dessen Biosynthese der Biosynthese der Glycopeptidantibiotika der Vancomycin-Gruppe von Antibiotika ähnelt. Zudem konnten im *Streptomyces sp*. DSM 11171 Genom weitere NRPS und Polyketidsynthase (PKS) Gencluster identifiziert und annotiert werden.

Abstract:

Investigation of the antibacterial activity and the biosynthesis gene cluster of the peptide antibiotic feglymycin

Feglymycin is a linear 13-mer peptide produced by *Streptomyces* sp. DSM 11171 containing largely the non-proteinogenic Hpg (4-hydroxyphenylglycine) and the non-proteinogenic Dpg (3,5-dihydroxyphenylglycine) amino acids and an interesting alternation of D and L amino acids. It shows structural homogies to the glycopeptides of the vancomycin group of antibiotics and the glycodepsipeptide antibiotics ramoplanin and enduracidin. Feglymycin additionally shows an interesting biological activity. It possesses antibiotic activity against MRSA (multi-resistant *Staphylococcus aureus*) strains *in vivo* and inhibits syncytium formation in HIV infection *in vitro*. Due to its molecular mass and structural analogies to known inhibitors of the cell-wall biosynthesis, i.e. vancomycin and ramoplanin, feglymycin was tested as cell-wall biosynthesis inhibitor. In these tests feglymycin showed no effect on the membrane-bound second and third step of the peptidoglycan biosynthesis but the experiments indicated an inhibition of earlier biosynthetic steps.

Aim of this work was to investigate the antibacterial activity of feglymycin on the bacterial cell-wall biosynthesis in more detail and to identify the biological target. Additionally the feglymycin biosynthesis gene cluster was investigated. Feglymycin was tested in a LC-MS one-pot assay against the isolated enzymes MurA-F from *E. coli.* Dereplication revealed that feglymycin specifically inhibits the enzymes MurA (enolpyruvyl-UDP-GlcNAc synthase) and MurC (UDP-*N*-acetyl-muramyl-L-alanine ligase). In *in vitro* assays with the enzymes MurA and MurC from gram-negative *E. coli,* a K_i value of 0.33 +/- 0.04 µM was determined for the MurC enzyme and a K_i value of 3.4 +/- 1.1 µM for the MurA enzyme. Further investigations showed that feglymycin also inhibits the MurA (IC_{50} = 3.5 +/- 1.3 µM) and MurC (IC_{50} = 1.0 +/- 0.6 µM) enzyme from gram-positive *Staphylococcus aureus*. The inhibition mode of feglymycin was found to be non-competitive with the binding of PEP (phosphoenolpyruvate) and UDP-GlcNAc (UDP-*N*-acetylglucosamine) in case of the MurA enzyme and non-competitive with binding of UDP-MurNAc (UDP-*N*-acetylmuramic acid), ATP (adenosine-triphosphate) and L-alanine in case of the MurC enzyme. Feglymycin is therefore the first natural compound found to inhibit the MurC enzyme showing a non-competitive inhibition type. Circular dichroism (CD) experiments with the isolated enzymes MurA and MurC from *E. coli* and feglymycin indicated a possible allosteric effect of feglymycin.

Furthermore the feglymycin production by *Streptomyces sp*. DSM 11171 and feglymycin detection by LC-MS were optimized. Sequencing of the genome of *Streptomyces sp*. DSM 11171 allowed the idenfitication of the feglymycin biosynthesis gene cluster. Annotation of the gene cluster showed that feglymycin is a non-ribosomal synthesized peptide (NRPS) closely related to the glycopeptides of the vancomycin group of antibiotics. Additionally further NRPS and polyketide synthase (PKS) gene clusters were identified in the *Streptomyces sp*. DSM 11171 genome and annotated.

Teile der vorliegenden Arbeit wurden bereits veröffentlicht:

Publikationen:

"**Feglymycin is an inhibitor of the enzymes MurA and MurC of the peptidoglycan biosynthesis pathway**"
Saskia Rausch, Anne Hänchen, Alexander Denisiuk, Marius Löhken, Tanja Schneider, Roderich D. Süssmuth
ChemBioChem, **2011,** *8*, 1171-1173.

Poster:

"**Feglymycin inhibits the enzymes MurA and MurC of the peptidoglycan biosynthesis pathway"**
Saskia Rausch, Anne Hänchen, Alexander Denisiuk, Marius Löken and Roderich Süßmuth
10th German Peptide Symposium, FU-Berlin, 7.03-10.03.2011

"**Feglymycin inhibits the enzymes MurA and MurC of the peptidoglycan biosynthesis pathway"**
Saskia Rausch, Anne Hänchen, Alexander Denisiuk, Marius Löken and Roderich Süßmuth
Bayer PhD student Course, Köln, 10.-14.07.2011

Vorträge:

"**Antimicrobial activity of the peptide antibiotic Feglymycin"**
Saskia Rausch, Anne Hänchen, Alexander Denisiuk, Marius Löken and Roderich Süßmuth
International workshop, DGMS „New Developments of Lysosomal Storage Disease Diagnostics & Therapeutics, Protein – Carbohydrate Interactions, Konstanz, 3-5.10.2011

“It is the search for the truth, not possession of the truth which is the way of philosophy. Its questions are more relevant than its answers, and every answer becomes a new question.”

Karl Theodor Jaspers, Way to Wisdom: An Introduction to Philosophy

“It’s a bacteria-eat-man world out there, filled with a nearly endless variety of germs that see us as spawning grounds.”

W. Wayt Gibbs, Nanobodies

Die vorliegende Arbeit wurde unter der Leitung von

Herrn Prof. Dr. Roderich Süßmuth

In der Zeit vom September 2008 bis August 2011 am Institut für Chemie der Fakultät II der Technischen Universität Berlin angefertigt.

Danksagungen:

Mein besondere Dank gilt meinen Doktorvater Prof. Roderich Süssmuth für meine Aufnahme in den Arbeitskreis Süßmuth, das interessante Promotionsthema und die exzellente Betreuung und Förderung wärend meiner Promotionszeit. Ich bin dankbar für das mir von ihm entgegengebrachte Vertrauen und das freundschaftliche Verhältnis, dass das Arbeiten auch in besonders stressigen Zeiten noch angenehm machte. Ich bin ebenfalls dankbar für die vielen Möglichkeiten die mir geboten wurden so viele verschiedene Methoden zu erlernen und so vielfältige und spannende Projekte zu bearbeiten. Insbesondere möchte ich mich auch für die intensive Betreuung und den Versuch bedanken „mir noch den Feinschliff zu verpassen“ unter anderem durch sein ständig offenes Ohr für Disskussionen und Fragen, das Präsentationstraining im Mitarbeiterseminar und auf verschiedenen Tagungen und die viele, viele Zeit, die er für die Korrektur und Durchsicht von Artikeln, Vorträgen, Arbeitsberichten und auch für dieser Arbeit investiert hat.

Mein zweiter besonderer Dank gilt meinen Kollegen und ehemaligen Kollegen. Durch das freundschaftliche Verhältnis und das gute Arbeitsklima konnte wir einige Labordramen überstehen und es fand sich immer jemand der bereit war einem wissenschaftlichen oder methodischen mit Rat und Tat zur Seite zu stehen. Namentlich Dr. Heiko Schadt, Dr. Elvira Gottardi, Jonny Nachtigal, Dr. Maik Henkel, Dr. Anne Hänchen, Dr. Joanna Krawczyk, Dr. Wolfgang Müller, Dr. Stefan Pohle, Dr. Georg Sambeth, Dr. Agnes Mühlenweg, Dr. Srinivas Banala, Eva Mösker, Nicole Sattler, Manuela Hügelland, Annette Poch, Jane Müller, Dr. Soleiman Helaly, Todor Baravov, Diana Matthes, Marius Löhken, Florian Oldach, Benjamin Landmann, Bartlomiej Krawczyk, Bahar Kalyon (née Yanova), Viven Schubert, Alexander Pesic, Alexander Denisiuk, Paul Ensle, David Wagner, Stefanie Uhlmann, Kamil Stelmaszyk, Ginka Völler (née Kazakova), Julian Kretz, Anja Kuthning, Sebastian Müller, Sophia Zobel und Rashed al Toma.

Ich danke herzlichst Prof. Dirk Schwartzer dafür, dass er sich bereit erklärt hat das Zweitgutachten für diese Arbeit zu erstellen.

Ich danke herzlichst meiner Kollegin Eva Mösker für die Einarbeitung und die Hilfestellungen in die Massenspektrometrie und HPLC-Techniken. Für ihr stetts

offenes Ohr zu allen analytischen Fragestellungen und nicht zuletzt für ihre Einarbeitung und ihre Mitarbeit am Salmochelin-Projekt.

Insbesonders danke ich auch meiner ehemaligen Kollegin Dr. Anne Hänchen für die tolle Zusammenarbeit beim Feglymycin-Projekt. Für ihre Bereitschaft und ihr Vertrauen mir ihr in langen Wochen synthetisiertes Feglymycin für meine verschiedenen teils abenteuerlichen und nicht immer erfolgreichen Experimente zur Verfügung zu stellen bis ich es schließlich geschafft hatte funktionierende Assays zu etablieren.

Meinen Kollegen Alexander Denisiuk und Marius Löhken danke ich für ihre Bereitschaft sich an die Synthese von UDP-MurNAc zu machen und diese trotz aller Schwierigkeiten auch durchzuziehen. Ich bin ihnen sehr dankbar für die viele Arbeit die sie darauf verwendet haben.

Ich danke Todor Baramov und Kamil Stelmaszyk für ihre Mitarbeit im Salmochelin-Projekt und ihr tolle und schnelle Mithilfe als unsere erste These zur Struktur des Siliziumkomplexes plötzlich widerlegt wurden.

Ich danke meinem ehemaligen Kollegen Dr. Wolfgang Müller und meinem Kollegen Bartlomiej Krawczyk für die wissenschaftliche Disskussion und die Hilfestellung bei proteinbiochemischen Fragestellungen. Bartek möchte ich zudem für sein großartiges kleines Computerprogramm zur nicht-linearen Regression danken.

Ich danke meinen Kollegen Jane Müller und Diana Matthes für ihre Beratung bei molekularbiologischen Fragen und meinen ehemaligen Kollegen Dr. Stefan Pohle für die Einführung in die Genomannotation.

Ich danke Dr. Agnes Mühlenweg, Anette Poch und Lara Michel Mata für die Mitarbeit am Feglymycin-Gencluster-Projekt.

Ich danke Prof. Dr. Hans-Georg Sahl und Dr. Tanja Schneider für die erfolgreiche Kooperation im Feglymycin-Projekt.

Ich danke Prof. Mookie Baik und Prof. Klaus Hantke für die Kooperation im Salmochelin-Projekt.

Ich danke Prof. Ulrich Koert und Dr. Philipp Reiß für die Durchführung des Ionenkanal-Experimentes.

Nicht zuletzt danke meiner Familien und meinen Freunden für ihre Unterstützung und ihr Verständis dafür, dass ich kaum mehr Zeit für sie hatte. Und dafür, dass sie mich trotzdem nicht vergessen haben.

Contents

1 Introduction

1.1 Short story of antibiotics and their discovery

The era of antibiotics from microorganisms started with the discovery of penicillin by Alexander Fleming (Fleming 1929). For his discovery Fleming was later, together with Howard W. Florey and Ernst B. Chain, two other antibiotic pioneers, decorated with the Nobel Prize. In the 1940ies the production of penicillin was industrialized and the success soon led to the discovery of further antibiotics. Antibiotics, first reserved only for the military, became available to a larger public and reduced the mortality rates of infectious diseases (Alanis 2005) e.g. tuberculosis so significantly that they took a lot of these illnesses their threat. Most of the major classes of antibiotics used today like the tetracyclines, the chlorampenicols and the glycopeptide antibiotics were already discovered between 1940 and 1960 (Figure 1.1). In the end of the 1960ies screening programs started to fail to discover new antibiotics and the emergence of antibiotic resistance started to be a problem. To overcome this problem and in order to generate new antibacterially active substances, semi-synthetic modification of known antibiotics became popular. Semisynthesis proofed a good method to generate therapeutics improved in stability, tolerance and less prone to induce resistance. However by the 1980ies this method seemed exhausted (Fernandes 2006). The success of the antibiotic ciprofloxacin (Ciprobay, Bayer AG) synthetically derived from nalidixic acid led to the intensive investigation and synthesis of further fluoroquinolone antibiotics (Oliphant, Green 2002). At the same time automatable screening of small-molecule libraries became fashionable (Fernandes 2006). These screening efforts were extended by the use of combinatorial libraries and by high-throughput screenings focusing on specific bacterial target proteins. Simultaneously new bacterial targets were investigated. These screenings led to a large number of very effective protein inhibitors. However a lot of these molecules showed no activity *in vivo* or did not meet the requirements in toxicity, stability and permeability. It became obvious that the best inhibitor is not necessarily the best antibiotic (Peláez 2006). The realization that nature, driven by thousands of years of evolution may have created the best lead structures recently led to the concept of diversity-oriented synthesis of more nature-akin compounds (Newman 2008) but also to a return to long ago discovered but not followed up antibiotics (Fernandes 2006).

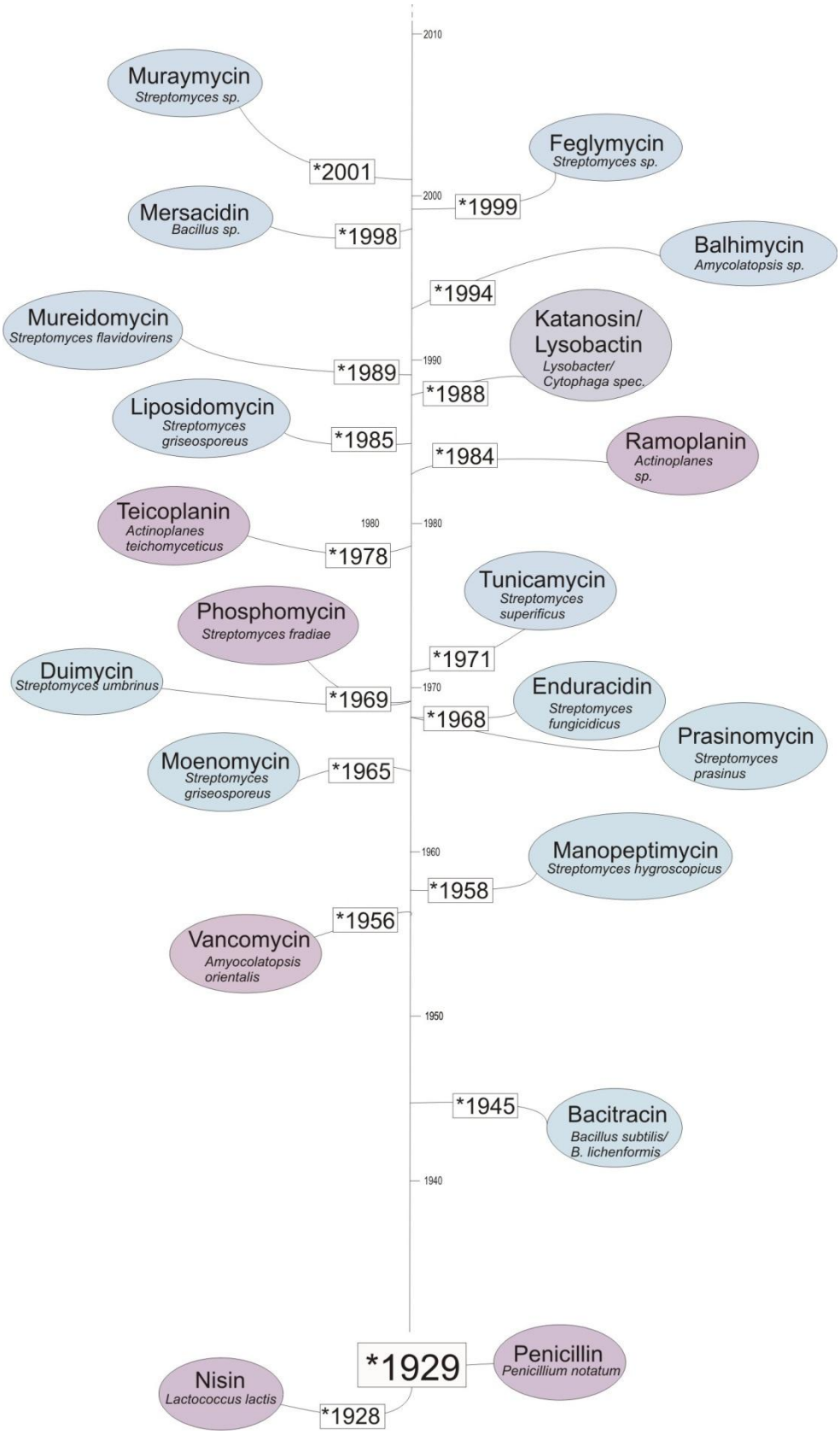

Figure 1.1: Time line of the discovery of cell wall biosynthesis inhibitors.

1.2 Recent approaches to the discovery of new antibiotics

In reflection that synthetic screening methods failed some approaches went back to the isolation of natural compounds (van Lanen, Shen 2006). Mathematic calculations number the percentage of so far cultured and investigated bacteria only around 1 % of the actual natural biodiversity. For the genus *Streptomyces* e.g. a possible total number of 100.000 different compounds were predicted; much more than up to now discovered (Watve et al. 2001). New cultivation methods were suggested to help studying until now “unculturable” strains (Vartoukian et al. 2010) but also to reinvestigate long known antibiotic producers. Also well-known antibiotic producers might contain some new surprises, as genome sequencing of several of these strains revealed that long known strains often possess several unknown gene clusters (Bentley et al. 2002). Genetic methods and new cultivation methods might help to activate so far hidden antibiotics (Peláez 2006). More sensitive and fractionated screening methods might also help as some antibiotics might only escaped detection due to low titer production.

A particular focus has lately been put on marine organisms. Marine microbes have just recently been started to be explored but already raise great expectations as sources for new bioactive compounds. Arguments in favor of are the harsh and competitive natural environment marine microbes are exposed to and the finding that a lot of the bioactive compounds found in marine invertebrate actually origin from symbiotic marine bacteria (Zhang et al. 2005; Peláez 2006). Also other more exotic sources for antibiotics have been explored like the antimicrobial peptides produced in animals, insects and plants (Bulet et al. 2004). The finding of antimicrobial compounds in the brain of cockroaches and locust (Lee et al. 2011; Khan et al. 2008) lately attracted a great deal of attention even outside of the scientific community.

An approach still waiting for a break-through success beside proof of concept is metagenomics. Metagenomics means the subcloning of DNA fragments of non-cultivatable environmental strains via plasmids, cosmids or BACs into *E. coli* and *Streptomyces* strains creating large metagenomic libraries to discover new active gene clusters (Daniel 2004; Peláez 2006). The compounds thus far identified from these metagenomic approaches turned out to be structurally rather simple (Gillespie et al. 2002; Brady et al. 2001). Beside discovering of new gene clusters the transfer of identified gene clusters into stains more easy accessible to molecular biological

methods (heterologous expression) can also help to characterize and modify a natural compound (van Lanen, Shen 2006).

A rather new and courageous approach is combinatorial biosynthesis. Combinatorial biosynthesis takes advantage of the modular biosynthesis assembly lines of non-ribosomally synthesized peptides and polyketides from various polyketide synthases. The idea is the *de novo* biosynthesis of new natural products by changes in the arrangement of the modules e. g. by site-directed mutagenesis (Wilkinson, Micklefield 2007). Combinatorial biosynthesis could not fulfill the high hope put into this technology as it soon became obvious that the biosynthetic modules cannot be exchanged freely without limit. Limitations by not well-known molecular-recognition and proof-reading mechanisms often led to low or no production of the reprogrammed NRPS and PKS *in vivo* (Wilkinson, Micklefield 2007). However the increasing knowledge of NRPS and PKS systems might open this possibility or even the *de novo* biosynthesis of PKS or NPRS from a building block kit of modules in future (Leman et al. 2007).

Another interesting new approach focuses on *in vivo* screening. Instead of only screening for antibacterial activity with living bacterial cells or only screening against a specific target in an *in vitro* screening this approach combines the advantages of both screening methods. These new screening arrays use bacterial strains where the target gene is either over- or underexpressed. These modified strains can render resistance or hypersensitivity to a specific active compound. Compound that fail to penetrate the cell wall fail to bring positive results and at the same time only compounds active against the specific target or closely associated targets are selected (Peláez 2006; DeVito et al. 2002). A similar approach has been previously been introduced for screening of cytotoxic compounds like anticancer drugs with mutated yeast stains (Giaever et al. 1999). Even if not all of these approaches might be fruitful they certainly will broaden our knowledge of producers and biosynthesis of natural compounds.

1.3 Antibiotic Resistance

In 1945 Sir Alexander Fleming warned in an interview with the New York Times that the inappropriate use of penicillin might cause the selection of resistant mutant strains (Alanis 2005). History proofed him right. Only few years after its discovery

penicillin resistance started to emerge (Alanis 2005). Now, 50 years later antibiotic resistance is wide-spread and the incident of multi-drug-resistant “superbugs” is a new threat for society. Antibiotic resistant strains first emerged in hospitals and for years seemed to be a pure hospital problem. However lately there are increasing reports of spread of antibiotic resistant strains outside of hospitals in communities (Martin et al. 2002; Calva et al. 1996) indicating an ubiquitous spread. Multi-resistant strains do not only increase the mortality and the costs of treatment but are often also more aggressive than the wild type strain and can cause severe infections also in young and healthy individuals instead of predominantly attacking immuno-compromised persons (Fernandes 2006). Additionally strains formally considered non-pathogenic like *Enterococci* have gained antibiotic resistance and are becoming increasingly established as cause of hospital-acquired infections (Cetinkaya et al. 2000). At the same time the number of new antibiotics approved for medical use in humans (Alanis 2005) and also the chemical variation of the new antibiotics decreased (Lipsitch et al. 2002) over the years (Donadio et al. 2010), making some scientist doubtful if we will manage future biological threats or instead enter into a post-antibiotic era (Alanis 2005).

1.4 Antibiotics and pharma

Beside the growing difficulty to find new antibiotic classes the decrease of newly licensed antibiotics and the lack of variety in new antibiotics are caused by the shrinking effort of industry in the field of antiinfective research (Donadio et al. 2010). A lot of “big pharma” companies bid farewell from antibiotic research due to the low-market potential of the discovery and commercialization of new antibiotics while only some small pharma firms and universities keep alive antiinfective research (Boggs, Miller 2004). The reason for the withdrawal is an unprofitable risk benefit analysis for antibiotics. While discovery and development can take between seven to ten years and is very risky and cost-intensive as e.g. clinical controls are much stricter than for example for cancer medication, the time to make money out of a new invention is short and regulated. When put on the market a race with the time starts. Pharmaceutical companies have a general financial interest to sell as many drugs as possible before the patents expire and the market is overrun with generics (Williams, Bax 2009). This however is in discrepancy with the today’s awareness to use new

antibiotics as last resort antibiotics to delay emerge of resistance (McGowan 2004). Additionally in contrast to high profit drugs in target areas like diabetes and cancer antibiotics are only prescribed for a very limited time span until the patient is fully cured from the bacterial infection. Also emerge of resistance reduces the frequency an antibiotic can be applied. A last resort antibiotic that lost its activity against multi-resistant strains also loses its job (Fernandes 2006). The shrinking of the antibiotic pipeline (Clarke 2003) definitely presses the urge for rethinking. Possible solutions might be a public funding of antibiotic research, less stiff regulations (Boggs, Miller 2004), clinical trails more suitable for antibiotics and an extension of patent terms (Fernandes 2006).

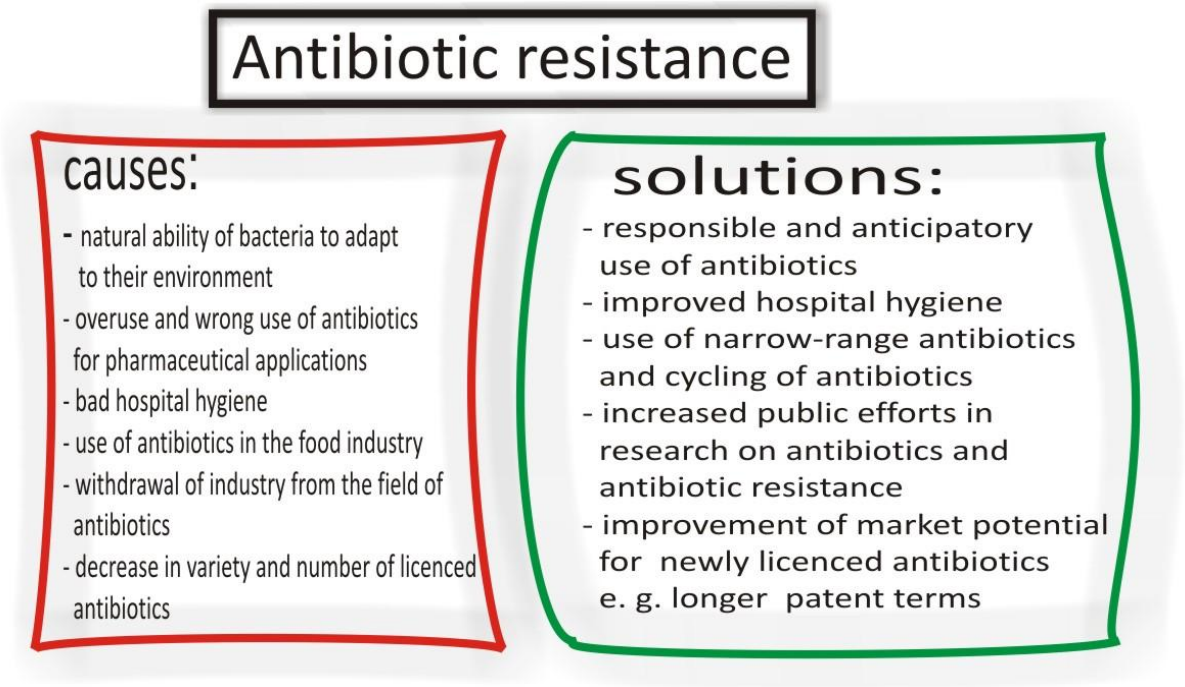

Figure 1.2: Causes of antibiotic resistance and solutions.

1.5 Causes of antibiotic resistance

Antibiotic resistance is to a certain extend a homemade problem (Figure 1.2). Inappropriate, incorrect and overuse of antibiotics for medical treatments are one main cause. Another cause is the intensive use of antibiotics in the food industry (Lipsitch et al. 2002). Antibiotics are especially used in animal feed but are even applied to control plant diseases (Barbosa, Levy 2000).

Antibiotic resistance can be naturally obtained by mutation or acquired by gene transfer from other bacteria. Unfortunately resistance gene can often be found in transposons or on plasmids, therefore especially mobile genome regions. Genetic

exchange between bacteria normally appears by conjugation, transformation or transduction (Knippers 1985). In case of conjugation genes are transferred on a plasmid through a tubular channel termed pilus between two neighboring bacteria. Transformation describes the ingestion and incorporation of free DNA fragments from the surrounding by a recipient bacterium. Transductions results from an error of a bacteriophage (Knippers 1985). The bacteriophages can accidentally pack DNA of their bacterial host instead of virus DNA into the phage envelope and inject it into another bacterium (Alanis 2005). The high multiplication and mutagenesis rates as well as the possibility to transfer genetic material between different bacterial species give bacteria the possibility to adapt very fast to environmental changes. The use of antibiotics results in a selective pressure causing a direct mutagenesis towards the formation of resistance mechanisms and their spread within the bacterial community.
There are different approaches to reduce the occurrence and spread of resistance in future. One of the most important is perhaps an improvement of hospital hygiene to stop the spread and breading of resistant bacteria (Pittet 2003). The other is a responsible administration of antibiotics both for humans and in the food industry. New “last resort” drugs should only be administered in cases of emergency when no other antibiotics can be used. Another approach might be the use of more narrow-range antibiotics and the cycling of antibiotics in their application (Kollef 2006). The hope that bacteria will lose their resistance when relieved from selective pressure, therefore a reversal of resistance, might have been too optimistic. Studies on this topic showed that resistance once obtained seems to be rather stable (Barbosa, Levy 2000). However a more responsible handling and the awareness of possible risks might delay the rise of resistance and the spread of multi-resistant strains in future.

1.6 Bacterial cell wall

The bacterial cell wall biosynthesis is an interesting target for antibiotics. Prokaryotic cells possess both, cell membranes and cell walls as barriers and as boundary separating the cytoplasm from its surroundings. Some bacteria also have an additional covering layer called capsule. Cell membranes consist of a lipid bilayer with integrated or peripheral membrane proteins and, according to the fluid mosaic model of Singer and Nicolson (Singer, Nicolson 1972), the cell membrane is fluid and allows the diffusion of lipids and proteins in the plane of the membrane. In contrast to

the very flexible cell membrane, the cell wall has a more rigid structure. It provides both mechanical stability and protection. At the same time, it also allows the selective translocation of substances from the cytoplasm to the extracellular space through special channels, transporters and pores. A key component of bacterial cell walls is peptidoglycan, a polymer comprised of chains of repeating units of *β*-(1,4)-linked *N*-acetylglucosamine-*N*-acetylmuramic disaccharides crosslinked by a pentapeptide stem. The pentapeptide stem is crosslinks to the peptide stem of another glycan chain thus resulting in the three dimensional structure of the polymer (Meroueh et al. 2006). There are two general types of bacterial cell walls: Gram-positive and Gram-negative cell walls distinguishable by the so called Gram staining with crystal violet (also hexamethyl pararosaniline chloride) (Gram 1884). The membrane of Gram-negative bacteria consists only of an thin layer of peptidoglycan surrounded by a second lipid bilayer containing a lot of lipoproteins and connected at the extracellular site to lipopolysaccharides (LPS) (Baron 1996). The LPS (lipopolysaccharides) are recognized by the immune system and often act as endotoxins and can cause severe disease reactions like sepsis in a Gram-negative bacterial infection (Raetz, Whitfield 2002). LPS is not found in Gram-positive bacteria. Gram-positive bacteria, in contrast, have a thick peptidoglycan layer containing additionally teichoic acids (TA) and lipoteichoic acids (LTA). In contrast, the cell wall of Gram-negative bacteria contains no teichoic acids. Lipoteichoic acids consist of teichoic acids and ribitol phosphate anchored by a lipid anchor in the cell membrane. They can cause pathogenic reactions comparable to LPS.

1.7 Peptidoglycan biosynthesis

The synthesis of peptidoglycan is often described in three stages. The first two stages occur in the cytoplasm and are finalized by the transport of the so called Park's Nucleotide (UDP-*N*-acetylmuramyl-L-alanyl-D-glutamyl-meso-diaminopimelyl-D-alanyl-D-alanine) to the other side of the membrane, which is the periplasm in Gram-negative and the extracellular space in Gram-positive organisms. In the subsequent third biosynthetic stage, the peptidoglycan building blocks are connected by enzymatic transglycosylations and transpeptidation reactions.

The enzymes MurA-MurF catalyze the initial stages of the peptidoglycan biosynthesis toward Park's Nucleotide (Figure 1.3). The MurA enzyme catalyzes the coupling of

UDP-GlcNAc (UDP-*N*-acetyl-glucosamine) with PEP (phosphoenolpyruvate) to yield EP-UDP-GlcNAc (UDP-*N*-acetyl-glucosamine-enolpyruvate). EP-UDP-GlcNAc is then reduced by the MurB enzyme, using NADPH as a reducing agent, to UDP-MurNAc (UDP-*N*-acetylmuramic acid). UDP-MurNAc is the substrate for the MurC enzyme, which adds L-alanine to UDP-*N*-acetylmuramic acid in an ATP-driven reaction. The synthesis of Park's nucleotide is continued by addition of D-Glu (D-glutamate) by the MurD enzyme and *meso*-Dap (*meso*-diaminopimelic acid) in case of Gram-negatives, or L-Lys (L-lysine) in case of Gram-positives by the MurE enzyme in ATP-dependent steps. Finally, D-Ala-D-Ala (D-alanyl-D-alanine) is added by the MurF enzyme and the biosynthesis of the Park's nucleotide is completed (Kahne et al. 2005). The second stage involves the enzymes MraY and MurG and results in the synthesis of the so called Lipid II. The Park's nucleotide is transferred by the MraY enzyme onto a lipid carrier creating lipid I. Lipid I is further modified by the glycosyltransferase MurG to form lipid II (Winn et al. 2010). Lipid II is then flipped in a still not fully understood way from the cytoplasmic site to the periplasm or extracellular space respectively. The third stage of peptidoglycan biosynthesis takes place in the extracellular space (or periplasm) and starts with the transfer of the disaccharide pentapeptide to the GlcNAc sugar of an existing peptidoglycan strand. This reaction is catalyzed by various transglycosylases. The immature and mechanically weak peptidoglycan strands are than stabilized by cross-linking of the pentapeptides of different strands. The crosslinking is carried out by a family of transpeptidases that catalyze amide bond formation of the δ-NH_2-group of lysine and the carbonyl carbon of the D-Ala-D-Ala-amide bond of the pentapeptide resulting in the release of the second D-Ala (Kahne et al. 2005).

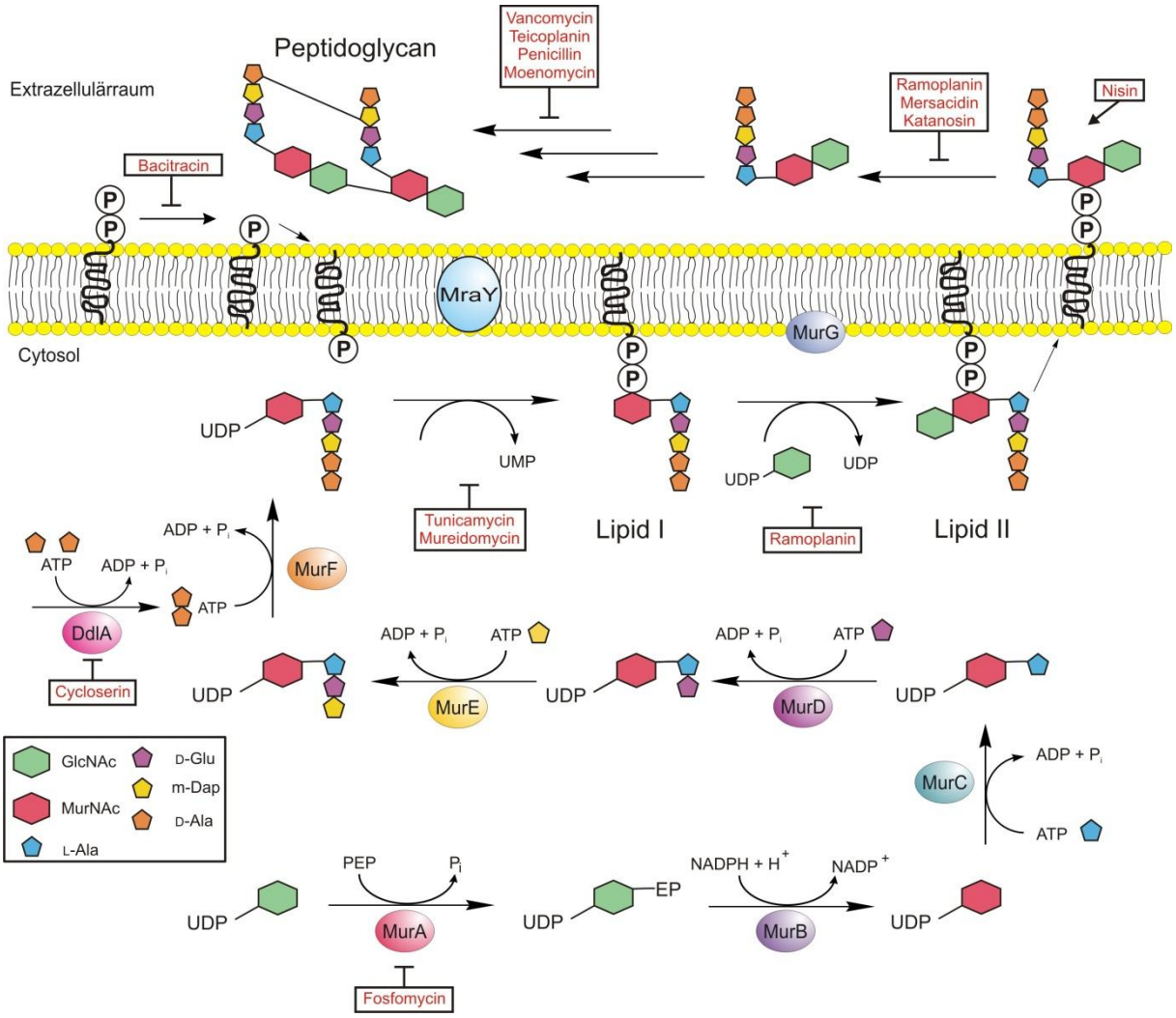

Figure 1.3: Scheme of the peptidoglycan biosynthesis and known antibiotics of the peptidoglycan biosynthesis.

1.8 Enzymes of the initial step of peptidoglycan biosynthesis

The enzymes MurA-F catalyze the first steps of peptidoglycan biosynthesis (Figure 1.4) and are all soluble cytoplasmic enzymes and very well studied in numerous publications (Schönbrunn et al. 1996; Benson et al. 1993; Jin et al. 1996; Bertrand et al. 1997; Gordon et al. 2001; Yan et al. 2000). For all of them crystal structures have been obtained (mostly from *E. coli*), for most of them even multiple crystal structure e.g. of proteins from divers bacterial sources or co-crystals of the enzymes with different substrates and inhibitors. The first enzyme MurA (UDP-*N*-acetylglucosamine enolpyrovyltransferase, also termed MurZ) catalyzes the transfer of enolpyruvate from PEP to UDP-GlcNAc to form EP-UDP-GlcNAc under the release of one equivalent phosphoric acid (Brown et al. 1994). This reaction is very unusual and the

only other enzyme known to transfer enolpyruvyl from PEP is the *S*-enolpyruvateshikimate-3-phosphate synthase (EPSPS) involved in the shikimate pathway in bacteria, fungi and plants (Holländer, Amrhein 1980). MurA and EPSPS are also structurally very similar but there are mechanistic differences that also result in susceptibility to different inhibitors. MurA is inhibited by phosphomycin (Figure 1.5) that has no effect on EPSPS. In contrast EPSPS can be effectively inhibited by the herbicide glyphosate, which has no effect on MurA (Holländer, Amrhein 1980; Schönbrunn et al. 1996). During the MurA reaction a PEP-enzyme intermediate is formed. The highly conserved Cys115 (in the *E. coli* enzyme) attacks the C2 position of PEP resulting in phospholactoyl-MurA. PEP is not released unless the second substrate UDP-GlcNAc is present (Brown et al. 1994). The reaction mechanism also explains why MurA is inhibited by phosphomycin. Phosphomycin is attacted by MurA like PEP but due to the epoxide motif the reaction stops after the attack and the active site of the enzyme is irreversibly blocked (Marquardt et al. 1994). The MurA enzyme consists of two globular domains connected by a double stranded hinge (Schönbrunn et al. 1996). Each domain consists again of three subdomains. The overall six subdomains are structurally very similar. Each of them consists of two α-helices and four β-sheets. The UDP-GlcNAc sugar is bound in the hinge region while PEP is bound at a flexible loop of one of the two domains. The reaction is expected to be accompanied by a conformational change (Schönbrunn et al. 1996).

MurB (UDP-*N*-acetylenolpyrovylglucosamine reductase) is a flavoprotein. It contains a non-covalently bond FAD cofactor that functions a redox intermediate. It facilitates the transfer of hydride from the cosubstrate NADPH to the enolpyruvyl moiety of EP-UDP-GlcNAc. The enolpyruvyl motif therefore is reduced to a lactyl ether to yield UDP-MurNAc (Benson et al. 1993). The kinetic mechanism is proposed to be a ping pong bi bi mechanism (Dhalla et al. 1995). Therefore NADPH is expected to be bound first and released before the second substrate EP-UDP-GlcNAc is bound and released. Both substrates are expected to share the same binding site (Dhalla et al. 1995). The MurB enzyme consists of three domains which are structurally inhomogeneous. All three domains possess a mixture of α-helices and β-sheets. The active site, containing the FAD cofactor, is placed in a cavity formed by all three domains (Timothy E Benson et al. 1996; Farmer et al. 1996).

The MurC protein (UDP-*N*-acetylmuramate-L-alanine ligase) catalyzes the transfer of L-alanine to UDP-*N*-acetylmuramate. L-alanine is linked to the carboxyl group of the

lactyl ether of the muramyl sugar under the release of one water molecule. The energy for the reaction is provided by the conversion of one molecule ATP to ADP and P_i. The MurC protein consists of three globular inhomogeneous domains. All three consist of both α-helices and β-sheets. The first domain shows similarities to the Rossmann fold, found in many nucleotide binding proteins, and is assumed to possess the structural requirements to bind the substrate UDP-MurNAc-Ala. The second domain is expected to bind ATP due to similarities to structures of other ATP or GTP binding proteins and the third domain shows a classical Rossmann fold. The active site is expected in an opening between all three domains (Spraggon et al. 2004). MurC is a self-associating protein and exists in equilibrium between the monomeric and the dimeric form, which are both active. The K_d value of the association was determined as 1.1+/- 0.4 µM at 37 °C. The oligomerization is not stabilized by disulfide bridges or influenced by the substrates. The role of the oligomerization for the protein is also not known (Jin et al. 1996).

MurD (UDP-MurNAc-L-alanine: D-glutamate ligase) transfers the amino acid D-glutamate onto the glycopeptide. MurD is structurally very similar to MurC. It possesses the same three globular domains and strong similarities also exist in the arrangement of the domains (Bertrand et al. 1997).

MurE (UDP-MurNAc-L-alanyl-: D-glutamate: *meso*-diaminopimelate/ L-lysine ligase) transfers either *meso*-Dap or L-Lys onto the UDP-MurNAc-dipeptide. The enzyme is not promiscuous but two different forms with different substrate specificity exist in Gram-positive and Gram-negative bacteria. MurE and MurF (UDP-MurNAc-tripeptide D-alanyl-D-alanine ligase), the latter adds adds the L-alanyl-L-alanine residue, share a similar three-dimensional structure with the other two Mur ligases (Gordon et al. 2001; Yan et al. 2000). Only MurF somehow structurally sticks out of this group. While the central and C-terminal domain show high similarity to the MurD enzyme, the *N*-terminal domain has no homology to the other Mur enzymes or any other protein (Gordon et al. 2001).

In summary the Mur ligases show an overall high structural homology beside only low sequence similarity (10-20 %). Together with the folylpoly-γ-L-glutamate synthetase (FGS) of *Lactobacillus casei* they form the Mur ADP forming ligase superfamily (Gordon et al. 2001). Especially the ATP binding site is highly conserved. The amide formation is expected to be initiated by a phosphorylation of the carboxyl group of the growing peptide chain to yield a mixed anhydride followed by a nucleophilic attack of

the NH_3-group of the incoming amino acid resulting in the formation of a tetrahedral intermediate which later collapses under release of the phosphate group (Bertrand et al. 1997).

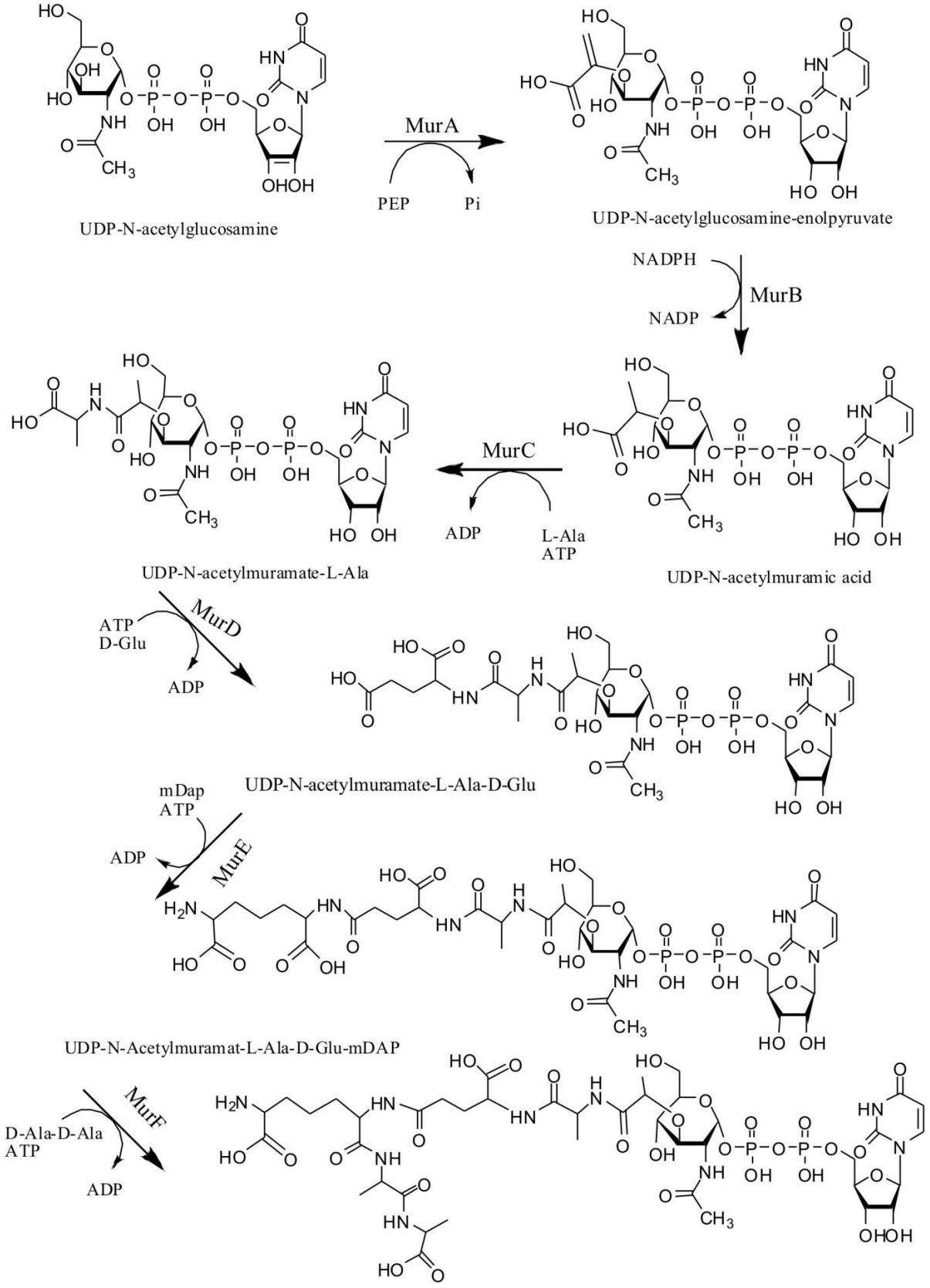

Figure 1.4: Reactionschemes of the initial steps of peptidoglycan biosynthesis.

1.9 Inhibitors of the cytoplasmic steps of peptidoglycan biosynthesis

Phosphomycin (also 3-methyloxiran-2-yl-phosphonic acid) is today the only known natural compound inhibitor of the enzyme cascade MurA-F (Figure 1.4). It was first isolated in 1969 and instantly found to be an inhibitor of the cell wall biosynthesis due to its triggering of spheroplast formation in some susceptible bacteria cells. It is expected to utilize the bacterial L-α-glycerophosphate transport system but has only very low toxicity in humans (Hendlin et al. 1969). Phosphomycin inhibits the MurA enzyme by covalently attacking the Cys residue of the active site. Besides an only moderate K_i value of 8.6 µM, phosphomycin is a very competent inhibitor and forms a stable enzyme-inhibitor complex due to the covalent bond between MurA and inhibitor (Marquardt et al. 1994). The moderate K_i value might results from the fact that the binding of phosphomycin is highly dependent on the presence of UDP-GlcNAc. As Baum et al. described it displays an significantly lower IC_{50} value of 0.4 µM in presence of UDP-GlcNAc compared to a much higher IC_{50} value of 8.8 µM in absence of UDP-GlcNAc (Baum et al. 2001). As phosphomycin preferably binds to the MurA-UDP-GlcNAc complex the inhibition mode probably matches best with an uncompetitive inhibition (Marquardt et al. 1994). Besides the inhibitor kinetics also biosynthesis has been clarified. Interestingly it was found that the last step, the epoxydation is catalyzed by a unique non-haem iron dependent monooxygenase (Higgins et al. 2005). Phosphomycin is a broad range antibiotic active against both Gram-negative and Gram-positive bacterial strains including *MRSA* and *VRSA*. Due to all this desirable qualities it established itself as an often used antibiotic especially applied against urinary tract infections. *Mycobacterium tuberculosis* is however not susceptible to phosphomycin because the *M. tuberculosis* MurA enzyme employs an Asp residue in the active site instead of Cys (Higgins et al. 2005). Self-resistance of phosphomycin-producing strains is conferred by mono- or diphosphorylation of phosphomycin. Also glutathione-modifications have been described likewise resulting in an inactive product (Kobayashi et al. 2000).

By phage-display recently a peptide inhibitor of the MurF enzyme was identified. The inhibitory effect however was very low and an *in vivo* activity not described (Paradis-Bleau et al. 2008). Another inhibitor targeting the early steps of peptidoglycan biosynthesis despite not targeting the Mur enzymes is cycloserine (Figure 1.5). Cycloserine targets both the alanine racemase and the D-alanine ligase responsible

for the supply of D-alanyl-D-alanine, the substrate of the MurF enzyme (Lambert, Neuhaus 1972). Cycloserine is active against many bacteria including *M. tuberculosis* but rarely used due to strong side effects (Ducati et al. 2006). Remarkably cycloserine is however applied to treat anxiety disorders and depressions. Cycloserine binds to the *N*-methyl-D-aspartate receptor (NMDA) in the amygdala expected to be connected with fear conditioning (Davis et al. 2005).

Strong efforts have been made in the synthesis of new inhibitors for the enzymes MurA-F. However none of these non-natural inhibitors resulted until today in a clinically used antibiotic. A lot of the synthetic inhibitors are substrate- or transition-state analogues (Emanuele, JR. et al. 1996; Tanner et al. 1996) but beside these also new more unexpected structures were identified (El Zoeiby et al. 2003).

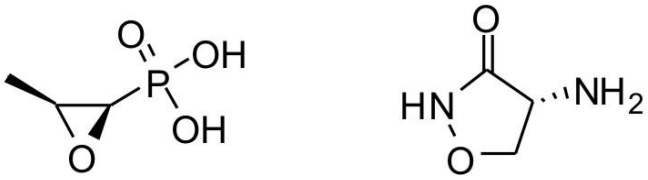

Phosphomycin Cycloserin

Figure 1.5: The natural inhibitors of the initial steps of peptidoglycan biosynthesis: phosphomycin and cycloserin.

For MurA three different inhibitors; a cyclic disulfate (RWJ-3981, Figure 1.6), a pyrazolopyrimidine (RWJ-110192, Figure 1.6) and a purine analogue (RWJ-140998, Figure 1.6) were indentified by screening of a chemical library (Baum et al. 2001). The IC_{50} values were found to be 0.2-0.9 µM and therefore significantly lower than for phosphomycin (8.8 µM) and a different binding mode compared to phosophomycin was postulated. Interestingly the inhibitory effect of all three inhibitors could be suppressed by addition of DTT (Baum et al. 2001). Beside the promising *in vitro* results *in vivo* tests showed only moderate antibacterial activity with MIC between 4-32 µg/ml and further experiments with tritiated UDP-GlcNAc, thymidine, uridine and amino acids indicated that the *in vivo* activity may not result from the specific inhibition of MurA as DNA, RNA and protein synthesis were also found to be inhibited by these compounds (Baum et al. 2001). Likewise by chemical screening a moderate MurA inhibitor derived from 5-sulfonoxy-anthranilic acid (T6361R/T6362R, Figure 1.6) was identified and characterized by co-crystallization with the enzyme. Interestingly

the inhibitor was found not to bind site specifically but to block conformational changes between the open and closed form of the enzyme (Eschenburg et al. 2005).

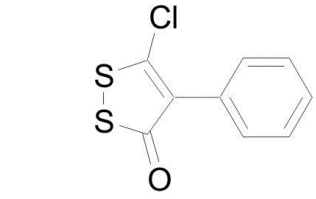

RWJ-3981, Baum et al. 2001

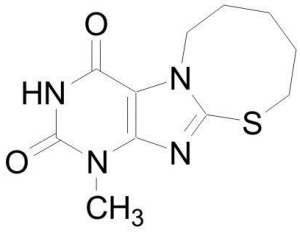

RWJ-140998, Baum et al. 2001

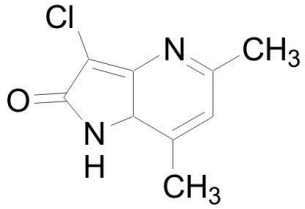

RWJ-110192, Baum et al. 2001

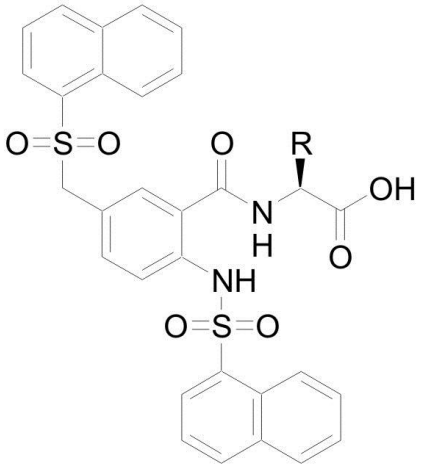

T6361 R = CH_2COOH
T6362 R = CH_2CH_2COOH
Eschenburg et al. 2005

Figure 1.6: Synthetic inhibitors of the MurA enzyme: RWJ-3981, RWJ-110192, RWJ-140998 and T6361R/T6362R.

To inhibit the MurB enzyme a number of 4-thiazolidinone inhibitors were synthesized as surrogates of the diphosphate moiety of EP-UDP-GlcNAc. Some showed a moderate activity *in vitro*, *in vivo* tests were however not reported (Figure 1.7) (Andres et al. 2000). A more successful approach was the synthesis of a library of 3,5-dioxopyrazolidines as inhibitors of the MurB enzyme from *E. coli* and *S. aureus* by Yang and coworkers (Figure 1.7) (Yang et al. 2006). These compounds showed antibacterial activity with MIC values between 0.25 µg/ml and 16 µg/ml against *MRSA*, vancomycin-resistant *Enterococcus faecialis* and *Streptococcus pneumoniae*. The best inhibitor of MurB gave a K_D of 260 nM. Some of the inhibitors showed additionally a moderate inhibitory effect on MurA and MurC enzymes from *E. coli*. A crystal structure of the complex of the inhibitor with the MurB enzyme from *E. coli* indicated a binding in the active site of MurB and an interaction with the FAD cofactor (Yang et al. 2006).

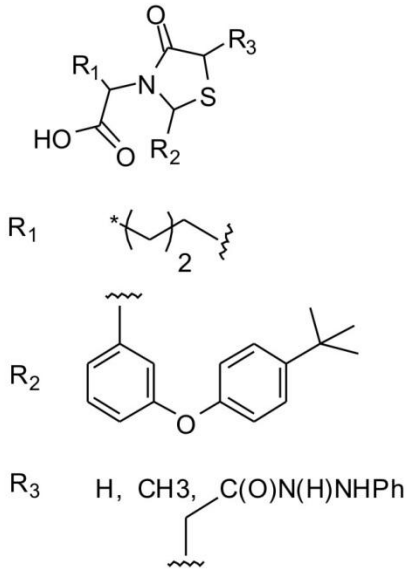

Some of the 4-thiazolidinones inhibitors, Andres et al. 2000

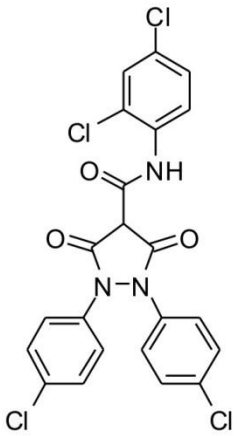

3,5-Dioxopyrazolidines, Yang et al. 2006

Figure 1.7: Synthetic inhibitors of the MurB enzyme: 4-thiazolidinones and 3,5-dioxopyrazolidines.

As inhibitors of the enzymes MurC-F mostly phosphinate inhibitors mimicking transition state analogues of the tetrahedral intermediate formed during amide formation were studied (Figure 1.8). These often showed a very good inhibitory action (El Zoeiby et al. 2003). Examples comprise a MurC inhibitor by Marmor et al. (Figure 1.8) (Marmor et al. 2001), a MurD inhibitor by Tanner et al. (Tanner et al. 1996), a MurE inhibitor by Zeng et al. (Zeng et al. 1998) and a MurF inhibitor by Miller et al. (Miller et al. 1998). *In vivo* activity of these compounds however was not even tested or appeared not promising to perform further studies. Beside the phosphinate inhibitors mostly substrate analogues were tested with only unsatisfying results for further investigation of their antibacterial potential (El Zoeiby et al. 2003).

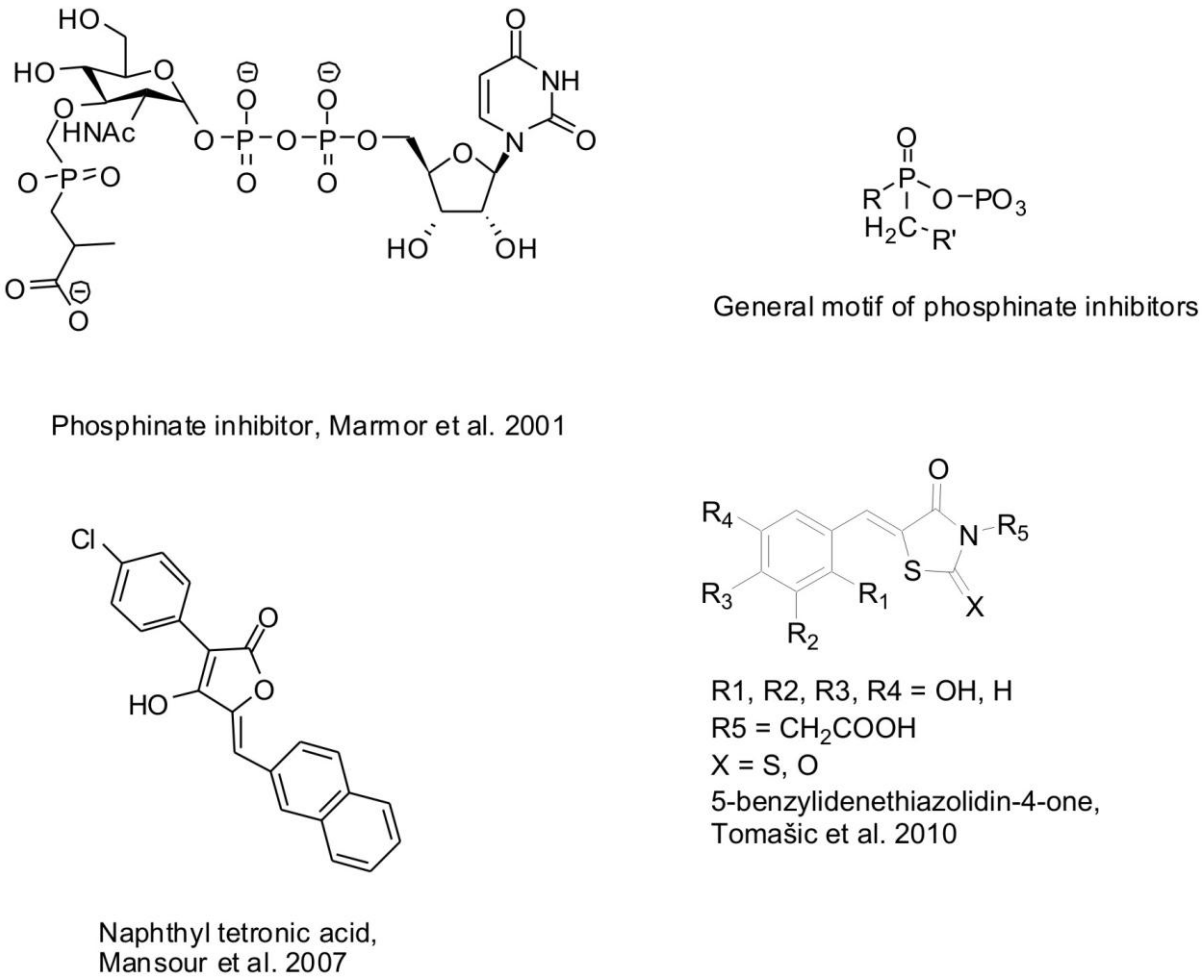

Figure 1.8: Structure of the phosphinate inhibitors and multitarget inhibitors of the Mur enzymes.

Additionally to inhibition of the single enzymes efforts lately were made to find multitarget inhibitors of the Mur enzymes. Mansour et al. investigated napthyl tetronic acids as multitarget inhibitors of the enzymes MurA-F (Figure 1.8). These compounds showed an inhibitory effect on the MurB enzyme in low µM range and also an antibacterial activity with MIC values between 2 µg/ml and 64 µg/ml on *E. coli* and *S. aureus* but less efficiency against the other Mur enzymes (Mansour et al. 2007). Tomašić et al. synthesized a number of 5-benzylidenethiazolidin-4-one derivatives from which some showed multitarget inhibition of the enzymes MurD-F (Figure 1.8). These compounds were tested against *E. coli*, *S. aureus*, *E. faecalis* or *P. aeruginosa* however none of them had any considerable antibacterial effect on these bacteria strains (Tomašić et al. 2010).

1.10 The enzymes of the second stage of peptidoglycan biosynthesis

The second stage of peptidoglycan biosynthesis takes place in the cytoplasm at the inner face of the cell membrane and involves the enzymes MraY and MurG. MraY (phospho-MurNAc-peptapeptide translocase) transfers the UDP-MurNAc-pentapeptide onto a membrane anchored undecaprenyl phosphate ($C_{55}P$) under release of UMP. The product of the MraY reaction is lipid I (undecaprenyl-pyrophosphate MurNAc-pentapeptide). In the subsequent reaction the glycosyltransferase MurG transfers a GlcNAc sugar from UDP to the 4'-hydroxy group of MurNAc under formation of a *β*-1,4-linkage. The undecaprenyl-pyrophosphate disaccharide pentapeptide is termed Lipid II. MraY is an intregral membrane protein and MurG is a membrane associated enzyme (Winn et al. 2010). Their membrane localization and the difficulty to generate the substrates for the MraY and MurG enzyme reactions are probably the reasons why enzyme assays were not available and both enzymes were not characterized in detail until recently. The MraY protein possesses homologies to several hexosamine-1-phosphate transferase enzymes both in prokaryotes and eukaryotes (Winn et al. 2010). The enzyme kinetics of MraY was first studied in 1996 in a fluorescence assay with isolated Park's nucleotide and the enzyme was solubilized by high amount of the detergent TritonX-100 (Brandish et al. 1996a). Topological studies of MraY revealed ten transmembrane α-helices and five cytoplasmic and six periplasmic domains (Bouhss et al. 1999). By sequence alignments three highly conserved aspartic acid residues were identified on the cytoplasmic side and found to be essential for MraY activity (Lloyd et al. 2004).

The MurG enzyme was not sequenced before 1990 and first overexpressed in 1998 (Ha et al. 2001). Assays to study the MurG enzyme were established both by semi-synthesis (Auger et al. 1997; Auger et al. 2003) and total synthesis of Lipid I (Ha et al. 1999). Membrane association was bypassed by addition of Triton-X 100. Lately also crystal structures of the MurG enzyme were obtained. The MurG enzyme consists of two domains which possess a strong structural similarity in spite of low sequence similarity. Both adopt an α/β sheet motif, the so called Rossmann fold. It is postulated that both substrates bind to a different domain in the course of the MurG reaction. Astonishingly MurG has strong homologies to the T4 phage *β*-

glycosyltransferase and only little homologies to any other studied glycosyltransferases (Ha et al. 2001).

1.11 Inhibitors of the second stage of peptidoglycan biosynthesis

A considerable number of inhibitors of the MraY enzyme have been described. Best known are perhaps the MraY inhibitors tunicamycin, mureindomycin and liposidomycin. The inhibition occurs supposable by substrate analogy to the UDP-MurNac-pentapeptide. Beside these analogies differences in structure, mechanism of inhibition and target specificity have been described (Brandish et al. 1996b). Tunicamycin, isolated in 1971 from *Streptomyces superificus,* active against Gram-positive bacteria, yeast and fungi consists of a uracil moiety, GlcNAc, an 11-carbon aminodialdose (tunicamine) and a fatty acid chain linked to the amino group (Figure 1.9). Different homologues exist, which differ in the length of the fatty acid chain (Takatsuki et al. 1971). Tunicamycin was found to be a reversible inhibitor of both MraY and the mammalian UDP-GlcNAc-dolichyl-phosphate-GlcNAc-1-phosphate transferase, involved in the biosynthesis of glycoproteins in eukaryotic cells (Heifetz et al. 1979). Due to its toxicity towards eukaryotes tunicamycin is not employed as an antibiotic but it is used as an experimental tool as it induces unfolded protein response as a cellular stress response (Mitra et al. 2002). Mureindomycin and liposidomycin, in contrast, specifically inhibit the bacterial enzyme with a different binding kinetics than tunicamycin (Brandish et al. 1996b). Mureindomycin, a mixture of homologous peptidyl nucleoside antibiotics was first isolated from *Streptomyces flavidovirens* in 1989 (Isono et al. 1989a). Beside one Met and two Tyr residues it contains 2-amino-3-*N*-methylaminobutyric acid (AMBA) as well as uracil or dihydrouracil, respectively (Figure 1.9). Mureindomycin was found to exhibit an especially high activity against *Pseudomonas* while liposidomycin possess a good activity against Mycobacteria including multi-drug resistant *Mycobacterium tuberculosis*. Liposidomycin is a uracil-nucleoside antibiotic isolated 1985 from *Streptomyces griseosporeus* in Japan (Isono et al. 1985). Later it was grouped together with the structurally very similar natural product caprazamycin (Hirano et al. 2008) and more simple structured FR900493 (Hirano et al. 2007) as 6´-*N*-alkyl-5´-*β*-*O*-aminoribosylglycyluridine antibiotics. Further related antibiotics are muraymycin

(McDonald et al. 2002), pacidamycin (Fronko et al. 2000), capuramycin (Yamaguchi et al. 1986) and napsamycin (Chatterjee et al. 1994).

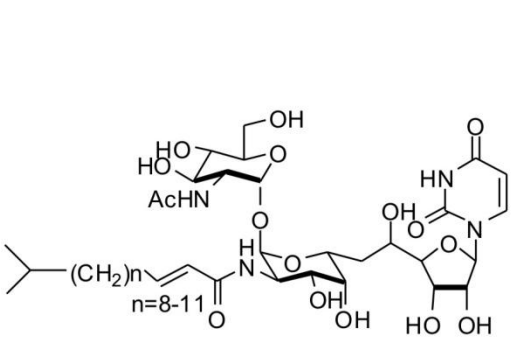

Tunicamycin

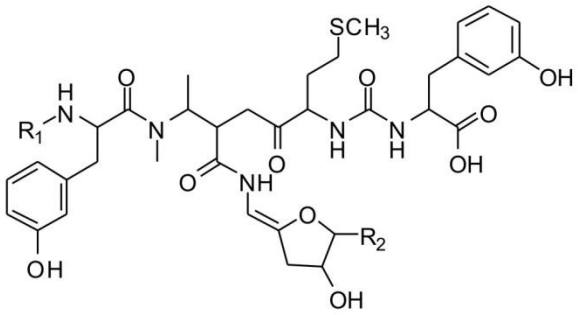

Mureidomycin

	R_1	R_2
A	H	Uracil
B	H	Dihydrouracil
C	Glycine	Uracil
D	Glycine	Dihydrouracil

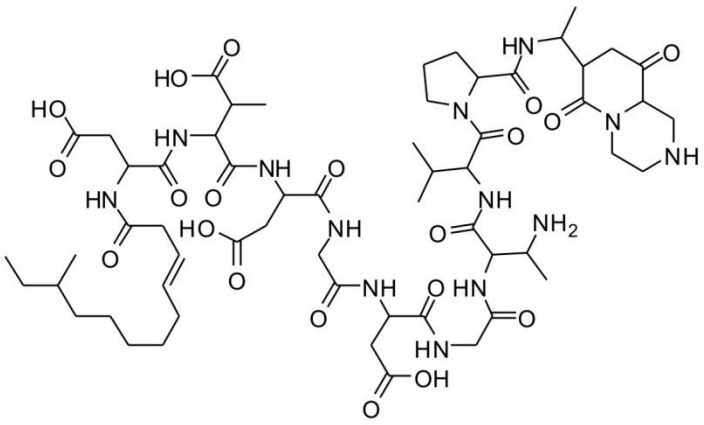

Amphomycin

Figure 1.9: Inhibitors of the second stage of peptidoglycan biosynthesis: tunicamycin, mureidomycin and amphomycin.

Amphomycin, an undecepeptide antibiotic, also inhibits the MraY catalyzed reaction (Figure 1.9) (Tanaka et al. 1979). More detailed studies revealed that the inhibition results from a Ca^{2+} dependent complexation of the C_{55}-isoprenyl phosphate (Banerjee 1987). Due to its more general mechanism of action it inhibits all glycosylations of dolicyl phosphate and therefore like tunicamycin also eukaryotic glycopeptide biosynthesis.

The natural MraY inhibitors have inspired the synthesis and semisynthesis of a number of artificial inhibitors (Kimura, Bugg 2003). Lin at al. e.g. synthesized a

number of muraymycin inhibitors that however were not tested *in vivo* (Lin et al. 2002). A modification of capuramycin of Bogatcheva and coworkers in contrast was able to improve *in vitro* activity of the compound (Bogatcheva et al. 2011).

For the MurG enzyme less inhibitors are known. Ramoplanin is known to inhibit the MurG enzyme additionally to its inhibitory effect on the third stage of peptidoglycan biosynthesis (McCafferty et al. 2002). Recently efforts were made to identify synthetic MurG inhibitors (Hu et al. 2004; Trunkfield et al. 2010). A donor displacement screen in the group of Walter identified seven MurG inhibitors with IC_{50} values against *E. coli* MurG of 1-6 µM. *In vivo* tests were however not reported (Figure 1.10) (Hu et al. 2004). Transition state analogues synthesized by Trunkfield and coworkers were less successful. Most compounds showed only little or no effect on *E. coli* MurG (Trunkfield et al. 2010).

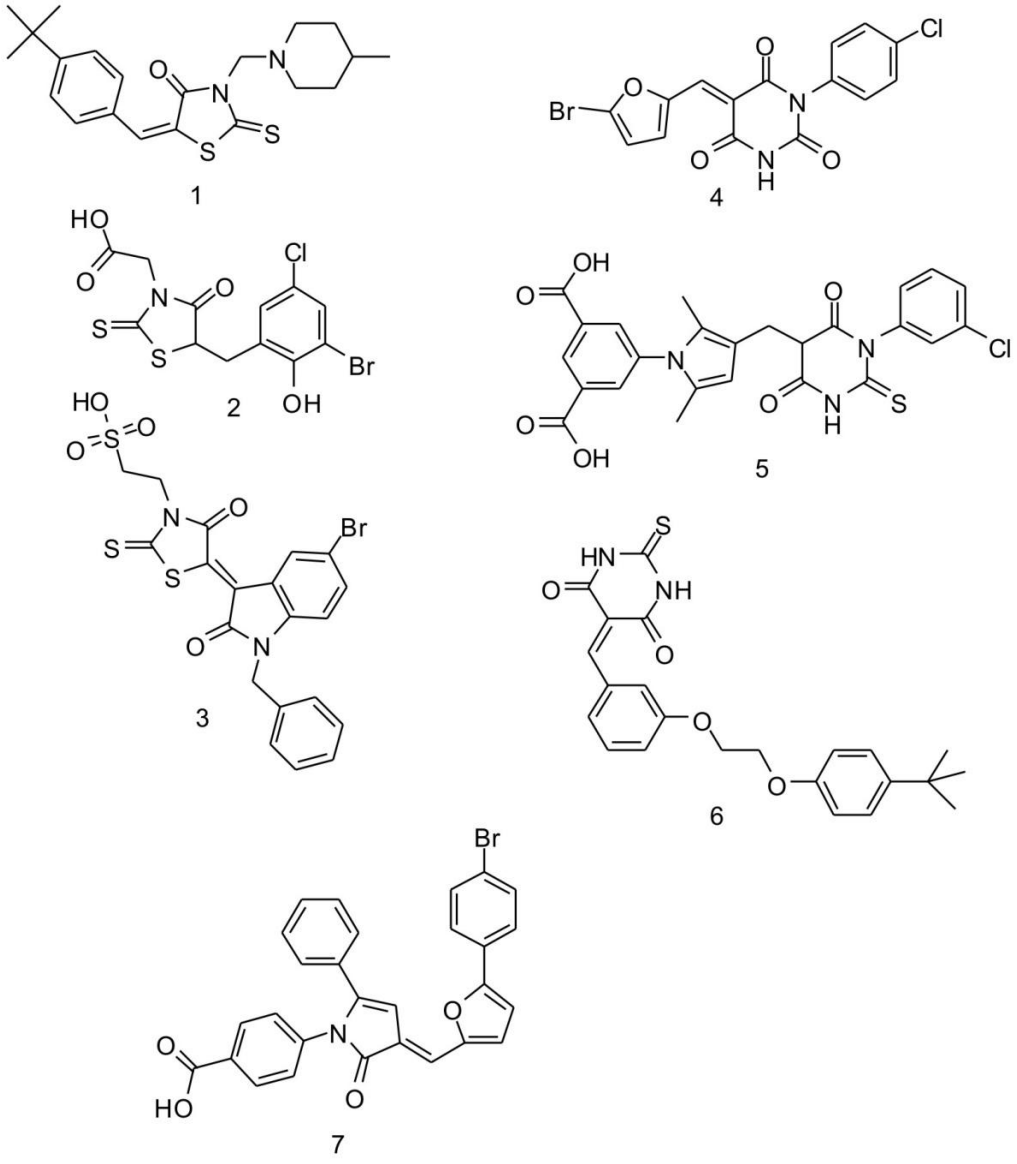

Figure 1.10: Synthetic inhibitors of the MurG enzyme (Hu et al. 2004).

1.12 The enzymes of the third stage of peptidoglycan biosynthesis

The last stage of peptidoglycan comprises only two reactions, a transglycosylation and a transpeptidation. Due to the extensive formation of a network structure it might be however considered enzymatically most complex and is also least understood. This is due to the fact that the two reactions are catalyzed by a larger group of different enzymes known as penicillin-binding proteins (PBP). In this context it is interesting to note, that *E. coli* e.g. can produce 12 different PBP (O'Daniel et al. 2010). The group of PBPs were initially characterized for they ability to bind penicillin (Spratt 1977) and are traditionally further classified by their molecular weight as high or low molecular weight PBP. Some of the high molecular weight PBP contain both transglycosylase and transpeptidase domains (Lovering et al. 2007), the other PBP seem to catalyze only one of the two reactions (Kahne et al. 2005). The high molecular weight PBPs are mainly responsible for peptidoglycan polymerization, but some are also believed to play a role in cell morphogenesis and to interact with proteins involved in the cell cycle (Sauvage et al. 2008). The low molecular weight PBPs, in contrast, are related to cell separation and peptidoglycan maturation and recycling (Sauvage et al. 2008). Both high and low molecular weight PBP are membrane anchored (O'Daniel et al. 2010).

Table 1.1: Natural product inhibitors of peptidoglycan biosynthesis in the order they are mentioned in the text.

Antibiotic	Target	activity
Initial stage of peptidoglycan biosynthesis		
Phosphomycin	MurA	K_i: 8.6 μM *E. coli* MurA (Baum et al. 2001)
Cycloserin	Alanine-racemase and D-alanine ligase	K_i: 6.5 * 10^{-4}M *E. coli* alanine racemase (Lambert, Neuhaus 1972)
Second stage of peptidoglycan biosynthesis		
Tunicamycin	MraY and mammalian UDP-GlcNAc-dolichyl-phosphate-GlcNAc-1-phosphate transferase	K_i: 0.55 μM *E. coli* MraY (Brandish et al. 1996b)

Liposidomycin B	MraY	IC_{50} = 0.05 μg/mL for *E. coli* MraY (Hirano et al. 2008)
Mureidomycin A	MraY	K_i: 0.04 *10 μM *E. coli* MraY (Brandish et al. 1996b) MIC = 1.56 μg/mL against antibiotic-resistant *Pseudomonas aeruginosa* (Isono et al. 1989b)
Caprazamycin	MraY	IC_{50} = 0.05 μg/mL *E. coli* MraY; MIC = 3.13 μg/mL against multi-drug-resistant *Mycobacterium tuberculosis* (Hirano et al. 2008)
Muraymycin	MraY	IC_{50} = 0.027 μg/mL *E. coli* MraY; MIC 2 to 16 μg/mL against *Staphilococcus* (McDonald et al. 2002)
Pacidamycin	MraY	MIC 1 to 125 μg/mL against *Pseudomonas aeruginosa* (Fronko et al. 2000)
Capuramycin	MraY	MIC 12.5 μg/mL against *Streptococcus pneumoniae* and MIC 3.2 μg/mL against *Mycobacterium smegmatis* (Yamaguchi et al. 1986)
Napsamycin	MraY	MIC 12 to 25 μg/mL against *Pseudomonas aeruginosa* (Chatterjee et al. 1994)
Amphomycin	MraY	IC_{50} = 20 μg/ml MraY (Tanaka et al. 1979)
Ramoplanin	MurG; Lipid II, different binding site than vancomycin	MIC 2. μg/mL against *MRSA* (McCafferty et al. 2002)
Final stage of peptidoglycan biosynthesis		
Penicillin	Transpeptidase	IC_{50} = 0.5 μg/mL binding to *S. aureus* PBP1, MIC 0.03 μg/mL against penicillin suseptable *Streptococcus pneumoniae* (Kosowska-Shick et al. 2010)
Moenomycin	Transglycosylation	MIC 0.01-0.3 μg/mL against *S. aureus* (Ostash, Walker 2010), K_D = 54.2 nM *E. coli* PBP1 (Cheng et al. 2008)

Prasinomycin	Transglycosylation	MIC 0.15 µg/mL against *S. aureus* (Ostash, Walker 2010)
Marcabomycin	Transglycosylation	MIC 0.05 µg/mL against *S. aureus* (Ostash, Walker 2010)
Diumycin	Transglycosylation	MIC 0.02 µg/mL against *S. aureus* (Brown et al. 1974)
Vancomycin	Lipid II, complexes D-Ala-D-Ala moiety	K_D 1,6 µM D-Ala-D-Ala derivates (Rao et al. 1998), MIC 1.4 µg/mL against *S. aureus* (Peschel et al. 2000)
Balhimycin	Lipid II, complexes D-Ala-D-Ala moiety	MIC 1.4 µg/mL against *S. aureus* (Peschel et al. 2000)
Chloroeremomycin	Lipid II, complexes D-Ala-D-Ala	MIC 0.057 µg/mL against *M. luteus* (Allen, Nicas 2003)
Teicoplanin	Lipid II, complexes D-Ala-D-Ala	MIC 1.3 µg/mL against *S. aureus* (Peschel et al. 2000)
A40926	Lipid II, complexes D-Ala-D-Ala	MIC 0.06 µg/mL against *S. aureus* and 2 µg/mL against *Neisseria gonorhoeae* (Goldstein et al. 1987)
A47934	Lipid II, complexes D-Ala-D-Ala	MIC 0.06 µg/mL against *S. aureus* and 8 µg/mL against *Neisseria gonorhoeae* (Goldstein et al. 1987)
Ramoplanin	Lipid II, different binding site than vancomycin; MurG	MIC 0.38–1.5. µg/mL against *MRSA* and 0.1–1.5 µg/mL against *VRE* (Brumfitt et al. 2002)
Enduracidin	Lipid II, different binding site than vancomycin	MIC 0.78 µg/mL against *S. aureus* (Tsuchiya et al. 1968)
Janiemycin	Lipid II, different binding site than vancomycin	MIC 0.05 µg/mL against *S. aureus* (Brown et al. 1974)
Nisin	Pore formation	MIC 0.06 µg/mL against *L. lactis* (Sun et al. 2009), MIC 1.5-16 mg/L against *MRSA* and MIC 1.5-16 mg/L against *VRE* (Brumfitt et al. 2002)
Epidermin	Pore formation	MIC 0.3 µg/mL against *S. carnosus* (pRB473/pTepiQ10 (Otto et al. 1998)

Mersacidin	Lipid II, different binding site than vancomycin	MIC 0.1 µg/mL against *M. luteus* (Brötz et al. 1998)
Actagardin	Lipid II, different binding site than vancomycin	MIC 0.8 µg/mL against *M. luteus* (Brötz et al. 1998)
Mannopeptimycin	Lipid II, different binding site than vancomycin	MIC 4-128 µg/mL against *MRSA* (Singh et al. 2003)
Bacitracin	C_{55}-isoprenyl pyrophosphate	MIC 2-16 mg/L against *MRSA* and MIC 12-125 mg/L against *VRE* (Brumfitt et al. 2002)
Katanosin	Transglycosylation different to vancomycin	MIC 0.39-0.78 µg/mL against *S. aureus* (Shoji et al. 1988)
Plusbactin	Transglycosylation different to vancomycin	MIC 0.4-1.6 µg/mL against *MRSA* (Shoji et al. 1992)

1.13 Inhibitors of the third stage of peptidoglycan biosynthesis

The enzymes of the third stage of peptidoglycan biosynthesis are highly qualified as targets for antibiotics. Not only are they essential and specific for bacteria but they are additionally highly accessible (at least in Gram-positive bacteria), also for compounds that cannot penetrate the cell wall, due to the fact that they are localized in the extracellular phase in Gram-positive and the periplasm in Gram-negative bacteria (Lovering et al. 2007). Furthermore despite of the high number of different PBP most of them are targeted by the same antibiotics due to the high degree of conservation of the active domains. Probably because of these favorable properties for drug design a lot of effort has been put in the discovery, synthesis and semisynthesis of new inhibitors (Malabarba et al. 1997). But also nature seems to favor the third stage of peptidoglycan biosynthesis as a considerable number of natural compound inhibitors inhibit the last stage of cell wall biosynthesis (Kahne et al. 2005). There are roughly three different classes of antibiotics inhibiting the final stage of peptidoglycan biosynthesis: inhibitors of the transpeptidases, inhibitors of the transglycosylases and antibiotics binding to the substrate of the transpeptidase/transglycosylase reaction (Kahne et al. 2005). The β-lactam antibiotics belong to the first mentioned class, a member of the second class is moenomycin and vancomycin is a representative of the last class. Beside these three distinct types there are still further inhibitors that can be regarded as inhibitors of the

third step of peptidoglycan biosynthesis. For example bacitracin that inhibits the regeneration of C_{55}-isoprenyl pyrophosphate, the lipid carrier of the disaccharide pentapeptide, and lantibiotics like nisin that interact with lipid II and induce pore formation.

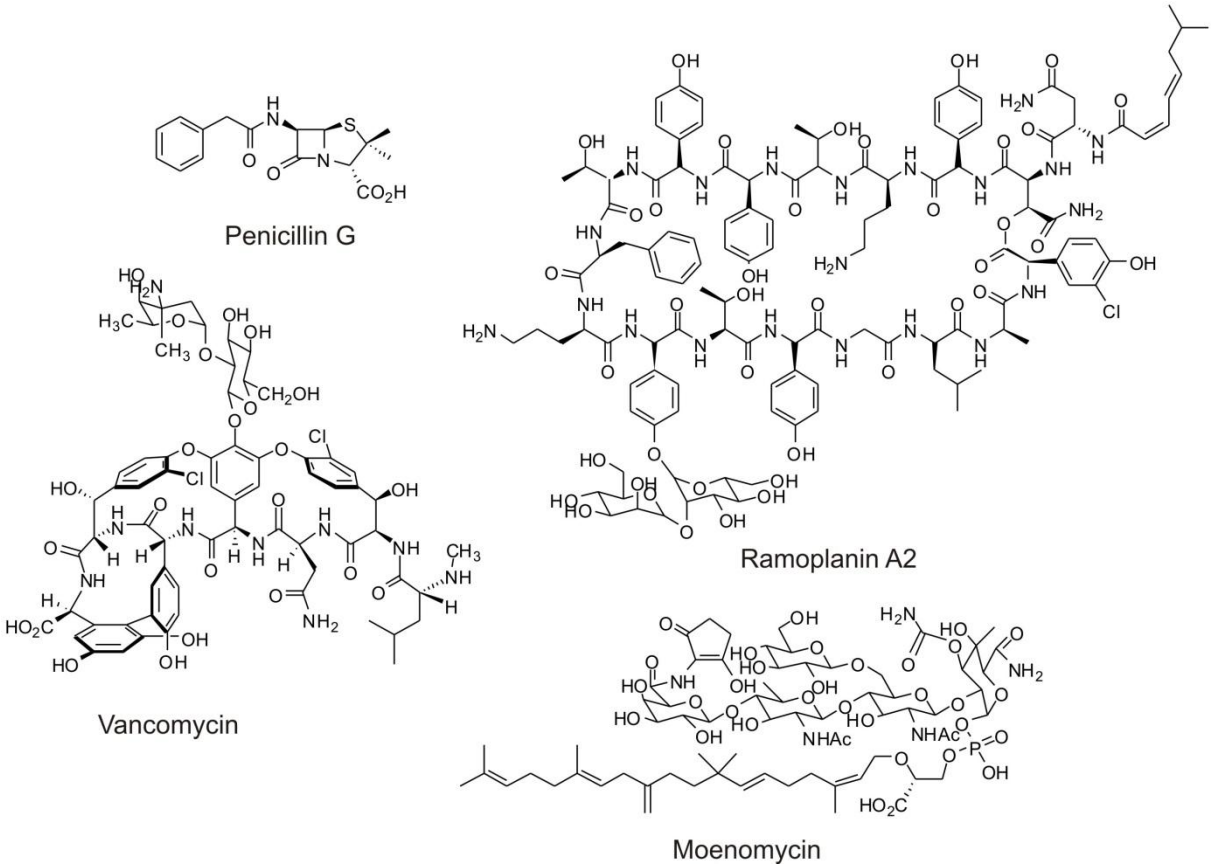

Figure 1.11: The inhibitors of the third stage of peptidoglycan biosynthesis penicilin, ramoplanin, vancomycin and moenomycin.

1.14 The β-lactam antibiotics

β-lactam antibiotics bind to the active center of the transpeptidases (Frère et al. 1974). Among these penicillin (Figure 1.11) is probably the most renowned member of this complex group of antibiotics. The observance of its antibiotic effect by Alexander Fleming in 1929 (Fleming 1929) is often considered the start of the era of antibiotics (Fernandes 2006). β-lactam antibiotics are both produced by filamentous fungi like *Penicillium notatum* (Fleming 1929) and Gram-positive as well as Gram-negative bacteria (Brakhage et al. 2005). β-lactam antibiotics divide in a large number of structurally diverse antibiotics that all share the β-lactam motife in their structure. Worth mentioning are certainly clinically important β-lactam antibiotic subgroups, like the cephalosporins, the carbapenems and the monobactams which

are less prone to cause allergies than the Penicillin antibiotics (Pegler, Healy 2007; Frumin, Gallagher 2009). Beside allergies the biggest problem with the clinical treatment with β-lactam antibiotics is the wide spread of β-lactam resistance. β-lactam resistance was first reported in 1940 (Abraham, Chain 1940) and is based on enzymatic hydrolysis of the β-lactam ring by β-lactamases. Since the first discovery of β-lactam resistance a large number of different β-lactamases have been described. A problematic factor of β-lactam resistance is that especially Gram-positives can produce large quantities of β-lactamases, which they export. Thus, they can protect a whole bacteria colony against the antibiotic threat. Also the plasmid-mediated host-to-host transfer of β-lactam resistance is quite common (Theuretzbacher 1998). The fast spread and effectiveness of some β-lactamases even trigger labels like “superbug” as has been used in the popular press for a multi-drug resistant Gram-negative *Enterobacteriaceae* carring a particularly efficient metallo-β-lactamase 1 (NDM-1) (Kumarasamy et al. 2010; Wandtner 16.09.2010). β-lactam resistance can be bypassed by the application of combination drugs, e.g. a β-lactam antibiotic and a β-lactamase inhibitor. Examples are the high selling drug augmentin (Glaxo Smith Kline) a combination of amoxicillin with the β-lactamase inhibitor clavulamic acid. Further examples are piperacillin and tazobactam in the commercial antibiotic tazocin (Wyeth) and the combination of β-lactamase inhibitor sulbactam with cefoperazone (Sulperzone) or amplicillin (Sultamicillin) (Saudagar et al. 2008). However this solution predicatively has a time-limit as resistance to β-lactamase inhibitors starts to emerge (Papp-Wallace et al. 2010).

1.15 The Moenomycin-type antibiotics

The members of the moenomycin family of antibiotics are very effective inhibitors of the transglycosylation step with MIC values around 1-100 ng/mL (Lovering et al. 2007; Cheng et al. 2008; Ostash, Walker 2010). Moenomycin (Figure 1.11, also bambermycin, flavomycin or flavophospholipol), eponym of this family was isolated in 1965 (Wallhausser et al. 1965) and 1969 (Schacht, Huber 1969) and is a glycolipid antibiotic. Further moenomycin like antibiotics are prasinomycin, macabomycin and duimycin (Lugtenberg et al. 1972; Brown et al. 1974). Moenomycin consists of a pentasaccharide linked by 3-phosphoglyceric acid to a C25 isoprenoid chain (moenocinol) (Baizman et al. 2000) and is the only bacterial secondary product

known containing 3-phosphoglyceric acid (Ostash, Walker 2010). Due to poor pharmacokinetic properties monomycin so far has not been considered for clinical use. It however is applied as additive in animal feed (Kahne et al. 2005). Acquired resistances against moenomycin are not known, however a natural resistance of some *E. faecium* strains was reported (Butaye et al. 2003). A mechanism conveying moenomycin resistance is also unknown (Ostash, Walker 2010).

1.16 The Vancomycin-type antibiotics

Vancomycin (Figure 1.11) is the best known member of a family of antibiotics also called glycopeptide antibiotics. Vancomycin was discovered by McCormick in 1956 from *Amycolatopsis orientalis* (McCormick et al. 1955-1956). The structure however was not elucidated before 1978 (Sheldrick et al. 1978) probably due to the fact that vancomycin and its related glycopeptides exhibit a very complex structure and possess a lot of modifications like crosslinking, glycosylation, lipidation, methylation, halogenation or sufonylation. Beside distinct differences in the nature of their modification all vancomycin antibiotics, at first sight, show a closely related structure: A heptapeptide scaffold cycled or branched by extensive oxidative cross-linking (Kahne et al. 2005). The peptide scaffold contains an altering number of non-proteinogenic amino acids like 4-hydroxyphenylglycine (Hpg), 3,5-dihydroxyphenylglycine (Dpg) and β-hydroxy-chlorotyrosine (Cht). Other important members of the group of vancomycin antibiotics are balhimycin (Pelzer et al. 1999), complestatin (Chiu et al. 2001), chloroeremomycin (also termed LY264826) (Rolston et al. 1990; van Wageningen et al. 1998), teicoplanin (Li et al. 2004), A40926 (Sosio et al. 2003) and A47934 (Pootoolal et al. 2002). Identfication of the gene clusters of many members of the group of vancomycin antibiotics proved that they are synthesized by non-ribosomal peptide synthetases. Vancomycin inhibits the cell wall biosynthesis by binding tightly to the D-Ala-D-Ala terminus of a growing peptidoglycan chain in the late stages of the peptidoglycan biosynthesis (Reynolds 1989). It shows a bad permeability for the cytoplasmic membrane (Perkins, Nieto 1970) and also for the outer membrane of Gram-negative bacteria (Kahne et al. 2005) wherefore it is only applied to Gram-positive bacteria. All glycopeptide antibiotics are generally considered to act by the same mode of action. However there is a growing awareness of differences in the mode of action and mechanism of resistance to

different glycopeptides (Kahne et al. 2005). Complestatin i.e. was reported to possess an anticomplement and a neuroprotective activity (Kaneko et al. 1980). Vancomycin and teichoplanin are considered as last resort antibiotics and especially used for patients suffering from bacterial infections with *MRSA* because for several decades of usage no vancomycin resistance emerged. However resistance to vancomycin by vancomycin-resistant *Enterococci* has spread since the end of the 1980ies (Cetinkaya et al. 2000) and lately also resulted in emergence of vancomycin-resistant *MRSA* (so called *VRSA*) (Chang et al. 2003). Vancomycin resistance is generally enabled by the remodeling of the D-Ala-D-Ala terminus of peptidoglycan to D-Ala-D-Lac and conferred by a resistance cassette of five genes *VanRSHAX. VanR* and *VanS* code for a two-domain response regulator and a transmembrane sensor kinase and have regulatory function. VanH converts pyruvate to D-Lac and VanA links D-Lac and D-Ala. D-Ala-D-Lac is accepted by the normal MurF enzyme. VanX cleaves of the ordinary D-Ala-D-Ala terminus and hence reduces the amount of possible target for the glycopeptide antibiotics (Walsh et al. 1996). Different phenotypes of resistant strains with different susceptibility to different glycopeptide antibiotics were observed and termed VanA, VanB and VanC. Interestingly VanB strains are still susceptible to teicoplanin while VanA strains are not, although both carry the complete resistance cassette. Later it was found that vancomycin but not teicoplanin induces the VanS senor kinase in VanB strains which has been suggested to be associated with the membrane localization of teicoplanin due to its accessory lipid chain (Kahne et al. 2005).

A lot of semisynthetic derivates of the glycopeptide antibiotics have been described and synthesized; some of which had an increased *in vivo* activity also against vancomycin-resistant strains (Nicas et al. 1995; Al-Nawas, Shah 1998; Goldstein et al. 2004, Allen, Nicas 2003).

1.17 Ramoplanin

Closely related to the vancomycin group of antibiotics, but no members are the glycodepsipeptide antibiotics ramoplanin and enduracidin. Ramoplanin (Figure 1.11), produced by *Actinoplanes* sp., was discovered in 1984 in a screening for new cell wall inhibitors in Italy (Pallanza et al. 1984). Ramoplanin is a 17 amino acid cyclic peptide with an attached fatty acid chain and several non-proteinogenic Hpg amino

acids. It additionally carries amino acids modified by β-hydroxylation, chlorination and glycosylation. Ramoplanin has a broad-spectrum activity against Gram-positive bacteria with MIC values around 2.0 µg/mL (McCafferty et al. 2002). It binds to lipid I and lipid II but instead of the D-Ala-D-Ala motif targets the disaccharide and the attached pyrophosphate motif of Lipid II (Cudic et al. 2002). Crystal structures showed the formation of an amphipathic dimer able to interact with the membrane (Hamburger et al. 2009). Additionally it was found that ramoplanin can inhibit the MurG enzyme *in vitro*, but it is not clear if this activity also plays a role *in vivo*, as the MurG enzyme is located at the inner face of the cell membrane and it is still unknown if ramoplanin can get there (McCafferty et al. 2002). The different mode of action compared to the vancomycin antibiotics and the good tolerance of ramoplanin in humans makes it a good candidate for the therapy of infection with *VRE* strains (Emerson, Marzella 2007). Semisynthetic approaches report the exchange of the lipidic part by a carboxylic acid to increase tolerability in intravenous injections which resulted in slight decrease of the biological activity of some bacteria strains (Ciabatti et al. 2007).

Enduracidin and janiemycin (Brown et al. 1974) are further cell wall inhibitors that are structurally closely related to ramoplanin. For enduracin in addition an antiviral activity (McCafferty et al. 2002) and an activity against the human prolyl endopeptidase (Kimura et al. 1997) has been reported.

1.18 Lantibiotic cell wall biosynthesis inhibitors

Another famous group of peptide antibiotics are the lantibiotics. The name lantibiotics derives from lathionine. A lathionine motif formally can be regarded as the crosslinking of two alanine residues by a thioether bridge. The lantibiotics are a larger group of peptides ribosomal produced by Gram-positive bacteria and some of them target the bacterial cell wall biosynthesis (Chatterjee et al. 2005).

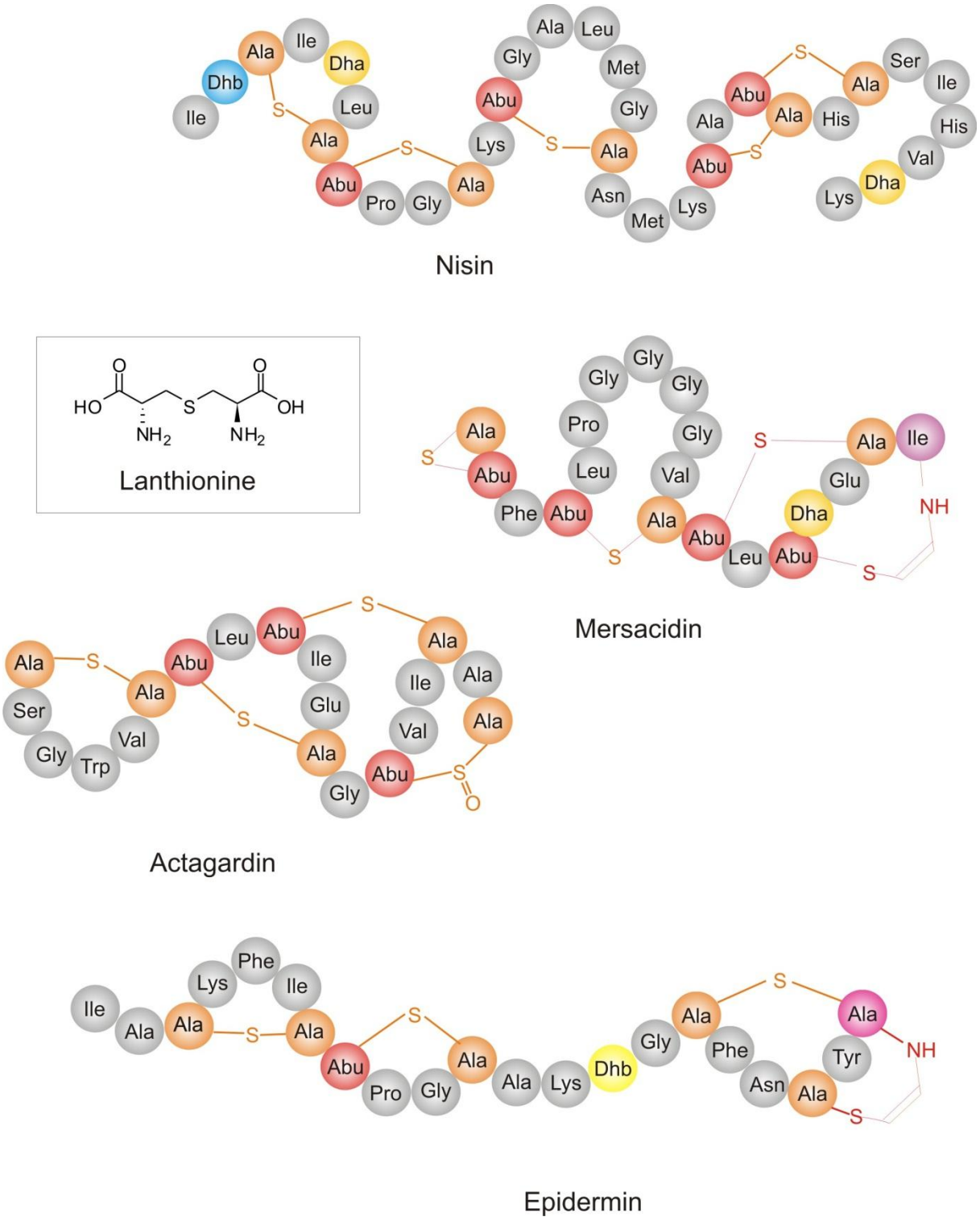

Figure 1.12: The lantibiotic inhibitors of the peptidoglycan biosynthesis nisin, mersacidin, actagardin and epidermin.

Besides the lathionine motif they can contain further modifications likewise introduced posttranslationally. Lantibiotics are generally classified in type A or type B lantibiotics according to their topology. An additional subgroup is the two component lantibiotics. Another way to classify lantibiotics is the classification according to the modifying

enzymes. The most prominent member of the group of lantibiotics is probably Nisin produced by *Lacococcus lactis* and first discovered in 1928 (Figure 1.12) (Rogers, Whittier 1928). Nisin is used as a food preservative and induces pore formation in the bacterial cell membrane. It is a type A lantibiotic and has an amphipathic screw-like structure (Chatterjee et al. 2005). Nisin contains 34 amino acids, one lathionine ring, four methyllantionine rings and three modified amino acids (one 2,3-didehydroalanine and two 2,3-didehydrobutyrines). Interestingly it was found that nisin interacts with the lipid II molecule to facilitate the integration into the cell membrane. The interaction with lipid II might help to adopt the right conformation for pore formation and explain the higher effectiveness of nisin compared to other pore forming antibiotics (Brötz, Sahl 2000). For the lantibiotic epidermin (Figure 1.12) the same mode of action as for nisin is considered. Epidermin host resistance is provided by the export of epidermin out of the cell by specific ABC transporters (Otto et al. 1998). Non-host strains were reported to gain nisin resistance by physiological adoption, therefore changes in the composition of the cell membrane. Lately in non-host strains a nisin resistance protein was discovered that was able to proteolytically inactive nisin *in vitro* and by this also provide nisin resistance (Sun et al. 2009).

The lantibiotics mersacidin (Figure 1.12) and actagardin (Figure 1.12) also inhibit the bacterial cell wall biosynthesis. They are shorter than nisin and possess a more globular three-dimensional structure and are therefore classified as type B lantibiotics (Chatterjee et al. 2005). Both mersacidin and actagardin inhibit the transglycosylation step by binding to lipid II (Brötz et al. 1998). The lipid II binding domain recognized by mersacidin and actagardin is very similar to the motif recognized by ramoplanin. Also the backbone fold is very much similar to the peptide backbone of ramoplanin (McCafferty et al. 2002). A paralleled evolution might therefore have led to a similar mode of action in different antibiotic classes.

1.19 Further inhibitors of the later stages of peptidoglycan biosynthesis

Further inhibitors of the final stages of peptidoglycan biosynthesis that do not belong to the above mentioned groups and families are mannopeptimycin, bacitracin and the katanosins.

Mannopeptimycin (Figure 1.13) is another peptide cell wall inhibitor active against a variety of Gram-positive bacteria first discovered in 1958 and re-discovered in 2003 (Singh et al. 2003). It is a cyclic glyco-hexapeptide and was also found to inhibit the transglycosylation by binding to Lipid II, possibly at a different binding site than vancomycin and ramoplanin (Ruzin et al. 2004).

The peptide antibiotic bacitracin (Figure 1.13), produced by *Bacillus subtilis* and *Bacillus licheniformis,* was first isolated in 1945 (Johnson et al. 1945). Instead of only one antibiotic *Bacillus* normally produces a mixture of closely related structures of which bacitracin A is the main component. Bacitracin A is a 12 amino acid peptide with an *N*-terminal pentapeptide and a *C*-terminal seven amino acid lactam ring. The structure of bacitracin slightly resembles to a lariat. It exhibits a thiazoline ring between a Cys and an Ile residue at the *N*-terminal end, which is important for its antibiotic activity (Stone, Strominger 1971). Bacitracin A forms a complex with the C_{55}-isoprenyl pyrophosphate and by this inhibits the regeneration of the lipid carrier of Park`s nucleotide. Interestingly the complexation requires a metal ion as cofactor (Stone, Strominger 1971). Furthermore bacitracin can bind to the major grove of the DNA and is also referred to as a potential proteinase inhibitor (Pfeffer et al. 1991). Bacitracin is industrially used in animal feed, for antibiotic ointments and for antibiotic treatment during chemotherapy. Resistance to bacitracin can occur by increased *de novo* synthesis of the C_{55}-isoprenyl phosphate. E.g. strong amplification of a C_{55}-isoprenyl kinase responsible for phosphorylation of C_{55}-isoprenol was found to confer resistance to bacitracin (Cain et al. 1993).

Katanosin A and katanosin B (Figure 1.13, also lysobactin), isolated 1988 from the genus *Cytophaga* (Shoji et al. 1988), are 11 amino acids cyclic depsipeptides and also possess a so called “lariat” structure with a linear dipeptide part and macro cycle part of nine amino acids. They additionally possess five non-proteinogenic amino acids one D-Arg and four β-hydroxylated amino acids. The katanosins are active agains *VRE* and seem to inhibit the transglycosylation differently to vancomycin. The mode of action was not studied yet in detail but a mode of action similar to ramoplanin or mannopeptimycin is expected (Maki et al. 2001; Breukink, de Kruijff 2006). The total synthesis of katanosin was published at the same time by Nussbaum et al (von Nussbaum et al. 2007) and Campagne (Campagne 2007). Due to its expedient qualities the katanosin derivatives were studied further by the Bayer AG (Leverkusen, Germany) to gain a possible clinical antibiotic (von Nussbaum et al.

13.04.2007). The homologous antibiotic plusbactin, isolated 1992 from *Pseudomonas* (Shoji et al. 1992) is expected to act in the same way as katanosin.

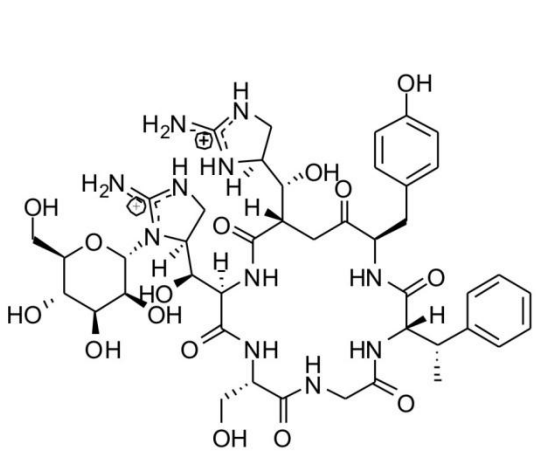

Mannopeptimycin β

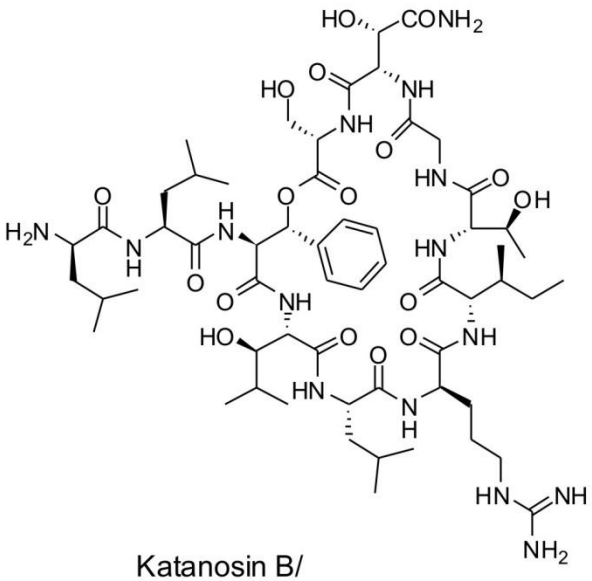

Katanosin B/
Lysobactin

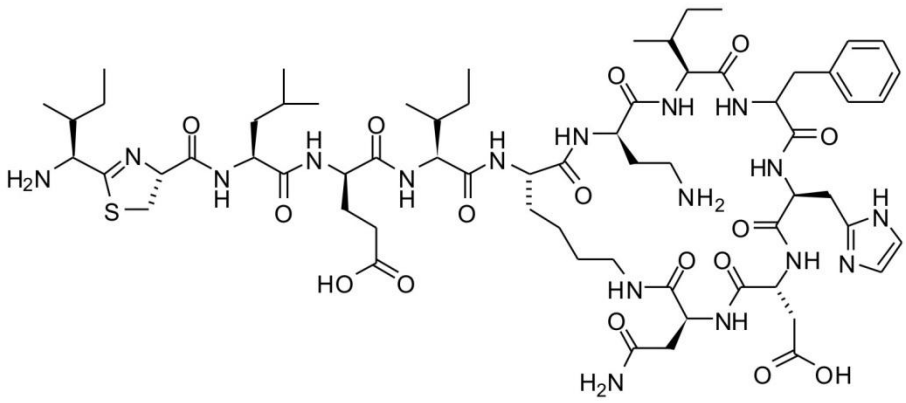

Bacitracin

Figure 1.13: The inhibitors mannopeptimycin, katanosin and bacitracin.

1.20 Feglymycin

The isolation and structure elucidation of feglymycin from *Streptomyces* sp. DSM 11171 was first published in 1999 by Vertesy (Figure 1.14). Additionally an antibacterial activity against *Staphylococcus* strains and a strong inhibition of syncytium formation in HIV infection *in vitro* was described (Vértesy et al. 1999). Feglymycin is a linear 13er peptide containing largely non-proteinogenic Hpg (4-hydroxyphenylglycine) and the non-proteinogenic Dpg (3,5-dihydroxyphenylglycine) amino acids and an interesting alternation of D and L amino acids. Hpg and Dpg can

also be found in members of the group of glycopeptide antibiotics, the ramoplanin group of antibiotics and the lipohexapeptide arylomycin (Luo et al. 2009). Feglymycin however sticks out of this listing for having a much more simple structure. Cystals structures revealed an antiparallel double-helical dimer formation of two feglymycin molecules (Figure 1.14). Similar antiparallel double-stranded β-helices are also formed by other D-L alternating peptides and also by the peptide antibiotic gramicidin A (Bunkóczi et al. 2005). The specific structure of gramicidin A enables the molecule to form channels in phospholipid membranes (Wallace 1986).

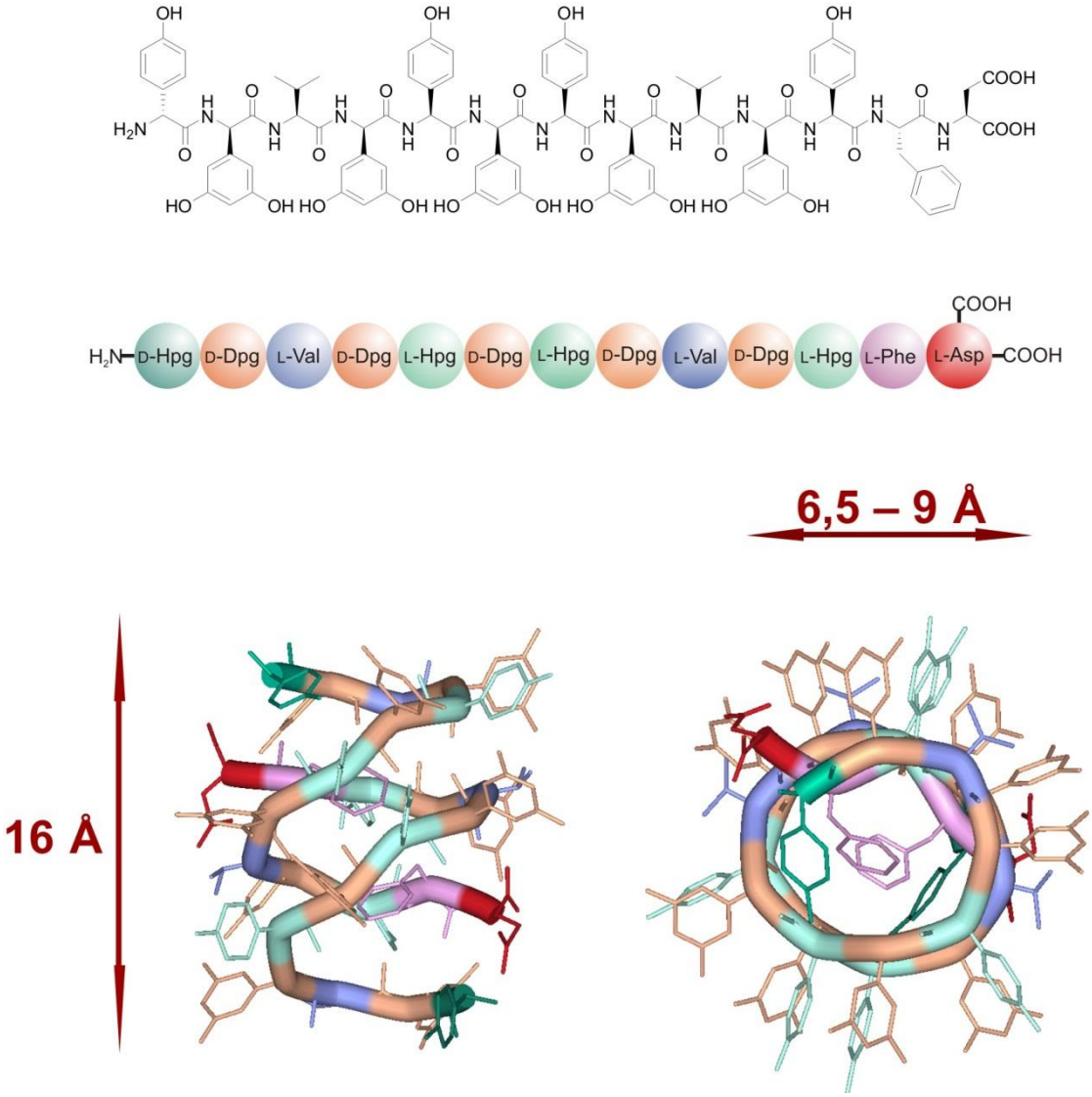

Figure 1.14: Structure and amino acid sequence of the tridecapeptide feglymycin and the crystal structure of feglymycin.

For feglymycin a similar mode of action is however not expected as the dimer would be too short to span the membrane and the channel is additionally blocked by phenylalanine side chains. Instead a function as ion carrier was proposed (Bunkóczi

et al. 2005). In 2009 the total synthesis of feglymycin was achieved and a more detailed investigation of the antibacterial and antiviral activity conducted. Anti-HIV-1 activity was tested against MT-4 cell lines. For feglymycin an IC_{50} value of 1.9 µg/ml was determined with no cytotoxic effects at 100 µg/ml. Besides feglymycin also the *N*-terminal Cbz-protected heptamer fragment of feglymycin and the Cbz-protected heptamer fragment with a methyl group at the *C*-terminal end showed an anti-HIV-1 activity around 8 µg/ml and low cytotoxic effects (Dettner et al. 2009). Feglymycin was also tested against different *MRSA* strains and showed IC_{80} values around 0.7-2.3 µg/ml and MICs (minimal inhibitory concentration) between 1-4 µg/ml. Feglymycin was additionally tested against Gram-negative *E. coli* and *E. faecalis*, Gram-positive *Streptococcus pyogenes* and *Mycobacterium smegmatis* as well as the yeast strains *Candida albicans*. The antibacterial activity against these strains was found to exceed a MIC of 64 µg/ml and was therefore not determined (Dettner et al. 2009).

1.21 Non ribosomal peptide synthetases (NRPS)

The large number of non-proteinogenic amino acids in feglymycin indicates that feglymycin might be a non-ribosomal synthesized peptide. Also the glycopeptide antibiotics and the glycodepsipeptide antibiotics ramoplanin and enduracidin are synthesized by NRPS (non-ribosomal peptide synthetases) (Kahne et al. 2005). The non-ribosomal peptide synthesis allows bacteria and fungi to overcome structural restrictions of the ribosomal peptide synthesis. Ribosomal peptide synthesis is largely restricted to the proteinogenic amino acids with only very few exceptions and to posttranslational modification. For NRPS, in contrast, incorporation of non-proteinogenic amino acids, the formation of branched and cyclic structures or modification like methylation, glycosylation and halogenation are more rule than exception. Non-ribosomally synthesized peptides are often very active compounds with interesting bioactivities and speculative applications. Beside antibiotics, immunosuppressives like cyclosporin (Borel et al. 1977), cytostatics like bleomycin A2 (Twentyman 1983), toxins like thaxomin A (Healy et al. 2002) and iron-chelators like enterobactin belong to the non-ribosomally synthesized peptides (Raymond et al. 2003b). NRPS are big multi-enzyme complexes with modular organization. One module normally corresponds to one amino acid. The modules again contain of several domains that possess a conserved structure. A typical module contains of the three domains C – A – T (Figure 1.15) (Schwarzer et al. 2003).

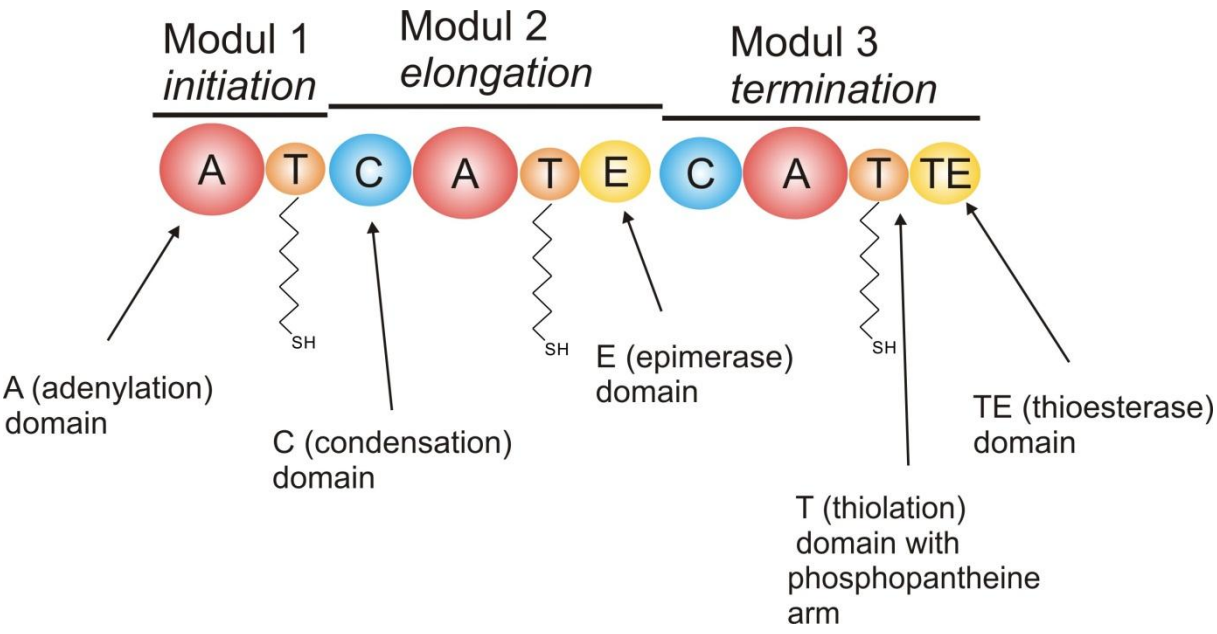

Figure 1.15: Organization of a hypothetical three-modular NRPS with one E-domain.

The A-domain (adenylation domain) is responsible for the recognition and activation of the amino acid substrate. Like during ribosomal peptide synthesis the amino acids first need to be activated by transfer of AMP from ATP onto the carboxyl group of the amino acid forming the aminoacyl adenylate (Schwarzer et al. 2003). The A-domain however has no further similarities to aminoacyl-tRNA-synthetases but instead structural similarities to the firefly luciferase as has been shown for an A-domain of the NRPS gramicidin A (Conti et al. 1997). The sequences of the binding pocket of A-domains activating the same substrate are often strongly conserved. Comparison of the sequence of an A-domain with sequences of known A-domains therefore often allows a relatively good prediction of the preferred substrate (Bachmann, Ravel 2009b).

The T-domain (thiolation domain) also called PCP (peptidyl carrier protein) is responsible for the transport of the amino acid and the growing peptide chain between the different domains. It needs the 4-phosphopantethein (4'PP) cofactor from coenzyme A to be active which is supplied by the 4-phosphopantetheinyl transferase (Sfp). The C-domain (condensation domain) is responsible for the formation of the peptide bond. Beside the A-domain also the C-domain has some substrate specificity (Schwarzer et al. 2003). The modules are normally arranged linear in direct correspondence to the amino acid sequence of the non-ribosomal peptide. This is also called colinearity or type A NRPS. Type B NRPS are iterative

NRPS and type C NRPS are non-linear NRPS. Iterative NRPS are NRPS were every module is used more than once (Schwarzer et al. 2003). An example for an iterative NRPS is the enniatin synthetase. The enniatin synthetase contains of only two modules that catalyze the synthesis of the cyclohexadepsipeptide enniatin in three reaction cycles (Glinski et al. 2002).

The first module of an NRPS is called initiation module and normally lacks the C-domains. The last module of an NRPS normally contains an additional Te-domain behind the PCP and is called termination module. The Te-domain releases the finished peptide chain. It can also introduce further modifications like macrocyclisation or functions as a storage position in iterative NRPS (Schwarzer et al. 2003). Another change to the usual domain arrangement can be the insertion of E-domains (epimerase domains) behind the T-domain. E-domains can convert L-amino acids into D-amino acids. Incorporation of D-amino acid however can also occur by recognition of D-amino acid by D-amino acid specific A-domains. Further modification are the replacement of the C-domain by a Cy-domain (heterocyclization domain) able to introduce heterocycles like thiazolines or oxazolines e. g. in the yesiniabactin biosynthesis gene cluster (Pfeifer et al. 2003) or an *N*-methylation domain inserted in the A-domain e. g. in cyclosporine (Dittmann et al. 1994). Heterocycles like thiazolines and oxazolines however not specific for NRPS but can also be introduced in ribosomal synthesized peptides as has been shown for the ribosomal synthesized cytotoxin Streptolysin S (Mitchell et al. 2009).

1.22 Mass spectrometry

Mass spectrometry allows the separation of ions by their mass to charge ration (*m/z*). It is used for identification, quantification and structure elucidation of analytes. Mass spectrometers are often used on-line hyphenated to chromatographic systems like HPLC or GC. A mass spectrometer commonly consists of an ion source, a mass analyzer and a detection unit. Typical ion sources are e.g. ESI (electrospray ionization), MALDI (matrix-assisted laser desorption/ionization) and ICP (inductively coupled plasma). The mass analyzer separates ions by their *m/z* value using an electric or/and magnetic field. Commonly applied mass analyzers are time-of-flight (TOF), Quadrupole or ion trap systems. Ions are detected by electron multipliers or micro channel plate detectors.

1.23 TOF mass spectrometer

Time-of-flight (TOF) mass spectrometers measure the time an ion needs to pass through a long flight tube. The ions are accelerated in the flight tube by an electric field. For ions bearing the same charge the velocity and therefore the time of flight depends only on the molecular mass (Wiley, McLaren 1955). The very fast detection needed to differentiate the minor flight time discrepancies is mostly provided by a time to digital converter (TDC) that allows resolutions down to a few picoseconds (ps). To increase the dynamic range often multiple TDCs are used. Time-lag-focusing is applied to compensate the time spread of ions produced early and late in the ionization event. Ions are not directly accelerated in the flight tube but are delayed for some nanoseconds (ns) after ionization (delayed extraction). Some TOF mass spectrometers possess a reflectron. The reflectron uses an electrostatic field to reflect the ions like a mirror. If a gradient instead of a simple electric field is applied the resolution can be increased. Additionally the reflectron increases the flight distance in a given flight tube. Because of the very high resolution and the ability to detect also large molecular masses TOF mass spectrometry is often applied for biological samples or proteomics.

1.24 Quadrupole mass spectrometer

A quadrupole analyzer (Q) normally consists of four parallel hyperbolic metallic rods. The quadrupole serves as a mass filter. By applying oscillating electric fields on the rods only ions with a specific mass are able to pass and to proceed to the detector. To record a full mass scan the quadrupole has to serve as a mass filter over time for different molecular masses. The quadrupole then sequentially scans every *m/z* value separately. Due to the dedicated measurement time for a single molecular mass the detection time for every *m/z* value becomes lesser for full mass scan compared to a single ion scan. Very high specificity can be achieved with triple quadrupole (QQQ) mass spectrometers. Triple quadrupole mass spectrometers have three quadrupoles arranged in series (Figure 1.16) (de Hoffmann 1996). The first and the third quadrupole commonly work as mass filters. The second quadrupole is the collision

cell and often actually a hexapole. It is filled with an inert gas like helium, argon or nitrogen and allows the controlled fragmentation of the precursor ions.

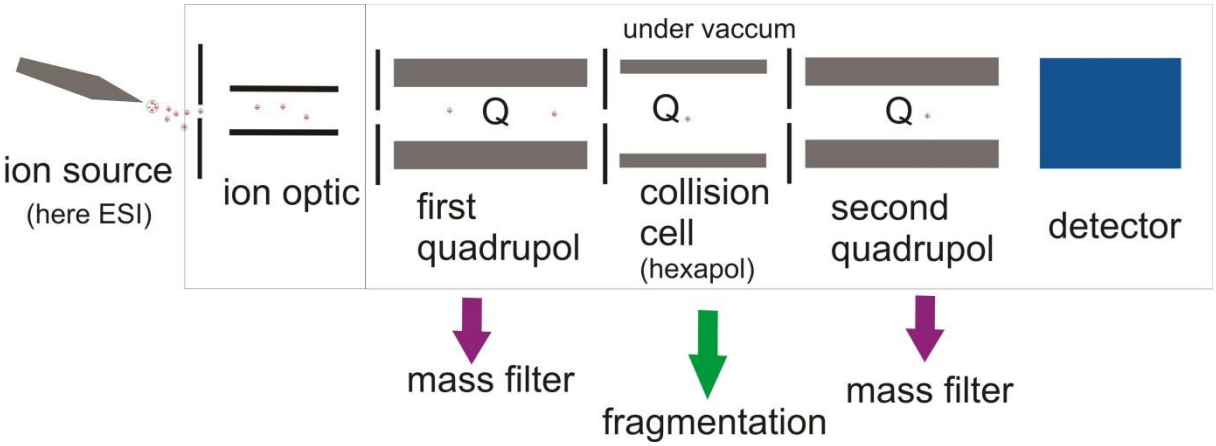

Figure 1.16: Scheme of a triple quadrupole (QQQ) mass spectrometer.

1.25 Ion trap mass spectrometer

Ion trap (IT) mass spectrometers use a quadrupole ion trap or an orbitrap to separate ions by mass. In ion trap mass spectrometer selected ions are trapped, accumulated and controlled ejected. A three dimensional quadrupole ion trap consists of two parallel hyperbolic rods and one hyperbolic ring electrode which is arranged between the rods. Ions are trapped by a field induced oscillation in three dimensional electric fields. In a linear ion trap ions are trapped in a two dimensional electric field.

The orbitrap mass spectrometry technique was invented by Alexander Marakov in 2000 (Makarov 2000). In the orbitrap mass spectrometer the electric field is not applied to a hyperbolic rod but to a spindle-shaped electrode. Ions circulate in orbits around the electrode. The orbits additionally move back and forth along the spindle (lateral movement). These oscillations are inversely proportional to the square root of the *m/z*. Orbitrap mass spectrometer have an especially high mass accuracy of 2-5 ppm and a very high resolving power (up to 150.000). Orbitrap mass spectrometry therefore is used to determine exact masses of molecules (Hu et al. 2005).

1.26 MSMS and SRM measurements

MSMS also termed *product ion scan* is performed to characterize or identify a substance, especially proteins, by mass spectrometry. For MSMS so called tandem mass spectrometry is applied. A specific precursor mass is isolated from other molecular masses and fragmented in a collision cell to produce a number of product

ions (Yost, Enke 1978). The molecular mass of the product ions is characteristic of the substance, wherefore substances can be identified by their specific fragmentation pattern also called *mass fingerprint*. The fragmentation can also be used to characterize a chemical structure. A fragment of *m/z* 91 for example is characteristic of aromatic substances.

In SRM (single reaction monitoring) experiments a specific precursor mass is isolated from the other masses and fragmented. Only one specific product ion whose signal is indicative for a substance is detected. SRM is the most sensitive mode of operation, because the ions are filtered both for a specific precursor ion and for a specific product ion. SRM experiments are primarily performed with triple quadrupole mass spectrometer. The first quadrupole isolates the precursor, the second one act as a collision cell and the last quadrupole isolates a specific product ion. With the help of a calibration curve that has to be best created with the same substance or an internal standard under identical conditions, SRM measurements can enable the absolute quantification of a substance. If multiple SRM are run for the same precursor ion one speaks of MRM (multiple reaction monitoring). MRM relies of the detection of several specific product ions instead of just one and therefore allows even better specificity and reliability especially for quantitative applications (de Hoffmann, Stroobant 2007).

2 Materials

2.1 List of abbreviations

A	adenine
ACN	acetonitrile
L-Ala	L-alanine
D-Ala-D-Ala	D-alanyl-D-alanine
Amp	ampicillin
AP	alkaline phosphatase
APS	ammonium persulfate
ATP	adenosine triphosphate
BCIP	5-bromo-4-chloro-3-indolyl phosphate
BSA	bovine serum albumin
C	cytosine
$CaCl_2$	calcium chloride
$CaCO_3$	calcium carbonate
C-18	octadecylsilane
Cys	cysteine
meso-Dap	*meso*-diaminopimelic acid
dH_2O	deionized water
DMSO	dimethyl sulfoxide
DNA	desoxyribonucleic acid
dNTP	desoxyribonucleoside triphosphate
Dpg	3,5-dihydroxyphenylglycine
DTT	dithiothreitol
EDTA	ethylenediaminetetraacetic acid
e.g.	*exempli gratiā* (for example)

EIC	entracted ion current
EP-UDP-GlcNAc	UDP-*N*-acetyl-glucosamine-enolpyruvate
ESI	electrospray ionization
g	gram
g	earth's gravitational acceleration
G	guanine
GlcNAc	*N*-acetylglucosamine
D-Glu	D-glutamate
GTP	guanosine triphosphate
h	hours
HCOOH	formic acid
His-Tag	6-histidine-tag
HPLC	high performance liquid chromatography
Hpg	4-hydroxyphenylglycine
IC_{50}	half maximal inhibitory concentration
IC_{80}	concentration of 80 % inhibition
IgG	immunoglobulin G
IPTG	Isopropyl-β-D-1-thiogalactopyranoside
Kan	kanamycin
K_M	inverse of enzyme affinity; equivalent to the substrate concentration at which the rate of conversion is half of V_{max}
KCl	potassium chloride
KH_2PO_4	potassium dihydrogen phosphate
L	liter
µL	microliter
LC	liquid chromatography

LDH	lactic dehydrogenase
Lipid I	undecaprenylpyrophosphoryl-*N*-acetylmuramoyl-pentapptide
Lipid II	undecaprenylpyrophosphoryl-*N*-acetylglucosamine-*N*-acetylmuramoyl-pentapptide
NaCl	sodium chloride
NADH	nicotinamide adenine dinucleotide (reduced)
NBT	nitro blue tetrazolium chloride
$(NH_4)_2SO_4$	ammonium sulfate
NADPH	nicotinamide adenine dinucleotide phosphate (reduced)
m/z	mass-to-charge ratio
M	molar
MeOH	methanol
MIC	minimum inhibitory concentration
mL	milliliter
µM	micromolar
mg	milligram
µm	micrometer
mM	millimolar
MurA	enolpyruvyl-UDP-GlcNAc synthase
MurB	UDP-*N*-acetylenolpyruvoylglucosamine reductase
MurC	UDP-*N*-acetyl-muramyl-L-alanine ligase
MurD	UDP-*N*-acetylmuramoylalanine-D-glutamate ligase
MurE	UDP-*N*-acetylmuramoyl-L-alanyl-D-glutamate-2,6-diaminopimelate ligase
MurF	UDP-*N*-acetylmuramoyl-tripeptide-D-alanyl-D-alanine ligase

MurG	UDP-*N*-acetylglucosamine-*N*-acetylmuramyl-pentapptide pyrophosphoryl-undecaprenol *N*-acetylglucosamine transferase
MraY	phospho-*N*-acetylmuramoyl-pentapptide-transferase
$MgCl_2$	magnesium chloride
$MgSO_4$	magnesium sulfate
$MnCl_2$	manganese chloride
MOPS	3-(*N*-morpholino)propanesulfonic acid
MPa	megapascal
MS	mass spectrometry
MSMS	product ion scan
MWCO	molecular weight cut off
NRPS	non-ribosomal peptide synthetase
OD	optical density
ORF	open reading frame
PCR	polymerase chain reaction
PEP	phosphoenolpyruvate
PK	pyruvate kinase
PKS	polyketide synthase
pM	picomolar
PMSF	phenylmethylsulfonyl fluoride
$RbCl_2$	rubidium chloride
RNA	ribonucleic acid
RP	reverse phase
RT	room temperature
SDS	sodium dodecyl sulfate
SIM	single ion monitoring

TEMED	*N*,*N*,*N*',*N*'-tetramethylendiamin
Tris	tris(hydroxymethyl)aminomethane
TFE	trifluoroethanol
Triton X-100	polyethylene glycol *p*-(1,1,3,3-tetramethylbutyl)-phenyl ether
TOF	time-of-flight
U	uridine
UDP	uridinediphosphat
UDP-GlcNAc	UDP-*N*-acetylglucosamine
UDP-MurNAc	UDP-*N*-acetylmuramic acid
UV	ultra violett light
V_{max}	maximum reaction rate
VIS	visible light
X-Gal	bromo-chloro-indolyl-galactopyranoside

2.2 List of used bacteria strains

strain	antibiotic resistance	description	company
E. coli DH5α	none	strain for cloning *endA1* gene mutation → decreased nuclease activity	Life Technologies
E. coli BL21	none	protein expression strain *lon* and *ompT* gene mutation →decreased protease activity	Novagen
E. coli K12	none	wild type	-
E. coli ET12567	chloramphenicol	methylation deficient *E. coli* strain	-
E. coli ET12567+pUZ8002	chloramphenicol, kanamycin	*E. coli* donor strain for *Streptomyces* conjugation	
Streptomyces sp. HAG 4675 DSM 11 171	phosphomycin	feglymycin producing strain	-

2.3 Media

2.3.1 *E. coli* media

LB

0.5 % yeast extract	5.0 g
1 % tryptone	10.0 g
1 % NaCl	5.0 g
dH_2O	add 1 L

For agar plates add 17 g agar per 1 L medium.

TY

1 % yeast extract	10.0 g
1.6 % tryptone	16.0 g
0.5 % NaCl	5.0 g
dH_2O	add 1 L

For agar plates add 17 g agar per 1 L medium.

2.3.2 *Streptomyces* media:

E1 medium

glucose	20.0 g
soluble starch	20.0 g
yeast extract	5.0 g
pharma medium	2.5 g
$MgSO_4$ x 7 H_2O	1.0 g
KH_2PO_4 x 3 H_2O	1.3 g
NaCl	3.0 g
$CaCO_3$	3.0 g
tap water	add 1 L

Adjust pH to 6.8

GYM medium

glucose	4.0 g
yeast extract	4.0 g
malt extract	10.0 g
dH_2O	add 1 L

Adjust pH to 7.2.

For agar plates add 12 g agar and 2 g $CaCO_3$ per 1 L medium.

HA medium

bacto yeast extract	4.0 g
malt extract	10.0 g
glucose	4.0 g
dH_2O	add 1 L

Adjust pH to 7.3 with NaOH. Add 1 mM $CaCl_2$ after autoclaving. For agar plates add 20 g agar.

M9 minimal medium

Prepare first M9 salt medium

Na_2HPO_4 x 7 H_2O	64.0 g
KH_2PO_4	15.0 g
NaCl	2.5 g
NH_4Cl	5.0 g
dH_2O	add 1 L

Dilute 200 mL of sterile M9 salt medium in 700 mL sterile dH_2O. Add 2 mL of sterile 1 M $MgSO_4$, 20 mL of 20 % glucose, 100 µL of sterile 1 M $CaCl_2$.

MS medium

mannit	20.0 g
soy flour	20.0 g
dH_2O	add 1 L

For agar plates add 21 g agar per 1 L medium.

N-Z-amine medium

glucose	10.0 g
soluble starch	20.0 g
yeast extract	5.0 g
N-Z-amine	5.0 g
$CaCO_3$	1.0 g
dH_2O	add 1L

Adjust pH to 7.2. For agar plates add 15 g agar per 1 L medium.

Paper medium

malt extract	20.0 g
yeast extract	2.0 g
glucose	10.0 g
$(NH_4)_2HPO_4$	0.5 g
dH_2O	add 1L

Adjust pH to 6.0. For agar plates add 20 g agar per 1 L medium.

TSB (tryptone soya broth)

tryptone soya broth powder	30.0 g
dH_2O	add 1L

YEME (yeast extract-malt extract medium)

yeast extract	3.0 g
bacto-peptone	5.0 g
malt extract	3.0 g
glucose	10.0 g
sucrose	340.0 g
dH_2O	add 1 L

Add 5 mM $MgCl_2 \times 6H_2O$ after autoclaving.

2.4 Buffers

2.4.1 Buffers for the production of competent *E. coli* cells

TJB1

RbCl	3.00 g
$MnCl_2$ x $4H_2O$	2.37 g
potassium acetat	0.74 g
$CaCl_2$ x $2H_2O$	0.36 g
glycerine	37.5 mL
dH_2O	add 250 mL

Adjust carefully to pH 5.8 with HCl. Sterilize buffer by filtrations.

TJB2

MOPS	0.20 g
RbCl	0.12 g
$CaCl_2$ x $2H_2O$	1.10 g
glycerine	15.0 mL
dH_2O	add 100 mL

Adjust carefully to pH 7.0 with NaOH. Sterilize buffer by filtrations.

2.4.2 Buffers for agarose gel electrophoresis

10 x TAE buffer

Tris	48.4 g
acetic acid (96 %)	11.4 mL
EDTA	7.2 g
dH_2O	add 1 L

Adjust pH to 7.9

2.4.3 Buffers for SDS-PAGE

Sample buffer

1 M Tris/HCl pH 6,8	3.75 mL
SDS	1.2 g
glycerin	6 mL
bromophenol blue	6 mg
dH_2O	add 13.5 mL

Add 100 mM DTT freshly before use.

10 x Electrophoresis buffer

Tris	31.0 g
glycine	144.0 g
SDS	10.0 g
dH_2O	add 1 L

Separating gel buffer

250 mM Tris/HCl pH 6.8

Stacking gel buffer

1,5 M Tris/HCl pH 8.8

APS stock solution

100 mg/mL APS in dH_2O

Separating gel (for 2 gels)

H_2O	3.4 mL
separating gel buffer	2.5 mL
Rotiphorese 30 % (37.5:1)	4.0 mL
10 % SDS	100 µL
APS stock solution	50 µL
TEMED	25 µL

Add APS and TEMED only directly before pouring the gel.

Stacking gel (for 2 gels)

H_2O	3.05 mL
stacking gel buffer	1.25 mL
Rotiphorese 30 % (37.5:1)	0.65 mL
10 % SDS	50 µL
APS stock solution	25 µL
TEMED	12.5 µL

add APS and TEMED only directly before pouring the gel

Comassie blue stain solution

serva blue R250	0.86 g
ethanol	250 mL
acetic acid (96 %)	50 mL
dH_2O	add 500 mL

2.4.4 Buffers for Western Blotting

Blotting buffer

Tris/HCl	3.03 g
flycerine	4.4 g
methanol	200 mL
dH_2O	add 1 L
Adjust pH to 8.3	

TNT buffer

Tris/HCl	2.42 g
NaCl	29.22 g
Tween20	500 µL
dH_2O	add 1 L
Adjust pH to 7.5	

AP buffer

Tris/HCl	12.1 g
NaCl	5.84 g
$MgCl_2$ x 6 H_2O	1.02 g
dH_2O	add 1 L
Adjust pH to 9.5	

10 % Thimerosal stock solution

Dissolve 1 g thimerosal in 10 mL water. Store at 4 °C in the dark.

BCIP stock solution

Dissolve 10 mg/mL BCIP in 100 % dimethylformamide. Store at – 20 °C.

NBT stock solution

Dissolve 50 mg/mL NBT in 70 % dimethylformamide. Store at – 20 °C.

2.4.5 Buffers for CD spectroscopy

Phosphate buffer (0.1 M)

pH	Volume of 1 M K_2HPO_4 (mL)	Volume of 1 M KH_2PO_4 (mL)
5.8	8.5	91.5
6.0	13.2	86.8
6.2	19.2	80.8
6.4	27.8	72.2
6.6	38.1	61.9
6.8	49.7	50.3
7.0	61.7	38.5
7.2	71.7	28.3
7.4	80.2	19.8
7.6	86.6	13.4
7.8	90.8	9.2
8.0	94.0	6.0

Prepare at 25 °C and dilute in 1L dH_2O.

2.5 Vectors, primers and proteins

Table 2.1: List of used vectors

name	antibiotic resistance/marker	description	company
pDrive	ampicillin, kanamycin	direct cloning vector vector map (Appendix 6.1)	Quiagen
pEt24a(+)	kanamycin	protein expression vector, T7-promotor, C-terminal His-Tag vector map (Appendix 6.2)	Novagen
pEt28a(+)	kanamycin	protein expression vector, T7-promotor, N- and C-terminal His-Tag vector map (Appendix 6.3)	Novagen
pEt21a(+)	ampicillin	T7-promotor, C-terminal His-Tag vector map (Appendix 6.4)	Novagen
pUZ8002	kanamycin	Carries *tra* gene → coding for transfer protein Tra allowing intergeneric conjugation	in house
pK18mobapra	apramycin	Vector to induce specific knock-out mutants in *Streptomyces* vector map (Appendix 6.5)	in house

Table 2.2: Table of used primers

gene	forward primer (5'→3')	reverse primer (3'→5')
murA (E. coli)	CGCGCCATATGATGGATAAATTTCGTGTTCAGG	AGAGCTCGAGTTCGCCTTTCACACGCTCAA
murB (E. coli)	GGCGGAATTCATGAACCACTCCTTAAAAC	GCGGCTCGAGTGAAATTGTCTCCACTGCG
murC (E. coli)	GCGCCATATGATGAATACACAACAATTGGC	AGAGCTCGAGGTCATGTTGTTCTTCCTCCG

murD (E. coli)	GGCGGAATTCATGGCTGATTATC AGGGTAAA	AGAGCTCGAGACCTAACTCCTTCGC CAGAC
murE (E. coli)	GCGTGCATATGGTGGCAGATCG TAATTTGCG	AGAGCTCGAGTGCAATCACCCCCAG CAGAC
murF (E. coli)	GCGCGAATTCATGATTAGCGTAA CCCTTAG	GCGCCTCGAGACATGTCCCATTCTC CTGTA
murA (S. aureus)	TTTGCTAGCGATAAAATAGTAAT CAAAGGTG	TAACTTGCATAATTGCTAGAGCTCTC A
murC (S. aureus)	GCGCCATATGTTAAAACGCATTT TTCATGCCTAATTTA	GCGCCTCGAGATGACACACTATCAT TTTGTCGGAATT
murD (S. aureus)	GGCGCCATATGATGCTTAATTAT ACAGGG	GCGCCTCGAGATAAGATGGTAAATG GGCAC

Table 2.3: Table of overexpressed proteins

protein	calculated MW in Dalton	protein sequence
MurA *(E. coli)*	46,013	MMDKFRVQGPTKLQGEVTISGAKNAALPILFAALLAEEPVEIQNV PKLKDVDTSMKLLSQLGAKVERNGSVHIDARDVNVFCAPYDLVK TMRASIWALGPLVARFGQGQVSLPGGCTIGARPVDLHISGLEQL GATIKLEEGYVKASVDGRLKGAHIVMDKVSVGATVTIMCAATLAE GTTIIENAAREPEIVDTANFLITLGAKISGQGTDRIVIEGVERLGGG VYRVLPDRIETGTFLVAAAISRGKIICRNAQPDTLDAVLAKLRDAG ADIEVGEDWISLDMHGKRPKAVNVRTAPHPAFPTDMQAQFTLLN LVAEGTGFITETVFENRFMHVPELSRMGAHAEIESNTVICHGVEK LSGAQVMATDLRASASLVLAGCIAEGTTVVDRIYHIDRGYERIEDK LRALGANIERVKGELEHHHHHH
MurB *(E. coli)*	40,573	MNHSLKPWNTFGIDHNAQHIVCAEDEQQLLNAWQYATAEGQPV LILGEGSNVLFLEDYRGTVIINRIKGIEIHDEPDAWYLHVGAGENW HRLVKYTLQEGMPGLENLALIPGCVGSSPIQNIGAYGVELQRVCA YVDSVELATGKQVRLTAKECRFGYRDSIFKHEYQDRFAIVAVGLR LPKEWQPVLTYGDLTRLDPTTVTPQQVFNAVCHMRTTKLPDPKV NGNAGSFFKNPVVSAETAKALLSQFPTAPNYPQADGSVKLAAG WLIDQCQLKGMQIGGAAVHRQQALVLINEDNAKSEDVVQLAHHV RQKVGEKFNVWLEPEVRFIGASGEVSAVETISLEHHHHHH
MurC *(E. coli)*	56,985	MGSSHHHHHHSSGLVPRGSHMMNTQQLAKLRSIVPEMRRVRHI HFVGIGGAGMGGIAEVLANEGYQISGSDLAPNPVTQQLMNLGATI YFNHRPENVRDASVVVVSSAISADNPEIVAAHEARIPVIRRAEMLA ELMRFRHGIAIAGTHGKTTTTAMVSSIYAEAGLDPTFVNGGLVKA AGVHARLGHGRYLIAEADESDASFLHLQPMVAIVTNIEADHMDTY QGDFENLKQTFINFLHNLPFYGRAVMCVDDPVIRELLPRVGRQTT TYGFSEDADVRVEDYQQIGPQGHFTLLRQDKEPMRVTLNAPGR HNALNAAAAVAVATEEGIDDEAILRALESFQGTGRRFDFLGEFPL EPVNGKSGTAMLVDDYGHHPTEVDATIKAARAGWPDKNLVMLF QPHRFTRTRDLYDDFANVLTQVDTLLMLEVYPAGEAPIPGADSR SLCRTIRGRGKIDPILVPDPARVAEMLAPVLTGNDLILVQGAGNIG KIARSLAEIKLKPQTPEEEQHDLEHHHHHH
MurD *(E. coli)*	51,858	MGSSHHHHHHSSGLVPRGSHMASMTGGQQMGRGSEFMADYQ GKNVVIIGLGLTGLSCVDFFLARGVTPRVMDTRMTPPGLDKLPEA VERHTGSLNDEWLMAADLIVASPGIALAHPSLSAAADAGIEIVGDI ELFCREAQAPIVAITGSNGKSTVTTLVGEMAKAAGVNVGVGGNIG LPALMLLDDECELYVLELSSFQLETTSSLQAVAATILNVTEDHMD RYPFGLQQYRAAKLRIYENAKVCVVNADDALTMPIRGADERCVS

		FGVNMGDYHLNHQQGETWLRVKGEKVLNVKEMKLSGQHNYTN ALAALALADAAGLPRASSLKALTTFTGLPHRFEVVLEHNGVRWIN DSKATNVGSTEAALNGLHVDGTLHLLLGGDGKSADFSPLARYLN GDNVRLYCFGRDGAQLAALRPEVAEQTETMEQAMRLLAPRVQP GDMVLLSPACASLDQFKNFEQRGNEFARLAKELGLEHHHHHH
MurE *(E. coli)*	54,507	MADRNLRDLLAPWVPDAPSRALREMTLDSRVAAAGDLFVAVVG HQADGRRYIPQAIAQGVAAIIAEAKDEATDGEIREMHGVPVIYLSQ LNERLSALAGRFYHEPSDNLRLVGVTGTNGKTTTTQLLAQWSQL LGEISAVMGTVGNGLLGKVIPTENTTGSAVDVQHELAGLVDQGA TFCAMEVSSHGLVQHRVAALKFAASVFTNLSRDHLDYHGDMEH YEAAKWLLYSEHHCGQAIINADDEVGRRWLAKLPDAVAVSMEDH INPNCHGRWLKATEVNYHDSGATIRFSSSWGDGEIESHLMGAFN VSNLLLALATLLALGYPLADLLKTAARLQPVCGRMEVFTAPGKPT VVVDYAHTPDALEKALQAARLHCAGKLWCVFGCGGDRDKGKRP LMGAIAEEFADVAVVTDDNPRTEEPRAIINDILAGMLDAGHAKVM EGRAEAVTCAVMQAKENDVVLVAGKGHEDYQIVGNQRLDYSDR VTVARLLGVIALEHHHHHH
MurF *(E. coli)*	52,195	MGSSHHHHHHSSGLVPRGSHMASMTGGQQMGRGSEFMISVTL SQLTDILNGELQGADITLDAVTTDTRKLTPGCLFVALKGERFDAH DFADQAKAGGAGALLVSRPLDIDLPQLIVKDTRLAFGELAAWVRQ QVPARVVALTGSSGKTSVKEMTAAILSQCGNTLYTAGNLNNDIG VPMTLLRLTPEYDYAVIELGANHQGEIAWTVSLTRPEAALVNNLA AAHLEGFGSLAGVAKAKGEIFSGLPENGIAIMNADNNDWLNWQS VIGSRKVWRFSPNAANSDFTATNIHVTSHGTEFTLQTPTGSVDVL LPLPGRHNIANALAAAALSMSVGATLDAIKAGLANLKAVPGRLFPI QLAENQLLLDDSYNANVGSMTAAVQVLAEMPGYRVLVVGDMAE LGAESEACHVQVGEAAKAAGIDRVLSVGKQSHAISTASGVGEHF ADKTALITRLKLLIAEQQVITILVKGSRSAAMEEVVRALQENGTCL EHHHHH
MurA *(S. aureus)*	44,995	MDKIVIKGGNKLTGEVKVEGAKNAVLPILTASLLASDKPSKLVNVP ALSDVETINNVLTTLNADVTYKKDENAVVVDATKTLNEEAPYEYV SKMRASILVMGPLLARLGHAIVALPGGCAIGSRPIEQHIKGFEALG AEIHLENGNIYANAKDGLKGTSIHLDFPSVGATQNIIMAASLAKGK TLIENAAKEPEIVDLANYINEMGGRITGAGTDTITINGVESLHGVEH AIIPDRIEAGTLLIAGAITRGDIFVRGAIKEHMASLVYKLEEMGVEL DYQEDGIRVRAEGELQPVDIKTLPHPGFPTDMQSQMMALLLTAN GHKVVTETVFENRFMHVAEFKRMNANINVEGRSAKLEGKSQLQ GAQVKATDLRAAAALILAGLVADGKTSVTELTHLDRGYVDLHGKL KQLGADIERIND
MurB *(S. aureus)*	33,783	MINKDIYQALQQLIPNEKIKVDEPLKRYTYTKTGGNADFYITPTKN EEVQAVVKYAYQNEIPVTYLGNGSNIIIREGGIRGIVISLLSLDHIDV SDDAIIAGSGAAIIDVSRVARDYALTGLEFACGIPGSIGGAVYMNA GAYGGEVKDCIDYALCVNEQGSLIKLTTKELELDYRNSIIQKEHLV VLEAAFTLAPGKMTEIQAKMDDLTERRESKQPLEYPSCGSVFQR PPGHFAGKLIQDSNLQGHRIGGVEVSTKHAGFMVNVDNGTATDY ENLIHYVQKTVKEKFGIELNREVRIIGEHPKES
MurC *(S. aureus)*	52,402	MGSSHHHHHHSSGLVPRGSHMTHYHFVGIKGSGMSSLAQIMHD LGHEVQGSDIENYVFTEVALRNKGIKILPFDANNIKEDMVVIQGNA FASSHEEIVRAHQLKLDVVSYNDFLGQIIDQYTSVAVTGAHGKTS TTGLLSHVMNGDKKTSFLIGDGTGMGLPESDYFAFEACEYRRHF LSYKPDYAIMTNIDFDHPDYFKDINDVFDAFQEMAHNVKKGIIAW GDDEHLRKIEADVPIYYYGFKDSDDIYAQNIQITDKGTAFDVYVDG EFYDHFLSPQYGDHTVLNALAVIAISYLEKLDVTNIKEALETFGGV KRRFNETTIANQVIVDDYAHHPREISATIETARKKYPHKEVVAVFQ PHTFSRTQAFLNEFAESLSKADRVFLCEIFGSIRENTGALTIQDLID KIEGASLINEDSINVLEQFDNAVVLFMGAGDIQKLQNAYLDKLGM KNAFLEHHHHHH
MurD *(S. aureus)*	53,203	MGSSHHHHHHSSGLVPRGSHMMLNYTGLENKNVLVVGLAKSG YEAAKLLSKLGANVTVNDGKDLSQDAHAKDLESMGISVVSGSHP LTLLDNNPIIVKNPGIPYTVSIIDEAVKRGLKILTEVELSYLISEAPIIA VTGTNGKTTVTSLIGDMFKKSRLTGRLSGNIGYVASKVAQEVKPT

		DYLVTELSSFQLLGIEKYKPHIAIITNIYSAHLDYHENLENYQNAKK QIYKNQTEEDYLICNYHQRQVIESEELKAKTLYFSTQQEVDGIYIK DGFIVYKGVRIINTEDLVLPGEHNLENILAAVLACILAGVPIKAIIDSL TTFSGIEHRLQYVGTNRTNKYYNDSKATNTLATQFALNSFNQPII WLCGGLDRGNEFDELIPYMENVRAMVVFGQTKAKFAKLGNSQG KSVIEANNVEDAVDKVQDIIEPNDVVLLSPACASWDQYSTFEERG EKFIERFRAHLPSYLEHHHHHH

Sequences marked in blue do not belong to the original protein sequence. The blue sequences are additional sequences added by the pEt24a(+), pEt28a(+) or pEt21 vectors.

Table 2.4: Reaction kits

name	company
PCR Purfication Kit	Qiagen GmbH, Hilden, Germany
PCR Cloning Kit	Qiagen GmbH, Hilden, Germany
A-Addition Kit	Qiagen GmbH, Hilden, Germany
GeneJET Plasmid Miniprep Kit	Fermentas GmbH, St. Leon-Rot, Germany
GeneJET Gel Extraction Kit	Fermentas GmbH, St. Leon-Rot, Germany

Table 2.5: Purchased enzymes

enzyme	company
Taq-DNA polymerase	Fermentas GmbH, St. Leon-Rot, Germany
Herculase II Fusion DNA polymerase	Agilent Technologies Deutschland GmbH, Böblingen, Germany
antarctic phosphatase	New England Biolabs Inc., Ipswich, England
T4 DNA ligase	New England Biolabs Inc., Ipswich, England
L-lactic dehydrogenase type II isolated from rabbit muscle	Sigma-Aldrich Chemie GmbH, Munich, Germany

pyruvate kinase isolated from rabbit muscle	Sigma-Aldrich Chemie GmbH, Munich, Germany

2.6 Chemicals

All common reagents and chemicals were purchased from Sigma-Aldrich or Carl Roth GmbH and were not considered for the following list.

reagent	company
BugBuster Protein Extraction Reagent	Novagen, EMD Chemicals Inc.,Gibbstown, USA

2.7 Equipment

equipment	**company**
refrigerator	Liebherr GmbH, Ochsenhausen, Germany
freezer	Privileg GmbH, Stuttgart, Germany
Varioklav 300 EP-Z (autoclave)	Thermo Fisher Scientific GmbH, Dreieich, Germany
Sano Clav typ LaM-20 (benchtop autoclave)	A. Wolf SANOclav GmbH, Bad Überkingen-Hausen, Germany
Forma – 86 °C ULT Freezer	Thermo Fisher Scientific GmbH, Dreieich, Germany
Holten horizontal Lavin Airflow clean bench	Thermo Fisher Scientific GmbH, Dreieich, Germany
Multitron II (shaker)	Infors GmbH, Einsbach, Deutschland
Privileg 8022 L microwave	Privileg GmbH, Stuttgart, Germany
thermomixer comfort	Eppendorf Vertrieb Deutschland GmbH, Wesseling-Berzdorf, Germany

Microcentrifuge 5415 D	Eppendorf Vertrieb Deutschland GmbH, Wesseling-Berzdorf, Germany
refrigerated bench-top centrifuge 5810 R	Eppendorf Vertrieb Deutschland GmbH, Wesseling-Berzdorf, Germany
constant climate chamber	Binder GmbH, Tuttlingen, Germany
heating oven	Binder GmbH, Tuttlingen, Germany
Pricisa XR 1255 M (balance)	Precisa Gravimetrics AG, Dietikon, Switzerland
Ultraspec 2100 pro (UV-Vis spectrometer)	GE, Munich, Germany
Heidolph Laborota 4000 efficient (rotary evaporator)	Heidolph Instruments GmbH & Co. KG, Schwabach, Germany
Sensoquest labcycler (PCR machine)	Sensoquest Biomedizinische Elektronik GmbH, Göttingen, Germany
sub cell horizontal electrophoresis systems	Bio-Rad Laboratories Inc., Munich, Germany
Bio View transilluminator UXT-20M1SR	Bio step GmbH, Jahnsdorf, Germany
Bio-Rad Power Pac HC (power source)	Bio-Rad Laboratories Inc., Munich, Germany
SIM-AMINCO French Pressure Cell Press	Polytec GmbH, Waldbronn, Germany
His Trap FF crude 5 mL	GE, Munich, Germany
Mini-Protean tetra vertical electrophoresis system	Bio-Rad Laboratories Inc., Munich, Germany
Trans-Blot semi-dry transfer cell	Bio-Rad Laboratories Inc., Munich, Germany
Infinite M200 microplate reader	Tecan Group Ltd., Männedorf, Switzerland

ultrasonic bath	Merck eurolab GmbH, Darmstadt, Germany
Agilent 1200 analytical LC system	Agilent Technologies Deutschland GmbH, Böblingen, Germany
Agilent 1100 preparative LC system	Agilent Technologies Deutschland GmbH, Böblingen, Germany
ÄKTApurifier UPC 10 system	GE, Munich, Germany
Micromass Q-TOF 2 mass spectrometer	Waters GmbH, Eschborn, Germany
Triple Quad LS/MS 6460 system	Agilent Technologies Deutschland GmbH, Böblingen, Germany
Exactive mass spectrometer	Thermo Fisher Scientific GmbH, Dreieich, Germany
Grace Grom-SIL 120 ODS-5 ST 10 µm, 250 mm x 20 mm (preparative HPLC)	Grace Davison Discovery Sciences - Alltech Grom GmbH, Worms, Germany
Phenomenix Luna C18, 5µm, 100 mm x 4.6 mm (analytical HPLC)	Phenomenix Inc., Aschaffenburg, Germany
Grace Grom-Sil 120 ODS-5 ST, 3 µm 100 mm x 2.0 mm (Q TOF 2)	Grace Davison Discovery Sciences - Alltech Grom GmbH, Worms, Germany
Eclipse Plus C18 column, 1.8 µM, 2.1 mm x 50 mm (Triple-Quad)	Agilent Technologies Deutschland GmbH, Böblingen, Germany
Eclipse XDB C-18 column, 5 µm, 4.6 mm x 150 mm (Orbitrap)	Agilent Technologies Deutschland GmbH, Böblingen, Germany
His Load 16/60 Superdex 75 prep grade	GE, Munich, Germany
JASCO J715 CD-spectrometer	Jasco Europe, Cremella, Italy
Quartz cuvettes	Hellma GmbH & Co. KG, Müllheim, Germany

2.8 Common usage

Basic materials were not considered for the following lists.

material	company
MF-Millipore, membrane filter, 0.22 µM	Millipore GmbH, Schwalbach, Germany
Spectra/Por dialysis membrane MWCO 12,000-14,000	Spectrum Europe B.V., Breda, The Netherlands
Amicon Ultra Ultracel 30 K, MWCO 30,000 centrifugal filter devices	Millipore GmbH, Schwalbach, Germany

3 Methods

3.1 Molecular biological techiques

3.1.1 Primer design

PCR primers were designed with the help of the Clone Manager Suit 7 (Sci-Ed software http://www.scied.com). The melting temperature of the primers ranged from 54 to 65 °C and was chosen as close as possible for a primer pair.

3.1.2 PCR

The polymerase chain reaction (PCR) was performed both with the *Taq*-polymerase and the Herculase II fusion polymerase. The Herculase II fusion polymerase was used mostly for cloning to improve the accuracy of the amplification, the *Taq*-polymerase for test PCRs.

The *Taq*-polymerase was originally isolated from *Thermus aquaticus* and is a thermostable DNA polymerase with a temperature optimum at 72 °C. The *Taq*-polymerase however does not possess a proof-reading function and can be overstrained by GC-rich sequences. The Herculase polymerase allows a higher fidelity and better amplification of GC-rich sequences, due to fusion of a *Pfu*-based DNA polymerase to a high affinity DNA-binding domain. The *Pfu*-polymerase, originally isolated from *Pyrococcus furiosus,* possesses a proof-reading function and can therefore provide a higher accuracy than the *Taq*-polymerase. *Taq*-polymerase and *Pfu*-polymerase also differentiate in their produced overhangs. *Taq*-based polymerases produce PCR products with A-overhangs, so called “sticky ends”. *Pfu*-based polymerases, in contrast, produce PCR products without overhangs, so called “blunt ends”.

Isolated genomic DNA, plasmid DNA or bacterial cultures were used as templates for the PCR reactions. For colony PCR bacterial colonies were picked with plastic tips into the PCR reaction mix. The success of the PCR reaction was checked by agarose gel electrophoresis. 3-5 µL of the PCR product were mixed 2:1 with sample buffer and run on an agarose gel along with a molecular weight marker to allow an estimation of the molecular weight of the PCR product.

PCR mix for the *Taq*-DNA polymerase

2.5 µL	10 x Taq PCR buffer
0.5 µL	dNTP mix (10 mM each)
0.5 µL	forward primer (25 pM)
0.5 µL	reverse primer (25 pM)
0.125 µL	*Taq* DNA Polymerase
1 µL or 0.5 µL	liquid culture, genomic DNA oder plasmid DNA
dH_2O	ad 25 µL total volume

PCR mix for the Herculase II DNA polymerase

10 µL	5 x Herculase PCR buffer
1 µL	dNTP mix (25 mM each)
1 µL	forward primer (25 pM)
1 µL	reverse primer (25 pM)
1 µL	Herculase DNA Polymerase
1 µL or 0.5 µL	Liquid culture, genomic DNA oder plasmid DNA
dH_2O	ad 50 µL total volume

PCR programme

step	temperature	time
1.	95 °C	5 min
2.	95 °C	1 min
3.	55 °C	15 s
4.	72 °C	1 min 30 s
5.	→ step 2. (35 x)	
6.	72 °C	5 min
7.	16 °C	10 min

3.1.3 Agarose gel electrophoresis

Agarose gel electrophoresis was applied to separate DNA molecules by size. 1 % agarose was suspended in TAE buffer and boiled in a microwave oven until the solution cleared. 0.5 µg/mL ethidium bromide was added to the clear solution and the solution was poured into horizontal gel trays. The gel was cooled at RT until a rigid gel formed. DNA samples were mixed 2:1 with sample buffer. The gel chamber was filled with TAE buffer and the DNA samples were loaded into the gel slots. To allow an estimation of the molecular weight of the DNA sample, a molecular weight marker was run along with the DNA sample. The gels were run at 85 V until the sample buffer had crossed three quarters of the gel. The gel was documented using a UV gel detection system.

3.1.4 Quantification of PCR products and plasmids

PCR products and plasmids were quantified spectroscopically with an UV spectrophotometer at the wavelength of λ = 260 nm. An absorbance of 1 with 1 cm path length at λ = 260 nm equals 50 µg/mL DNA. Additionally the ratio of 260 nm/280 nm was determined. A 260 nm/280 nm ratio of 1.8-2.0 indicates pure protein. A 260 nm/280 nm ratio above 2.0 indicates RNA contamination and a ratio below 1.8 indicates protein contamination.

3.1.5 Production of chemically competent *E. coli* cells

Chemically competent *E. coli* cells were prepared according to the method described by Hanahan (Hanahan 1983). An overnight *E. coli* culture was picked from a glycerol stock in 3 mL of YT medium and incubated for 12 h at 37 °C with shaking. A main culture was prepared by inoculating 200 mL of YT medium with 1 mL of the overnight culture and incubated at 37 °C with shaking until an OD_{600} value of 0.4-0.5 was reached. The main culture was cooled for at least 10 min on ice and centrifuged for 5 min at 4 °C and 4,000 g. The cell pellet was resuspended in 30 mL of ice-cold TJB1 medium and stored for further 5 min on ice. After incubation in TJB1, the cells were pelleted again by centrifugation as described before. Afterwards the cell pellet was resuspended in 2 mL of ice-cold TJB2 medium and immediately aliquoted in 100 µL aliquots and transferred to – 80 °C. Chemically competent *E. coli* cells were stored at – 80 °C until usage.

3.1.6 Heat shock transformation of chemically competent *E. coli* cells

Chemically competent *E. coli* cells were thawed on ice. Up to 10 µL of plasmid DNA was carefully mixed with the competent cells and incubated for 30 min on ice. A heat shock was applied by transferring the cells for 30 s to a heating block of 42 °C. After the heat shock, the cells were stored for further 5 min on ice before they were diluted in 250 µL LB medium and incubated for 1 h at 37 °C with shaking. The bacterial solution was plated on agar plates with LB medium and an antibiotic and stored overnight at 37 °C to select successfully transformed cells.

3.1.7 Creating an intermediate cloning vector

Genes of interest were amplified by PCR (see PCR 3.1.2). Primers were designed with restriction sites to allow later on cloning into the expression vectors pEt24a(+) and pEt28a(+). The PCR products were isolated using a Quiagen PCR Purification Kit following the manufacturer's instructions. The isolated PCR products were cloned into a pDrive cloning vector with the use of the Qiagen PCR Cloning Kit following the manufacturer's instructions. The pDrive vector carries ampicillin and kanamycin resistance genes and a *LacZΔM15* gene coding for a β-galactosidase. β-galactosidase can hydrolyze X-gal into galactose and 5-bromo-4-chloro-indoxyl which

in presence of oxygen turns into a blue dye. The *β-galactosidase* gene is disrupted by ligation of a DNA insert into the cloning site. Positive clones therefore cannot express β-galactosidase. The production of β-galactosidase can be induced with IPTG. In presence of IPTG and X-gal negative clones therefore have a blue color while positive clones remain white. Positive clones can therefore be selected by color in the so called “blue/white selection”. The pDrive vector is supplied by the manufacturer in linear form with U-overhangs at each end. The U-overhangs allow a precise ligation of PCR products with A-overhangs. The use of PCR products with “blunt ends” however can significantly decrease the cloning efficiency. Genes amplified with Herculase II DNA polymerase therefore were modified with a Quiagen A-Addition Kit following the manufacturer’s instruction to generate A-overhangs. The ligation was performed with 50 ng of pDrive cloning vector and a three times molar ratio of PCR product with the supplied ligase and enzyme buffer in a total reaction volume of 10 µL. After incubation for 1-2 h at 16 °C 5-10 µL of the ligation mix were transformed into chemically competent *E. coli DH5α* cells (see heat shock transformation of chemically competent cells). Positive clones were selected by plating the cells on LB agar plates containing 50 µg/mL Kan, 50 µM IPTG and 80 µg/mL X-gal and incubated overnight at 37 °C. To improve the blue/white selection the plates were incubated a second time at 4 °C for at least 1 h. Selected positive clones were analyzed by colony PCR and restriction analysis. Constructs verified by PCR and restriction analysis were isolated using the GeneJET Plasmid Miniprep Kit following the manufacturer’s instructions. DMSO stocks of successfully transformed colonies were prepared by mixing 900 µL of cell solution with 100 µL of sterile DMSO and transferring the cells to – 80 °C. DMSO stocks were stored at - 80 °C.

3.1.8 Creating a protein expression vector

Genes of interest were cloned from the intermediate cloning vector into the pEt24a(+) and the pEt28a(+) expression vector. The pEt24a(+) and the pEt28a(+) vector possess a kanamycin resistance gene and a cloning/expression region controlled by a T7 expression system. The bacteriophage *T7* promoter is induced by the T7 RNA polymerase. When induced the *T7* promoter is so active, that after some hours nearly 50 % of the cell total protein content can be made up of the desired product. The pEt24a(+) and the pEt28a(+) vector contain a copy of a T7 RNA polymerase that is

under the control of a *lacUV5* promoter. The *lacUV5* is normally repressed and no T7 RNA polymerase and therefore no product is expressed. In presence of lactose or the lactose analogue IPTG the *lacUV5* promoter is induced and the T7 RNA polymerase is expressed. Induction with IPTG (normally with an IPTG concentration between 100-500 µM) leads thus to a very strong transcription of the inserted gene within a few hours. The cloning region of both the pEt24a(+) and the pEt28a(+) vector is designed in a way to allow the production of a fusion protein carrying a His-tag to facilitate protein purification.

E. coli DH5α cells containing the empty pEt24a(+) or pEt28a(+) expression vectors were picked from glycerol stocks into 10 mL LB medium with 50 µg/mL Kan and incubated overnight at 37 °C with shaking. pEt24a(+) and pEt28a(+) plasmids were isolated using the GeneJET Plasmid MiniPrep Kit following the manufacturer's instructions. 1-2 µg of the expression vectors pEt24a(+) and pEt28a(+) were digested in a 50 µL reaction mixture containing 1 µL each of the appropriate restriction enzymes and the appropriate buffer at 37 °C for 4 h. For double digests optimal enzyme buffers were selected with the help of the Fermentas DoubleDigest Tool (http://www.fermentas.com/en/tools/doubledigest) and enzyme concentrations were used as recommended by the manufacturer. Similarly, pDrive plasmids containing the genes of interest were isolated and digested with the appropriate restriction enzymes. Digestion products were separated by agarose gel electrophoresis (see agarose gel electrophoresis). The digested pEt24a(+) and pEt28a(+) vectors and the genes of interest were cut out of the gel and isolated from the gel with the GeneJET Gel Extraction Kit following the manufacturer's instructions. Before ligation, the vector fragments were dephosphorylated with antarctic phosphatase following the manufacturer's instruction to prevent self-ligation. The dephosphorylated vector fragments and the gene fragments were joined together using the T4 DNA ligase following the manufacturer's instructions. The ligation was performed with 50 ng of vector and a 6-12 times molar ratio of PCR product with 1 µL ligase in the supplied enzyme buffer in a total reaction volume of 20 µL. After incubation at 16 °C for 4-12 h, the ligation products were transformed into chemically competent *E. coli DH5α* cells. Positive clones were selected by plating the transformed cells on LB agar plates containing 50 µg/mL Kan and storing at 37 °C overnight. Selected positive clones were analyzed by colony PCR and restriction analysis. Constructs verified by PCR and restriction analysis were isolated using the GeneJET Plasmid Miniprep Kit

following the manufacturer's instructions and sent for sequencing to LGC genomics (LGC Genomics GmbH, Berlin, Germany) to confirm the correctness of the inserted gene. DMSO stocks of successfully transformed colonies were prepared by mixing 900 µL of cell solution with 100 µL of sterile DMSO and transferring the cells to – 80 °C. DMSO stocks were stored at – 80 °C. Constructs verified by sequencing were transferred into the *E. coli BL21* cells. The success of the transformation was verified by colony PCR. DMSO stocks were generated also from successfully transformed *BL21* cells and stored at – 80 °C.

3.1.9 Restriction analysis

Restriction analysis was performed to identify a DNA sequence on the basis of size of the restriction fragments generated by digest with a specific restriction enzyme. Successful cloning of a gene into a vector for example can be verified by cutting the plasmid both within the sequence of the gene and within the sequence of the vector. The Clone Manager Suit 7 (Sci-Ed software http://www.scied.com) was used to select suitable restriction enzymes and predict the size of the restriction fragments. For the restriction analysis 5 µL of isolated plasmid was digested in 20 µL reaction mixes containing each 0.5 µL of the selected restriction enzymes and the matching restriction buffer for at least 2 h at 37 °C. The digestion products were analyzed by agarose gel electrophoresis.

3.1.10 Construction of Plasmids for the Generation of knock-out mutants

The genes *ORF7, ORF26, ORF27, DpgD* from *Streptomyces* sp. DSM 11171 genomic DNA were amplified by PCR reactions with the Herculase II fusion DNA polymerase using a forward primer introducing an EcoRI restriction site and a reverse primer introducing an XbaI restriction site. The amplified genes were digested by EcoRI and XbaI and ligated into the Streptomyces knock-out vector pK18mobapra. Each recombinant plasmid was analysed by restriction analysis and PCR. Correctness of inserted gene fragments was verified by sequencing by LG genomics (LGC Genomics GmbH, Berlin, Germany) and the obtained sequence showed complete identity with the corresponding *Streptomyces* sp. DSM 11171 genes (www.expasy.ch). The resulting constructs were transformed into *E. coli*

ET12567+pUZ8002, selected with chloramphenicol (34 µg/mL), kanamycin (50 µg/mL) and apramycin (100 µg/mL) and stored at -80 °C.

3.1.11 Preparation of *Streptomyces* sp. DSM 11171 spore solution

Streptomyces sp. DSM 11171 was plated from cryostocks on HA agar plates for 3-4 days until spore formation was visible. The spores were detached from the agar plates with 9 mL of 0.1 % Tween20 solution, transferred into a sterile plastic tube and resuspended by intense vortexing for at least 1 min. The spore solution was than filtrated through sterile cotton batting and the spores were pelleted by centrifugation for 5 min at 4,000 rpm at 4 °C. Spores were resuspended in 1 mL 20 % glycerine solution and stored at -80 °C until usage.

3.1.12 Conjugation of *Streptomyces* sp. DSM 11171 to generate knock-out mutants

The *E. coli* ET12567+pUZ8002 strains containing the recombinant plasmids were grown in 20 mL LB medium supplemented with chloramphenicol (34 µg/mL), kanamycin (50 µg/mL) and apramycin (100 µg/mL) at 37 °C to an OD_{600} of 0.4-0.6, harvested and washed two times with the same volume fresh LB medium and resuspended in 2 ml LB. 50 µL fresh *Streptomyces* sp. DSM 11171 spore solution was resuspended in 2xYT (16.0 g/L tryptone, 10.0 g/L yeast extract, 5.0 g/L NaCl, pH 7.0) medium, heat shocked for 10 min at 50 °C and mixed with 500 µL of *E. coli* solution. The *Streptomyces E. coli* mixture was plated on MS agar plates and incubated for at 28 °C. After 24 h the plates were coated with NB soft agar (8.0 g/L nutrient broth, 5.0 g/L agar) with apramycin (1 mg/mL) and phosphomycin (1 mg/mL) and grown at 28 °C for additional 3-4 days. Successful conjugates were transferred on HA agar plates with apramycin (25 µg/mL) and phosphomycin (400 µg/mL) and analysed by restriction analysis and PCR and stored as spores at -80 °C.

3.1.13 Analysis of the genomic data

The Feglymycin genome cluster was analyzed with the help of the artemis genome annotation tool (http://www.sanger.ac.uk/resources/software/artemis/) (Rutherford et al. 2000), the NCBI blast tool (http://blast.ncbi.nlm.nih.gov/Blast.cgi) and the

NRPS/PKS analysis tool of the university of Maryland (http://nrps.igs.umaryland.edu/nrps/) (Bachmann, Ravel 2009a).

3.2 Biochemical techniques

3.2.1 SDS-PAGE

Sodium dodecyl sulfate acryl amide gel electrophoresis (SDS-PAGE) allows the separation of proteins according to their molecular weight. By running protein samples together with a protein marker the molecular weight of a sample can be estimated. 12 % acryl amide gels were prepared according to the method of Laemmli (Laemmli 1970). First a 12 % separation gel was prepared, poured into a vertical gel tray and left at RT until a rigid gel formed. To prevent the separation gel from drying, it was meanwhile covered with a layer of isopropanol. After the separation gel had polymerized, the isopropanol was removed and the separation gel was covered with the 4 % stocking gel. Protein samples were mixed 1:1 with sample buffer and transferred for 5-10 min to a 95 °C heating block. The electrophoresis chamber was filled with electrophoresis buffer and the protein samples were loaded into the gel slots along with a molecular weight marker. The gels were run for 1.5 h at 100 V. Afterwards the gels were stained with comassie blue staining solution for 1 h with shaking. The gel was destained with tap water overnight. To accelerate the destaining, the gels were heated one or more times for 1 min in water in a microwave oven.

3.2.2 Small scale protein expression

To test the protein expression under different expression conditions a small scale protein expression followed by a small scale protein preparation was performed. Bacterial cultures were prepared by picking a bacterial culture from an agar plate or a DMSO stock into 2-3 mL of LB medium containing 50 µg/mL Kan and incubation overnight at 37 °C with shaking. As main culture 50 mL of LB medium containing 50 µg/mL Kan was inoculated with 500 µL bacterial culture and incubated at 37 °C with shaking until an OD_{600} of 0.5-0.6 was reached. Protein expression was induced with ITPG concentrations between 0 and 500 µM and the main culture was incubated for further 3 h at 37 °C, for 1 d at 17 °C or for 2-3 d at 14 °C with shaking. The main culture than was used for small scale protein preparation.

3.2.3 Small scale protein preparation

Small scale protein preparation was performed with help of the BugBuster Protein Extraction Reagent. 5 mL of bacterial culture was pelleted by centrifugation for 5 min at 4 °C with 4,000 rpm. The cell pellet was thoroughly resuspended in 500 µL of BugBuster Protein Extraction Reagent and incubated for 20-30 min at RT with shaking to allow complete lysis of the cell wall. The crude cell lysate was centrifuged for 20 min at RT with 16,000 rpm and the supernatant, containing the soluble proteins, was separated from the pellet. Both supernatant and pellet were analyzed by SDS-PAGE.

3.2.4 Large scale protein expression

Large scale protein expression was performed with larger amounts of bacterial culture to enable the purification of larger amounts of protein. Bacteria cultures were prepared by picking a bacterial culture from an agar plate or a DMSO stock into 2-3 mL of LB medium containing 50 µg/mL kan and incubation overnight at 37 °C with shaking. As main culture 0.5-1 L of LB medium containing 50 µg/mL kan was inoculated with 2 mL preparatory culture and incubated at 37 °C with shaking until an OD_{600} of 0.5-0.6 was reached. For the Mur proteins it was found that they were all expressed at least partially soluble at 37 °C. The main culture was induced with 500 µM of IPTG and incubated for further 3 h at 37 °C with shaking. Afterwards the main culture was transferred to 17 °C and incubated overnight with shaking at lower temperature to improve the solubility of the expressed proteins.

3.2.5 Large scale protein preparation

1 L bacterial culture was pelleted by centrifugation for 20 min at 4,000 rpm. The cell pellet of the 1 L culture was taken up in 15 mL of lysis buffer. Salt concentration, pH and additives like $MgCl_2$, β-mercaptoethanol or Triton X-100 may influence the solubility and stability of a protein. A suitable lysis buffer had to be individually determined for every protein. Low imidazole concentrations were added to the lysis buffer to prevent unspecific binding to the Ni^{2+}-sepharose columns. For proteins with a low affinity to Ni^{2+}-sepharose however also low imidazole concentration decrease binding. For MurA, MurC and MurD from *E. coli* and MurA and MurD from *S. aureus*

a simple lysis buffer was used (20 mM Tris/HCl pH 8.0, 500 mM NaCl, 10 mM $MgCl_2$, 20 mM imidazole and 1 mM PMSF, freshly added). For MurB, MurE and MurF from *E. coli* and MurC from *S. aureus* a lysis buffer with a lower imidazole concentration containing additionally Triton X-100 and glycerine was used (20 mM Tris/HCl pH 8.0, 500 mM NaCl, 10 mM $MgCl_2$, 10 mM imidazole, 1 % Triton X-100, 1 % glycerine and 1 mM PMSF, freshly added). For MurB from *S. aureus* a similar lysis buffer with lower salt concentration was used (20 mM Tris/HCl pH 7.5, 75 mM NaCl, 20 mM $MgCl_2$, 10 mM imidazole, 1 % glycerine, 1 % Triton X-100 and 1 mM PMSF, freshly added). Cells were lyzed by passing through a French press twice. Cell debris was removed by centrifugation for 20 min at 12,000 rpm at 4 °C. The supernatant containing the soluble proteins was used for protein purification.

3.2.6 Protein purification

The recombinant proteins were purified by affinity chromatography. Affinity chromatography of proteins carrying a His-Tag is enabled by the fact that the imidazole group of histidine specifically binds Ni^{2+}-ions. The soluble protein fraction of the large-scale protein preparation was loaded on a 5 mL His-Trap Ni^{2+}-sepharose column using an Äkta LC system with on-line UV-detection at λ = 280 nm and eluted by a linearly increasing imidazole concentration with a standard flow of 1 ml/min and a pressure of 0.2-0.4 MPa. Before loading the protein fraction, the column was washed with 5 column volumes of water and equilibrated with 5 column volumes of binding buffer. All buffers were filtrated with a 0.22 µm membrane filter prior to being applied on the Äkta LC system. The binding buffer was in most cases identically to the lysis buffer. Only in those cases of the lysis buffers containing Triton X-100, the Triton X-100 concentration of the binding buffer was chosen 10 times lower than the Triton X-100 concentration of the lysis buffer (0.1 % Triton X-100 instead of 1 %). The protein fraction was loaded with a flow rate of 1 mL/min and at a column pressure below 0.5 MPa. After loading the sample, the column was first washed with 8 column volumes of binding buffer. Bound proteins eluted by linearly increasing the imidazole concentration to a total concentration of 250 mM imidazole. For the MurB proteins from *E. coli* and *S. aureus* a lower flow rate of 0.5 mL /min was chosen to increase binding.

3.2.7 Protein dialysis

By protein dialysis the high imidazole and salt concentrations resulting from the protein purification protocol were removed. Protein-containing fractions were transferred into a dialysis membrane tubing with a molecular weight cut-off of 12,000-14,000 Da and dialyzed with stirring in 1 L of dialysis buffer (20 mM Tris/HCl pH 7.0, 50 mM NaCl, 10 mM $MgSO_4$, 1 mM DTT and 20 % glycerine) at 4 °C for 24 h. If necessary the proteins were concentrated with an Amicon Ultra centrifugal filter devices with a MWCO of 30 kDa following the manufacturer's instructions.

3.2.8 Spectroscopic determination of the protein concentration

Protein concentration was determined by UV-Vis spectroscopy at a wavelength of λ = 280 nm. Aromatic amino acids like tyrosine, tryptophan, histidine and phenylalanine are mainly responsible for the absorption of proteins at λ = 280 nm. From the aromatic amino acids tryptophan has the biggest share in the absorption at λ = 280 nm. Protein concentrations were calculated from the specific absorbance of the protein. Specific absorbance of a protein was predicted with the help of the ProtParam tool of the ExPASy Proteomics Server (http://www.expasy.ch/tools/protparam.html).

3.2.9 Western blot

Western blot is an immunological technique to detect specific proteins with the help of antibodies. Western blotting is normally performed with two antibodies. The first antibody binds specifically to the target protein. The second antibody targets the first antibody and carries a marker to facilitate detection. The marker can be a linked protein e.g. alkaline phosphatase or horseradish peroxidase that catalyzes a reaction producing a colorimetric reaction product. Other used markers are e.g. radioactive isotopes or fluorophores. For Western blotting, proteins are first separated by SDS-PAGE (see SDS-PAGE). Because Antibody detection cannot be performed with an SDS gel the proteins are transferred from the unstained gel to a nitrocellulose membrane by means of electric current. This step has been termed blotting. The membrane is later blocked with BSA or milk powder to prevent unspecific binding of the antibody to the membrane. The Mur proteins were detected with an antibody produced in mice that specifically targets the His-Tag of the proteins. The second

antibody was an anti-mouse IgG antibody bound to alkaline phosphatase (AP). BCIP and NBT were used as substrates for AP. BCIP is hydrolyzed by the AP to form 5-bromo-4-chloro-indolyl and phosphate. 5-bromo-4-chloro-indolyl is further oxidized by oxygen to from the deep blue insoluble pigment 5,5′-dibromo-4,4′-dichloro-indigo (Knecht, Dimond 1984). NBT works as an oxidant and promotes the formation of 5,5′-dibromo-4,4′-dichloro-indigo.

After running the SDS gel, the gel and a nitrocellulose membrane of identical size were incubated for 20 min in the blotting buffer. Afterwards both were transferred to a semi-dry blotting gadget and blotted for 40 min at 15 V. The membrane was then transferred to the blocking solution (30 mL of TNT + 3 % BSA + 0.02 % (g/g) thimerosal). After 1 h, the blocking solution was replaced by a solution containing the first antibody (2.1 µL mouse anti-poly-histidine antibodies in 30 mL TNT + 1 % BSA + 0.02 % (g/g) thimerosal). The membrane was incubated with the first antibody for 1.5 h at RT or for 12 h at 4 °C. Unbound antibodies were removed by washing the membrane three times for 10 min with 30 mL of TNT (+ 1 % BSA) before it was incubated for additional 1.5 h with a solution containing the second antibody (6 µL goat anti-mouse IgG-alkaline phosphatase antibodies in 30 mL of TNT + 1 % BSA). After incubation with the second antibody the membrane was washed again three times for 10 min with 30 mL of TNT + 1 % BSA. To detect the bound antibodies the membrane was incubated with 15 mL of AP solution containing 300 µL of freshly added BICP solution and 135 µL of freshly added NBT solution. The AP reaction was stopped after the protein bands became visible by washing the membrane with tap water.

3.2.10 *In vitro* reconstruction assays of MurA-MurF

To investigate the inhibitory effect of feglymycin on the activity of the MurA-F enzymes from *E. coli* a one-pot assay was used. All reactions were performed in triplicate. A solution containing 20 mM Tris/HCl pH 7.0, 10 mM $MgCl_2$, 2 mM DTT, 400 µM UDP-GlcNAc, 400 µM PEP, 250 nM MurA and 50 µM feglymycin was prepared and incubated at 25 °C. As references a solution without feglymycin as a positive control and a solution without MurA as a negative control were prepared. For investigation of the MurB enzyme, the same solution as for the MurA reaction was prepared and incubated at 25 °C. After 2 h, additionally 400 µM NADPH, 100 nM MurB and 50 µM feglymycin were added. As references, a positive control without

feglymycin as well as a negative control without MurB was prepared. For investigation of the MurC enzyme, the same solutions as for the MurB reaction were prepared and incubated at 25 °C. After 2 h, additional 400 µM ATP, 400 µM L-Ala, 300 nM MurC and 50 µM feglymycin were added and reference samples were prepared as described for MurB. For investigation of the MurD enzyme, the same solutions as for the MurC reaction were prepared and incubated at 25 °C. After 2 h, additional 400 µM D-Glu, 400 µM ATP, 450 nM MurD and 50 µM feglymycin were added and reference samples were prepared. For the MurE enzyme, the same solutions as for the MurD enzyme were prepared and incubated at 25 °C. After 4 h, additional 1 mM *meso*-DAP, 1 mM DTT, 400 µM ATP, 350 nM MurE and 50 µM feglymycin were added and references were prepared. For the MurF enzyme, the same solutions as for the MurE enzyme were prepared and incubated at 25 °C. After 4 h, additional 1 mM D-Ala-D-Ala, 1 mM DTT, 400 µM ATP, 300 nM MurF and 50 µM feglymycin were added and references were prepared. All enzyme reactions were performed at 25 °C for 4 h. After 4 h, the enzyme reactions were stopped by addition of 1:2 ice-cold methanol. Both samples and reference samples were cooled for 10 min on ice and then centrifuged for 10 min at 15 000 g. The supernatant was analyzed by LC-ESI-MS (see LS-MS detection by means of ESI-TOF-MS and ESI-QQQ-MS) and high-resolving ESI-Orbitrap-MS (see high resolving ESI-MS).

3.2.11 MurA assay

The MurA assay was performed as a coupling assay with the MurB enzyme from *E. coli* similar to the assay previously described by Brown et al. (Brown et al. 1994). The MurB enzyme converts the product of the MurA reaction EP-UDP-GlcNAc to UDP-MurNAc accompanied by the spectrophotometrically detectable conversion of NADPH to $NADP^+$. The decrease of NADPH was read in 96 well plates at a detection wavelength λ = 340 nm at 20 s intervals with a UV-Vis reader (Tecan) for 20 min at 37 °C. All measurements were performed in triplicate and with controls (no substrate added). All V_{max} and K_m values were determined both under saturation with UDP-GlcNAc or PEP. The reaction buffer for the MurA enzyme from *E. coli* contained 50 mM Tris/HCl pH 7.0, 10 mM KCl, 3.5 mM DTT, 500 µM NADPH, 500 nM MurB, 200 µM PEP or 400 µM UDP-GlcNAc and 20 nM MurA and was preincubated for 5 min at 37 °C prior to starting the reaction. One substrate was always preincubated with the enzyme at a fixed concentration. The reaction was started by addition of the

second substrate. For determination of the IC_{50} values, the reaction mixture was preincubated for 5 min with 10 different concentrations of feglymycin (0- 50 µM), phosphomycin (0-250 µM) or bacitracin (between 0-250 µM). The reaction was started by addition of 400 µM UDP-GlcNAc (in case of feglymycin and bacitracin) or 200 µM PEP (in case of phosphomycin). To determine the time-dependence of the reaction, the reaction mixture was incubated with 5 µM feglymycin at 37 °C at different time intervals between 1 min and 20 min before it was started by addition of 400 µM UDP-GlcNAc. To determine the inhibition type and K_i-values, the reaction mixture was preincubated with 5-6 different feglymycin concentrations around the IC_{50} value (3.4 µM). The reactions were started either by addition of 10 different concentrations of PEP or UDP-GlcNAc (0-800 µM) while the other substrate was kept at a fixed concentration (400 µM). The reaction buffer for the MurA enzyme from *S. aureus* contained 20 mM Tris/HCl pH 7.5; 10 mM KCl; 2 mM DTT; 500 µM NADPH; 500 nM MurB; 400 µM PEP; 400 µM UDP-GlcNAc and 250 nM MurA. The determination of the V_{max}, K_m and IC_{50} values was performed as described for the MurA enzyme from *E. coli.*

3.2.12 Calculation of the V_{max}, K_m and K_i values

Linear fitting of the reciprocal of the substrate concentration and velocities are error-prone due to the fact that in a Lineweaver-Burk plot the lowest substrate concentration corresponds to the highest reciprocal values. Therefore, instead of the untransformed data, the V_{max} and K_M values determined by non-linear regression were inserted into the reciprocal Lineweaver-Burk equation (1) to obtain a linear function used for a Lineweaver-Burk plot. V_{max} and K_m non-linear least-squares fitting was performed with equation (1) and by the Levenberg–Marquardt algorithm implemented in the SciPy library (http://www.scipy.org) with a by Bartlomiej Krawczyk in-house written python program. K_i-values were calculated from the IC_{50} values as described by Copeland (Copeland 2000) for reversible non-competitive inhibitors.

$$\frac{1}{v} = \left(\frac{K_m}{V_{\max}} \frac{1}{[S]} \right) + \frac{1}{V_{\max}} \qquad (1)$$

The α value can be concluded from the interstion point of the lines in the Lineweaver-Burk plot. An α value of ~ 1 can be concluded if the converging lines in the Lineweaver-Burk plot intersted to the left of the y-axis and on the x-axis. Lines

that interst above the x-axis indicate an α value > 1 and lines that interst below the x-axis indicate an α value < 1 The K_i value was calculated from the IC_{50} value with the following equation (2) (Copeland 2000).

$$IC_{50} = \frac{[S] + K_m}{\frac{K_m}{K_i} + \frac{[S]}{\alpha K_i}} \quad \text{if } \alpha = 1 \;\; K_i = IC_{50} \qquad (2)$$

The k_{cat} value was calculated as V_{max}/c_{enzyme} with V_{max} in [M/s] and c_{enzyme} in [M].

3.2.13 MurC assay

The MurC assay was performed as a coupling assay monitoring the decrease of NADH with pyruvate kinase (PK) and lactic dehydrogenase (LDH) similar to the assay performed by Jin (Jin et al. 1996). The conversion of UDP-MurNAc to UDP-MurNAc-L-Ala is ATP-driven and accompanied by the formation of ADP. ADP and PEP serve as substrate for PK for the formation of pyruvate and ATP. Pyurvate, again, is used together with NADH by LDH to form lactat and NAD^+. The conversion of NADH to NAD^+ is spectrophotometrically detectable. The decrease of NADH was read in 96 well plates at λ = 340 nm at 20 s intervals with an UV-Vis reader (Tecan) for 20 min at 37 °C. All measurements were performed in triplicate and with controls (no substrate added). All V_{max} and K_m values were determined varying the L-Ala, ATP and UDP-MurNAc substrate concentration while the other two substrates were kept at saturation. The reaction buffer for the MurC enzyme from *E. coli* contained 50 mM Tris/HCl pH 8.0, 10 mM $MgCl_2$, 10 mM NH_4SO_4, 400 µM L-alanine or/and 400 µM ATP or/and 400 µM UDP-MurNAc, 2.5 mM DTT, 1 mM PEP, 1 mM NADH, 10 U/ml LDH, 10 U/ml PK, 20 nM MurC and was preincubated for 5 min at 37 °C prior to starting the reaction. Two substrates were always preincubated with the enzyme at a fixed concentration. The reaction was started by the addition of the third substrate. For determination of the IC_{50} values, the reaction mixture was preincubated for 5 min with 10 different concentrations of feglymycin (between 0-50 µM), β-chloro-L-alanine (between 0-250 µM) or bacitracin (between 0-250 µM). The reaction was started by addition of 400 µM UDP-MurNAc (in case of feglymycin) or 400 µM L-alanine (in case of β-chloro-L-alanine and bacitracin). To determine the time-dependence of the reaction, the reaction mixture was incubated with 0.5 µM feglymycin at different time intervals between 1 min and 20 min before the reaction was started by addition of

400 µM UDP-MurNAc. To determine the inhibition type and K_i-values, the reaction mixture was preincubated with 5 different feglymycin concentrations around the IC_{50} value (0.5 µM). The reactions were started either by addition of 10 different concentrations UDP-MurNAc, ATP or L-alanine (0-800 µM) while the other substrates were kept at fixed concentrations (400 µM). The reaction buffer for the MurC enzyme of *S. aureus* was the same as for the MurC enzyme from *E. coli* with a MurC *S. aureus* concentration of 200 nM. The determination of the V_{max}, K_m and IC_{50} values were performed analogously as described for the MurC enzyme from *E. coli*. Calculation of V_{max}, K_m, k_{cat} and K_i for MurC was performed as described above for the MurA enzyme (see Calculation of the V_{max}, K_m and K_i values).

3.2.14 Reversibility test

Reversibility of the inhibition of the MurA and MurC *E. coli* enzymes by feglymycin was tested using a comparative dilution analysis as described by Copeland (Copeland 2005). With the help of the comparative dilution analysis it should be tested if the inhibitor binds irreversibly to the enzyme, so that the enzyme stays inactive after contact with high concentrations of inhibitor, even after dilution to a much lower inhibitor concentrations. For this experiment, the enzyme in a concentration of about 100-fold higher than used for the activity assay (2 µM MurA/MurC) was incubated with an inhibitor concentration about 10-fold higher than the IC_{50} value (5 µM for MurC, 50 µM for MurA) for 20 min. After preincubation, the enzyme was either diluted 100-fold with reaction buffer without feglymycin or 100-fold with reaction buffer containing a 10-fold lower concentration of feglymycin (0.5 µM for MurC, 5 µM for MurA). Therefore the end concentration after dilution was 20 nM enzyme in the reaction buffer. The reaction was started by addition of 400 µM UDP-GlcNAc/UDP-MurNAc and the enzyme activity was detected within the first 4 min after dilution in intervals of 20 s as described above. All reactions were performed in triplicate.

3.3 Analytical techniques

3.3.1 Cultivation of *Streptomyces* sp. DSM 11171 strain for DNA sequencing

Streptomyces sp. DSM 11171 spores were seeded on GYM agar and grown for 2 d at 30 °C. A 1 cm x 1 cm piece of agar was cut out and transferred into 100 ml TSB

medium. After incubation for 2 days at 28 °C and 180 rpm the cells were harvested and frozen at - 80 °C. Isolation of genomic DNA and sequencing was carried out by LG genomics (LGC Genomics GmbH, Berlin, Germany).

3.3.2 Extraction of feglymycin from agar plates for LC-MS detection

Streptomyces sp. DSM 11171 spores were seeded on different agar plates and grown for 3 d at 30 °C. 50 µg of cell culture was scratched off the agar plates and resuspended in 500 µL 80 % MeOH (in dH_2O) and disrupted by 15 min incubation in an ultrasonic bath. The cell extract was centrifuged for 15 min at 15,000 rpm and the supernatant was analyzed by LC-MS.

3.3.3 Extraction of feglymycin from cell cultures for LC-MS detection

Streptomyces sp. DSM 11171 spores were seeded on GYM agar plates and grown for 2 d at 30 °C. A 1 cm x 1 cm piece of agar was cut out and transferred into 50 mL of TSB medium and incubated at 28 °C and 120 rpm. After two d 50 mL of E1 medium in a 250 mL flask were inoculated with 5 mL of the TSB culture und incubated at 28 °C and 120 rpm. After 7 d 1 mL of cell culture was harvested and pelleted by centrifugation at 5,000 rpm for 5 min. The cells were resuspended in 500 µL 80 % MeOH (in dH_2O) and disrupted by 15 min incubation in an ultrasonic bath. The cell extract was centrifuged for 15 min at 15,000 rpm and the supernatant was analyzed by LC-MS.

3.3.4 Isolation of preparative amounts of feglymycin

Streptomyces sp. DMS 11171 spores were seeded on a GYM agar plate and incubated for 2 d at 30 °C. A 1 cm x 1 cm piece of agar was then cut out and transferred into a 250 mL flask containing 50 mL of TSB medium und incubated at 28 °C and 120 rpm. After 2 d 200 mL of E1 medium in a 500 mL flask were inoculated with 20 mL of the TSB culture und incubated at 28 °C and 120 rpm. After 7 d the cells were pelleted by centrifugation for 20 min at 4,000 rpm at RT. The cell pellet was resuspended by vortexing in 100 mL of 80 % MeOH (in dH_2O) and disrupted by 30 min incubation in an ultrasonic bath. The cell extract was centrifuged for 30 min at 15,000 rpm and the supernatant was dried on a rotation evaporator.

The methanol extract was resolved in 2 mL MeOH and cleared by centrifugation for 15 min at 15,000 rpm. The supernatant was fractionated by RP-HPLC with a Grace Grom-SIL 120 ODS-5 ST column (10 µm, 250 mm x 20 mm) using the following gradient:

time (min)	% A (H_2O + 0.1 % HCOOH)	% B (MeOH + 0.1 % HCOOH)
0.0	95	5
40.0	60	40
40.1	0	100
45.0	0	100
45.1	95	5
50.0	95	5

Feglymycin eluted at a retention time Rt = 31 min. Fractions containing feglymycin were combined and methanol and water were evaporated at the rotary evaporator.

3.3.5 Isolation of preparative amounts of nocardamine

Streptomyces sp. DMS 11171 spores were seeded on a GYM agar plate and incubated for 2 days at 30 °C. A 1 cm x 1 cm piece of agar was then cut out and transferred into a 250 mL flask containing 50 mL of TSB medium und incubated at 28 °C and 120 rpm. After 2 d 200 mL of M9 minimal medium in a 500 mL flask were inoculated with 20 mL of the TSB culture und incubated at 28 °C and 120 rpm. After 3 d the cells were pelleted by centrifugation for 20 min at 4,000 rpm at RT. A column was prepared with 20 g of XAD-16 material and equilibrated with 10 column volumes of dH_2O. The supernatant was transferred on the column and incubated with the XAD-16 material for 20 min. The column was run with a flow rate of 1-2 mL/min. The XAD column was washed first with 200 mL dH_2O, then 200 mL 15 % MeOH (in dH_2O) and 200 mL 40 % MeOH (in dH_2O). Nocardamine was eluted from the XAD column with 200 mL 100 % MeOH. Methanol was evaporated at a rotary evaporator and the pellet was redissolved in 2-3 mL 100 % dH_2O and cleared by centrifugation for 15 min at 15,000 rpm. The supernatant was fractionated by RP-HPLC with a

Grace Grom-SIL 120 ODS-5 ST column (10 µm, 250 mm x 20 mm) and the following gradient:

time (min)	% A (H_2O + 0.1 % HCOOH)	% B (MeOH + 0.1 % HCOOH)
0.0	95	5
30.0	50	50
35.0	40	60
35.1	0	100
40.0	0	100
40.1	95	5
45.0	95	5

Nocardamine eluted at retention time of R_t = 30 min and demethylenenocardamine a lower homologue of nocardamine at retention time of R_t = 27.5 min. Fractions containing nocardamine and demethylenenocardamine were combined and methanol and water were dried at the rotary evaporator.

3.3.6 LS-MS detection with ESI-TOF-MS

Substrates and products of the Mur enzyme reactions were measured with LC-ESI-MS in negative ion mode. Enzymes were pelleted prior to the mass spectrometric analysis by addition of 2 volumes of ice-cold MeOH and centrifugation for 15 min at 15 000 g. The experiments were recorded on a QTof2 mass spectrometer coupled to an HPLC Agilent 1200. HPLC was performed using a C18 column (100 x 2 mm, 3 µM, Grace) with a flow rate of 0.3 mL/min using an optimized gradient. The gradient was 5 % aqueous ACN (0.1 % HCOOH) to 100 % ACN (0.1 % HCOOH) in 15 min and then isocratic at 100 % ACN (0.1 % HCOOH) for further 3 min. The following settings were found to be best for the detection of the MurA-F substrates and products:

capillary voltage	2.4 kV
cone voltage	45 V

desolvation temperature	350 °C
source temperature	120 °C
MCP	1750 V
TOF	9.1 kV
start mass	100
end mass	2800
scan time	0.5 s
inter-scan delay	0.1
ionization	negative

3.3.7 LS-MS detection of the MurA-F substrates and products with the TripleQuad LC-MS

LC-MS measurements were recorded on a TripleQuad LC/MS 6460 mass spectrometer coupled to an Agilent 1290 Infinity HPLC system. To detect full mass scans the setting MS2Scan was chosen. Enzymes were pelleted prior to the mass spectrometric analysis and the reaction mix was diluted by addition of 5 volumes of ice-cold MeOH and centrifugation for 15 min at 15 000 g. Analysis were performed by direct injection without column with a flow of 0.3 mL/min and water (0.1 % HCOOH) as solvent. Spectra were recorded for 1 min after injection. The following settings were found to be best for the detection of the MurA-F substrates and products:

scan type	MS2Scan
gas temperature	250 °C
gasflow	10 l/min
nebulizer	30 psi
sheath gas temperature	40 °C
sheath gas flow	11 l/min
capillary	3500 V
nozzle voltage	2000 V
start mass	500
end mass	1500
scan time	500 ms
fragmentor	120 V
ionization	negative

3.3.8 High resolving ESI-MS

High resolution mass spectra were recorded on an Orbitrap XL mass spectrometer or an Exactive Orbitrap mass spectrometer. Analysis were performed on an Eclipse XDB C-18 column (5 µm, 4.6 x 150 mm, Agilent) with a flow of 0.2 mL/min. Enzymes were pelleted prior to the mass spectrometric analysis and the reaction mix was diluted by addition of 10 volumes of ice-cold MeOH and centrifugation for 15 min at 15 000 g. The injection volume was 10 µL and the gradient was 5 % MeOH to 95 % MeOH in 25 min and then isocratic at 95 % MeOH for further 13 min. All samples were run in negative ion mode with a resolution of R = 100,000.

3.3.9 LC-MS detection of feglymycin with the TripleQuad LC-MS

LC-MS measurements were recorded on a TripleQuad LC/MS 6460 mass spectrometer coupled to an Agilent 1290 Infinity HPLC system. Enzymes were pelleted prior to the mass spectrometric analysis and the reaction mix was diluted by addition of 5 volumes of ice-cold MeOH and centrifugation for 15 min at 15 000 g. To

detect full mass scans the setting MS2Scan was chosen. The detection was optimized with the synthetic feglymycin (50 µM). Especially the Capillary and Nozzle Voltage as well as the Fragmentor tension had a strong influence on the yield of feglymycin detection. The following settings were found to be best for feglymycin detection:

scan type	MS2Scan
gas temperature	250 °C
gas flow	10 l/min
nebulizer	30 psi
sheath has temperature	40 °C
sheath gas flow	11 l/min
capillary	3000 V
nozzle voltage	2000 V
start mass	500
end mass	2200
scan time	500 s
fragmentor	180 V
ionization	negative

Analysis were performed on an Eclipse Plus C18 column (RRHD = 1.8 µM, 2.1 mm x 50 mm, Agilent) heated to 35 °C with a flow of 0.3 mL/min. The following gradient was used:

time (min)	% A (H_2O + 0.1 % HCOOH)	% B (ACN + 0.1 % HCOOH)
0	95	5
6	50	50
6.5	0	100
8	0	100
8.5	95	5
10	95	5

Feglymycin was detected at a retention time of R_t = 3.6 min. All measurements were repeated at least three times and performed with two different samples. Synthetic feglymycin (50 µM) was used as a reference.

3.3.10 MSMS measurement of feglymycin with the TripleQuad LC-MS

MSMS measurements were performed with the TripleQuad LC/MS 6460 coupled to an Agilent 1290 Infinity HPLC system. The two-fold negatively charge mass of feglymycin ($[M-2H]^{2-}$ = 948.8) was set as precursor ion. The settings were identical as for the full mass scan except for the following changes:

scan type	product ion scan
precursor ion	948.8 Da
start mass	100 Da
end mass	1200 Da
collision energy	35 V

Samples were measured with a gradient from 5 to 100 % ACN (0.1 % HCOOH) in water (0.1 % HCOOH) in 6.5 min (see LC-MS detection of feglymycin with the TripleQuad LC-MS).

3.3.11 SIM-MS measurements of feglymycin with the TripleQuad LC-MS

SIM (single ion monitoring)-measurements were performed with the two-fold negatively charged feglymycin ion ($[M-2H]^{2-}$ = 948.8) as detection mass. The SIM setting was found to provide the highest sensitivity for feglymycin detection. The settings were identical as for the full mass scan except for the following changes:

scan type	SIM
detection mass	948.8 Da

Samples were measured with a gradient from 5 to 100 % ACN (+ 0.1 % HCOOH) in water (+0.1 % HCOOH) in 6.5 min (see LC-MS detection of feglymycin with the TripleQuad LC-MS).

3.3.12 SRM MS measurements of feglymycin with the TripleQuad LC-MS

SRM measurements were performed with the two-fold negatively charged Feglymycin ion ($[M-2H]^{2-}$ = 948.8) and a collision energy of 35 V. The feglymycin product ion mass 287 Da was used for detection. A calibration curve was created by first measuring six different concentrations of synthetic feglymycin between 0-50 µM. The settings were identical as for the full mass scan except for the following changes:

scan type	MRM
precursor ion	948.8 Da
product ion	287 Da
dwell	500 ms
collision energy	35 V

Samples were measured with a gradient from 5 to 100 % ACN (+ 0.1 % HCOOH) in water (+0.1 % HCOOH) in 6.5 min (see LC-MS detection of feglymycin with the TripleQuad LC-MS).

3.3.13 CD spectroscopy

Optically active molecules absorb left- and right-handed circularly polarized light differently. This characteristic depends on the wavelength of the light. The difference in absorption of left- and right-handed circularly polarized light leads to the occurrence of elliptically polarized light. Amino acids, except for glycine, are optically active molecules. A protein therefore contains many optically active atoms which

contribute to its CD spectrum. The optical identity of a single amino acid however cannot be determined from a protein CD spectrum; however the CD spectrum of a protein can help to predict the secondary structure of a protein. This is due to the fact that the secondary structure elements α-helix, β-sheet and random coil all exhibit different and characteristic CD spectra. By comparison of CD spectrum of a protein with a set of CD spectra of proteins with known structures, the secondary structure of an unknown protein can be predicted.

CD spectra were recorded with a JASCO J715 CD-spectrometer from a wavelength of 190 nm - 300 nm in 0.5 nm steps with a quartz cuvette (1 mm layer, Hellma) at room temperature at a bandwidth of 1 nm. Each spectrum was generated from at least three individual wavelength scans. The molar ellipticity [θ] was calculated from the detected ellipticity θ [mdeg] with the following fomulare.

$$[\Theta] = \frac{\theta}{10 \times c \times l}$$

with l = layer thickness of the cuvette in [cm] and c = concentration in [mol/l].

To exchange the Tris-containing dialysis and storage buffer of the Mur enzymes to a 10 mM phosphate buffer pH 8.0 more suitable for CD spectrometry, a gel filtration was performed. The protein solutions were loaded on a Superdex 75 prep grade Gefi column using an Äkta LC system with on-line UV-detection. Before loading the protein fraction, the column was washed with 3 column volumes of water and equilibrated with 3 column volumes of phosphate buffer. The Mur enzymes eluted after ~ 0.4 column volumes. CD measurements were performed with 16 µM MurA of *E. coli* and 17.5 µM MurC of *E. coli*. Additionally to the pure enzymes the enzymes were measured together with an equimolar, a two-fold and a four-fold molar concentration of feglymycin. As reference the phosphate buffer without enzyme and the highest employed feglymycin concentration in phosphate buffer were measured. CD spectra of the proteins were also recorded in phosphate buffer with 20 % trifluoroethanol (TFE). Trifluoroethanol has a general supportive effect on the formation of helices in proteins and peptides (Myers et al. 1998).

4 Results

4.1 Cloning of the *murA-F* genes of *E. coli* and the *murC* and *murD* gene of *S. aureus* into *E. coli* protein expression vectors

To find the optimal PCR conditions for the different genes, test-PCRs were performed with the *Taq* DNA polymerase. In case of the *E. coli* genes liquid cultures of the wild type strain *E. coli* K12 were used as DNA template for the PCRs. The optimal annealing temperature for the different primer (see Table 2.2 list of used primers) was tested over a temperature gradient from 50° C – 56 °.C. The results of the PCR amplification were tested with agarose gel electrophoresis (**Figure** 4.1; Figure 4.2).

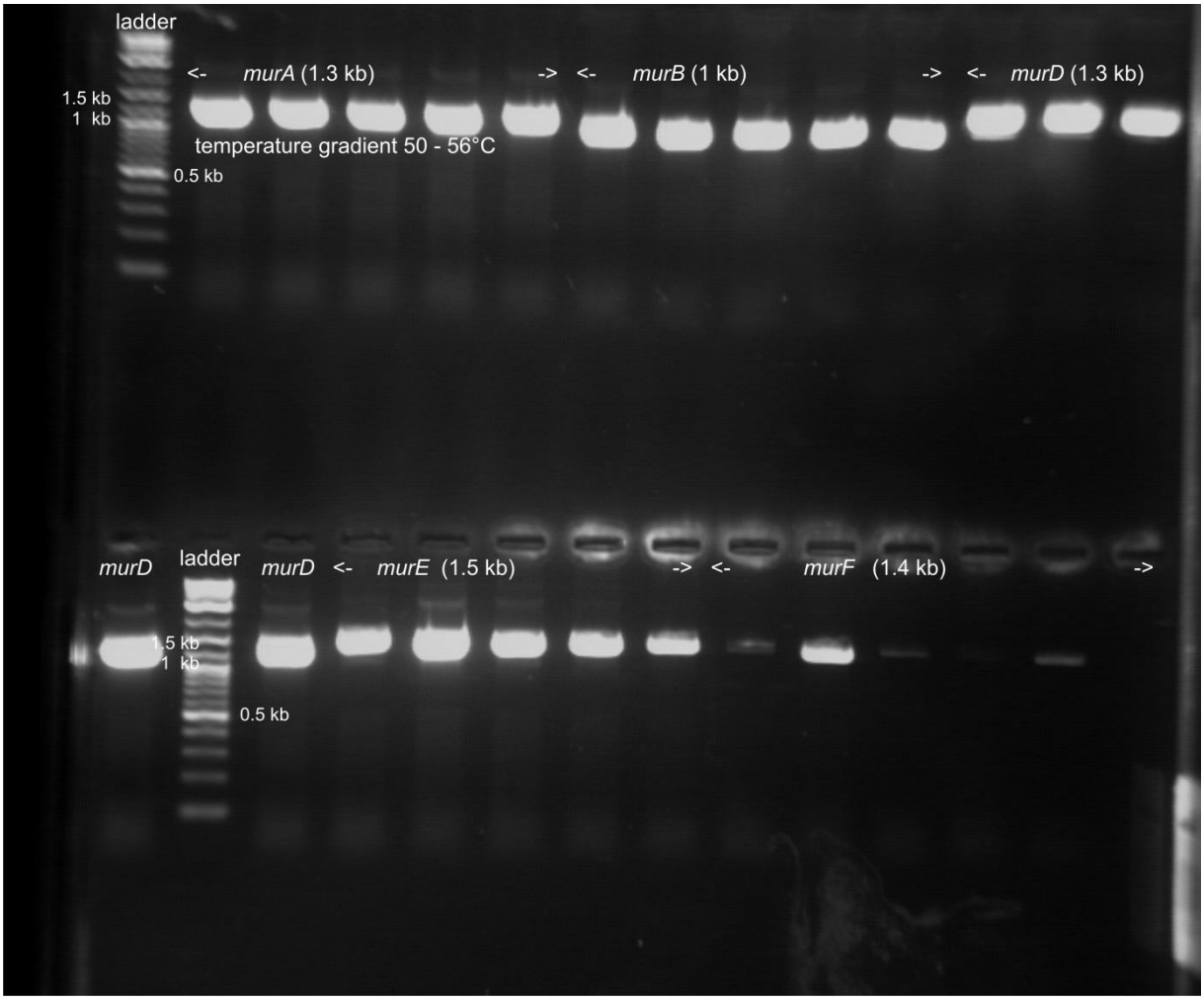

Figure 4.1: Test-PCRs with *Taq* DNA polymerase. Liquid cultures of *E. coli* K12 were used as templates for the genes *murA*, *murB*, *murD*, *murE* and *murF* from *E. coli*. The optimal annealing temperature was tested over a gradient from 50°C to 56°C in 0.5 °C steps.

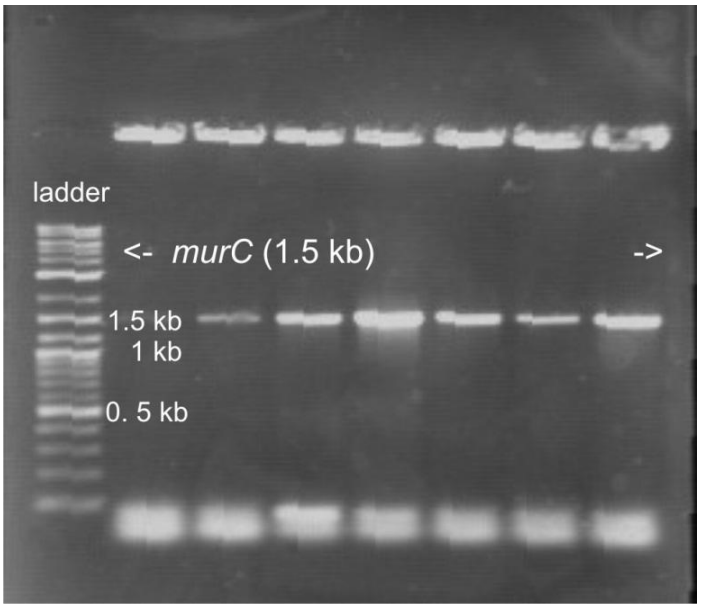

Figure 4.2: Test-PCRs with *Taq* DNA polymerase. Liquid cultures of *E. coli* K12 were used as templates for the *murC* gene from *E. coli*. The optimal annealing temperature was tested over a gradient from 50°C to 56°C in 0.5 °C steps**.**

In case of the *murC* and *murD* gene of *S. aureus*, *S. aureus* genomic DNA provided by Heiko Schadt (a former PhD student in the group of Prof. Roderich Süssmuth) was used as DNA template for the PCRs (see Table 2.2 list of used primers). The results of the PCR amplification were tested with agarose gel electrophoresis (Figure 4.3).

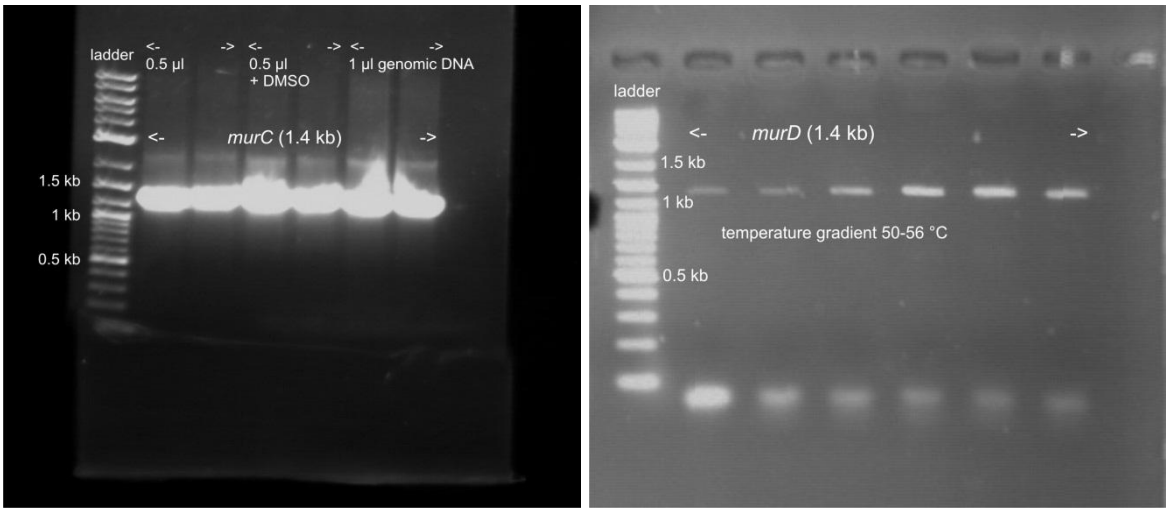

Figure 4.3: Test-PCRs with *Taq* DNA polymerase. *S.aureus* genomic DNA was used as a template for the genes *murC* (left picture) and *murD* (right picture) from *S. aureus*. For *murC*, different template concentrations (0.5-1 µl) and addition of DMSO to the PCR mix was tested at an annealing temperature of 54 °C. For *murD*, the optimal annealing temperature was tested over a gradient from 50°C to 56°C in 0.5 °C steps.

For the cloning step, the genes *murA*, *murB*, *murC*, *murD*, *murE* and *murF* from *E. coli* and *murC* and *murD* from *S. aureus* were amplified by PCR with a Herculase II fusion DNA polymerase using the optimized PCR conditions shown above (primers see Table 2.2 list of used primers). The success of the PCRs was checked by agarose gel electrophoresis and the PCR products were purified with a Quiagen PCR purification kit. The isolated DNA was quantified photometrically. The isolated PCR fragments were directly cloned into the pDrive vector using the PCR cloning kit and transformed into competent *E. coli DH5α* cells. The intermediate vectors were isolated with a GeneJET Plasmid Miniprep Kit. Successful cloning and transformation was confirmed for all genes by PCR and restriction analysis. The genes *murA* and *murE* from *E. coli* were cloned into the pEt24a(+) protein expression vector. The genes *murC* from *S. aureus*, *murD* from *E. coli*, *murD* from *S. aureus* and *murF* from *E. coli* were cloned into the pEt28a(+) protein expression vector. *MurB* from *E. coli* and *murC* from *E. coli* were cloned both in the pEt24a(+) and the pEt28a(+) protein expression vector. The expression vectors containing no insert and the intermediate vectors were digested with the appropriate restriction enzymes and inserts and plasmids were separated by agarose gel electrophoresis.The linearized expression vectors and the genes were isolated from the gel using a GeneJET Gel Extraction Kit, ligated with T4 DNA ligase and transformed into competent *E. coli DH5α* cells. The expression vectors were isolated with a GeneJET Plasmid Miniprep Kit. Successful cloning and transformation was confirmed for all genes by PCR and restriction analysis. The correctness of the inserted genes was additionally verified by sequencing by LCG genomics (Berlin). The correct expression vectors were than transformed into *E. coli* BL21 cells. Sucessful transformation was confimed for all genes by PCR.

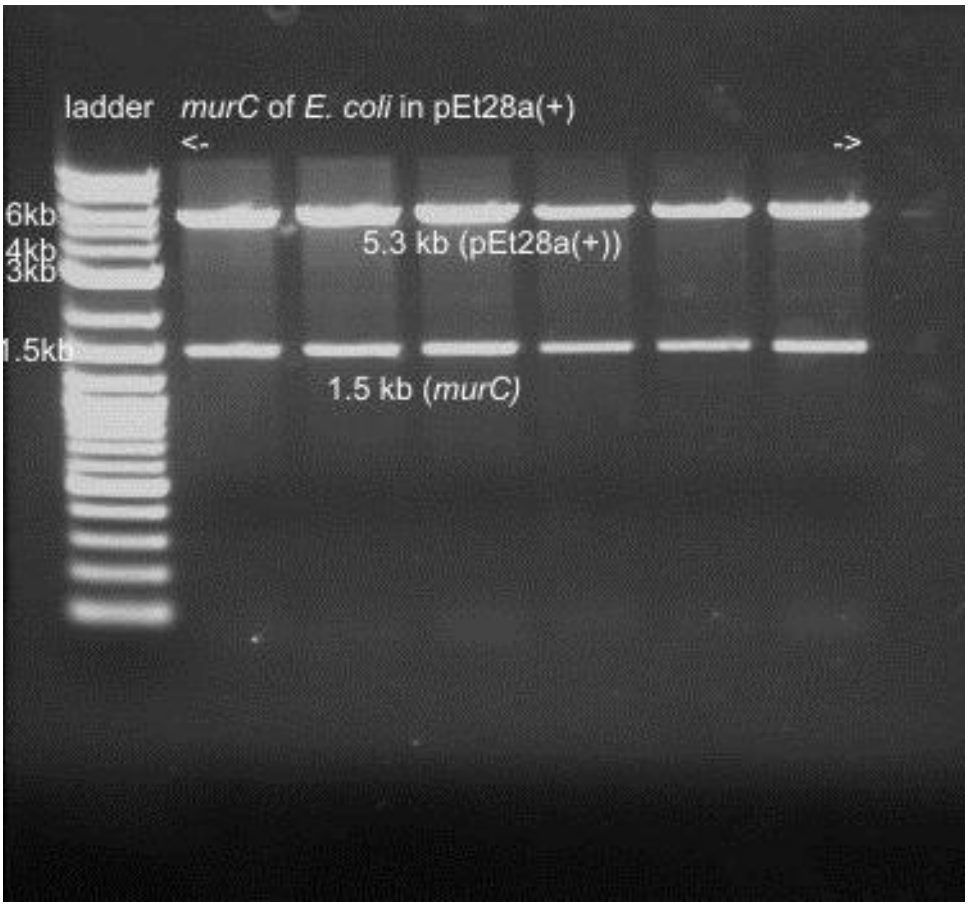

Figure 4.4: Restriction analysis of pEt28a(+) vectors containing the *murC* gene from *E. coli*. Both fragments (insert and linearized vector without insert) have the expected size.

The genes *murA* and *murB* from *S. aureus* already cloned in the appropriate *E. coli* protein expression vector pEt15b were a friendly gift by the group of Prof. H. G. Sahl (Bonn university).

4.2 Isolation of the heterologously and homologously expressed Mur enzymes

4.2.1 Protein test expression

The overexpression of the Mur enzymes was tested by small scale protein expression at different temperatures and with different IPTG concentrations. Proteins were isolated by small scale protein preparation from both the pellet and the supernatant fraction and analyzed by SDS-PAGE. All Mur enzymes were all found to be expressed at least partially soluble and in high concentration at 37 °C and after induction with an IPTG concentration of 250-500 µM.

4.2.2 Large scale expression and isolation

Large scale protein expression of the Mur enzymes was performed in LB medium at 37° C. 0.5-1 L bacteria culture were grown to an OD_{600} of 0.6-0.8 and protein expression was induced by addition of 250-500 µM IPTG. Cells were grown first for 3-4 h at 37° C (MurA, MurC, MurD) or directly transferred to 17° C (MurB, MurE, MurF) and incubated for further 24 h at 17 °C. Large scale protein preparation was performed with an optimized lysis buffer. For MurA, MurC and MurD from *E. coli* and MurA and MurD from *S. aureus* a simple lysis buffer was used. For MurB, MurE and MurF from *E. coli* and MurC from *S. aureus* a lysis buffer with a lower imidazole concentration containing additionally Triton X-100 and glycerin was employed. For MurB from *S. aureus* a similar lysis buffer with lower salt concentration was used. Proteins were purified by affinity chromatography with His Trap 5 mL columns (GE, Munich) using an ÄKTApurifier UPC 10 system (GE, Munich). High imidazole concentrations were removed by dialysis (see 3.2.5 large scale protein preparation, 3.2.6 protein purification, 3.2.7 protein dialysis).

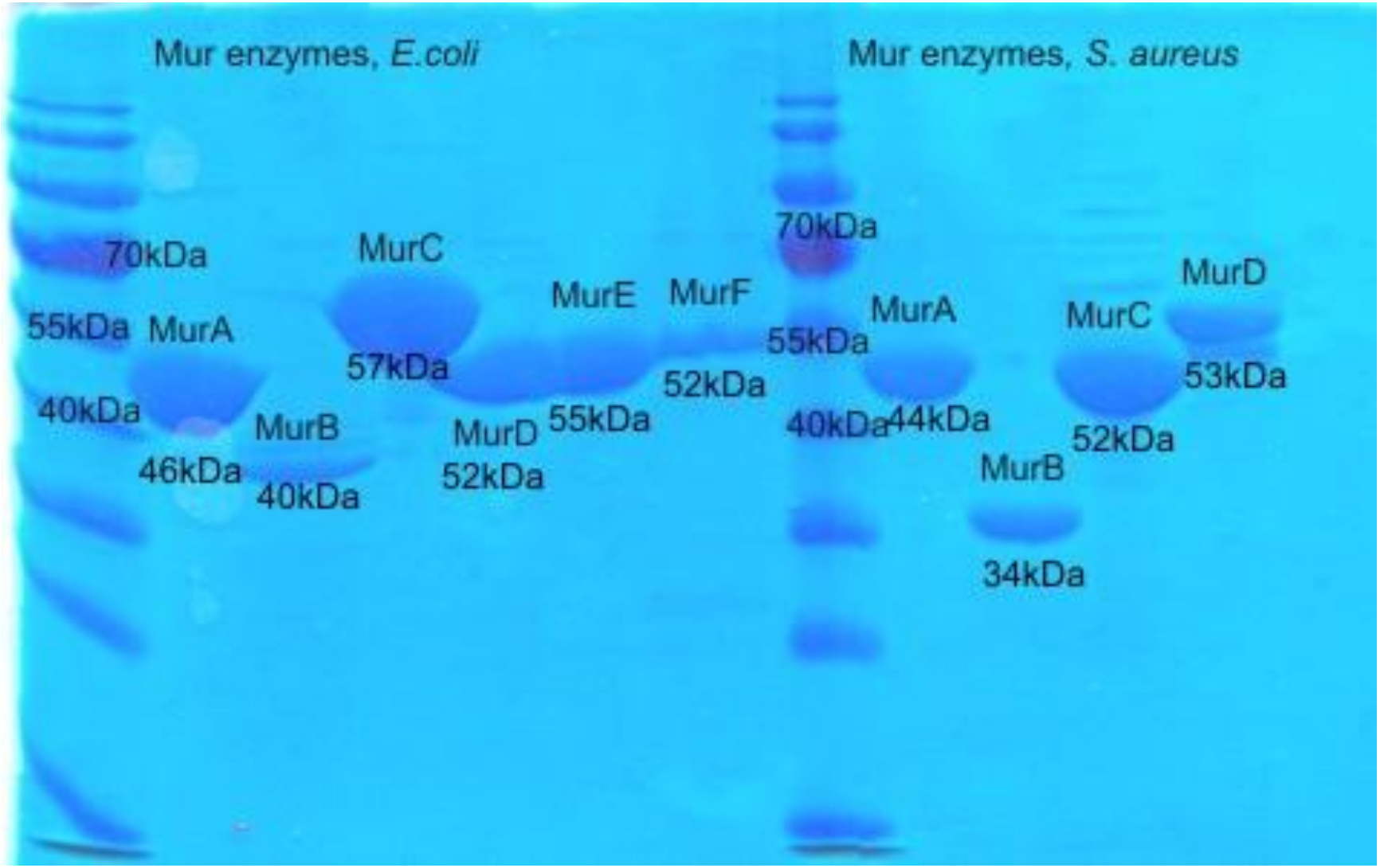

Figure 4.5: SDS-PAGE of the isolated enzymes MurA-F from *E. coli* and MurA-D from *S. aureus*.

MurA

The MurA enzymes both from *E. coli* and *S. aureus* showed a good solubility. From 1 L bacterial culture 16 mg of the *E. coli* enzyme (Figure 4.6) and 25 mg of the *S. aureus* enzyme were isolated. Interestingly the addition of low concentration of Triton X-100 to the lysis buffer and the addition of high salt concentrations (20 mM NH_4SO_4, 20 mM $MgCl_2$ and 200 mM NaCl) to the dialysis buffer led to a nearly total loss of activity of the *S. aureus* enzyme.

MurB

The MurB enzymes both from *E. coli* and *S. aureus* showed a very low solubility. From 1 L bacterial culture only 0.3 mg of the *E. coli* enzyme could be isolated with only poor purity when using the standard lysis buffer (Figure 4.7). The usage of an optimized lysis buffer with a lower imidazole (10 mM instead of 20 mM) concentration and an additional Triton X-100 concentration of 1 % and a decrease of flow rate of the Äkta LC system from 1 mL/min to 0.5 mL/min however helped to increase the protein yields to about 5 mg/L (Figure 4.8). The S*. aureus* enzyme was isolated with the same optimized buffer as the *E. coli* enzyme with yields of 19 mg/L.

MurC

The MurC enzyme from *E. coli* was isolated both as a construct with a C-terminal His-Tag (expressed in protein expression vector pEt24a(+)) and as a construct with both C- and N-terminal His-Tag (expressed in protein expression vector pEt28a(+)). The MurC construct with only C-terminal His-Tag showed only a very low binding affinity to the Ni^{2+} sepharose column and therefore could not be isolated. The MurC construct with both C- and N-terminal His-Tag in contrast was isolated in the very high concentration of more than 90 mg/L bacterial culture and good purity (Figure 4.9). Hence, the *S. aureus* enzyme was also expressed in the pEt28a(+) vector and likewise isolated in very high concentration and purity (38 mg/L).

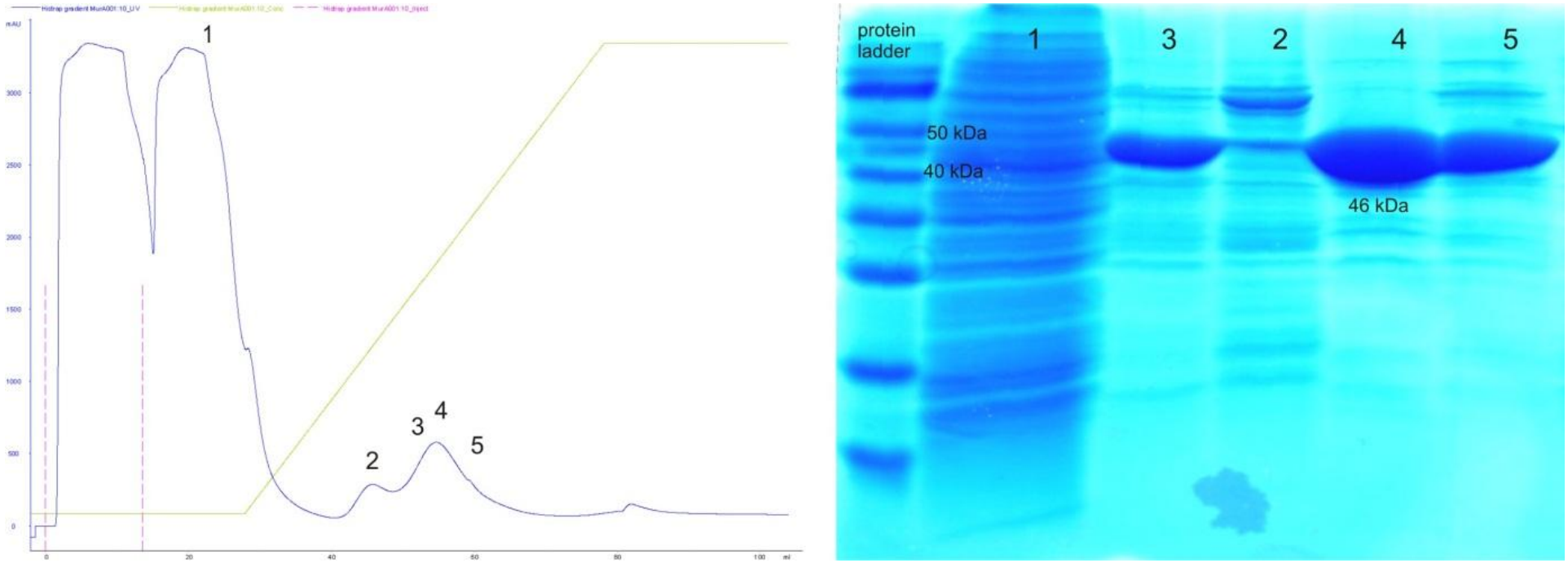

Figure 4.6: Isolation of the MurA enzyme from *E. coli* by affinity chromatography (His-Trap column). Left picture: affinity chromatography run detected at λ = 280 nm. Right picture: SDS-PAGE of different fractions of the affinity chromatography run. Fraction 1 contains the unbound proteins. Fraction 4 contains a high concentration of very pure MurA enzyme.

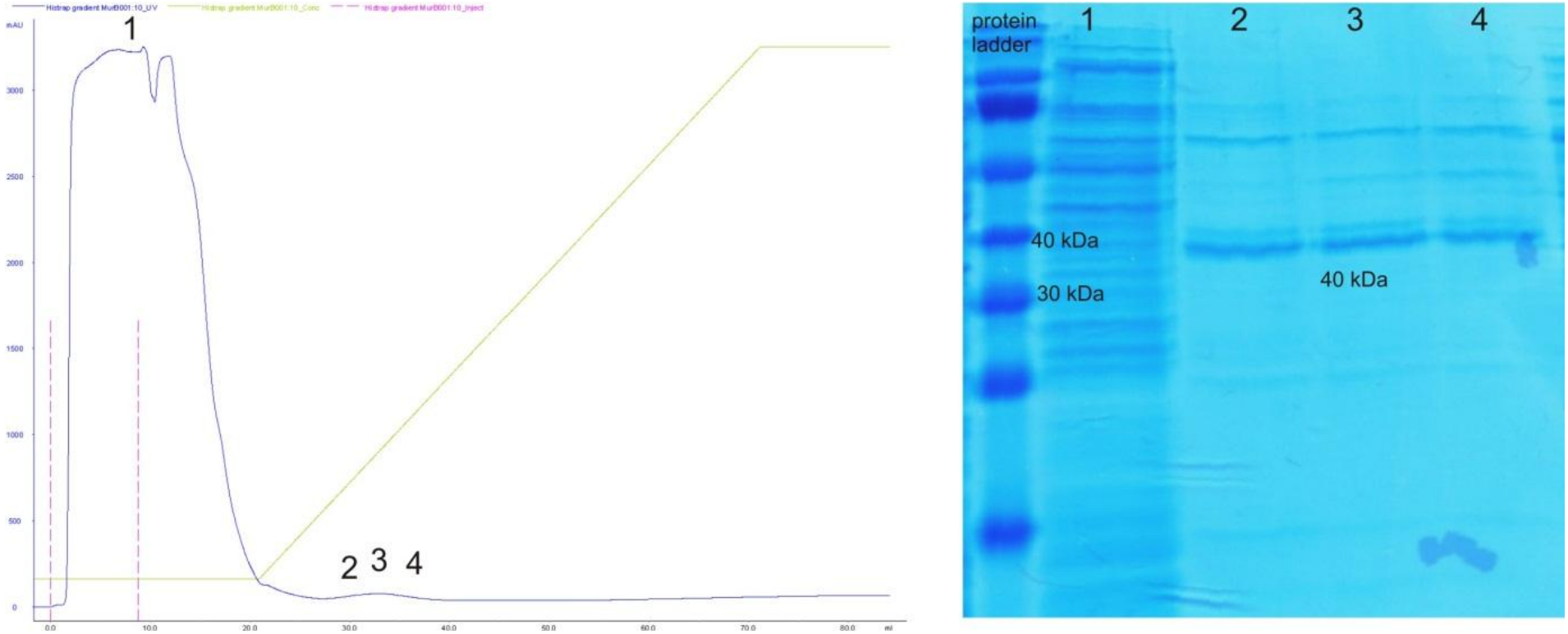

Figure 4.7: Isolation of the MurB enzyme from *E. coli* by affinity chromatography (His-Trap column) with standard lysis buffer (20 mM Tris/HCl pH 8.0, 500 mM NaCl, 10 mM MgCl2, 20 mM imidazole and 1 mM PMSF freshly added). Left picture: affinity chromatography run detected at λ = 280 nm. Right picture: SDS-PAGE of different fractions of the affinity chromatography run. Fraction 1 contains the unbound proteins. Fractions 2-4 contain low concentration of impure MurB enzyme.

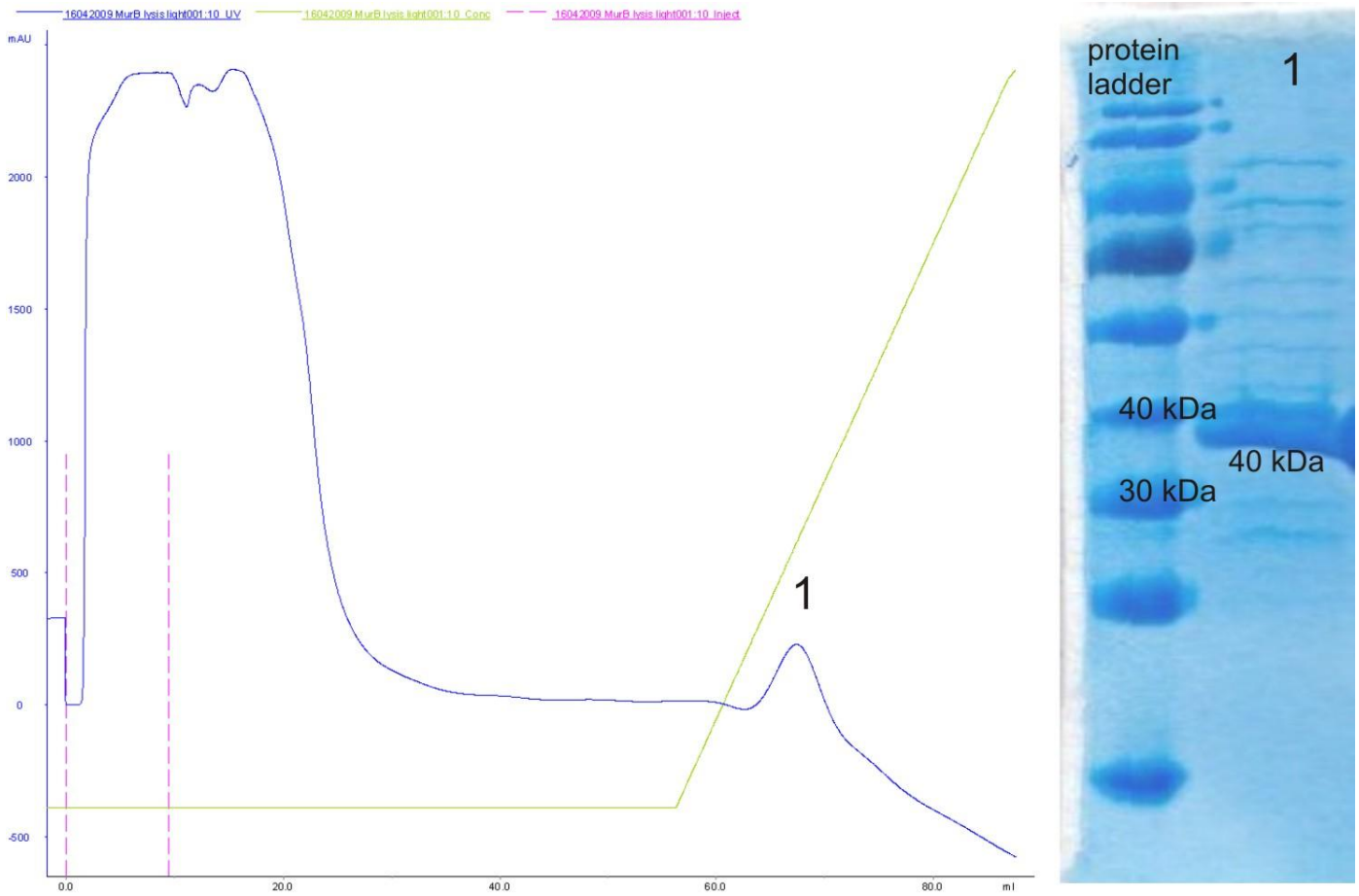

Figure 4.8: Isolation of the MurB enzyme from *E. coli* by affinity chromatography (His-Trap column) with an optimized lysis buffer (20 mM Tris/HCl pH 8.0, 500 mM NaCl, 10 mM MgCl2, 20 mM imidazole and 1 mM PMSF freshly added) and under optimized isolation conditions. Left picture: affinity chromatography run detected at λ = 280 nm. The absorption of Triton X-100 leads to a higher base line. Right picture: SDS-PAGE of a MurB protein fraction isolated by affinity chromatography.

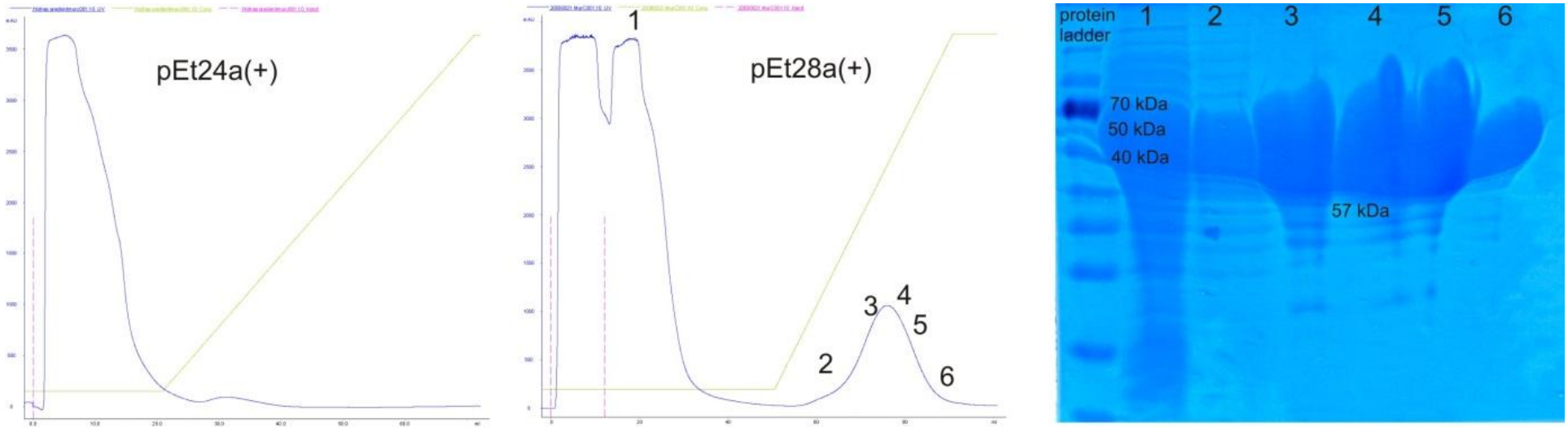

Figure 4.9: Isolation of the MurC enzyme from *E. coli* by affinity chromatography (His-Trap column). Left picture: affinity chromatography run detected at λ = 280 nm of the isolation of the pEt24a(+) construct (N-terminal His-Tag). Central picture: affinity chromatography run detected at λ = 280 nm of the isolation of the pEt28a(+) construct (C- and N-terminal His-Tag). Right picture: SDS-PAGE of different fractions of the affinity chromatography run of the pEt28a(+) construct. Fraction 1 contains the unbound proteins.Fraction 3-6 contained very high concentration of pure MurC enzyme.

MurD

The MurD enzymes both from *E. coli* and *S. aureus* showed a good solubility. 1 L bacterial culture yielded 28 mg of the *E. coli* enzyme (Figure 4.10) and 24 mg of the *S. aureus* enzyme.

MurE

The MurE enzyme from *E. coli* showed low solubility. Using an optimized lysis buffer with a lower imidazole concentration (10 mM instead of 20 mM) and an additional Triton X-100 of 1 % as used for the MurB enzyme however led to the isolation of concentrations as high as 18 mg/L bacteria culture of pure MurE enzyme (Figure 4.11).

MurF

The MurF enzyme from *E. coli* showed low solubility. Using an optimized lysis buffer with a lower imidazole concentration (10 mM instead of 20 mM) and an additional Triton X-100 of 1 % as used for the MurB enzyme however increased protein yield to 4.5 mg/ L bacteria culture of moderately pure MurF enzyme (Figure 4.11).

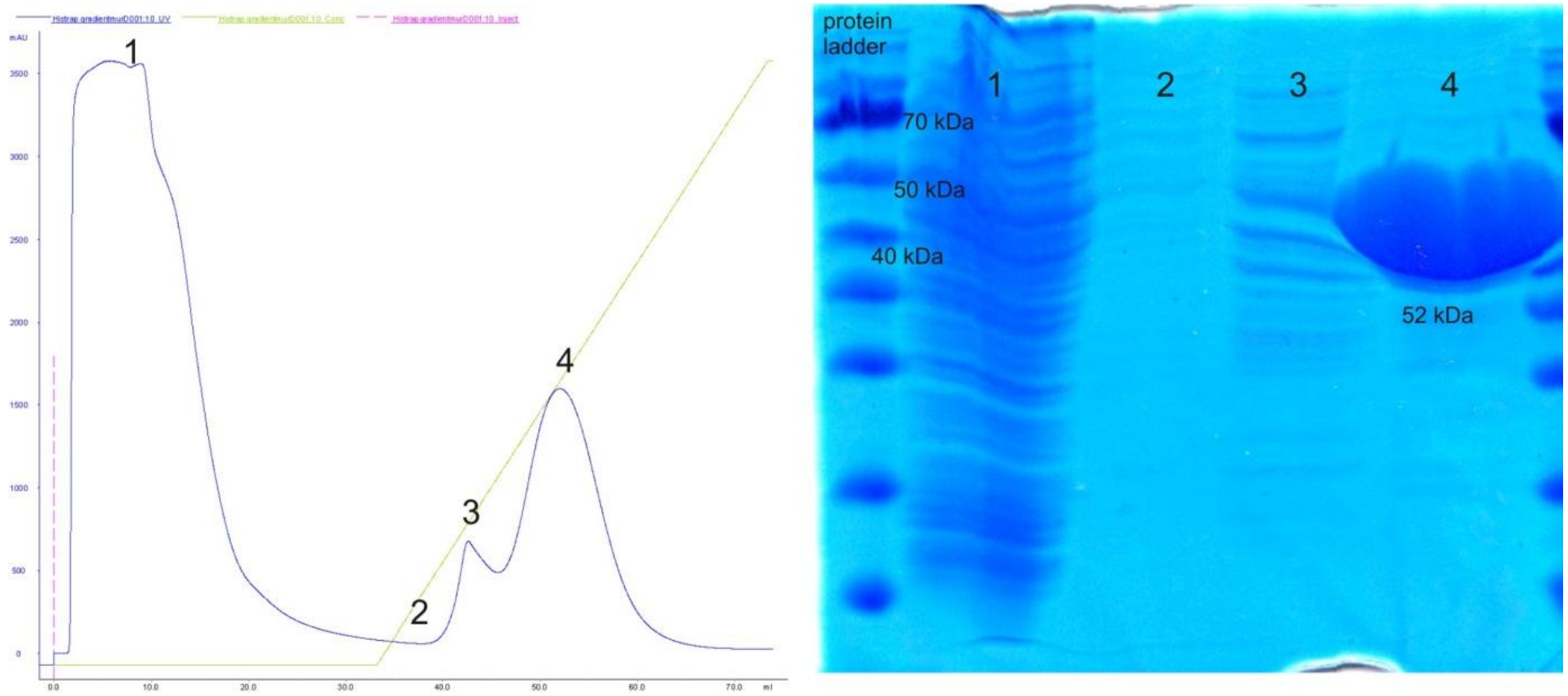

Figure 4.10: Isolation of the MurD enzyme from *E. coli* by affinity chromatography (His-Trap column). Left picture: affinity chromatography run detected at λ = 280 nm. Right picture: SDS-PAGE of different fractions of the affinity chromatography run. Fraction 1 contains the unbound proteins. Fraction 4 contains a very high concentration of very pure MurD enzyme.

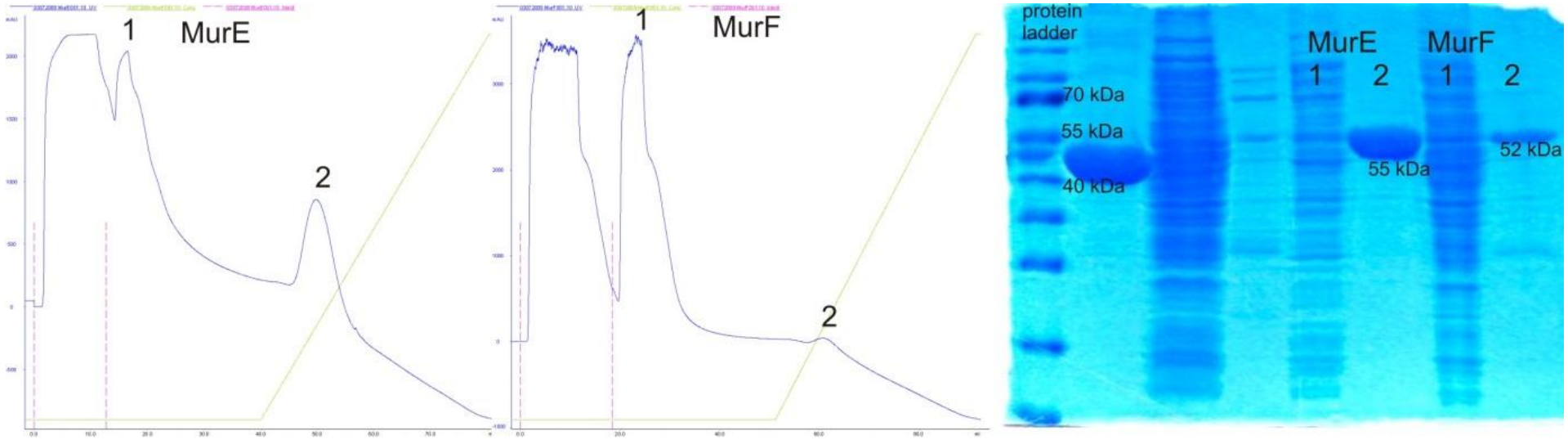

Figure 4.11: Isolation of the MurE and MurF enzymes from *E. coli* by affinity chromatography (His-Trap column)**.** Left picture: affinity chromatography run of the isolation of the MurE enzyme detected at λ = 280 nm. Central picture: affinity chromatography run of the isolation of the MurF enzyme detected at 280 nm. Right picture: SDS-PAGE of different fractions of the two affinity chromatography runs. Fractions 1 contains the unbound proteins. Fractions 2 contain the isolated proteins.

4.3 *In vitro* reconstitution assays of the MurA-MurF enzyme cascade

To investigate the inhibitory effect of feglymycin on the activity of the MurA-F enzymes from *E. coli* a one-pot assay was used. By using a one-pot assay, a fast screening of the Mur enzymes without the time-consuming isolation of the substrates for the enzymes MurB-MurF is facilitated. The stepwise and controlled stalling of the pathway allowed studying the effect of feglymycin to every single enzyme of the biosynthetic pathway. Enzymes in the pathway preceding the enzyme of interest were preincubated with substrate to allow the formation of a larger amount of product before the enzyme being studied and, optionally, the inhibitor were added. The enzyme and substrate concentrations were optimized to allow a near to complete conversion of substrates to products in the chosen time span, but not to high to be still able to observe also slight reductions of enzyme activity. The product of each enzyme reaction was detected by LC-ESI-TOF-MS (Figure 4.12) and high-resolving LC-ESI-Orbitrap-MS (Table 4.1). With LC-ESI-TOF-MS all masses were detected as single charged ions in negative ionization mode (Figure 4.12). With LC-ESI-Orbitrap-MS the larger enzyme products (UDP-MurNAc-L-Ala-D-Glc, UDP-MurNAc-L-Ala-D-Glc-*meso*-Dap and UDP-MurNAc-L-Ala-D-Glc-*meso*-Dap-L-Ala-L-Ala) were best detected as two-fold charged ions in negative ionization mode ($[M-2H]^{2-}$) while the small enzyme products were detected as singly charged ions ($[M-H]^{-}$). The theoretically calculated masses of the enzyme products correspond well to the masses detected with high resolution ESI-Oribitrap-MS (Table 4.1).

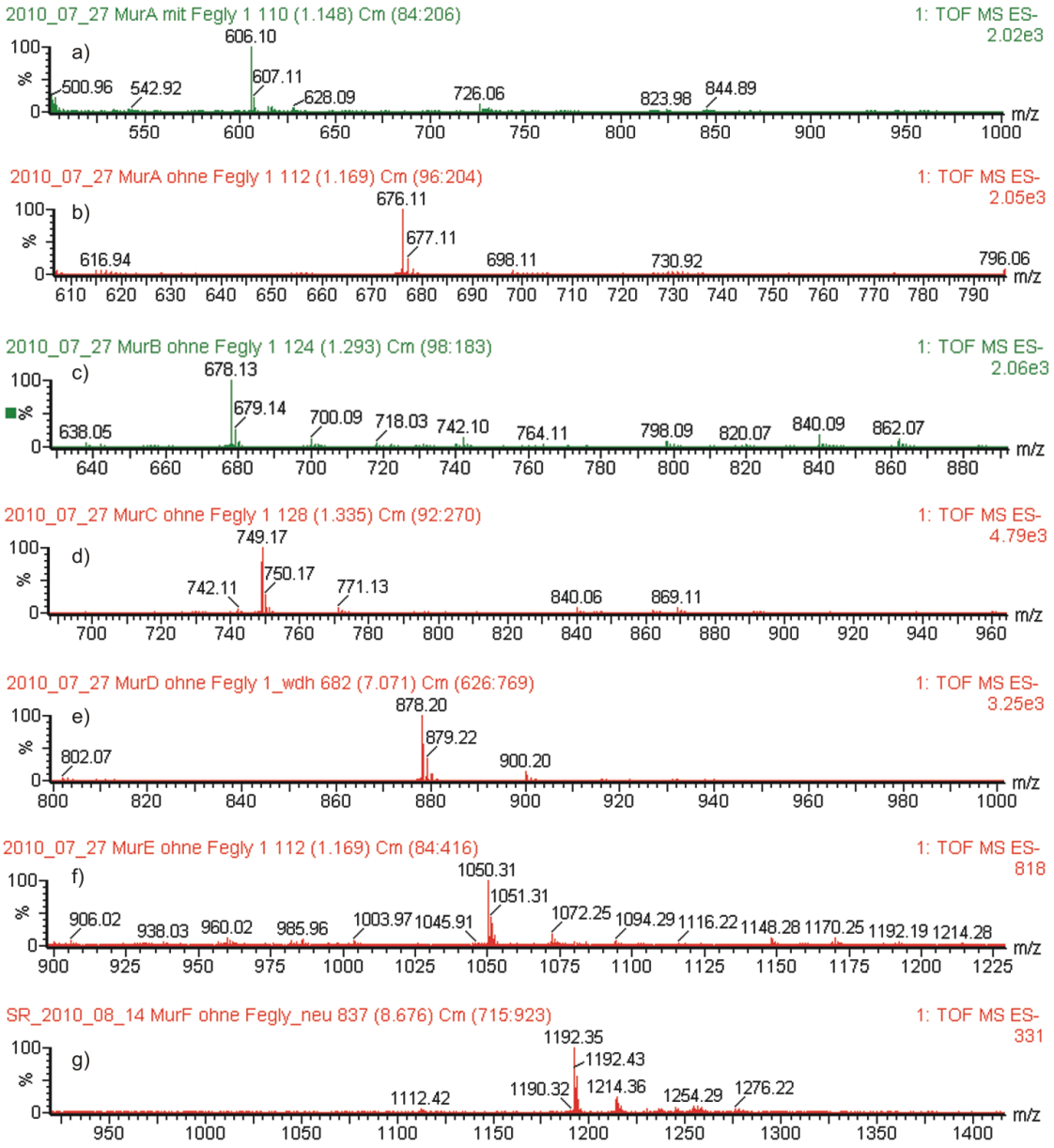

Figure 4.12: MS spectra of substrates and products of enzyme reactions MurA-F (*E. coli*) detected with the LC-ESI-TOF-MS in negative ionization mode. All masses were detected as $[M-H]^-$.

UDP-GlcNAc ($[M-H]^-$ = 606)

EP-UDP-GlcNAc ($[M-H]^-$ = 676)

UDP-MurNAc ($[M-H]^-$ = 678)

UDP-MurNAc-l-Ala ($[M-H]^-$ = 749)

UDP-MurNAc-l-Ala-d-Glc ($[M-H]^-$ = 878)

UDP-MurNAc-l-Ala-d-Glc-meso-Dap ($[M-H]^-$ = 1050)

UDP-MurNAc-L-Ala-d-Glc-meso-Dap-d-Ala-d-Ala ($[M-H]^-$ = 1192).

Table 4.1: Theoretical and found molecular masses detected with high-resolving LC-ESI-Orbitrap-MS.

	Theoretical mass	Mass detected
EP-UDP-GlcNAc ($C_{20}H_{29}O_{19}N_3P_2$)	$[M-H]^-$ = 676.0792	$[M-H]^-$ = 676.0787 (+ 0.01 mmu)
UDP-MurNAc ($C_{20}H_{31}O_{19}N_3P_2$)	$[M-H]^-$ = 678.0949	$[M-H]^-$ = 678.0944 (+ 0.03 mmu)
UDP-MurNAc-L-Ala ($C_{23}H_{36}O_{20}N_4P_2$)	$[M-H]^-$ = 749.1320	$[M-H]^-$ = 749.1318 (+ 0.39 mmu)
UDP-MurNAc-L-Ala-D-Glc ($C_{28}H_{43}O_{23}N_5P_2$)	$[M-2H]^{2-}$ = 438.5834	$[M-2H]^{2-}$ = 438.5830 (+0.12 mmu)
UDP-MurNAc-L-Ala-D-Glc-*meso*-Dap ($C_{35}H_{55}O_{26}N_7P_2$)	$[M-2H]^{2-}$ = 524.6258	$[M-2H]^{2-}$ = 524.6243 (- 0.96 mmu)
UDP-MurNAc-L-Ala-D-Glc-*meso*-Dap-D-Ala-D-Ala ($C_{41}H_{64}O_{28}N_9P_2$)	$[M-2H]^{2-}$ = 595.6629	$[M-2H]^{2-}$ = 595.6622 (- 0.18 mmu)

By performing the enzyme assays simultaneously in the presence and absence of the inhibitor feglymycin, the effect of feglymycin on every Mur enzyme was studied. All reactions were performed in triplicate. The enzyme reactions were stopped after a specific time and the samples were measured by LC-ESI-TOF-MS (Table 4.2). The experiment was also repeated and measured with LC-Triple-Quad-MS. The extracted substrate and product ion masses detected with LC-ESI-TOF-MS were quantified by their peak areas [cts]. Repeated LC-ESI-TOF-MS experiments with defined substrate and enzyme concentrations gave highly reproducible peak areas [cts]. The performed quantification from the peak area is only a relative and no absolute quantification. An absolute quantification would require calibration curves performed with defined concentrations of each reaction product as detected counts [cts] might vary between the different products due to differences in ionization yield. The detected peak areas [cts] are however good indicators for the relative amount and thus formation of the products of the enzyme reactions. The LC-ESI-TOF-MS data were chosen for the quantification because the variation of counts [cts] between the different reaction products and also between the different experiments was found to be lower than in case of the LC-Triple-Quad-MS data.

Table 4.2: Substrate and product formation by the enzymes MurA-F (*E. coli*) in the presence and absence of 50 µM feglymycin detected by LC-ESI-TOF-MS in negative ionization mode.

MurA	substrate mass $[M-H]^-$ = 606 peak area [cts]	product mass $[M-H]^-$ = 676 peak area [cts]
control (no feglymycin)	141.6 +/- 27.1*	622.7 +/- 100.7*
with 50 µM feglymycin	518.7 +/- 7.7*	17.7 +/- 1.5*
MurB	substrate mass $[M-H]^-$ = 676 peak area [cts]	product mass $[M-H]^-$ = 678 peak area [cts]
control (no feglymycin)	77.3 +/- 12.9	634.0 +/- 143.9
with 50 µM feglymycin	76. 7 +/- 17.2	600.3 +/- 145.2
MurC	substrate mass $[M-H]^-$ = 678 peak area [cts]	product mass $[M-H]^-$ = 749 peak area [cts]
control (no feglymycin)	23.7 +/- 2.3*	639.0 +/- 71.3*
with 50 µM feglymycin	693.3 +/- 212.4*	17.3 +/- 3.8*
MurD	substrate mass $[M-H]^-$ = 749 peak area [cts]	product mass $[M-H]^-$ = 878 peak area [cts]
control (no feglymycin)	3.0 +/- 1.0	1088.0 +/- 192.8
with 50 µM feglymycin	14.0 +/- 2.6	1241.3 +/- 349.2
MurE	substrate mass $[M-H]^-$ = 878 peak area [cts]	product mass $[M-H]^-$ = 1050 peak area [cts]
control (no feglymycin)	25.3 +/- 17.6	470.3 +/- 87.0
with 50 µM feglymycin	14.3 +/- 5.9	472.7 +/- 72.5
MurF	substrate mass $[M-H]^-$ = 1050 peak area [cts]	product mass $[M-H]^-$ = 1192 peak area [cts]
control (no feglymycin)	239.7 +/- 52.3	406.3 +/- 187.3
with 50 µM feglymycin	99.0 +/- 74.5	603.3 +/- 100.2

[cts] = peak area measured in arbitrary units with extracted ion chromatogram (EIC)

For MurA and MurC a significant decrease in product formation was detected with LC-ESI-TOF-MS in the presence of 50 µM feglymycin, indicating that both enzymes MurA and MurC are likely targets of feglymycin. In case of the MurA enzyme only 2.8 % of the product EP-UDP-GlcNAc is formed in presence of the inhibitor feglymycin within 2 h reaction time compared to the sample without inhibitor (17.7 +/- 1.5 peak area [cts] compared to 622.7 +/- 100.7 peak area [cts], see Table 4.2). Also the [cts] of the MurA substrate UDP-GlcNAc is significantly higher in presence of the inhibitor than in the control sample indicating, that the enzyme reaction was nearly totally repressed. In case of the MurC enzyme a very similar effect is visible. Only 2.7 % of the product UDP-MurNAc-L-Ala is formed in presence of feglymycin compared to the control (Table 4.2). At the same time the substrate concentration in presence of feglymycin is still about 30-times higher than in the control, indicating that the MurC reaction was nearly fully inhibited by feglymycin under the chosen conditions. For the other Mur enzymes, no significant changes of the product and substrate amount were detected in presence of feglymycin compared to the samples without feglymycin added. Only in case of the MurF enzyme differences between the samples with feglymycin and the samples without feglymycin were observed (Table 4.2). The peak area of the product mass of the control is lower than the peak area of the sample with feglymycin added. Also the peak area of the substrate mass of the control is higher than that of the sample with feglymycin. In case of the product mass, however the difference is still within the standard deviation. In case of the substrate mass the difference is slightly higher than the standard deviation. As a promoting effect of the MurF enzyme reaction by feglymycin seems unlikely, the effect might be an outlier.

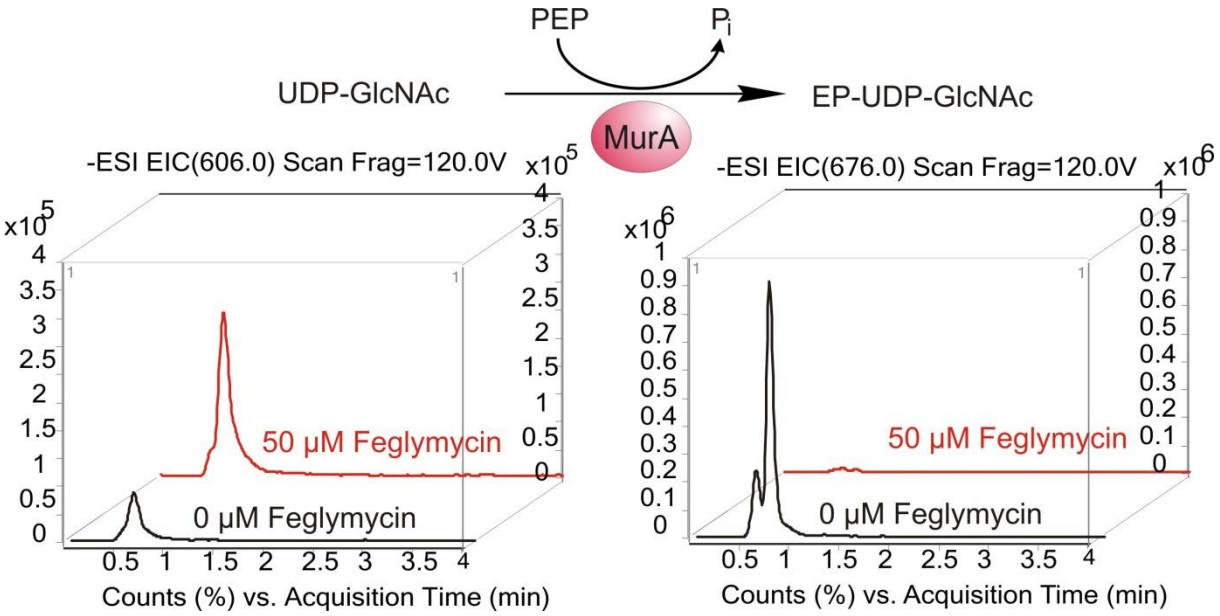

Figure 4.13: LC-MS chromatograms [EIC] of substrates and products of MurA *E. coli* enzyme reaction detected at the end point of the enzyme reaction with 0 µM feglymycin added (black) and with 50 µM feglymycin added (red) with the ESI-Triple-Quad-LC-MS in negative ionization mode. Left: EIC of UDP-GlcNAc ($[M-H]^-$ = 606) Right: EIC of EP-UDP-GlcNAc ($[M-H]^-$ = 676).

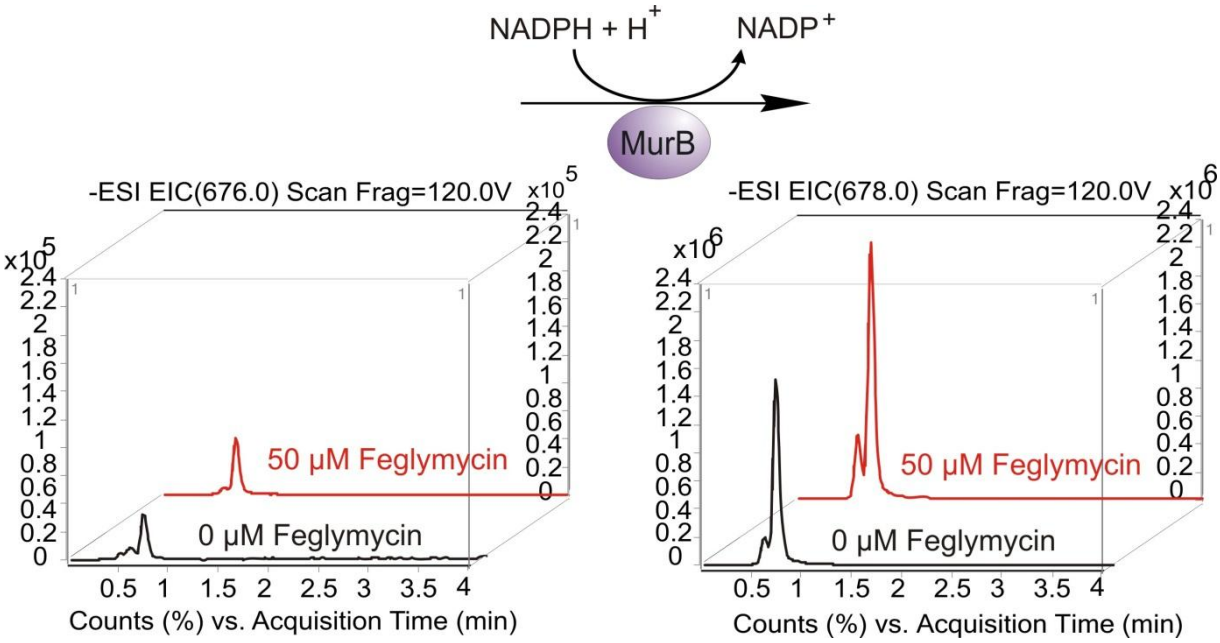

Figure 4.14: LC-MS chromatograms [EIC] of substrates and products of MurB *E. coli* enzyme reaction detected at the end point of the enzyme reaction with 0 µM feglymycin added (black) and with 50 µM feglymycin added (red) with the ESI-Triple-Quad-LC-MS in negative ionization mode. Left: EIC of EP-UDP-GlcNAc ($[M-H]^-$ = 676) Right: EIC of UDP-MurNAc ($[M-H]^-$ = 678).

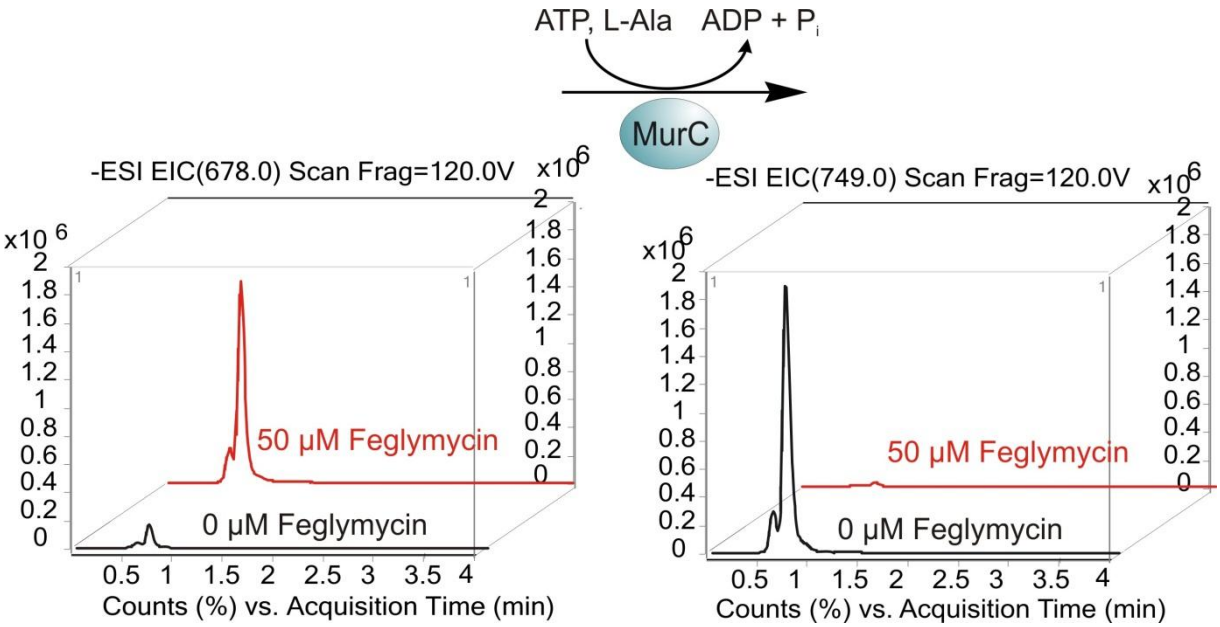

Figure 4.15: LC-MS chromatograms [EIC] of substrates and products of MurC *E. coli* enzyme reaction detected at the end point of the enzyme reaction with 0 µM feglymycin added (black) and with 50 µM feglymycin added (red) with the ESI-Triple-Quad-LC-MS in negative ionization mode. Left: EIC of UDP-MurNAc ([M-H]$^-$ = 678) Right: EIC of UDP-MurNAc-l-Ala ([M-H]$^-$ = 749).

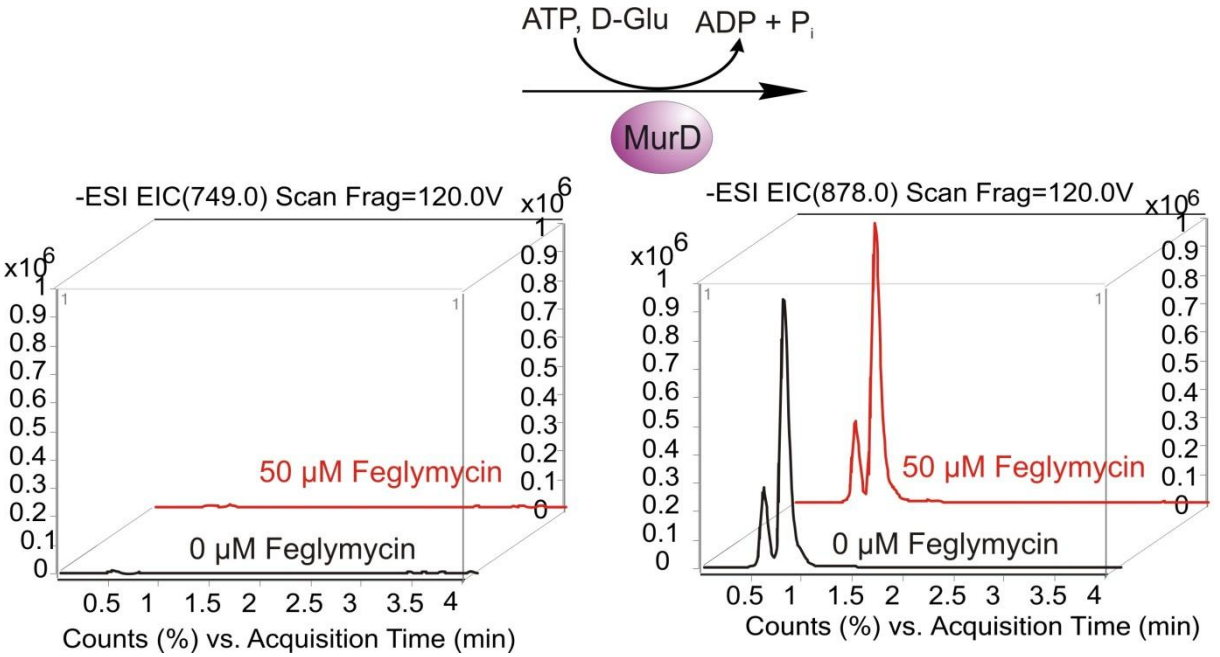

Figure 4.16: LC-MS chromatograms [EIC] of substrates and products of MurD *E. coli* enzyme reaction detected at the end point of the enzyme reaction with 0 µM Feglymycin added (black) and with 50 µM feglymycin added (red) with the ESI-Triple-Quad-LC-MS in negative ionization mode. Left: EIC of UDP-MurNAc-l-Ala ([M-H]$^-$ = 749) Right: EIC of UDP-MurNAc-l-Ala-d-Glu ([M-H]$^-$ = 878).

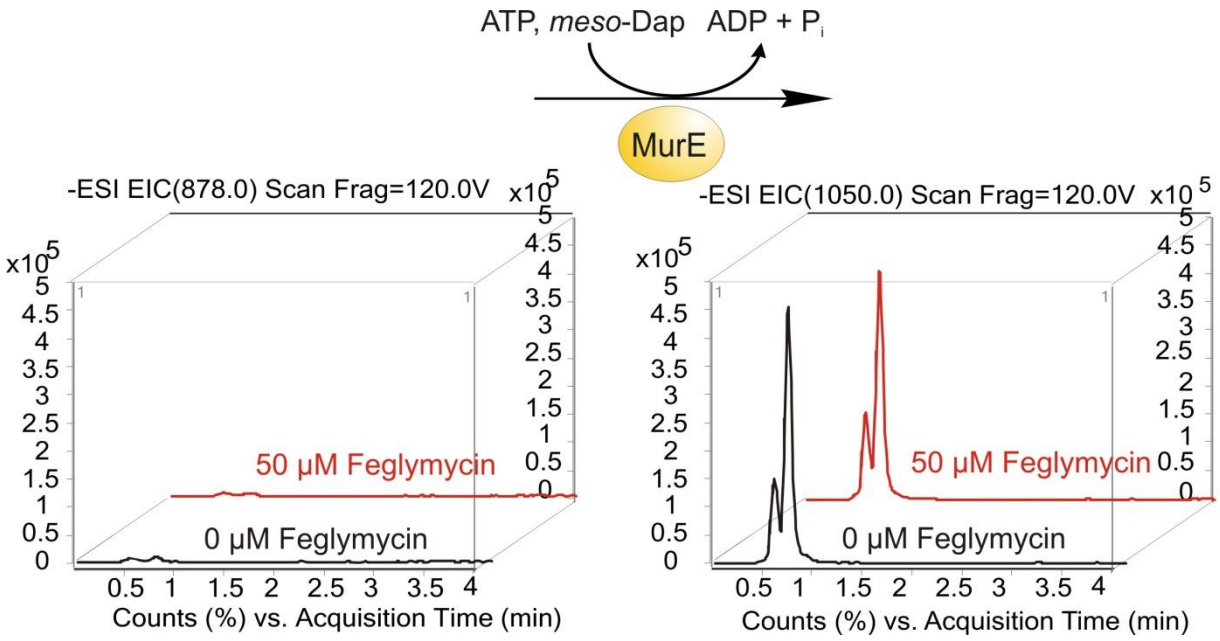

Figure 4.17: LC-MS chromatograms [EIC] of substrates and products of MurE *E. coli* enzyme reaction detected at the end point of the enzyme reaction with 0 µM feglymycin added (black) and with 50 µM feglymycin added (red) with the ESI-Triple-Quad-LC-MS in negative ionization mode. Left: EIC of UDP-MurNAc-l-Ala-d-Glu ($[M-H]^-$ = 878) Right: EIC of UDP-MurNAc-l-Ala-d-Glu-meso-Dap ($[M-H]^-$ = 1050).

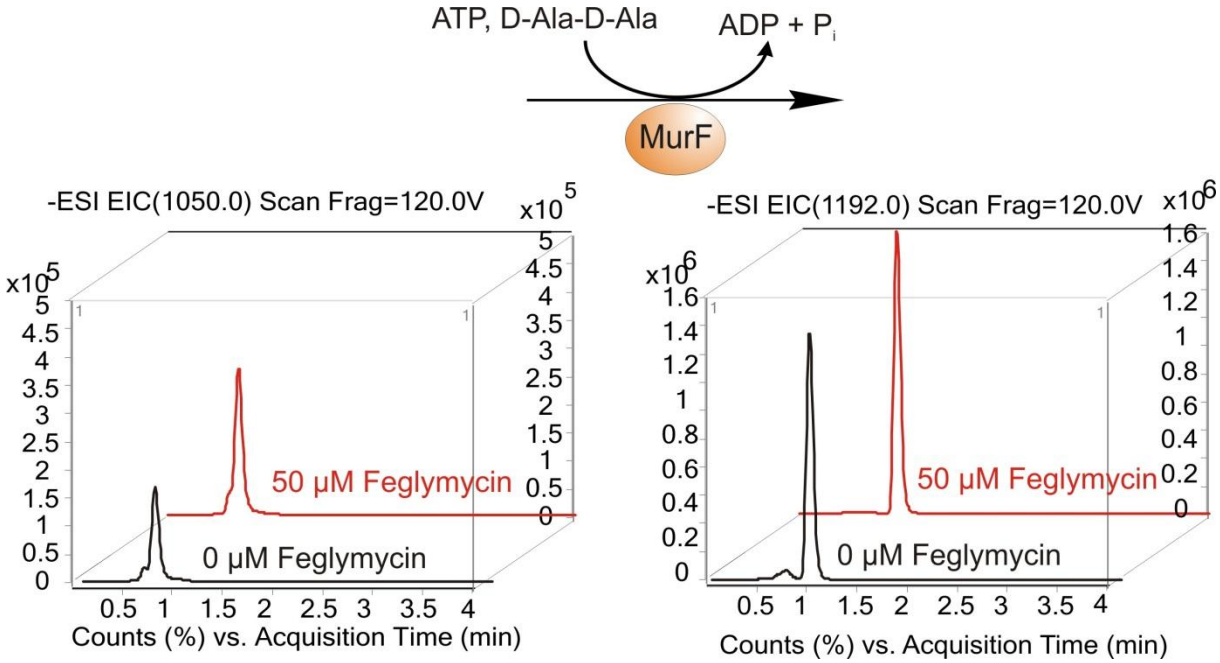

Figure 4.18: LC-MS chromatograms [EIC] of substrates and products of MurF *E. coli* enzyme reaction detected at the end point of the enzyme reaction with 0 µM feglymycin added (black) and with 50 µM feglymycin added (red) with the ESI-Triple-Quad-LC-MS in negative ionization mode. Left: EIC of UDP-MurNAc-l-Ala-d-Glu-meso-Dap ($[M-H]^-$ = 1050) Right: EIC of UDP-MurNAc-l-Ala-d-Glu-meso-Dap-d-Ala-d-Ala ($[M-H]^-$ = 1152).

The LC-Triple-Quad-MS results are paralleled to the results from the ESI-TOF-LC-MS. The peak areas of the substrates and products of the MurB, MurD, MurE and MurF reactions resemble strongly in form and height. Therefore no effect of feglymycin on the progress of these enzyme reactions can be observed. In case of the MurA and the MurC enzyme (Figure 4.13**,** Figure 4.15), however an accumulation of the substrate of the enzyme reaction in presence of feglymycin compared to the control is clearly visible.

4.4 UV-Vis Assays for determination of the kinetic parameters of the MurA and MurC enzymes from *E. coli* and *S. aureus*

By using a stepwise one-pot assay, a rapid screening of the Mur enzymes and their inhibition was facilitated. As the MurA and the MurC enzymes from *E. coli* were found to be sensitive to feglymycin a more detailed kinetic study of the inhibitory effect on these two enzymes was pursued. Enzyme coupling assays with UV-Vis detection were chosen due to the possibility to detect the enzyme reaction without having to stop the reaction before detection as it is necessary e.g. for LC-MS detection. As neither the substrate nor the product of the MurA and MurC reaction can be detected spectrophotometrically, the reactions were coupled to further enzyme reactions leading to a detectable product. In case of the MurA enzyme the reaction was coupled to the MurB enzyme, which catalyzes the spectrophotometrically detectable conversion of NADPH to $NADP^+$ as it has been described before by Brown et al. (Brown et al. 1994). In case of the MurC enzyme the reaction had to be coupled with two enzymes that do not belong to the same pathway, pyruvate kinase (PK) and lactate dehydrogenase (LDH). Coupling with PK and LDH has been used successfully before by Jin et al. (Jin et al. 1996). When couplings of enzymes are used, it has to be made sure that the rate of the reaction is actually determined by the enzymes intended to be measured. This can be assured by using an excess of coupling enzymes to ensure that the enzyme reaction that should be monitored is the limiting step of the enzymatic cascade. Both concentrations, of the MurA and the MurC enzyme, as well as of the coupling enzymes were optimized to concentrations where the onset of the reaction mainly depended on the concentration of MurA and MurC. Accordingly, all kinetic parameters were determined under saturation of all

substrates. Hence, the monitored substrate was measured as a pseudo first order reaction. To prevent effects due to sudden temperature changes of the enzyme, the reaction mixture containing the enzymes was always preincubated at 37°C. The reaction was started by addition of the substrate which was monitored.

4.4.1 Determination of IC_{50} values for MurA and MurC from *E. coli* and *S. aureus*

IC_{50} values were determined for the MurA enzymes both from *E. coli* and *S. aureus* as well as for the MurC enzymes both from *E. coli* and *S. aureus*. The IC_{50} value of feglymycin for the enzymes MurA from *E. coli* and *S. aureus* were both determined in comparison to the IC_{50} value of phosphomycin and bacitracin. Phosphomycin is a known irreversible inhibitor of MurA (Marquardt et al. 1994) and was used as a positive control. Bacitracin inhibits the third stage of cell wall biosynthesis (Stone, Strominger 1971) but has no effect on the enzymes MurA-F and was therefore used as a negative control. For the MurC enzyme *β*-chloro-L-alanine was used as a positive control and bacitracin again as a negative control. The L-alanine analogue *β*-chloro-L-alanine has been described before to possess inhibitory effects on the MurC enzyme (Liger et al. 1995). IC_{50} values were determined for all inhibitors with at least 10 different inhibitor concentrations and in triplicate (Table 4.3).

Table 4.3: Inhibition constants of various antibiotics on MurA and MurC.

	IC_{50} Feglymycin [µM]	IC_{50} Bacitracin [µM]	IC_{50} Phosphomycin [µM]	IC_{50} *β*-chloro-L-alanine [µM]
MurA *E. coli*	3.4 +/- 1.1	>250	6.2 +/- 2.8	n.d.*
MurA *S. aureus*	3.5 +/- 1.3	>250	0.2 +/- 0.1	n.d.*
MurC *E. coli*	0.3 +/- 0.1	>250	n.d.*	53.3 +/- 8.9
MurC *S. aureus*	1.0 +/- 0.6	>250	n.d.*	>250

* n.d. = not determinded.

The IC_{50} value of feglymycin was found to be about 3 µM, both for the *E. coli* and the *S. aureus* enzyme. The IC_{50} values of phosphomycin were found to be 6.2 +/- 2.8 µM for the *E. coli* enzyme which lies in the range of the described K_i value (Marquardt et al. 1994) and 0.2 +/- 0.1 µM for the *S. aureus* enzyme. The *S. aureus* enzyme therefore seemed to be more sensitive to phosphomycin than the *E. coli* enzyme

under *in vitro* conditions. The IC_{50} values of feglymycin for the MurC enzymes from *E. coli* and *S. aureus* were significantly lower than the IC_{50} values for *β*-chloro-L-alanine. Interestingly, *β*-chloro-L-alanine showed no inhibitory effect on the *S. aureus* enzyme at all. The IC_{50} values for feglymycin were with 0.3 +/- 0.1 µM for the *E. coli* enzyme and 1.0 +/- 0.6 µM for the *S. aureus* enzyme significantly lower than the IC_{50} values determined for the MurA enzymes. Bactracin showed no inhibitory effect on the MurA or MurC enzymes, as expected.

4.4.2 MurA assay

The UV-Vis MurA assay was performed both with the MurA enzyme from *E. coli* and *S. aureus*. V_{max} and K_M values were determined in dependence of both UDP-GlcNAc and PEP from at least three independent measurements with each at least 10 different substrate concentrations (Figure 4.19). V_{max} and K_M were calculated by non-linear fittings of the data. An average V_{max} and K_M value was calculated from the V_{max} and K_M values of the independent measurements (Table 4.4).

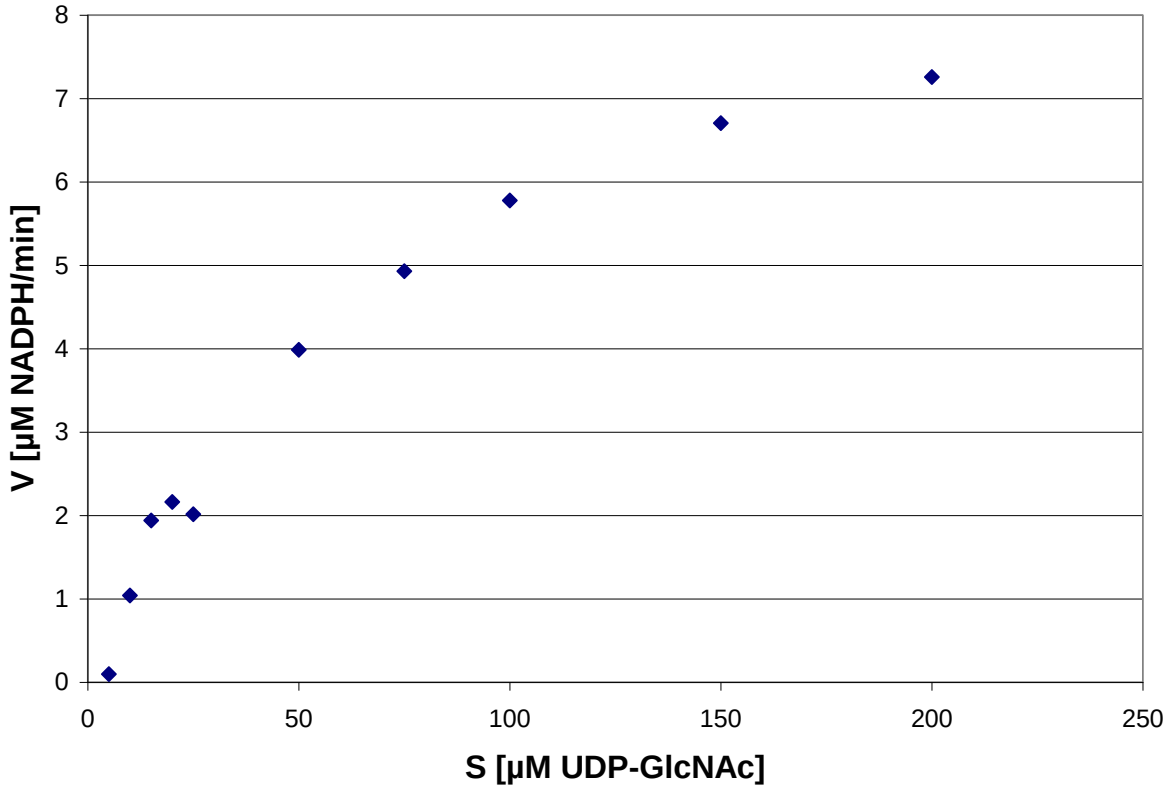

Figure 4.19: Michaelis-Menten-plot for the MurA enzyme from *E. coli*. The concentration of UDP-GlcNAc was varied [0-800 µM] while PEP [400 µM] was kept at a fixed concentration.

Table 4.4: Kinetic parameters obtained for the MurA enzymes from *E. coli* and *S. aureus*.

	V_{max} [µM/min]	K_M UDP-GlcNAc [µM]	K_M PEP [µM]	k_{cat} [s^{-1}]
MurA *E. coli*	9.3 +/- 0.3	60.4 +/- 9.8	48.5 +/- 18.8	7.7 +/- 0.2
MurA *S. aureus*	10.2 +/- 0.2	163.1 +/- 23.2	52.7 +/- 4.5	0.7 +/- 0.1

The k_{cat} value corresponds well to the values 8.9 s^{-1} (Dai et al. 2002) and 3.8 s^{-1} (Kim et al. 1996) previously described in the literature. The K_M values were calculated as 60.4 +/- 9.8 µM for UDP-GlcNAc and 48.5 +/- 18.8 µM for PEP. These values are higher than the values described before (Dai et al. 2002; Kim et al. 1996). The discrepancy in the K_M values may be due to differences in the enzyme assay used. The chosen UV-Vis coupling assay might not provide the necessary sensitivity to measure the exceedingly slow reactions at very low substrate concentrations. For the MurA enzyme from *S. aureus* a k_{cat} value of 0.7 +/- 0.1 s^{-1} was calculated. The enzyme was therefore found to be about 10-fold less active than the MurA enzyme from *E. coli*. The enzyme activity however corresponds to the values found by Du et al. for the MurA1 and MurA2 enzymes from *Staphylococcus pneumonia* (Du et al. 2000).

Inhibition type and K_i value were determined for the MurA enzyme from *E. coli* and the inhibitor feglymycin. To determine the inhibition type and K_i-values, the reaction mixture was preincubated with 5-6 different feglymycin concentrations around the IC_{50} value (3.4 µM). V_{max} and K_M values were determined in presence of the inhibitor in dependence of both UDP-GlcNAc and PEP from at least three independent measurements with each at least 10 different substrate concentrations (Figure 4.20).

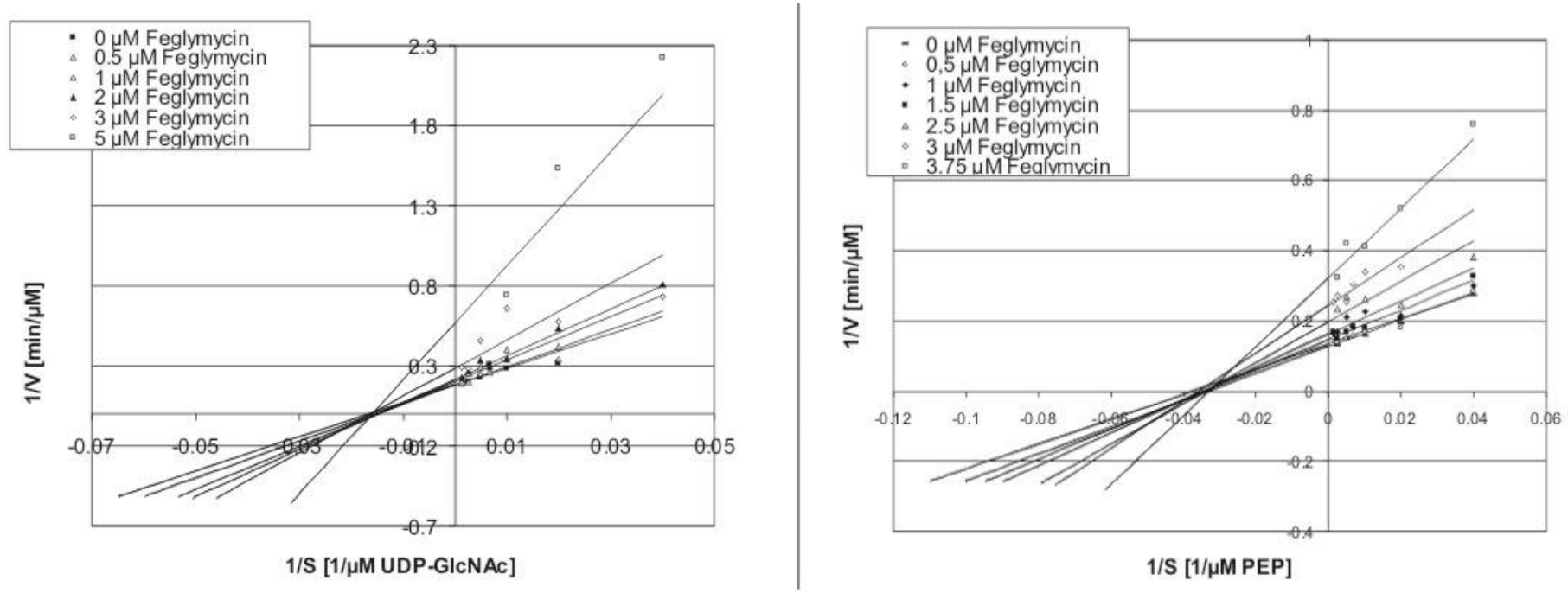

Figure 4.20: Lineweaver-Burk plot for MurA from *E. coli*. The initial velocities for the MurA enzyme were measured while one substrate and the feglymycin concentrations were varied and the other substrate was kept at a fixed concentration. The values for the graphs were derived from non-linear regression of the untransformed data fitted to the Michaelis-Menten equation. The double-reciprocal values of the untransformed data are displayed on the graphs as dots. The reciprocal plots indicate a non-competitive inhibition toward UDP-GlcNAc (left) and PEP (right).

4.4.3 MurC assay

In contrast to the MurA assay not all substrates for the MurC enzyme are commercially available. To be able to kinetically characterize the effect of feglymycin on the MurC enzyme *in vitro*, the substrate UDP-MurNAc however had to be provided. Sufficient amounts could be generated by Dipl.-Chem. Alexander Denisiuk and Dipl.-Chem. Marius Löhken (PhD students in the group of Prof. Roderich Süssmuth) applying a synthetic method published previously (Babic, Pecar 2008; Montoya-Peleaz et al. 2005; Takaku et al. 2006).

The UV-Vis MurC assay was performed both with the MurC enzymes from *E. coli* and *S. aureus*. V_{max} and K_M values were determined in dependence of both UDP-MurNAc, ATP and L-Ala from at least three independent measurements with each at least 10 different substrate concentrations (Figure 4.21). V_{max} and K_M were calculated by non-linear fittings of the data. An average V_{max} and K_M value was calculated from the V_{max} and K_M values of the independent measurements (Table 4.5).

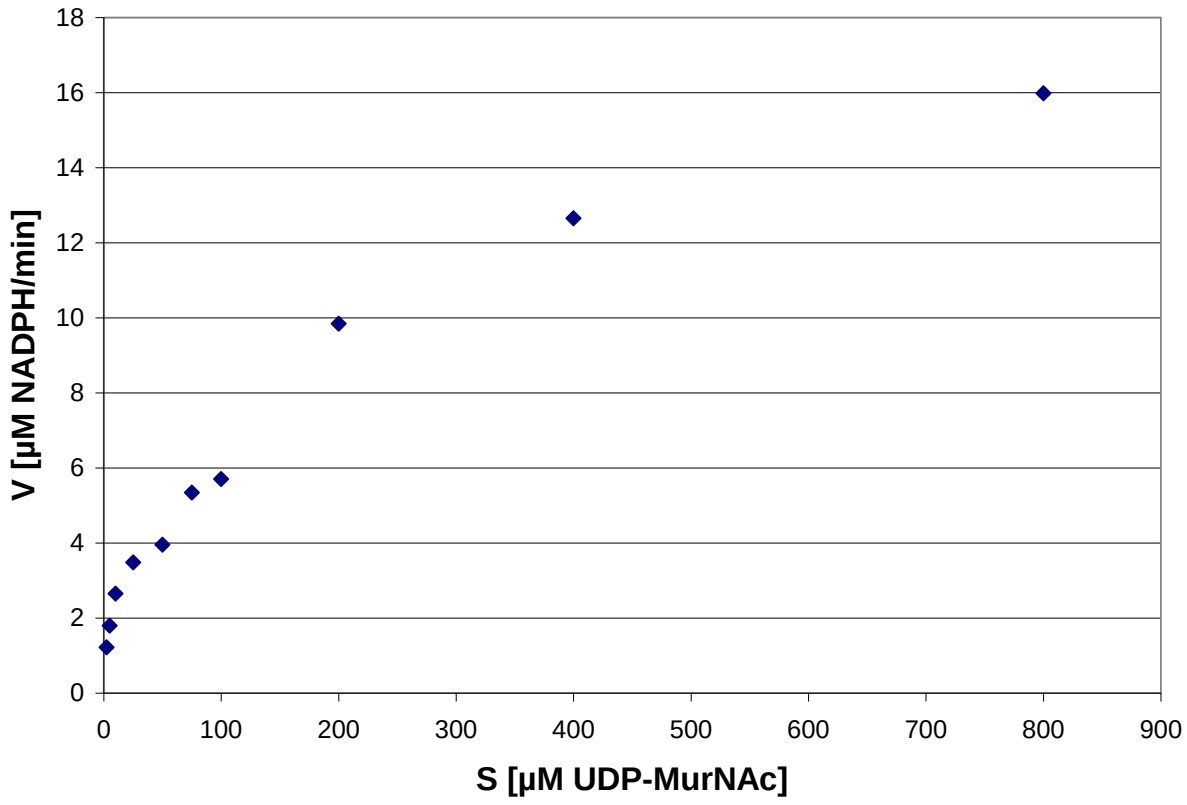

Figure 4.21: Michaelis-Menten-plot for the MurC enzyme from *E. coli*. The concentration of UDP-MurNAc was varied [0-800 µM] while the ATP [400 µM] and L-Ala [400 µM] were kept at a fixed concentration.

Table 4.5: Kinetic parameters obtained for the MurC enzymes.

	V_{max} [µM/min]	K_M UDP-MurNAc [µM]	K_M ATP [µM]	K_M L-alanine [µM]	k_{cat} [s^{-1}]
MurC *E. coli*	18.6 +/- 1.2	169.9 +/- 25.9	132.3 +/- 33.2	78.1 +/- 10.7	15.5 +/- 1.1
MurC *S. aureus*	16.3 +/- 0.5	263.1 +/- 12.9	280.2 +/- 53.8	221.6 +/- 89.0	1.4 +/- 0.1

The k_{cat} value of 15.5 +/-1.1 s^{-1} corresponds well to the k_{cat} value described before by Emanuele of 980 +/- 40 min^{-1} (= 16.3 +/- 0.7 s^{-1}) (Emanuele, JR. et al. 1996) while the K_M values for the MurC enzyme from *E. coli* are higher than the values described before in literature (Emanuele, JR. et al. 1996). The discrepancy in values can be explained in the same way as for the MurA enzyme. For the MurC enzyme from *S. aureus,* a k_{cat} value of 1.4 +/- 0.1 s^{-1} was calculated. Similar to the MurA enzyme from *S. aureus,* the MurC enzyme from *S. aureus* was therefore found to be about 10-fold less active than the *E. coli* enzyme.

Inhibition type and K_i value were determined for the MurC enzyme from *E. coli* and the inhibitor feglymycin. To determine the inhibition type and K_i-values, the reaction mixture was preincubated with 5-6 different feglymycin concentrations around the IC_{50} value (0.3 µM). V_{max} and K_M values were determined in presence of the inhibitor in dependence of both UDP-MurNAc, ATP and L-Ala from at least three independent measurements with each at least 10 different substrate concentrations (Figure 4.22).

Lineweaver-Burk plots were not created for the MurA and MurC enzymes from *S. aureus* as an analogue behaviour was expected. The similar inhibition constants of feglymycin towards the MurA and MurC enzymes from *E. coli* and *S. aureus* indicate an analogue mode of action.

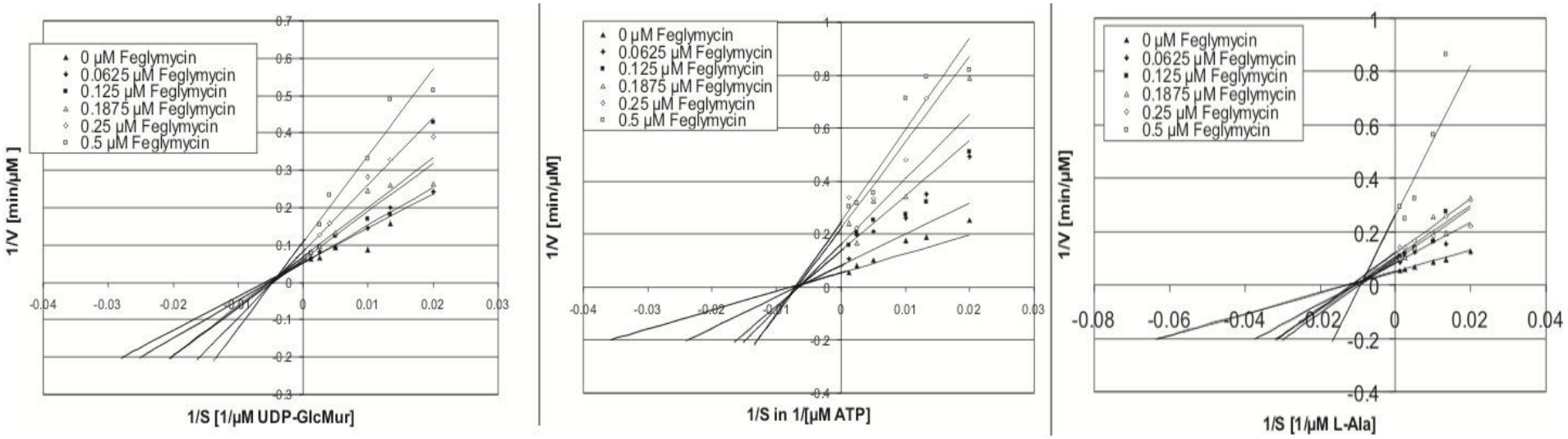

Figure 4.22: Lineweaver-Burk plot for MurC from *E. coli*. The initial velocities for the MurC enzyme were measured while one substrate and the feglymycin concentrations were varied and the other substrates were kept at a fixed concentration. The values for the graphs were derived from non-linear regression of the untransformed data fitted to the Michaelis-Menten equation. The double-reciprocal values of the untransformed data are displayed on the graphs as dots. The reciprocal plots indicate a non-competitive inhibition toward UDP-MurNAc (left), ATP (middle) and L-Ala (right).

4.4.4 Time-dependence experiments with feglymycin

Time-dependence experiments were performed to determine the rate of inhibition. MurA and MurC from *E. coli* were incubated for 1-20 min at 37 °C with a feglymycin concentration around the IC_{50} value before the reaction was started. All experiments reactions were performed in triplicate.

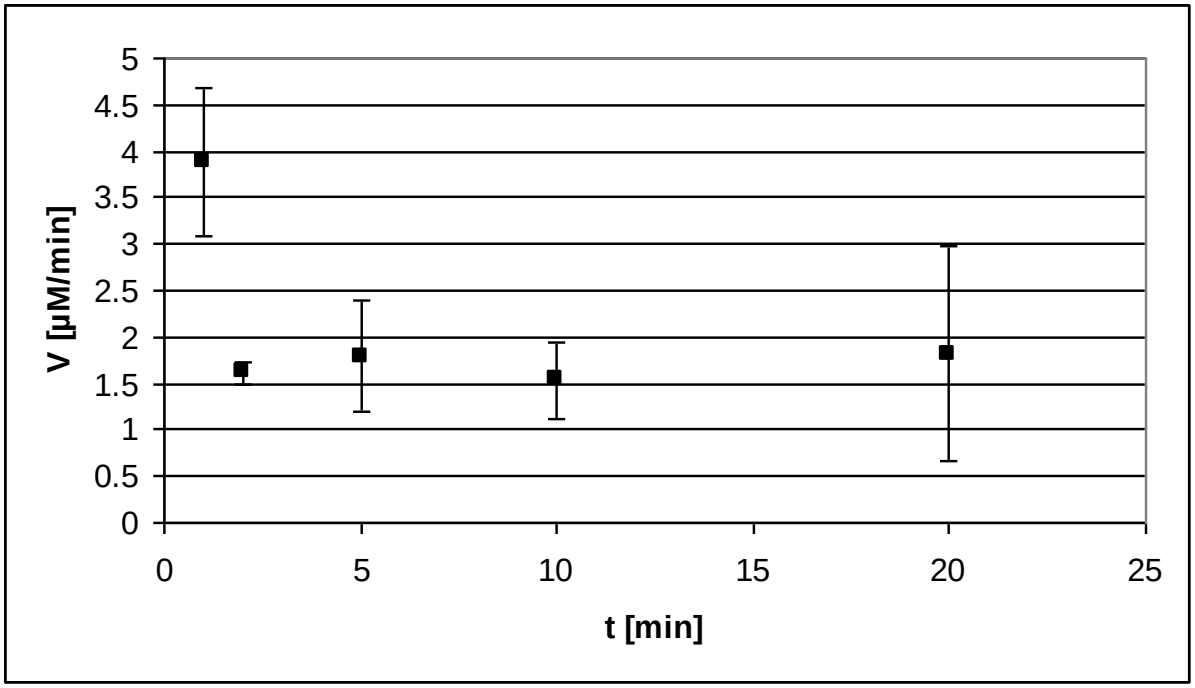

Figure 4.23: Time-dependence of the MurA (*E. coli*) inhibition by feglymycin.

The inhibition of MurA by feglymycin occurred within seconds. After ~2 min the maximal inhibitory effect is reached (Figure 4.23).

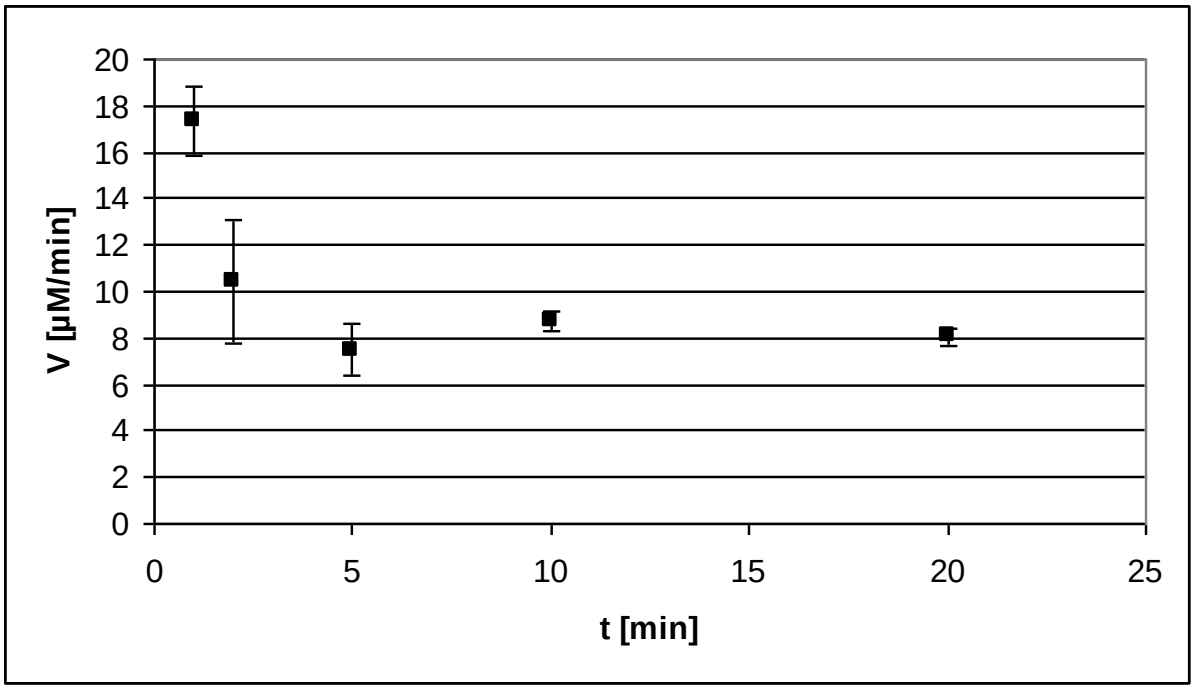

Figure 4.24: Time-dependence of the MurC (*E. coli*) inhibition by feglymycin.

The inhibition of MurC by feglymycin occurred after few minutes. After ~5 min the maximal inhibitory effect is reached (Figure 4.24).

4.4.5 Reversibility experiments with feglymycin

Reversibility of the inhibition of the MurA and MurC enzymes from *E. coli* by feglymycin was tested using a comparative dilution analysis as described by Copeland (Copeland 2005). With the help of the comparative dilution analysis it should be tested if the inhibitor binds irreversibly to the enzyme, so that the enzyme stays inactive after contact with high concentrations of inhibitor even after dilution to a much lower inhibitor concentration. The MurA enzyme was incubated with 50 µM feglymycin and the MurC enzyme with 5 µM feglymycin. The inhibitor concentration therefore was chosen about 10-fold higher than the IC_{50} values. After dilution of 1/100 the feglymycin concentration was expected to decrease to 0.5 µM (in case of the MurA enzyme) and 0.05 µM (in case of the MurC enzyme) therefore to feglymycin concentrations in range of the minimal inhibitory concentrations.

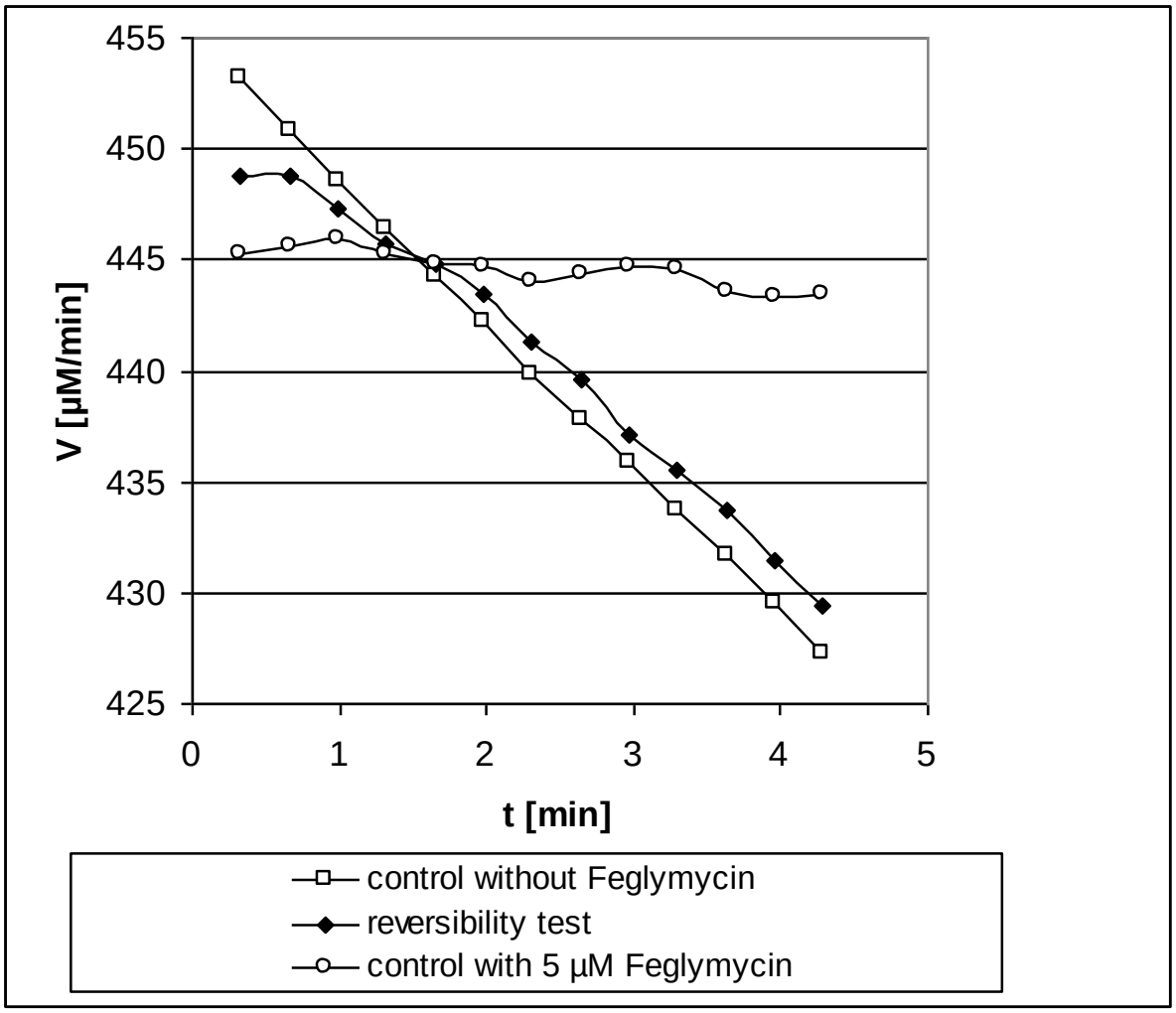

Figure 4.25: Reversibility of the feglymycin inhibition for the MurA enzyme from *E. coli*. The figure shows the decrease of NADPH over time. Initial reaction velocities were measured for a control without feglymycin (20 nM MurA in MurA reaction buffer), the reversibility test (a solution containing 2 µM MurA and 50 µM feglymycin was diluted 1/100 in MurA reaction buffer) and a control with 5 µM feglymycin (a solution containing 2 µM MurA and 50 µM feglymycin was diluted 1/100 in MurA reaction buffer with 5 µM feglymycin). The MurA-catalyzed reaction was started directly after dilution by addition of 400 µM UDP-GlcNAc and the initial reaction velocities detected at 20 s intervals with a UV-Vis reader for 4 min.

Table 4.6: Reversibility of the feglymycin inhibition for the MurA enzyme from *E. coli*.

	V_{max} [µM]/min
control without feglymycin	6.0 +/- 2.1
reversibility test*	5.5 +/- 1.2
control with 5 µM feglymycin*	0.5 +/- 0.2

* MurA was incubated in a concentration about 100-fold higher than used for the activity assay (2 µM) with an inhibitor concentration about 10-fold higher than the IC50 value (50 µM) for 20 min prior to

start of the measurement. After preincubation the enzyme was diluted 1/100 into reaction buffer without feglymycin (reversibility test) or with 5 µM feglymycin (control with 5 µM feglymycin). Subsequently the initial reaction velocities (V_{max}) were calculated.

The inhibition of the MurA enzyme seems to be rapidly reversible. Only about 1 min after the initiated strong dilution, the enzyme which had prior been incubated with a feglymycin concentration of 50 µM (reversibility test), reaches the same reaction velocity as the control without feglymycin and a much higher reaction velocity than the control diluted into reaction buffer containing 5 µM feglymycin (Figure 4.25, Table 4.6).

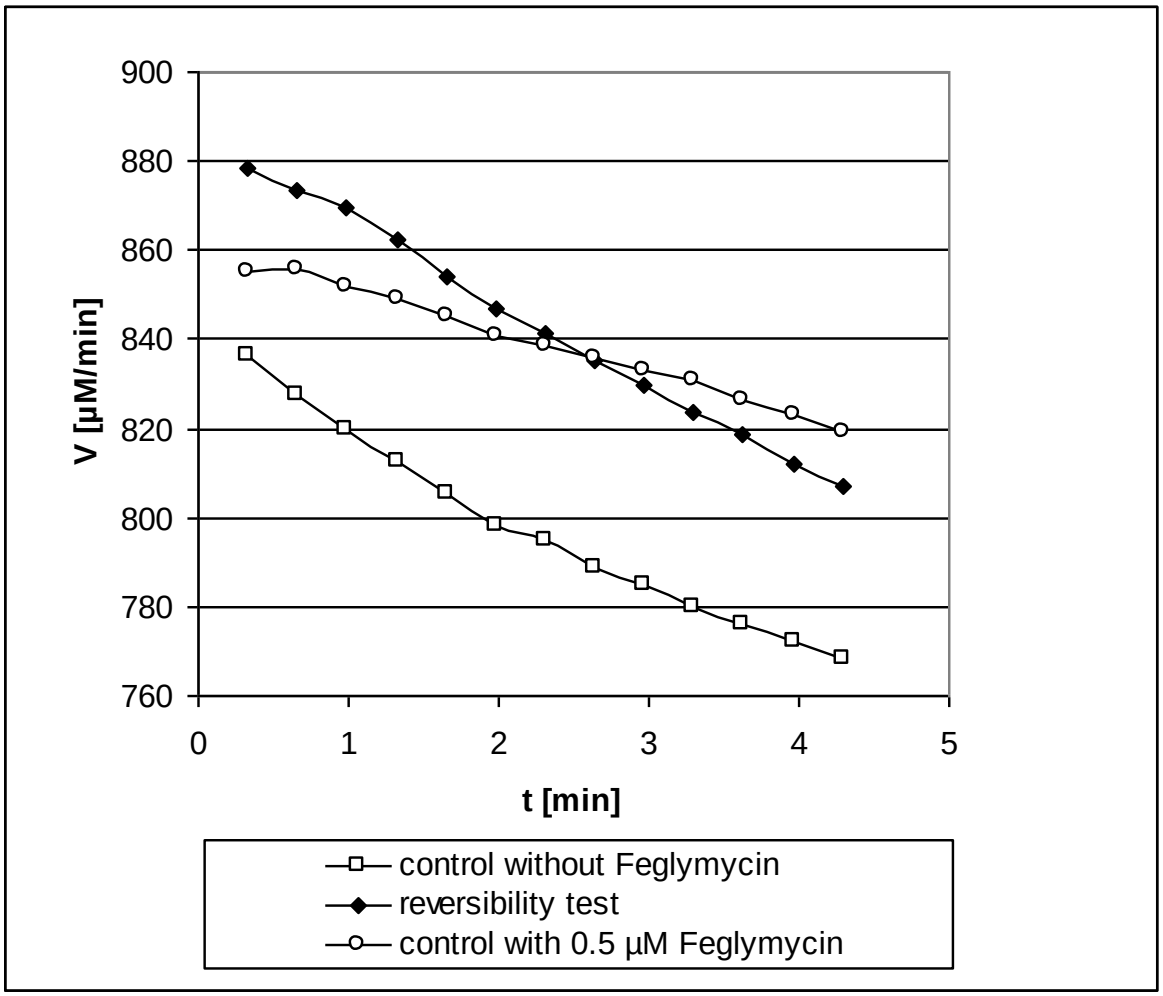

Figure 4.26: Reversibility of the feglymycin inhibition for the MurC enzyme from *E. coli*. The figure shows the decrease of NADH over time. Initial reaction velocities were measured of a control without feglymycin (20 nM MurC in MurC reaction buffer), the reversibility test (a solution containing 2 µM MurC and 5 µM feglymycin was diluted 1/100 in MurC reaction buffer) and a control with 0.5 µM feglymycin (a solution containing 2 µM MurC and 5 µM feglymycin was diluted 1/100 in MurC reaction buffer with 0.5 µM feglymycin). The MurC-catlyzed reaction was started directly after dilution by

addition of 400 µM UDP-MurNAc and the initial reaction velocities detected at 20 sec intervals with a UV-Vis reader for 4 min. Subsequently the initial reaction velocities (V_{max}) were calculated.

Table 4.7: Reversibility of the feglymycin inhibition for the MurC enzyme from *E. coli*.

	V_{max} [µM]/min
control without feglymycin	15.5 +/- 1.2
reversibility test*	15.1 +/- 1.0
control with 0.5 µM feglymycin*	7.2 +/- 2.9

* MurC was incubated in a concentration about 100-fold higher than used for the activity assay (2 µM) with an inhibitor concentration about 10-fold higher than the IC_{50} value (5 µM) for 20 min prior to start of the measurement. After preincubation, the enzyme was diluted 1/100 into reaction buffer without feglymycin (reversibility test) or reaction buffer with 0.5 µM feglymycin (control with 0.5 µM feglymycin).

The inhibition of the MurC enzyme seems to be rapidly reversible. Only about 1 min after the initiated strong dilution, the enzyme which had prior been incubated with a feglymycin concentration of 5 µM (reversibility test), reaches the same reaction velocity as the control without feglymycin and a much higher reaction velocity (2-fold) than the control diluted into reaction buffer containing 0.5 µM feglymycin (Figure 4.26, Table 4.7).

The reversibility experiments were not performed with the MurA and MurC enzymes from *S. aureus* as an analogue behaviour was expected. The similar inhibition constants of feglymycin towards the MurA and MurC enzymes from *E. coli* and *S. aureus* indicate an analogue mode of action.

4.4.6 CD measurements of the MurA and MurC enzymes from *E. coli*

CD spectra of MurA and MurC from *E. coli* were recorded in 10 mM phosphate buffer (pH 8.0). Additionally to the pure enzyme (16 µM MurA of *E. coli* and 17.5 µM MurC of *E. coli*) the enzymes were measured in presence of an equimolar concentration, a two-fold molar excess and a four-fold molar excess of feglymycin. As the addition of feglymycin to the enzymes caused a slight dilution of the enzyme solution the enzymes were additionally measured after a comparable dilution with phosphate buffer without feglymycin. In this context, it is known that trifluoroethanol (TFE) influences the three-dimensional structure of protein and especially promotes the formation of α-helices (Myers et al. 1998). The measurements were repeated in presence of 20 % TFE to test if the addition of TFE interferes with the effect of feglymycin on the three-dimensional structure of MurA and MurC. As reference, spectra of phosphate buffer without enzyme and feglymycin in phosphate buffer were recorded. Feglymycin has an α-helical structure in solution. For the used feglymycin concentrations the CD spectra of feglymycin were however so weak in comparison with the protein spectra that an unspecific additive effect of feglymycin on the protein spectra can be neglected. All experiments were performed twice. Additionally CD spectra of MurA and MurC were detected after 20 min at RT to rule out a change of ot fhe three-dimensional structure during the CD measurements due to temperature instability of the proteins.

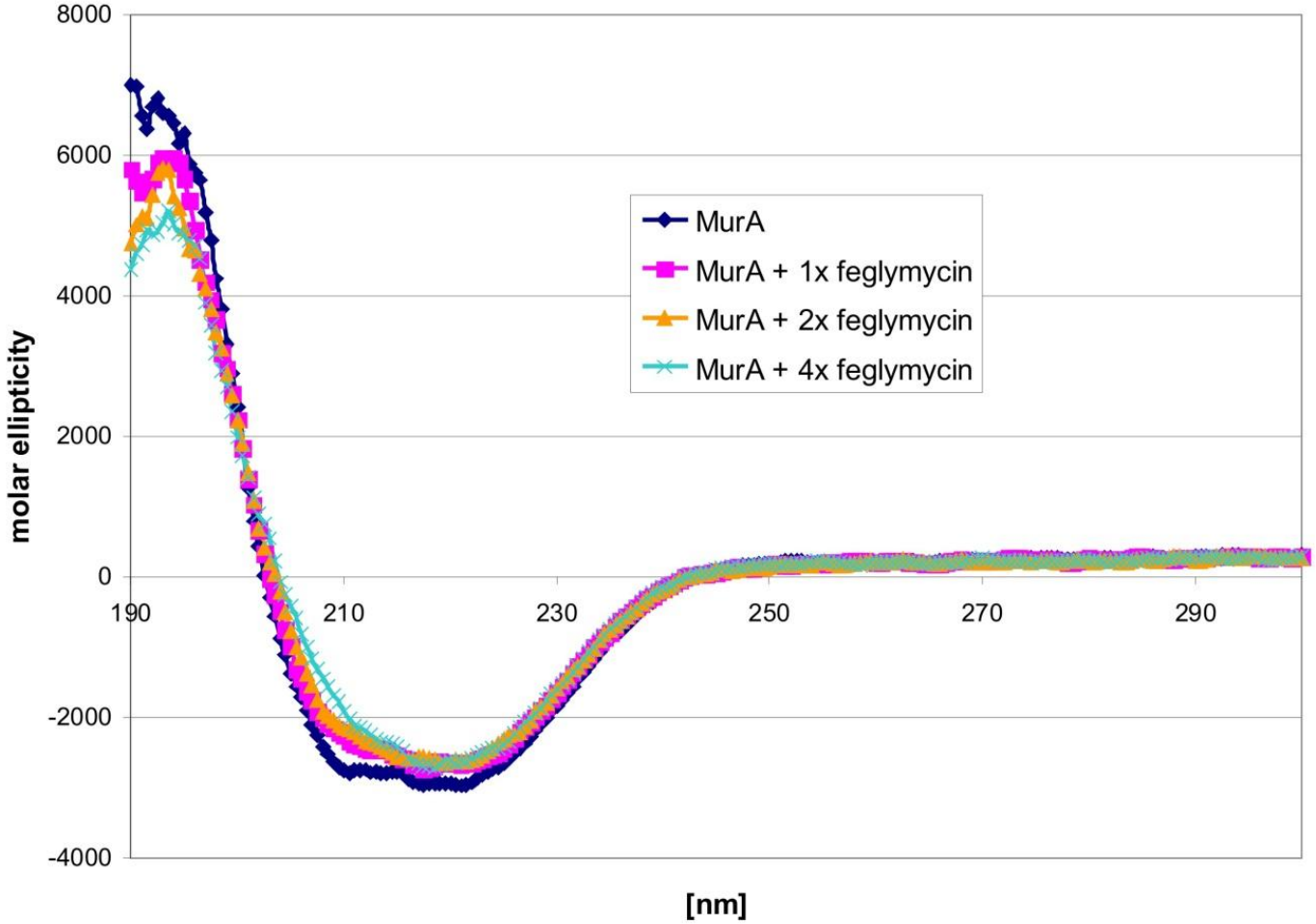

Figure 4.27: CD specta of MurA enzyme from *E. coli* in presence of different feglymycin concentrations. Blue: MurA (16 µM) in phosphate buffer (10 mM, pH 8.0), Pink: MurA (16 µM) in phosphate buffer (10 mM, pH 8.0) with an equimolar feglymycin concentration (16 µM). Orange: MurA (16 µM) in phosphate buffer (10 mM, pH 8.0) with a two-fold molar excess of feglymycin (32 µM). Turquoise: MurA (16 µM) in phosphate buffer (10 mM, pH 8.0) with a four-fold molar excess of feglymycin (64 µM).

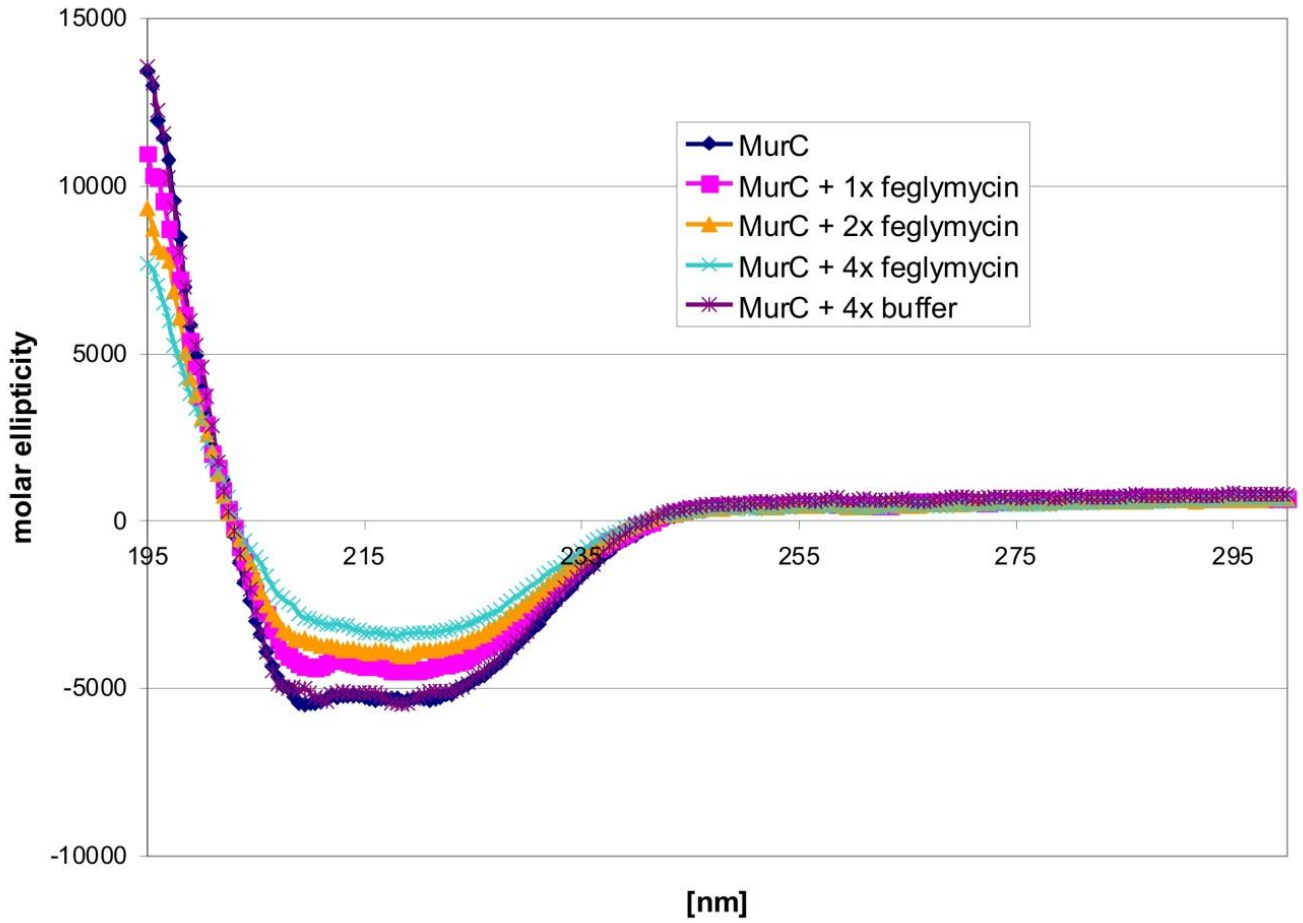

Figure 4.28: CD specta of MurC from *E. coli* in presence of different feglymycin concentration. Blue: MurC (17.5 µM) in phosphate buffer (10 mM, pH 8.0), Pink: MurC (17.5 µM) in phosphate buffer (10 mM, pH 8.0) with an equimolar feglymycin concentration (17.5 µM). Orange: MurC (17.5 µM) in phosphate buffer (10 mM, pH 8.0) with a two-fold molar excess of feglymycin (35 µM). Turquoise: MurC (17.5 µM) in phosphate buffer (10 mM, pH 8.0) with a four-fold molar excess of feglymycin (70 µM). Lilac: MurC (17.5 µM) in phosphate buffer (10 mM, pH 8.0) diluted with the same volume of phosphate buffer (10 mM, pH 8.0) as was added for the four-fold equimolare feglymycin concentration.

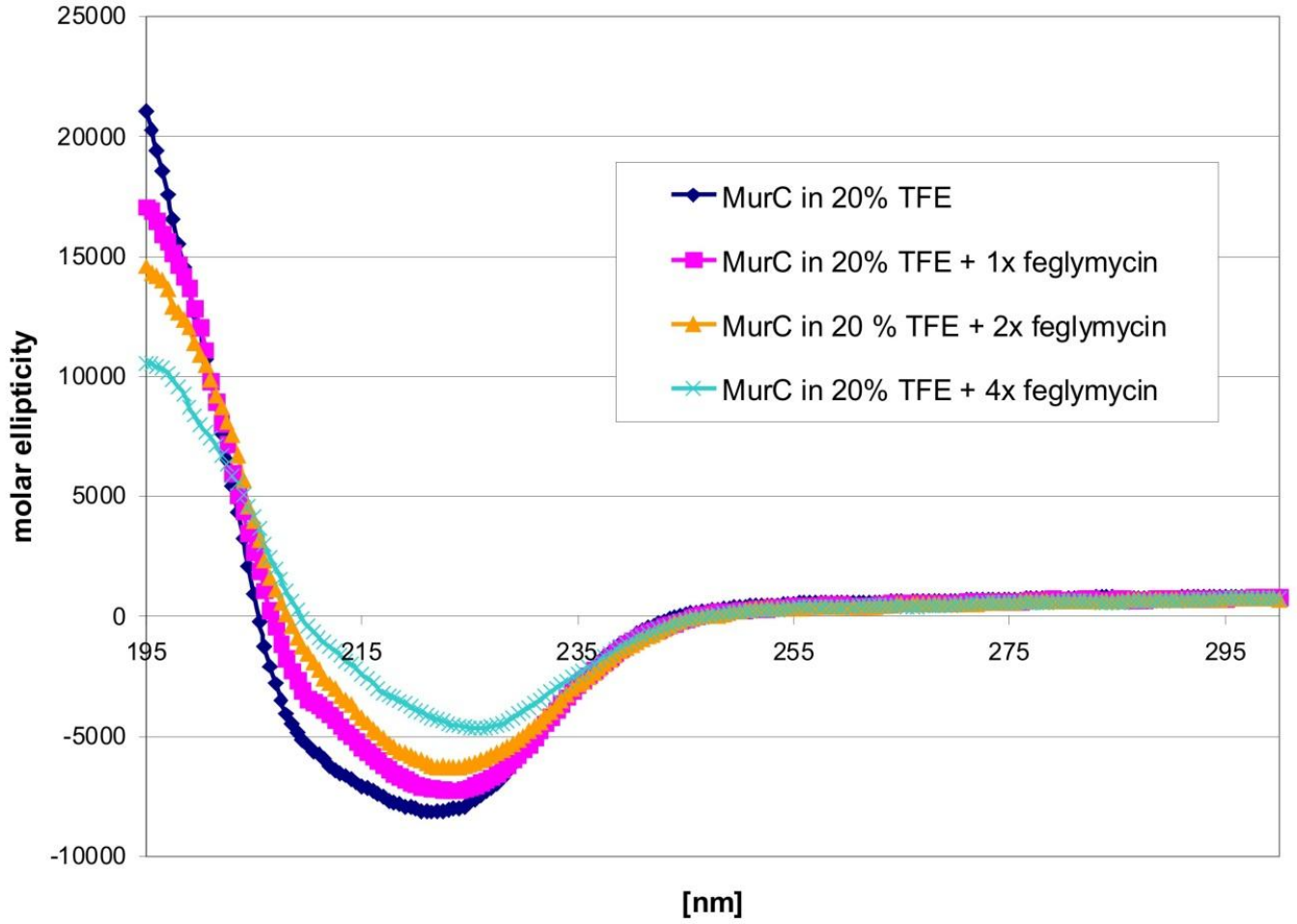

Figure 4.29: CD specta of MurC from *E. coli* in presence of different feglymycin concentrations and in the presence of 20 % (v/v) trifluoroethanol. Blue: MurC (17.5 µM) in phosphate buffer (10 mM, pH 8.0) with 20 % (v/v) TFE, Pink: MurC (17.5 µM) in phosphate buffer (10 mM, pH 8.0) with 20 % (v/v) TFE and an equimolar feglymycin concentration (17.5 µM). Orange: MurC (17.5 µM) in phosphate buffer (10 mM, pH 8.0) with 20 % (v/v) TFE and a two-fold excess of feglymycin (35 µM). Turquoise: MurC (17.5 µM) in phosphate buffer (10 mM, pH 8.0) with 20 % (v/v) TFE and a four-fold molar excess of feglymycin (70 µM).

The addition of feglymycin had only a minor influence on the CD spectra and hence overall conformation of the MurA enzyme (Figure 4.27). In case of the MurC enzyme however a significant influence of feglymycin is visible. The addition of feglymycin led to a flattening of the CD curve and a decrease of the molar ellipticity of the maxima at $\lambda = 210$ nm and $\lambda = 220$ nm. This effect increases with the concentration of feglymycin added, indicating that feglymycin might have an alterative effect on the tertiary structure of the MurC enzyme (Figure 4.28).

The addition of 20 % TFE to the MurC enzyme changes the CD spectrum. The absorption maximum at $\lambda = 210$ nm increases strongly and dominates the double maxima form of the native protein. However in presence of feglymycin a similar effect is visible as in absence of TFE. The addition of feglymycin leads to an increased flattening of the CD curve. In presence of TFE the effect is even more distinct (Figure 4.29). TFE therefore possibly might have a supporting effect inducing a change of the tertiary structure by feglymycin.

4.5 Optimization of the feglymycin production by *Streptomyces* sp. DSM 11171

The detection and mass spectrometric characterization of feglymycin with the LC-Triple-Quad-MS was optimized with synthetic feglymycin provided by Dr. Anne Hänchen (former member of the group of Prof. Roderich Süssmuth).

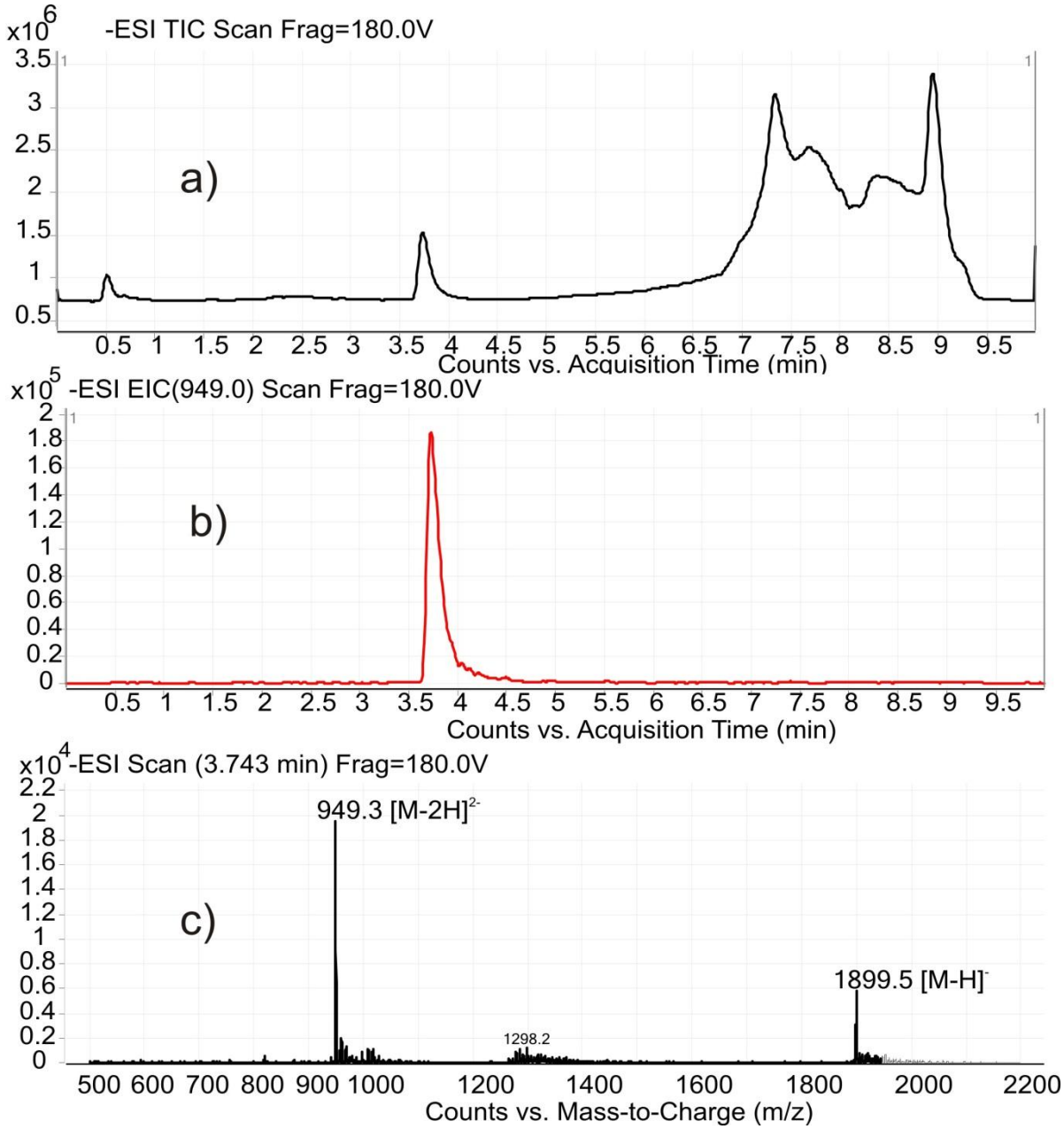

Figure 4.30: LC-Triple-Quad-MS detection of 50 µM synthetic feglymycin in negative ionization mode (injection volume 3 µl). a) total ion count (TIC), b) extracted ion chromatogram (EIC), c) mass spectrum recorded at R_t = 3.7 min.

A detection by single ion monitoring (SIM) of the two-fold charged molecular mass of feglymycin in negative mode ($[M-2H]^{2-}$ = 948.8) was found to provide the highest sensitivity and specificity for feglymycin (Figure 4.30, Figure 4.31).

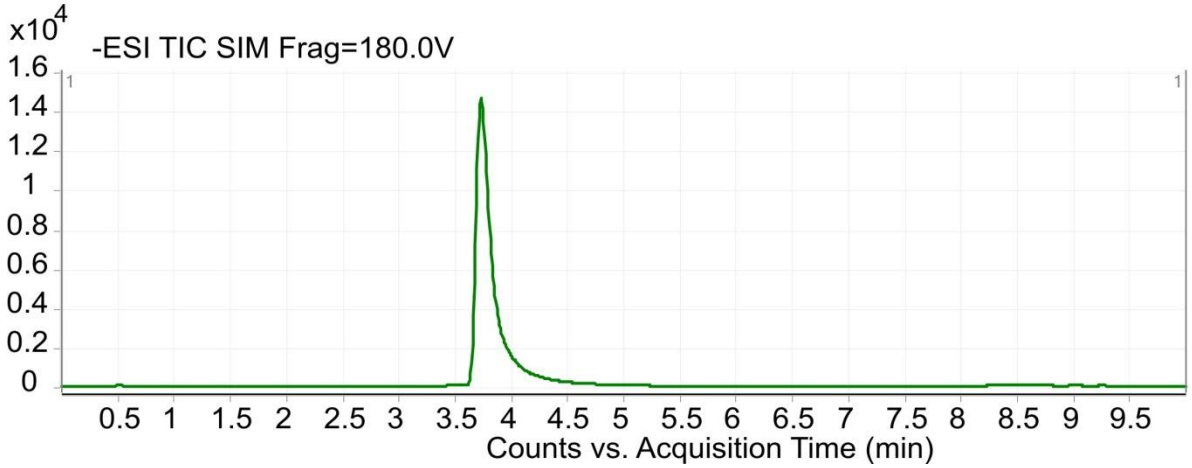

Figure 4.31: SIM-chromatogram by LC-Triple-Quad-MS detection of 50 µM synthetic feglymycin in negative ionization mode. The molecular mass of felgmycin 949.8 ($[M-2H]^{2-}$) is detected at a retention time of R_t = 3.8 min.

4.5.1 Production tests

Feglymycin production was tested both on agar plates and in liquid culture in different *Streptomyces* media. For production control on agar plates the media MS, GYM, N-Z-Amine and Paper were tested. The feglymycin producer stain was cultivated for 3 d at 28 °C on plate. Feglymycin was extracted from the agar plates and tested by LC-Triple-Quad-MS with SIM-measurements.

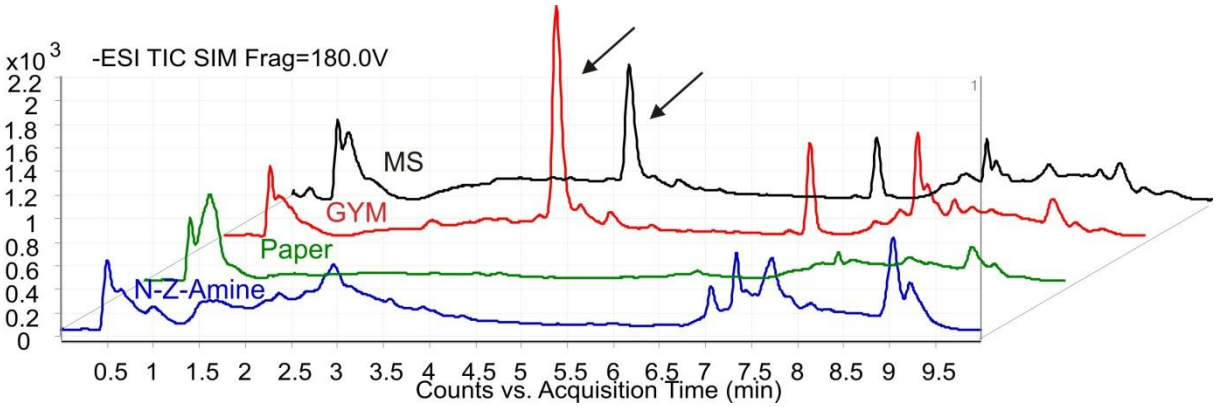

Figure 4.32: SIM-MS measurements of feglymycin with LC-Triple-Quad-MS in negative ionization mode of extracts from agar plates. black) MS medium, red) GYM medium, green) Paper medium, blue) N-Z-Amine medium. For MS medium and GYM medium a peak at the characteristic retention time of feglymycin was detected (R_t = 3.7 min).

In the agar plate extracts of both MS and GYM media a peak was detected by SIM-measurements at the characteristic retention time of feglymycin (R_t = 3.7 min) indicating a preferred feglymycin production on MS and GYM plates (Figure 4.32). The concentration of the produced feglymycin was however too low to allow verification by mass fingerprinting.

To test if feglymycin is produced in liquid culture the media GYM, E1, YEME, Paper and N-Z-Amine were tested. The feglymycin producer strain (*Streptomyces* sp. DSM 11171) was first cultivated for 3 d at 28 °C on GYM agar plates. A 1 cm x 1 cm piece of agar was transferred into 50 mL liquid medium (N-Z-Amine, Paper, YEME, E1 or GYM) and cultivated for 3 d at 28 °C with shaking. Feglymycin was extracted from the bacterial culture both from the cell pellet and the supernatant and tested by LC-Triple-Quad-MS with SIM-measurements.

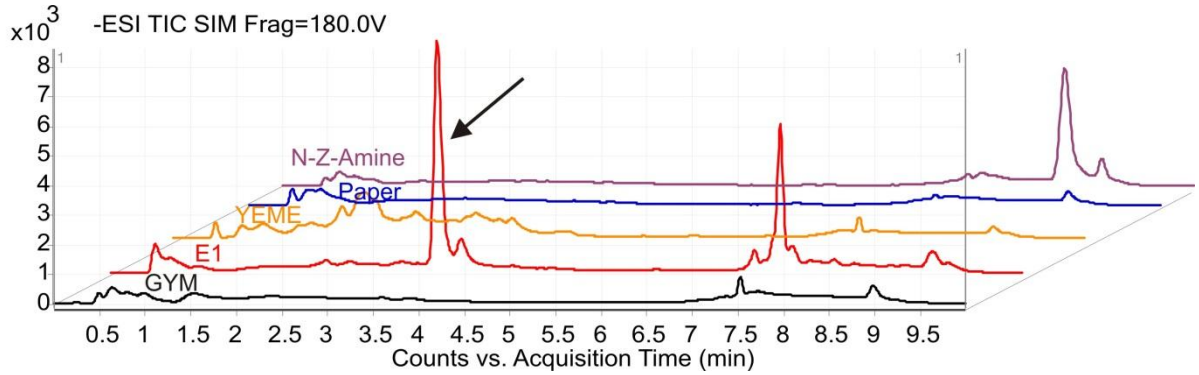

Figure 4.33: SIM-MS measurements of feglymycin with LC-Triple-Quad-MS in negative mode of extracts from cell pellets of liquid bacterial culture. Liquid culture media: black) GYM medium, red) E1 medium, yellow) YEME medium, blue) Paper medium, purple) N-Z-Amine medium. Only in E1 medium a peak at the characteristic retention time of feglymycin (R_t = 3.7 min) was detected.

In the liquid culture extracts only in the cell pellet of *Streptomyces* sp. DSM 11171 cultivated in E1 medium a peak was detected with SIM-measurements at the characteristic retention time of feglymycin indicating feglymycin production in E1 medium (Figure 4.33). These results were somewhat surprising as in literature feglymycin production in Paper medium after 3 d was reported (Vértesy et al. 1999). The concentration of the produced feglymycin was however too low to allow verification by mass fingerprinting. The production in E1 medium was further optimized by cultivating the strain first on GYM agar plates for 3 d at 28 °C, then in TSB medium for 3 d at 28 °C. This was followed by cultivation in E1 medium (as main culture). Additionally different cultivations periods were tested. Feglymycin production in the extracts of the cell pellet and the supernatant was tested with SIM-MS measurements and in addition quantified with SRM-MS measurements of feglymycin with TripleQuad LC-MS.

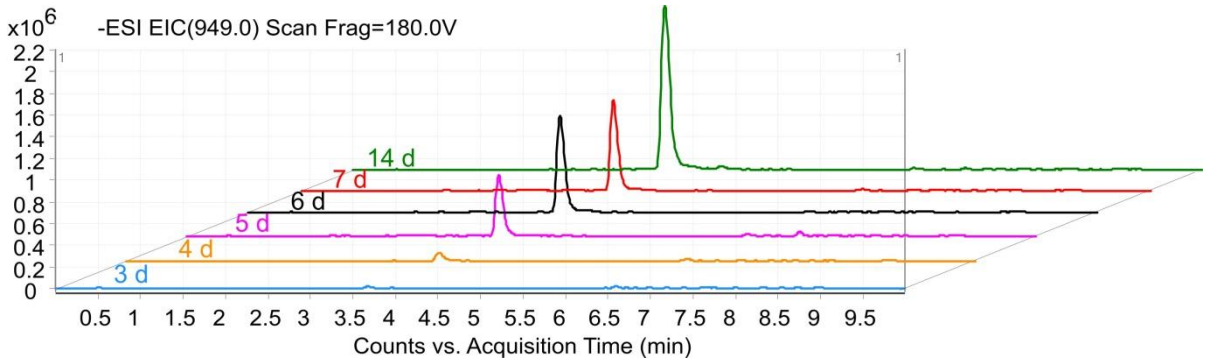

Figure 4.34: LC-Triple-Quad-MS of extracts extracted at different time points (3 d – 14 d) from cell pellets of *Streptomyces sp.* DSM 11171 cultivated in E1 medium. Displayed are EIC of the mass of the two-fold charged feglymycin molecular mass ($[M-2H]^{2-}$ = 949).

These experiments showed that feglymycin production increases in a late phase of Streptomyces growth. A strong production started after 5 d and production further increased until 14 d of cultivation (Figure 4.34) even though the bacteria started to die off after 7 d of cultivation (high number of broken cells visible in the microscope). The high concentration of feglymycin after 14 d of cultivation therefore might indicate that feglymycin is not metabolized by the bacteria and further indicates an unexpected stability of the antibiotic under the cultivation conditions applied.

4.5.2 Mass finger printing

The concentration of the feglymycin produced in E1 medium after 14 d of cultivation was high enough to allow verification of primary sequence by mass fingerprinting. The product ion spectra of synthetic feglymycin and wildtype extract were in excellent accordance (Figure 4.35). This is evidence that the *Streptomyces* sp. DSM 11171 is producing feglymycin.

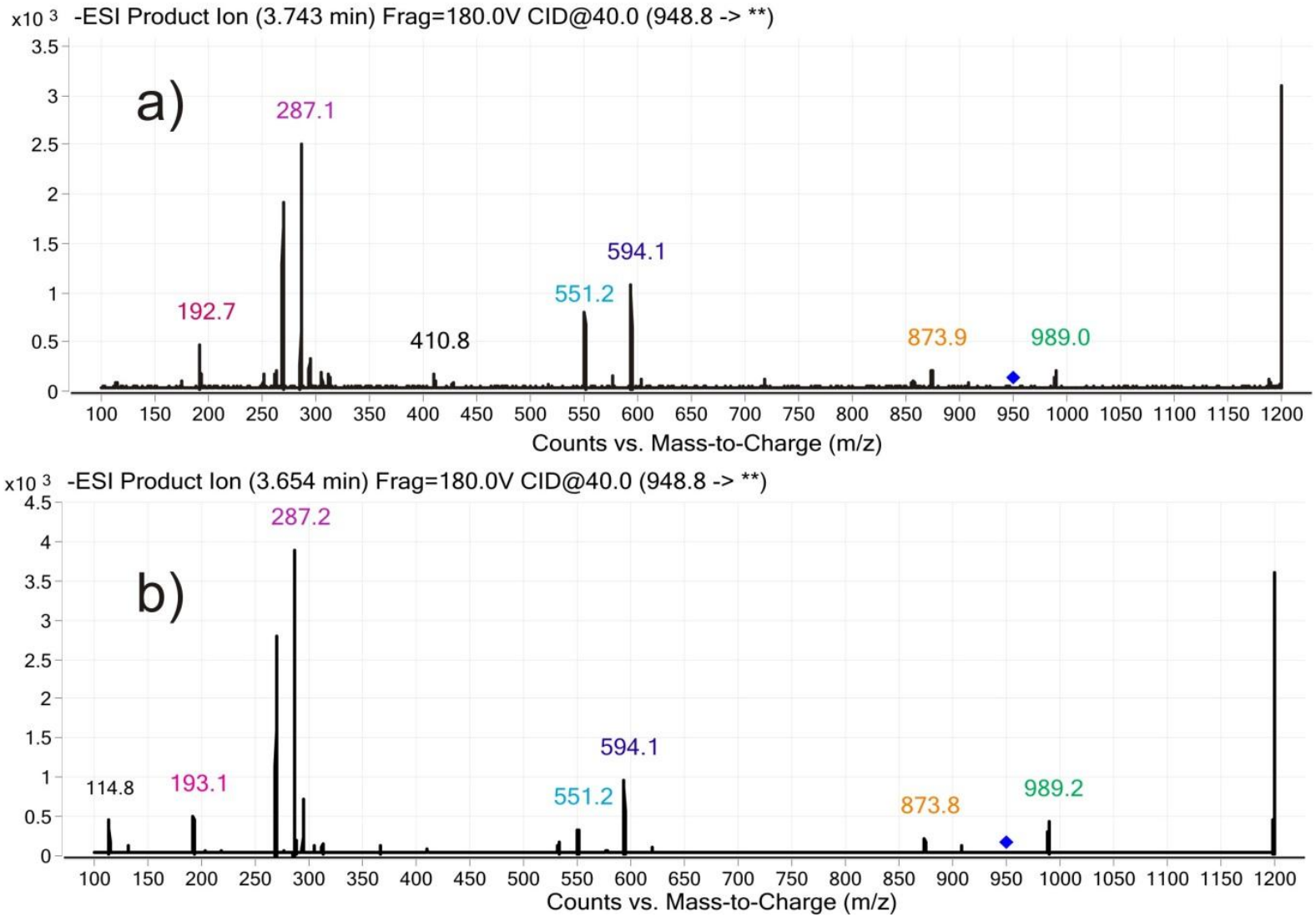

Figure 4.35: ESI-MSMS measurement (LC-Triple-Quad-MS) of a) 50 µM synthetic feglymycin (injection volume 5 µM) and b) feglymycin extracted from the cell pellet of *Streptomyces sp.* DSM 11171 cultivated for 14 d in E1 medium. Displayed are the mass spectra detected at R_t = 3.7 min.

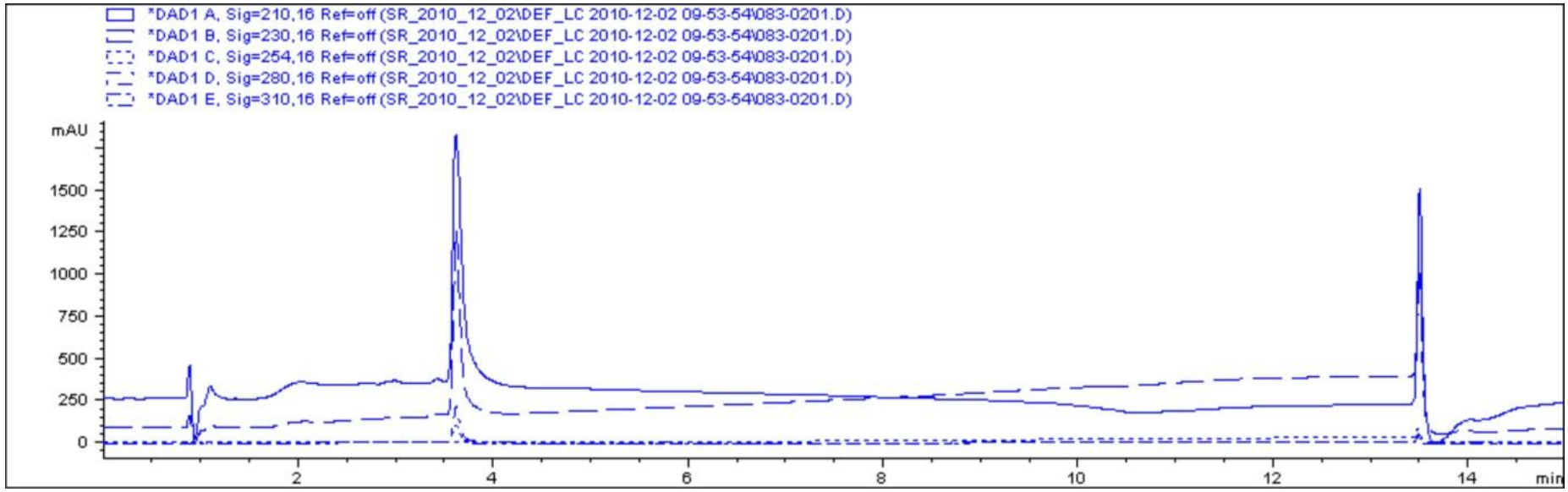

Figure 4.36: Analytical HPLC chromatogram of isolated feglymycin (detection at λ = 210, 230, 254, 280, 310). Feglymycin is detected at R_t = 3.7 min.

4.5.3 Isolation of preparative amounts of feglymycin

Feglymycin was isolated from the pellet of bacterial culture after 14 d of cultivation in E1 medium. Feglymycin was extracted from cell pellet with 80 % MeOH and was fractionated by preparative RP-HPLC. From 500 mL of bacterial culture 2.5 mg analytically pure feglymycin were isolated. Purity was verified by analytical HPLC (Figure 4.36) and mass spectrometry.

4.6 Annotation of the feglymycin gene cluster

20 g cell pellet of the *Streptomyces* sp. DSM 11171 cultivated for 3 d in TSB medium was send to LG genomics (LGC Genomics GmbH, Berlin, Germany) for sequencing. The genomic data was analyzed by means of the artemis annotation tool (Rutherford et al. 2000). The biosynthesis gene cluster was traced by searching genes characteristic for Hpg and Dpg biosynthesis. The genes constituting the gene cluster were analyzed with the NCBI blast tool (Mizyed et al. 2005). The obtained gene cluster is expected to span nearly 100 kb and includes up to 35 open reading frames (ORFs) (Figure 4.37). The feglymycin gene cluster is framed by coding DNA regions making it difficult to determine the borders of the gene cluster.

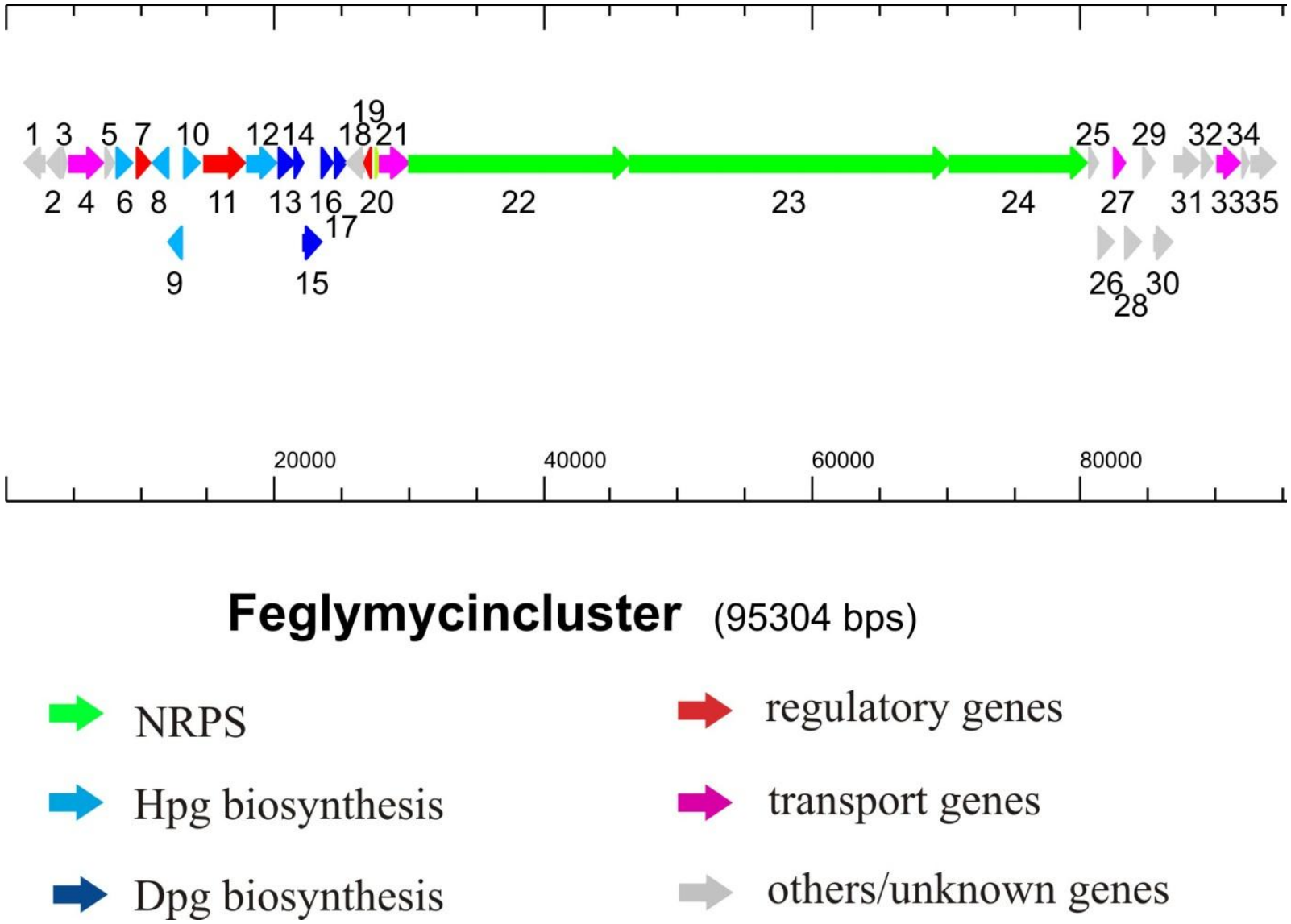

Figure 4.37: Organization of the feglymycin biosynthesis gene cluster.

Table 4.8: ORFs that were identified in the region of the feglymycin gene cluster.

ORF	size (aa)	best match source	entry	proposed function
1	531	*Streptomyces sviceus* ATCC 29083	ZP_06920919	secreted peptidase
2	358	*Streptomyces* sp. ACTE	ZP_06273624	Radical SAM domain protein
3	147	*Streptomyces* sp. Mg1	ZP_04997539	conserved hypothetical protein
4	799	*Streptomyces* avermitilis MA-4680	CAF60521	Putative efflux protein
5	225	*Saccharopolyspora erythraea*	ZP_06565737	SAM-dependent methyltransferases
6	355	*Actinoplanes teichomyceticus*	CAE53368	DAHP
7	335	*Actinoplanes teichomyceticus*	CAE53369	transcriptional regulator
8	379	*Streptomyces toyocaensis*	AAM80552	Hmo
9	366	*Streptomyces toyocaensis*	AAM80551	HmaS
10	398	*Streptomyces toyocaensis*	AAM80550	Pdh
11	969	*Actinoplanes teichomyceticus*	CAG15028	LuxR regulatory protein
12	775	*Streptomyces fungicidicus*	ABD65949	HpgT/Hmo fusions protein
13	388	*Streptomyces toyocaensis*	AAM80548	DpgA
14	217	*Streptomyces toyocaensis*	AAM80547	DpgB
15	435	*Streptomyces toyocaensis*	AAM80546.1	DpgC

ORF	size (aa)	source	entry	proposed function
16	270	*Streptomyces toyocaensis*	AAM80545	DpgD
17	269	*Frankia* sp. *CcI3*	YP_481545	putative esterase/lipase
18	418	*Frankia* sp. *EuI1c*	YP_004015376	histidine kinase
19	217	*Catenulispora acidiphila* DSM 44928	YP_003117332	Two component transcription regulator
20	74	*Gordonia bronchialis* DSM 43247	YP_003274808	MbtH-like short polypeptide
21	685	*Frankia* sp. CcI3	YP_481558	ABC transporter
22	5447	*Streptomyces violaceusniger* Tu 4113	ZP_07605823	non-ribosomal peptide synthase
23	7911	*Rhodococcus opacus* B4	YP_002782356	non-ribosomal peptide synthetase
24	3407	*Frankia* sp. CcI3	YP_481555.1	non-ribosomal peptide synthase
25	200	*Stackebrandtia nassauensis* DSM 44728	YP_003514660	hypothetical protein
26	390	*Frankia* sp. EuI1c	YP_004015373	peptidoglycan binding protein
27	257	*Frankia* sp. EuI1c	YP_004015372	ABC transporter
28	400	*Frankia* sp. EuI1c	YP_004015371	Putative ABC transporter
29	277	*Streptomyces* sp. C	ZP_07290192	D-aminopeptidase
30	451	*Streptomyces flavogriseus* ATCC 33331	ZP_05803769	putative peptidase
31	663	*Catenulispora acidiphila* DSM 44928	YP_003117332	putative peptidase
32	292	*Streptomyces coelicolor* A3(2)	NP_630572	LD-carboxypeptidase
33	596	*Streptomyces pristinaespiralis* ATCC 25486	ZP_06913570	ABC transporter
34	183	*Streptomyces griseoflavus* Tu4000	ZP_07309655	acetyltransferase
35	649	*Streptomyces kanamyceticus*	BAE95554	Tetratricopeptide

4.6.1 Biosynthesis of non-proteinogenic amino acids

The biosynthesis of Hpg and Dpg has been elucidated with the help of the gene cluster of chloroeremomycin, another vancomycin-like glycopeptides produced by *Amycolatopsis orientalis* (Hubbard et al. 2000; Choroba et al. 2000; Chen et al. 2001; Li et al. 2001), with the help of the balhimycin gene cluster from *Amycolatopsis mediterranei* (Pfeifer et al. 2001) and the complestatin biosynthetic gene cluster of *Streptomyces lavendulae* (Chiu et al. 2001). Genes highly homologous to a p-hydroxymandelate oxidase (Hmo), a p-hydroxymandelic acid synthase (Hmas), a p-hydroxyphenylglycine aminotransferase (HpgT) and a prephenate dehydrogenase (Pdh) were identified in the feglymycin gene cluster (Table 4.8). Hmo, Hmas, HpgT and Pdh have been described before to be responsible for the supply of the non-proteinogenic amino acid Hpg (Hubbard et al. 2000; Choroba et al. 2000; Chiu et al. 2001).

Both L-tyrosine and prephenate can accordingly be used as starting material for Hpg biosynthesis. Prephenate is converted by Pdh into *p*-hydroxyphenylpyurvate which in the next steps is transformed to L-*p*-hydroxymandelate by HmaS and oxidized by Hmo to *p*-hydroxybenzoylformate. L-Tyrosine and *p*-hydroxybenzoylformate are the substrate of a transamination catalyzed by HpgT generating L-*p*-hydroxyphenylglycine (Hpg) and *p*-hydroxyphenylpyruvate. *p*-Hydroxyphenylpyruvate later can be converted to Hpg in another round (Figure 4.38). The identified *Hmo*, *Hmas*, *HpgT* and *Pdh* genes of the feglymycin gene cluster show a strong similarity with previously described Hpg-biosynthesis genes from the teicoplanin gene cluster (Li et al. 2004; Sosio et al. 2003), the balhimycin gene cluster (Pelzer et al. 1999), the complestatin gene cluster of *Streptomyces lavendulae* (Chiu et al. 2001) and the A47934 gene cluster (Pootoolal et al. 2002) (Table 4.9).

Interestingly the HpgT protein was predicted to be an HpgT/Hmo fusion protein. The feglymycin gene cluster therefore consists two genes that might code for Hmo. The *Hmo*, *Hmas* and *Pdh* genes are arranged in line in the same order as described also for the A47934 gene cluster from *S. toyocaensis* (Pootoolal et al. 2002). The *S. toyocaensis* genes also possess the highest similarity to these genes. The gene coding for the HpgT/Hmo fusion protein is separated from the other three genes by one open reading frame. It shows the highest similarity with a predicted HpgT/Hmo fusion protein of the enduracidin producer *Streptomyces fungicidicus* (Yin, Zabriskie 2006).

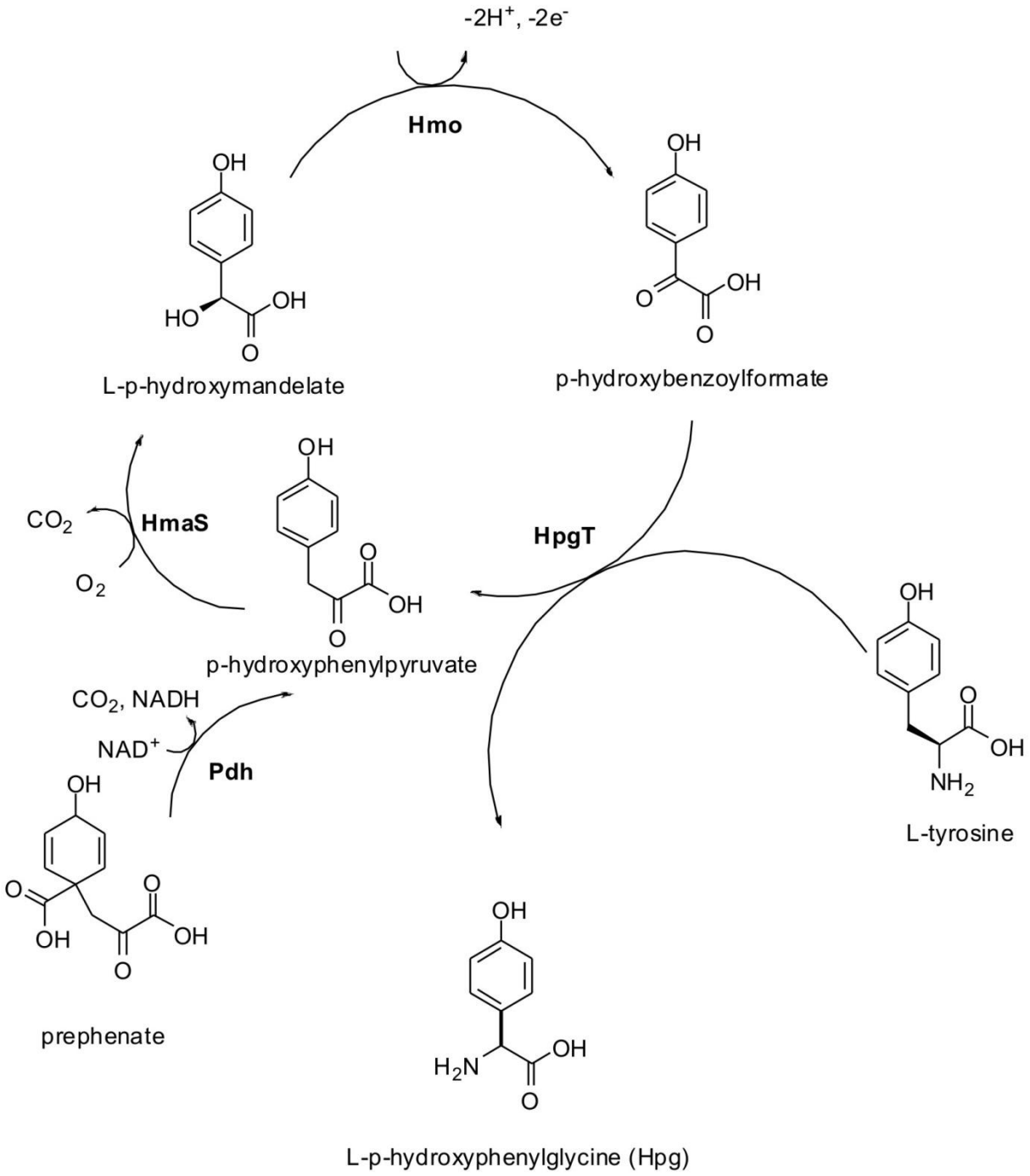

Figure 4.38: Scheme of the Hpg biosynthesis (figure according to Chiu et al. 2001).

ORF 6 codes for a 3-deoxy-D-arabinose-heptulosonate-7-phosphate synthase (DAHP synthase). The DAHP synthase is the first enzyme of the shikimate pathway leading to the biosynthesis of aromatic amino acids like tyrosine. A DAHP synthase has also been described in the teicoplanin gene cluster and has been justified with the high demand of tyrosine (Li et al. 2004). Feglymycin also contains a high number of amino acids originated from tyrosine wherefore the existence of an additional DAHP synthase in the feglymycin gene cluster seems to be reasonable.

The Dpg biosynthesis has been investigated mainly in the balhimycin producer *Amycolatopsis mediterranei* (Pfeifer et al. 2001) and the chloroeremomycin producer *Amycolatopsis orientalis* (Chen et al. 2001; Li et al. 2001). DpgA converts malonyl-CoA to 3,5-dihydroxyphenylacetyl-CoA which in the next step is converted to 3,5-dihydroxyphenylglyoxylate by DpgC (Figure 4.39). DpgB and DpgD were found to dramatically boost the activity of DpgA (Chen et al. 2001). The last step, a transamination of dihydroxyphenylglyoxylate to Dpg is expected to be catalyzed by the HpgT protein (Figure 4.39) (Chen et al. 2001). The feglymycin gene cluster contains four ORFs in line coding for DpgA, DpgB, DpgC and DpgD. A gene inactivation mutant of the *DpgD* gene led to abortion of feglymycin production indicating the importance of the gene for feglymycin production (Figure 4.41).

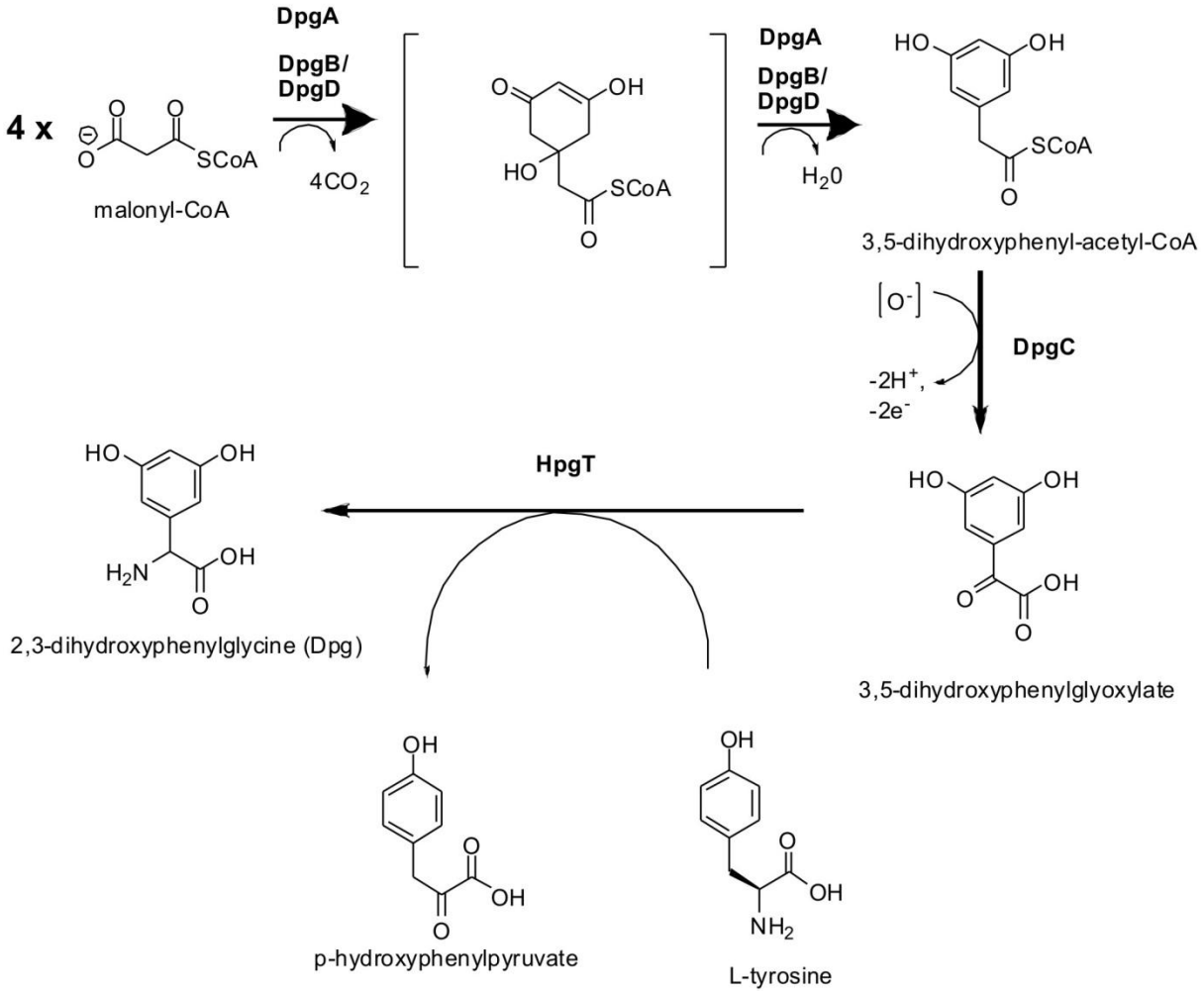

Figure 4.39: Scheme of the Dpg biosynthesis (figure according to Chen et al. 2001).

The ORFs have the same arrangement and highest similarity to the *DpgA-D* genes in *S. toyocaensis* (Table 4.9) (Pootoolal et al. 2002). The absence of an additional *HpgT* gene in the feglymycin gene cluster indicates that the transamination reaction

in the Dpg biosynthesis might be catalyzed by the same HpgT protein as in the Hpg biosynthesis thus indicating an interconnection of the Hpg and Dpg biosynthesis pathways in *Streptomyces* sp. DSM 11171. Such dual function has also been postulated for the Pgat protein of the balhimycin gene cluster (Pfeifer et al. 2001; Recktenwald et al. 2002).

Table 4.9: ORFs that were identified in the region of the feglymycin biosynthesis gene cluster that show a strong homology to ORFs of known NRPS gene clusters.

Reference		Li et al.(Li et al. 2004)	Pelzer et al. (Pelzer et al. 1999)	Pootoolal et al. (Pootoolal et al. 2002)	Chiu et al. (Chiu et al. 2001)	van Wageningen et al. (van Wageningen et al. 1998)	Yin et al.(Yin, Zabriskie 2006)
product	feglymycin	teichoplanin	balhimycin	A47934	complestatin	chloroeremomycin	enduracidin
strain	*Streptomyces* sp. DSM 11171	*Actinoplanes teichomyceticus*	*Amycolatopsis balhimycina*	*Streptomyces toyocaensis*	*Streptomyces lavendulae*	*Amycolatopsis orientalis*	*Streptomyces fungicidicus*
		tei	bal	sta	com	Cep	end
DAHP	ORF 6	ORF14*					
transcriptional regulator	ORF 7	x	bbr	StaQ	ComG	CZA382.26	ORF24
Hmo	ORF 8	ORF29*	hmo	Hmo	Hmo	ORF22	
HmaS	ORF 9	ORF28*	hmaS	HmaS	HmaS	ORF21	ORF25
Pdh (PD)	ORF 10	ORF24*	Pdh	Pdh	PD	ORF1	ORF23
LuxR regulatory protein	ORF 11	ORF16*					
HpgT/Hmo fusions protein	ORF12	ORF23*	pgat	HpgT	HpgT	PCZA361.25	ORF29
DpgA	ORF13	ORF17*	dpgA	DpgA		ORF27	
DpgB	ORF14	ORF18*	dpgB	DpgB		ORF28	
DpgC	ORF15	ORF19*	dpgC	DpgC		PCZA361.8	
DpgD	ORF 16	ORF20*	dpgD	DpgD		ORF30	
putative alpha/beta fold esterase/lipase	ORF 17	x	bhp			PCZA361.30	ORF34
histidine kinase	ORF 18	x					
two component transcription regulator	ORF 19	x		VanRst			
MbtH-like short polypeptide	ORF 20	ORF1*	orf1		ComE		ORF46
ABC transporter	ORF 21	x	abc	StaU	ComL	ORF2	ORF33
NRPS (FegA)	ORF 22	teiC	bpsB	StaC	ComC	CepB	

4.6.2 Annotation of the NRPS genes

NPRS genes of the feglymycin biosynthesis gene cluster were analyzed with the NCBI blast tool (Mizyed et al. 2005) and the NRPS/PKS analysis tool of the University of Maryland (Bachmann, Ravel 2009a). The NRPS region spans over about 50 kb and includes three ORFs that are organized collinearly. The first ORF22 contains four modules, the second one (ORF23) six modules and the last one (ORF24) three modules. The first module is a loading module with A-T domain structure, followed by 11 elongation modules and a release module with a C-terminal thioesterase domain. The number of modules precisely corresponds to the number of amino acids of feglymycin (Figure 4.40).

Table 4.10: Predicted amino acids (according to Bachmann, Ravel 2009a) and amino acid sequence of feglymycin.

module	predicted amino acid specificity of A-domain (Bachmann, Ravel 2009a)	predicted configuration	amino acid of feglymycin
1	Tyr	D	D-Hpg
2	Tyr	D	D-Dpg
3	Val	L	L-Val
4	Tyr	D	D-Dpg
5	Hpg	L	L-Hpg
6	Tyr	D	D-Dpg
7	Hpg	L	L-Hpg
8	Tyr	D	D-Dpg
9	Val	L	L-Val
10	Tyr	D	D-Dpg
11	Hpg	L	L-Hpg
12	Phe	L	L-Phe
13	Asp	L	L-Asp

The organization of the epimerase domains (E-domains) also corresponds to the organization expected from the chemical structure formula and configuration of amino acids of feglymycin. The stereochemical outcome of the feglymycin structure is reflected by the configurational sequence D-D-L-D for the first ORF, L-D-L-D-L-D for the second ORF and L-L-L for the last ORF. A prediction of the amino acid substrates of the amino adenylation domains (A-domains) with the PKS/NRPS analysis tool of the

University of Maryland (Bachmann, Ravel 2009a) resulted in the following sequence: Tyr-Tyr-Val-Tyr-Hpg-Tyr-Hpg-Tyr-Val-Tyr-Hpg-Phe-Asp.

Except for the misconstruction of the first Hpg and all Dpg residues the results are in perfect agreement with the structure of feglymycin (Table 4.10). The false interpretation of the Dpg residues and the D-Hpg residue might be explained by the low occurrence of these non-natural amino acids in NRPS clusters and hence in current NRPS databases. The first NRPS (ORF22) has strong homologies to NRPS ORFs of the related clusters like the TeiC protein in the teicoplanin gene cluster of *Actinoplanes teichomyceticus* (Li et al. 2004; Sosio et al. 2004), the BpsB protein in the balhimycin cluster of *Amycolatopsis bahimycina* (Pelzer et al. 1999) and the StaC protein in the gene cluster of A47934 producing *Streptomyces toyocaensis* (Pootoolal et al. 2002). In comparison with the homologous NRPS the position of ORF22 in the elongation cycle has shifted in the feglymycin gene cluster. While the homologous NRPS are the second (BpsB) or third NRPS (StaC, TeiC) in the elongation cycle, the NRPS in feglymycin is the first in the elongation process and contains the loading module. The second and third NRPSs of the feglymycin gene cluster (ORF23 and ORF24) have no strong homologies to NRPS of the related clusters. Instead the second NRPS shows a strong similarity to NRPS identified from different *Rhodococcus* strains but also the gramicidin synthetase LgrB from *Streptomyces albus* (Kessler et al. 2004). The third NRPS (ORF24) possesses strong similarities to NPRSs identified from different *Streptomyces* strains and *Rhodococcus* strains. An MbtH domain protein that can be found in similar form in nearly all related gene clusters was identified in ORF20. MbtH-like proteins were shown to influence amino acid activation and to work as integral components of bacterial non-ribosomal peptide synthases (Felnagle et al. 2010; Zhang et al. 2010).

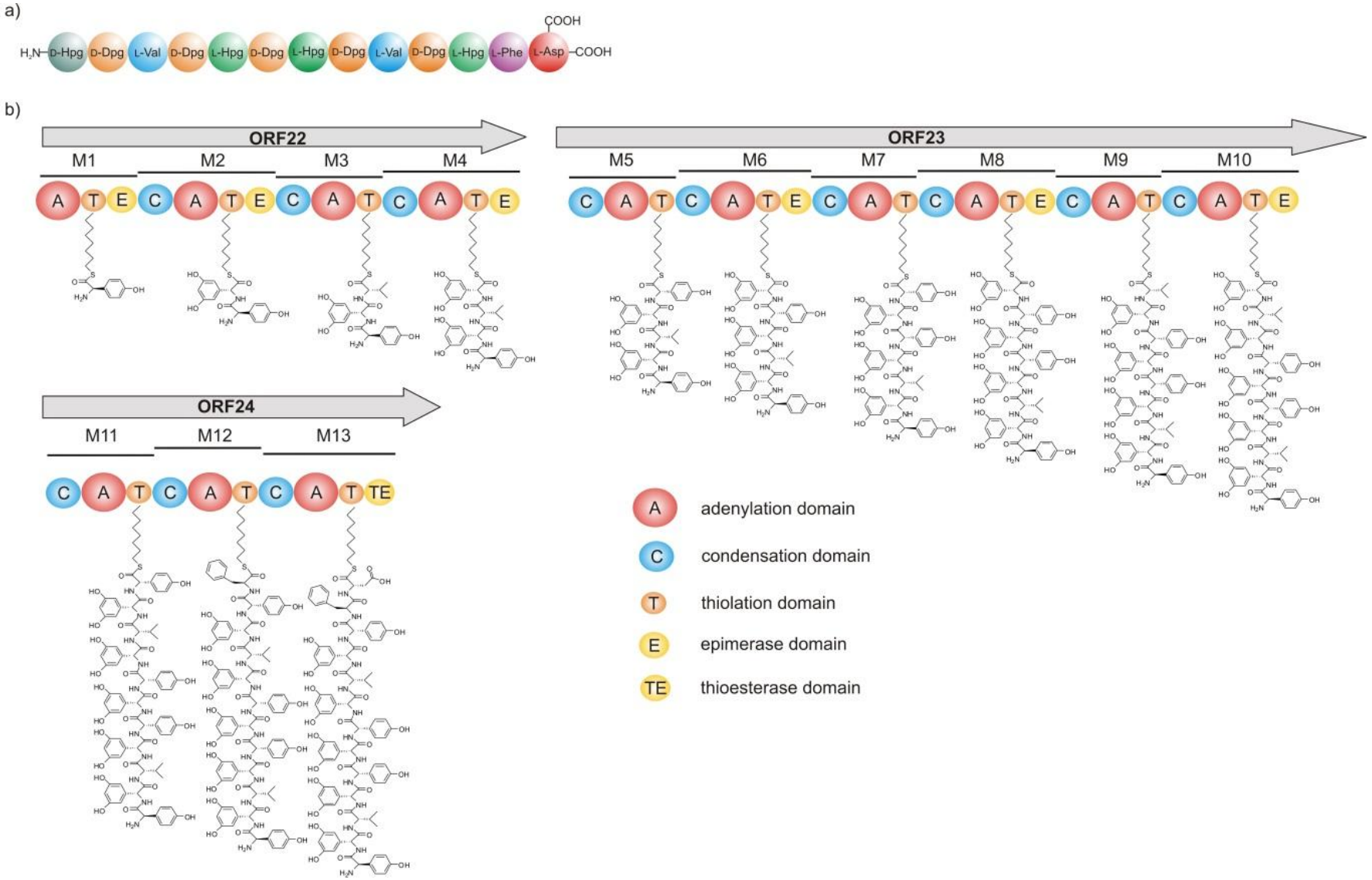

Figure 4.40: a) Ball-model of feglymycin. b) Organization of the NRPS genes and deduced biosynthesis assembly line for feglymycin.

4.6.3 Testing of gene inactivation mutants of the feglymycin gene cluster

Gene inactivation single crossover mutants of ORF 7, ORF13 (DpgA), ORF26 and ORF27 were generated by Dipl.-Ing. Lara Michel Mata (Diplomarbeit, TU Berlin 2011) and detected for feglymycin production by SIM-measurements with LC-Triple-Quad-MS (Figure 4.41). The wild type strain *Streptomyces* sp. DSM 11171 was used as positive control. The generated mutants possess an apramycin resistance cassette inserted in the corresponding position of the four genes. The gene inactivation mutants were therefore cultivated in E1 medium with 25 µg/mL apramycin and 400 µg/mL phosphomycin. Phosphomycin was added both to the gene inactivation mutants and the wild type, as it was found that *Streptomyces* sp. DSM 11171 has a natural phosphomycin resistance. The production controls were always performed with two different mutants and feglymycin production was tested both in 7 d, 10 d and 14 d old bacterial cultures. All measurements were performed in triplicate.

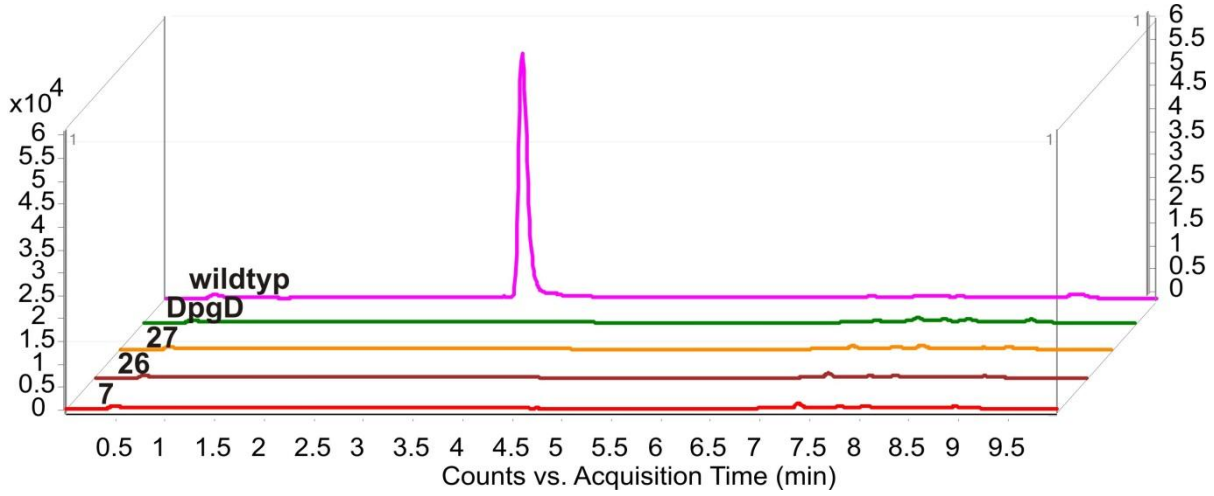

Figure 4.41: SIM-MS measurements of feglymycin with LC-Triple-Quad-MS in negative ionization mode of extracts from cell pellets of wild type and gene inactivation mutants of *Streptomyces sp.* DSM 11171 cultured for 10 d in E1 medium. pink) wild type, green) DpgA mutant, yellow) ORF27 mutant, purple) ORF26 mutant, red) ORF7 mutant. Only for the wild type strain a peak at the characteristic retention time of feglymycin (R_t = 3.7 min) was detected.

All four mutants failed to produce feglymycin in comparison to the wild type strain, indicating that these four genes are essential for feglymycin production and belong to the feglymycin gene cluster (Figure 4.41). To rule out a possible interference of the antibiotic apramycin with feglymycin production the experiment was repeated without

adding apramycin to the main culture of the knock-out mutants. The result was however the same.

4.6.4 Further genes identified in the feglymycin gene cluster

The feglymycin gene cluster contains several genes that can be connected to regulatory functions (Table 4.8). ORF7 has strong similarities to a transcription regulator with a ParB domain and ORF11 to a LuxR like transcription regulator. Both show the highest similarity to homologues in the teicoplanin gene cluster of *A. teichomyceticus* (Li et al. 2004; Sosio et al. 2004). ORF7 additionally has strong similarities to the StaQ transcription regulator described in the A47934 gene cluster of *S. toyocaensis* (Pootoolal et al. 2002) and to homologues in gene clusters of *A. balhimycina*, *S. lavendulae* and *S. fungicidicus*. The strong homology of these putative regulators to genes in related clusters indicates a high degree of conservation and an important role in regulation of the feglymycin gene cluster and related antibiotics. Experiments with an ORF7 gene inactivation mutant proofed that this transcription regulator is essential for feglymycin production (Figure 4.41). ORF18 codes for a histidine kinase and ORF19 for a two component transcription regulator. Both genes possibly are also involved in regulation of the feglymycin gene cluster. ORF19 shows similarities to the VanRst ORF found in *S. toyocaensis* (Pootoolal et al. 2002). In *S. toyocaensis* VanRst is expected to be associated with the regulation of the *VanH, VanA* and *VanX* resistance genes (Pootoolal et al. 2002). The *VanH, VanA and VanX* genes are predicted to be responsible for host resistance to vancomycin-like antibiotics by conversion of D-Ala-D-Ala in the peptidoglycan layer to D-Ala-D-lactate (Walsh et al. 1996). By inclusion of D-Ala-D-lactate instead of D-Ala-D-Ala in the peptidoglycan layer the inhibition of cell-wall biosynthesis due to binding of vancomycin-like antibiotics to the D-Ala-D-Ala motif can be bypassed. However no genes homologous to *VanH, A* and *X* were found in the feglymycin gene cluster nor in the genome sequence of *Streptomyces* sp. DSM 11171. The lack of the common host resistance cluster in *Streptomyces* sp. DSM 11171 corresponds to the previous finding, that feglymycin has a different mode of action compared to the vancomycin-like glycopeptides and that feglymycin does not inhibit the late stages of peptidoglycan biosynthesis. ORF19 also possess even stronger homology to the CutR regulator described to be responsible for the regulation of production of the polyketide antibiotic and pigment actinorhodin in *Streptomyces lividans* (Chang et al.

1996) and the CutR protein from *Streptomyces avermitilis* MA-4680 invovled in copper metabolism (Tseng, Chen 1991). ORF19 might therefore not be related to host resistance but possess a different regulatory function. ORF4 codes for a putative transmembrane efflux protein possibly involved in host resistance to feglymycin. Interesting was the finding of a protein with a peptidoglycan binding domain in ORF26 in close neighborhood to the NRPS genes. Remarkably ORF26 was found to be essential for feglymycin production (Figure 4.41). Peptidoglycan binding domains can be found in enzymes involved in the degradation of the bacterial cell wall (Briers et al. 2007). For ORF26 however no domains with lytic activity were predicted. Striking is also the high number of predicted peptidases in close distance of the feglymycin gene cluster e.g. ORF1, ORF29-32. A connection to the feglymycin gene cluster is however speculative.

Several genes were identified in the feglymycin gene cluster that might be connected to feglymycin transport. A predicted ABC-transporter ORF21 was found in close distance to the NRPS genes. ORF21 has strong homologies to a predicted ABC-transporter in the balhimycin gene cluster from *A. balhimycina* and the *StaC* gene in *S. toyocaensis* (Pootoolal et al. 2002). Homologous genes also exist in the gene clusters of *S. lavendulae* and *S. fungicidicus*. Two further putative ABC transporters can be found downstream of the feglymycin gene cluster in ORF27 and ORF28. A knock-out mutant of the ORF27 gene leads to the abortion of feglymycin production (Figure 4.41). ORF17 codes for a putative alpha/beta fold esterase or lipase. Homologues exist in the balhimycin (Pelzer et al. 1999) and the enduracidin gene cluster (Yin, Zabriskie 2006). The function however is unclear. ORF2 codes of a putative radical SAM domain protein and ORF4 for a putative SAM-dependent methyltransferase. It is however not certain that they are connected to the feglymycin biosynthesis.

4.7 Further gene cluster discovered in the genome of *Streptomyces* sp. DSM 11171

By searching the *Streptomyces* sp. DSM 11171 genome with the artemis gene annotation tool (Rutherford et al. 2000) for open reading frames with a size larger than 1000 bp five further likely NRPS and PKS gene cluster were identified. These gene clusters were also analyzed with the NCBI blast tool (Mizyed et al. 2005) and the NRPS/PKS analysis tool of the University of Maryland (Bachmann, Ravel 2009a). The clusters were denominated as “small NRPS cluster” (cluster II), “NRPS-PKS cluster” (cluster III), “small PKS clusters” (cluster IV), “siderophore cluster” (cluster V) and “one-modulare NRPS cluster” (cluster VI) on the basis of their most striking characteristics and will be referred to under this names in the following text.

4.7.1 Small NRPS gene cluster (cluster II)

The gene cluster named “small NRPS cluster” (cluster II) is expected to span over a region of nearly 30 kb (Figure 4.42). The gene cluster is framed by coding DNA regions making it difficult to precisely determine the borders of the gene cluster and to predict which genes belong to the biosynthesis of the expected NRPS product. The in the following described genes might therefore also not all be genes belonging to this cluster. A remarkable finding is the large number of possible tailoring enzymes. ORF6, ORF8 and ORF14 code for monooxygenases, two of which are located directly next to the NRPS encoding gene (ORF6, ORF8). ORF6 is predicted to be a cytochrome P450 monooxygenase which is highly homologous to previous identified monooxygenases e.g. in the pristinamycin gene cluster of *Streptomyces pristinaespiralis* (Mast et al. 2011). ORF8 codes for a FAD-dependent monooxygenase with about 40 % identity to a molybdenum-containing oxidoreductase found to be a tailoring oxidase in the biosynthesis of the antitumor antibiotic dynemicin, a member of the enediyne family produced by *Micromonaspora chersina* (Gao, Thorson 2008). Interestingly, in *Streptomyces* sp. DMS 11171 the oxidoreductase domain is linked to a possible C-domain. A further putative monooxygenase is located in ORF14 highly homologous to diverse F420-dependent oxidoreductases.

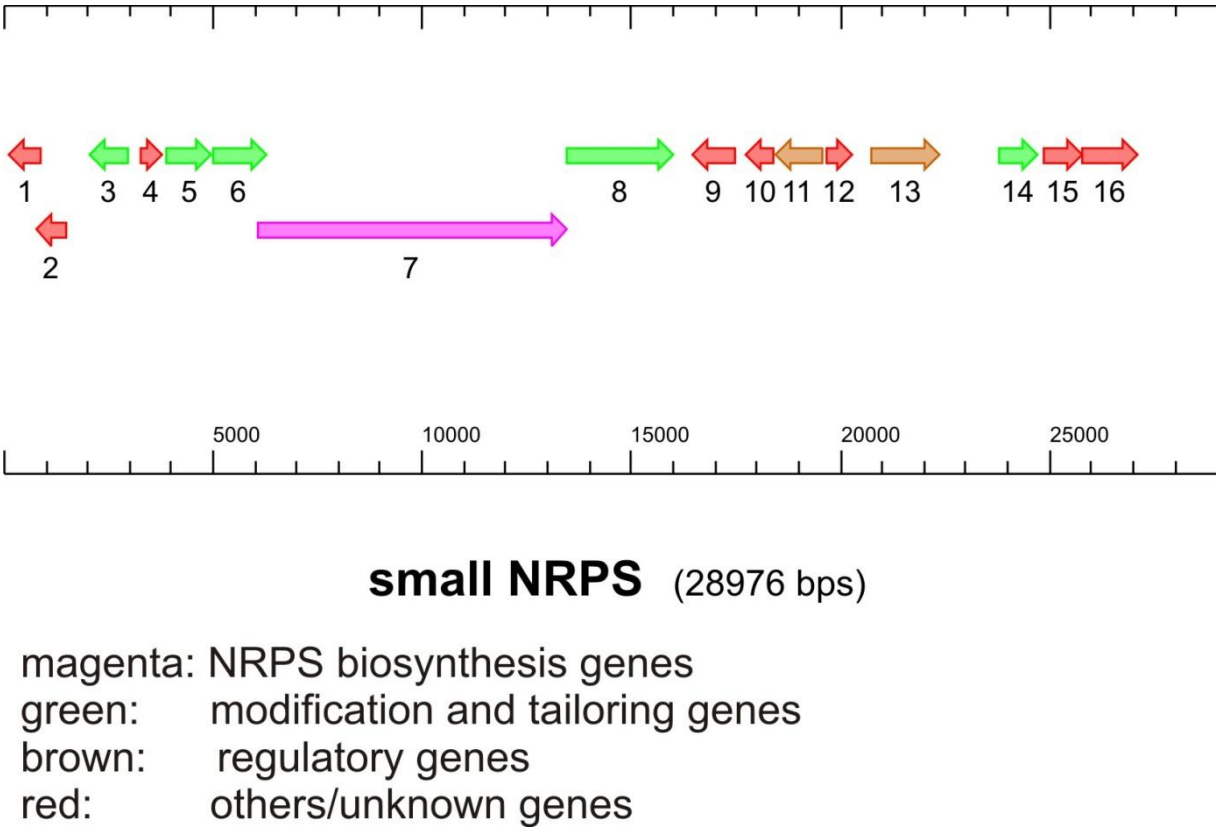

Figure 4.42: Arrangement of the small NRPS gene cluster (cluster II).

In close distance to the NRPS gene, in ORF5, additionally a SAM-dependent methyltransferase is located which shares about 70 % identity with an *O*-methytransferase described in the biosynthesis gene cluster of the PKS antibiotic rifamycin from *Amycolatopsis mediterranei* S699 (August et al. 1998) and the MitM and MitN *O*-methyltransferases described in the gene cluster of the antitumor antibiotic mitomycin C in *Streptomyces lavendulae* NRRL 2564 (Mao et al. 1999). *N*- and *C*-methylations are common modifications of nonribosomal peptides. There *S*-adenosylmethionine (SAM) is often the source of the methyl-group (Schwarzer et al. 2003). ORF15 and ORF16 both code for homocysteine *S*-methyltransferases. Homocysteine *S*-methyltransferases catalyse the conversion of SAM and L-homocysteine to *S*-adenosyl-L-homocysteine and L-methionine and also the back reaction and participate in the methionine metabolism (Balish, Shapiro 1967). Additional homocysteine *S*-methyltransferases present in this cluster might be justified by a higher demand of SAM due to a possible methylation of the NRPS product. ORF3 codes for a putative short-chain dehydrogenase/reductase possibly also involved in tailoring of the gene cluster product (Kallberg et al. 2002).

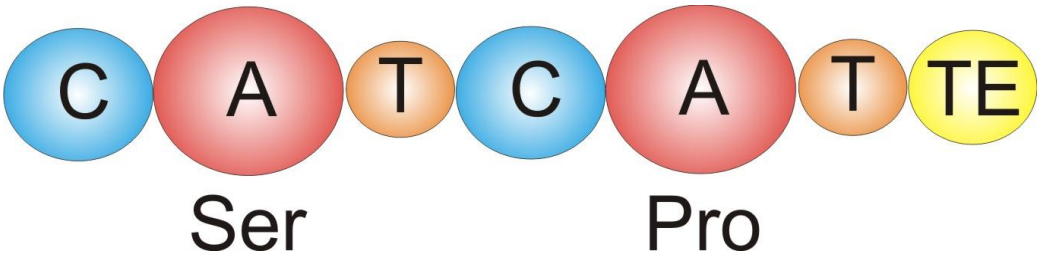

Figure 4.43: Organization of the NRPS genes and predicted amino acid specificities of the A-domains (according to Bachmann, Ravel 2009a).

The NPRS gene (ORF7) is predicted to have typical NRPS organization. The A-domains are predicted to accept L-Ser and L-Pro as substrates (Figure 4.43). The predicted peptide is therefore very short and apparently only contains proteinogenic amino acids. The large number of possible tailoring enzymes and the possibility of an iterative biosynthesis, could however hint to a di-, tri- or multimerization of the dipeptide by the Te-domain and to a strong tailoring.

ORF11 and ORF13 code for putative transcription regulators possibly involved in the regulation of the gene cluster. Beside the tailoring enzymes the small NRPS cluster contains further interesting enzymes (Table 4.11). E.g. a possible calcium binding enzyme in ORF4 with an EF hand domain. EF hand domain proteins can work as molecular switch and play a role in the calcium signaling in cells (Capozzi et al. 2006). ORF9 codes for a 3-oxoacyl-[acyl-carrier-protein (ACP)]-synthase highly homologous to a gene in the genome of the erythromycin producer *Saccharopolyspora erythraea* (Oliynyk et al. 2007) and ORF12 for an isochorismatase. The 3-oxoacyl-(ACP)-synthase uses Acetyl-CoA and Malonyl-CoA to form oxoacyl- and catalyzes the first step in the fatty acid biosynthesis. The isochorismatase catalysis the formation of 2,3-dihydroxy-2,3-dihydrobenzoate and pyruvate from isochorismate and plays a role in the biosynthesis of dihydroxybenzoate containing siderophores like enterobactin (Raymond et al. 2003a). ORF1, ORF2 and ORF10 code for highly conserved hypothetical proteins. The connection and interplay of all these interesting enzymes to the small NRPS biosynthesis is however difficult to predict.

Remarkably, no ABC-transporters and no MbtH-like protein could be identified in the region of the gene cluster.

Table 4.11: ORFs that were identified in the region of the small NRPS gene cluster (cluster II).

ORF		best match		
ORF	size (aa)	source	entry	proposed function
1	266	*Streptomyces clavuligerus* ATCC 27064	ZP_08219737	conserved hypothetical protein
2	229	*Streptomyces griseoflavus* Tu4000	ZP_07310245	conserved hypothetical protein
3	306	*Streptomyces* sp. Mg1	ZP_04996125	putative short-chain dehydrogenase
4	183	*Streptomyces* sp. Mg1	ZP_04996126	calcium-binding protein
5	358	*Streptomyces* sp. Mg1	ZP_04996127	SAM dependent methyltransferase
6	420	*Streptomyces* sp. Mg1	ZP_04996128	cytochrome P450 monooxygenase
7	2463	*Streptomyces* sp. Mg1	ZP_04996129	non-ribosomal peptide synthetase
8	844	*Streptomyces clavuligerus* ATCC 27064	ZP_06771754	probable FAD-dependent monooxygenase
9	341	*Streptomyces* sp. Mg1	ZP_04996133	3-oxoacyl-[acyl-carrier-protein] synthase
10	219	*Streptomyces ghanaensis* ATCC 14672	ZP_06581823	conserved hypothetical protein
11	414	*Streptomyces clavuligerus* ATCC 27064	ZP_06776081	putative transcriptional regulator
12	210	*Streptomyces* sp. e14	ZP_06711196	isochorismatase
13	545	*Streptomyces pristinaespiralis* ATCC 25486	ZP_06908802	bldA-regulated nucleotide binding protein
14	307	*Streptomyces griseus subsp. griseus* NBRC 13350	YP_001823089	putative F420-dependent oxidoreductase
15	305	*Streptomyces pristinaespiralis* ATCC 25486	ZP_06908798	homocysteine *S*-methyltransferase
16	480	*Streptomyces pristinaespiralis* ATCC 25486	ZP_06908798	homocysteine *S*-methyltransferase

4.7.2 NRPS-PKS cluster (cluster III)

The gene cluster named “NRPS-PKS cluster” is expected to span over a region of slightly more than 30 kb and contains four NRPS-like genes (ORF6, ORF7, ORF9, ORF10) and one PKS gene (ORF5) (Figure 4.44). Furthermore it contains several regulators, transporters and two possible peptidases and one 4-phosphopantetheinyl transferase (SFP, ORF2) (Table 4.12). The gene cluster is framed by coding DNA regions making it difficult to determine the borders of this cluster.

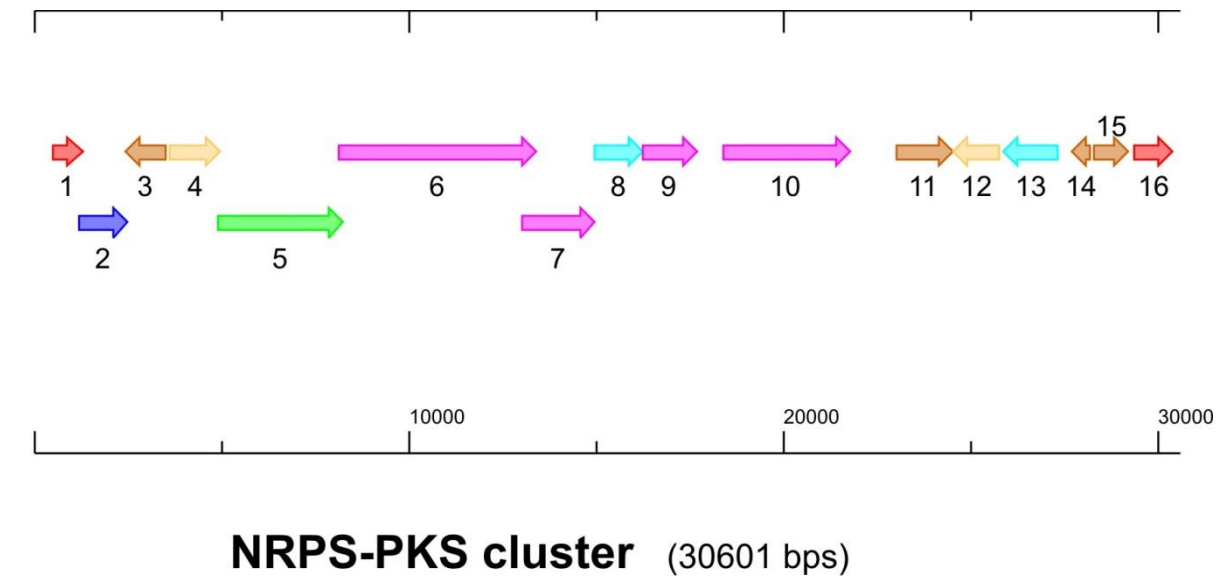

Figure 4.44: Arrangement of the NRPS-PKS gene cluster (cluster III).

4'-phosphopantetheinyl transferases (SFPs) can serve for both NRPS and PKS biosynthesis. The SFP activates NRPS and PKS by transferring a 4-phosphopantetheine (4'PP) cofactor from coenzyme A to the PCP (peptidyl carrier protein; NRPS) or ACP (acetyl carrier protein; PKS) (Lambalot, Walsh 1995). The putative SFP gene in ORF2 shows 45 % identity with the *ovmF* gene of the biosynthetic gene cluster of the PKS oviedomycin from *Streptomyces antibioticus* ATCC 11891 (Lombó et al. 2004). ORF1 codes for a highly conserved protein with an *S*-adenosyl methyltransferase domain. The existence of a methyltransferase might indicate a possible modification by methylation. Likewise, this assumption is supported by the presence of a homocysteine *S*-methyltransferase in ORF16.

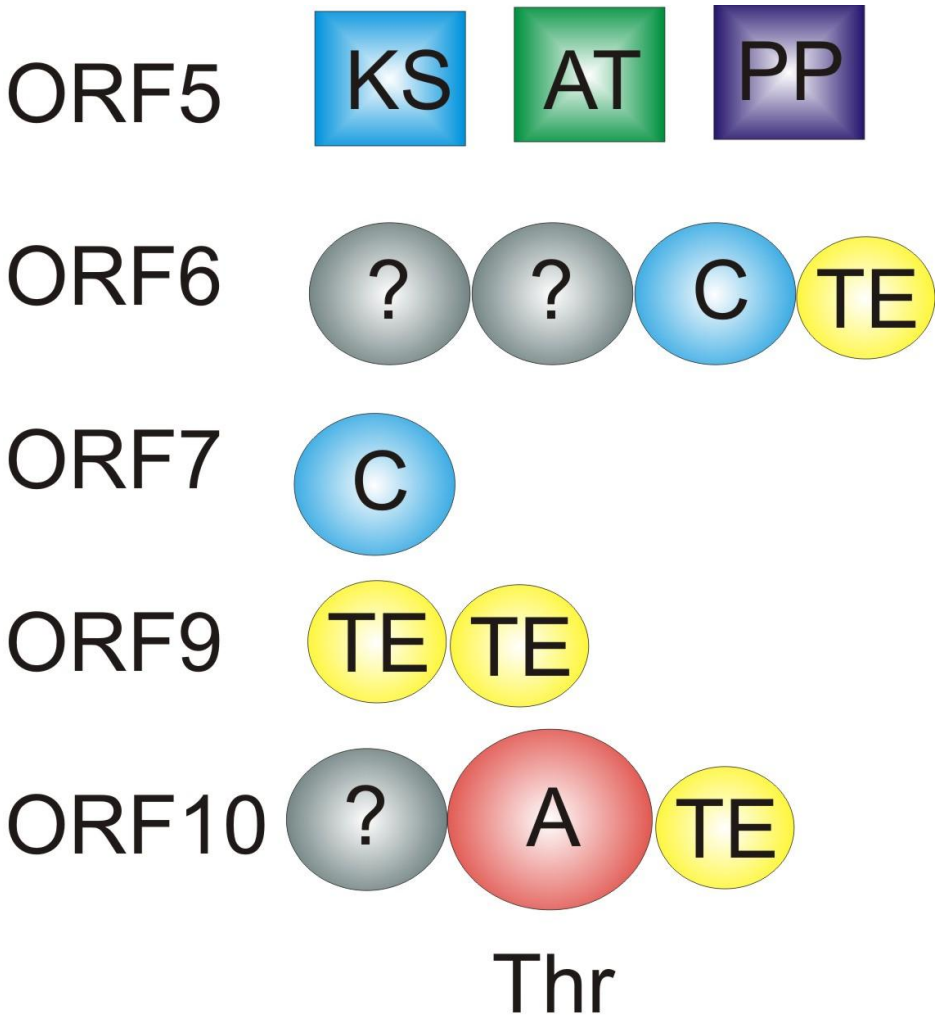

Figure 4.45: Organization of the NRPS (ORF6, ORF7, ORF9, ORF10) and PKS (ORF5) genes and predicted amino acid specificities of the A-domains (Bachmann, Ravel 2009a).

The PKS gene (ORF5) contains three typical PKS modules: a ketosynthase (KS) module, an acyltransferase (AT) module and a thioesterase (PP) module. The thioesterase was also predicted to be an acyl carrier protein (ACP). PKS biosynthesis normally requires three essential domains to form a *β*-keto ester intermediate: a KS, an AT and an ACP (Staunton, Weissman 2001). PKS biosynthesis genes can also contain a variety of further modifying domains like e.g. a ketoreductase (KR), a dehydratase (DH) and a enoyl reductase (ER) (Staunton, Weissman 2001), this is however not predicted for ORF5 (Figure 4.45).

The NRPS genes show no typical organization and the online prediction tool failed to predict the function of several of the NRPS modules. For the first NRPS gene two non-identifyable modules were predicted followed by a C-domain and a Te-domain. The C-domain in ORF6 was predicted to be untypically positioned directly next to the Te-domain. ORF7 was predicted to be a lone-standing C-domain and ORF9 two adjacent lone-standing Te-domains. For ORF10 the first module could not be identified. It might however be a C-domain as it is followed by an A-domain, predicted to accept Thr, and a Te-domain (Figure 4.45). ORF3, ORF11 and ORF15 are highly homologous to numerous putative transcription regulators and are possibly involved in regulation of the NRPS-PKS gene cluster. ORF14 might also be connected to regulation as it is predicted to be an ATP-binding protein and is about 40 % identical to the *ecaE* gene connected with gene regulation of the antibiotic actinorhodin in *Streptomyces coelicolor* (Huang et al. 2001). ORF3 and ORF12 are predicted to be transporters possibly involved in transport of the gene product out of the bacteria cell. ORF12 is about 60 % identical to a transporter identified in the gene cluster of the herbicide phosphinothricin tripeptide from *Streptomyces viridochromogenes* Tü494 (Schwartz et al. 2004).

ORF13 is predicted to be a possible lipase or esterase and ORF8 possesses a M18 peptidase aspartyl aminopeptidase domain and is highly homologous to diverse putative aminopeptidases. The connection of these two genes in the NRPS-PKS gene cluster is however uncertain.

Table 4.12: ORFs that were identified in the region of the NRPS-PKS gene cluster (cluster III).

ORF		best match		
ORF	size (aa)	source	entry	proposed function
1	260	*Streptomyces ghanaensis* ATCC 14672	ZP_04688780	conserved hypothetical protein
2	414	*Streptomyces pristinaespiralis* ATCC 25486	ZP_06907893	phosphopantetheinyl transferase
3	367	*Streptomyces roseosporus* NRRL 15998	ZP_04695889	LuxR family transcriptional regulator
4	498	*Streptomyces cf. griseus* XylebKG-1	ZP_08236170	major facilitator superfamily permease
5	1110	*Streptomyces cf. griseus* XylebKG-1	ZP_08236171	PKS
6	1753	*Streptomyces roseosporus* NRRL 15998	ZP_04695885	NRPS
7	632	*Streptomyces griseus subsp. griseus* NBRC 13350	YP_001823997	putative NRPS
8	427	*Streptomyces griseus subsp. griseus* NBRC 13350	YP_001823998	Aspartyl aminopeptidase
9	492	*Streptomyces cf. griseus* XylebKG-1	ZP_08236174	thioesterase
10	1131	*Streptomyces avermitilis* MA-4680	NP_824375	NRPS
11	487	*Streptomyces avermitilis* MA-4680	NP_822883	putative transcriptional regulator
12	424	*Streptomyces pristinaespiralis* ATCC 25486	ZP_06908448	transmembrane transporter
13	494	*Streptomyces hygroscopicus* ATCC 53653	ZP_07299637	lipolytic enzyme, G-D-S-L
14	146	*Streptomyces roseosporus* NRRL 15998	ZP_04697493	regulatory protein
15	299	*Streptomyces pristinaespiralis* ATCC 25486	ZP_06908070	transcription regulator
16	480	*Streptomyces pristinaespiralis* ATCC 25486	ZP_06908798	homocysteine *S*-methyltransferase

4.7.3 Small PKS cluster (cluster IV)

The gene cluster named “small PKS cluster” is expected to span over a region of nearly 30 kb and is, similarly to the previous described gene clusters, framed by coding DNA regions. It contains one PKS gene, several genes that can be related to fatty acid biosynthesis, further genes possibly involved in tailoring and one transporter gene (Figure 4.46).

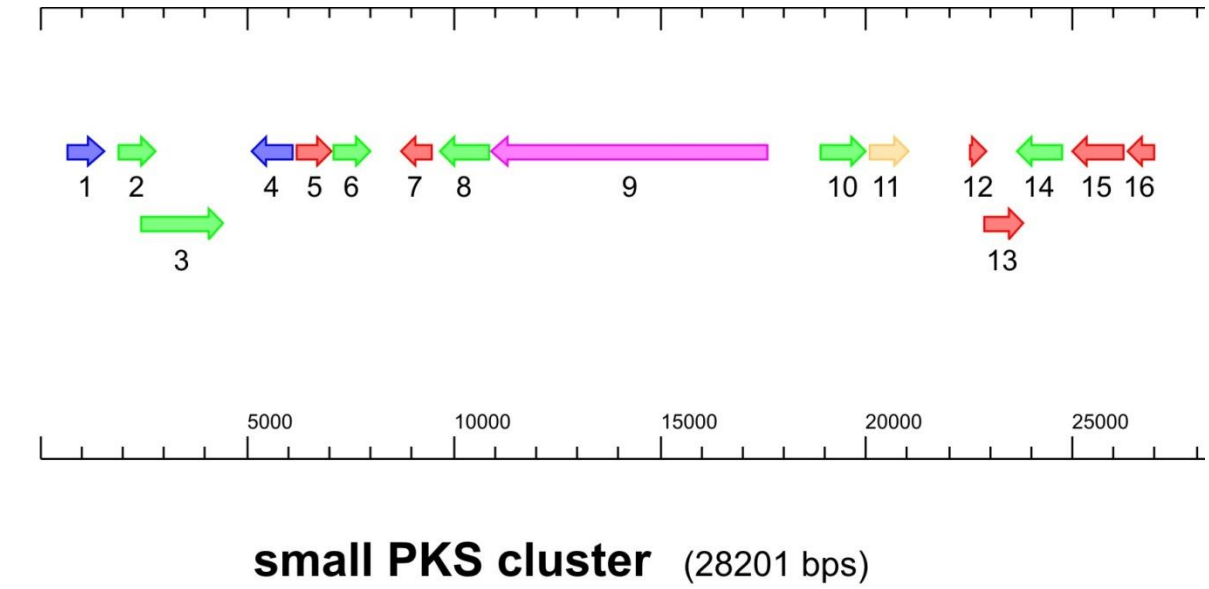

Figure 4.46: Arrangement of the small PKS gene cluster (cluster IV).

ORF1 codes for a putative 3-hydroxybutyryl-CoA dehydrogenase. 3-hydroxybutyryl-CoA dehydrogenases catalyze the convertion of 3-hydroxybutanoyl-CoA to 3-acetoacetyl-CoA using $NADP^+$ as proton acceptor and play a role in the *β*-oxidation of fatty acids (Colby, Chen 1992) and in the formation of short-chain fatty acid like butyrate (Seedorf et al. 2008). ORF4 is predicted to be an oxidoreductase and possesses a domain characteristic for 3-hydroxyisobutyrate dehydrogenases. 3-hydroxyisobutyrate dehydrogenases convert 3-hydroxy-2-methylpropanoate to 2-methyl-3-oxopropanoate (Rougraff et al. 1988). The butyrate metabolism provides precursors for the dicarboxyl acids used for polyketide biosynthesis (Liu, Reynolds 2001). The existence of genes connected to fatty acid biosynthesis, butyrate metabolism and related pathways in a PKS gene cluster therefore seems reasonable.

There are several genes in the gene cluster that could be involved in tailoring reactions of the gene product (Table 4.13). ORF2 and ORF3 are predicted to be 5-methyltetrahydropteroyltriglutamate-homocysteine methyltransferases catalyzing the reaction of 5-methyltetrahydropteroyltri-L-glutamate and L-homocysteine to tetrahydropteroyltri-L-glutamate and L-methionine connected to methionine metabolism. Interestingly, both share 50 % identity with a cobalamin-independent methionine synthase in the plant *Arabidopsis thaliana* (Ravanel et al. 2004). Analysis with the NCBI blast tool indicates that ORF2 and ORF3 might form a single protein but were disrupted by default sequencing. ORF6 codes for a putative hydrolase with about 40 % identity with the *lipE* gene in the gene cluster of antibiotic friulimicin in *Actinoplanes friuliensis* (Heinzelmann et al. 2005), about 35 % identity with tailoring enzymes in the vancomycin producer *Amycolatopsis orientalis* (a non-heme halogenase) (van Wageningen et al. 1998) and in the bahimycin producer *Amycolatopsis balhimycina* (a putative hydrolase) (Pelzer et al. 1999).

Three genes in the small PKS gene cluster hint to a connection to isoprenoid biosynthesis (Table 4.13). ORF10 is predicted to code for a polyprenyl diphosphate synthase and has 46 % identity with the PntB protein from *Streptomyces arenae* connected to sesquiterpenoid antibiotic pentalenolacton biosynthesis (Zhu et al. 2011). Polyprenyl diphosphate synthases catalyze the reaction of farnesyl diphosphate and isopentenyl diphosphate to polyprenyl diphosphate and are generally involved in isoprenoid biosynthesis (Okada et al. 1996). ORF8 and ORF14 also code for proteins that might be connected to isoprenoid biosynthesis. ORF8 is predicted to possess a geranyl geranyl reductase domain and ORF14 possesses 30 % identity with a terpene synthase of *Planobispora rosea* (Giardina et al. 2010).

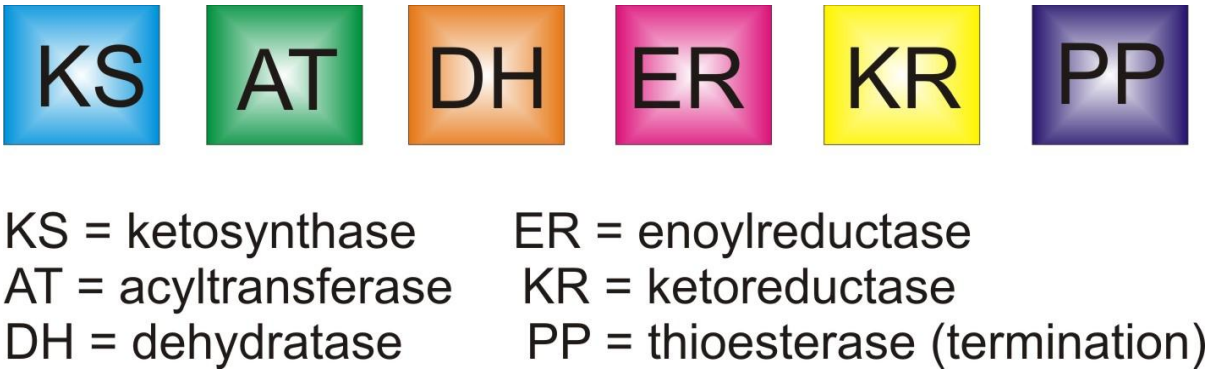

Figure 4.47: Organization of the PKS gene (ORF9).

The PKS gene contains the three domains essential for PKS biosynthesis: KS, AT and PP (ACP). Additionally it contains the domains that can introduce modifications to the keto group: DH, ER and KR (Figure 4.47). The gene cluster contains three genes that might be related to host resistance. ORF5 is predicted to contain a nucleotidyl transferase domain similar to the one in the nucleotidyl transferase in *Staphylococcus aureus* than confers bacterial resistance to the antibiotic kanamycin (Sakon et al. 1993). The kanamycin nucleotidyl transferase in *Staphylococcus aureus* inactivates kanamycin by transferring a nucleotidyl residue from a nucleoside triphosphate like ATP, GTP or UTP onto kanamycin (Sakon et al. 1993). ORF5 might confer host resistance to the unknown PKS in a similar way. ORF7 codes for a highly conserved hypothetical protein with a glycoxalase like domain and two potential metal-binding domains. Glyoxalase like structure can also be found in antibiotic resistance proteins like in the FosA protein that confers phosphomycin resistance (Bernat et al. 1997). ORF11 codes for a putative ABC transporter possibly involved in the export of the PKS product out of the cell. ORF12, ORF13, ORF15 and ORF16 code for conserved hypothetical proteins and there function is not clear. ORF12 is predicted to possess a SCP-like extracellular protein domain with unknown function (Yeats et al. 2003).

Table 4.13: ORFs that were identified in the region of the small PKS gene cluster (cluster IV).

ORF		best match		
ORF	size (aa)	source	entry	proposed function
1	290	*Streptomyces* sp. Mg1	ZP_04998790	3-hydroxybutyryl-CoA dehydrogenase
2	295	*Streptomyces clavuligerus* ATCC 27064	ZP_06776109	5-methyltetrahydropteroyltriglutamate--homocysteine methyltransferase
3	651	*Streptomyces roseosporus* NRRL 11379	ZP_04712500	5-methyltetrahydropteroyltriglutamate--homocysteine methyltransferase
4	322	*Streptomyces venezuelae* ATCC 10712	CCA55307	putative oxidoreductase
5	280	*Streptomyces* sp. Tu6071	ZP_08456800	putative nucleotide transferase domain
6	296	*Mycobacterium parascrofulaceum* ATCC BAA-614	ZP_06852772	possible hydrolase
7	247	*Streptomyces ghanaensis* ATCC 14672	ZP_06574548	conserved hypothetical protein
8	421	*Streptomyces bingchenggensis* BCW-1	ADI05134	putative geranyl geranyl reductase
9	2214	*Frankia* sp. EAN1pec	YP_001507667	PKS
10	364	*Streptomyces griseoaurantiacus* M045	ZP_08287721	putative polyprenyl diphosphate synthase
11	307	*Streptomyces ambofaciens* ATCC 23877	CAJ89729	putative ABC transporter ATP-binding subunit
12	120	*Salinispora tropica* CNB-440	YP_001161048	hypothetical protein
13	362	*Streptomyces ghanaensis* ATCC 14672	ZP_04690390	hypothetical protein
14	356	*Streptomyces ambofaciens* ATCC 23877	CAJ89725	terpene synthase
15	420	*Streptomyces subtropicus*	ADM87299	hypothetical protein
16	217	*Streptomyces* sp. Mg1	ZP_04995961	hypothetical protein

4.7.4 Siderophore cluster (cluster V)

The cluster termed “siderophore cluster” (cluster V) is expected to span over ~ 34 kb and to comprise 23 ORFs (Figure 4.48). Striking is the high number of genes than can be connected to siderophore biosynthesis, transport and regulation as well as the high homology of large parts of the gene cluster to the gene cluster of griseobactin in *Streptomyces sp.* ATCC 700974 (Patzer, Braun 2010) (Table 4.14).

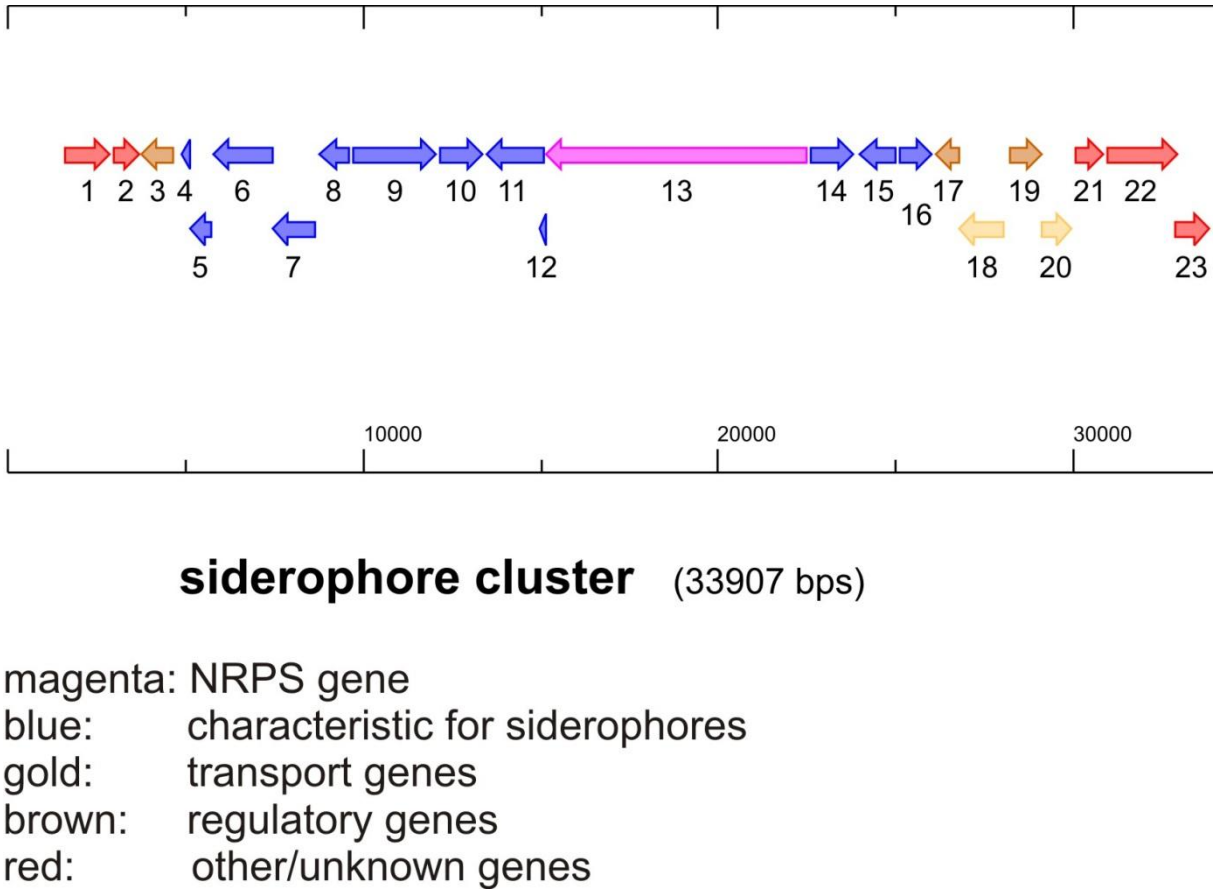

Figure 4.48: Arrangement of the siderophore gene cluster (cluster V).

ORF4-ORF16 are highly homologous (70-80 % identity) to genes in the gene cluster responsible for biosynthesis of the catechol-siderophore griseobactin (Table 4.14). Several genes can be connected to the biosynthesis and incorporation of dihydroxybenzoic acid. Dihydroxybenzoic acid possesses a catecholate moiety responsible for the iron complexation of the catecholate type siderophores (Raymond et al. 2003b). ORF7 is a predicted isochorismate synthase and ORF5 is a predicted isochorismatase. Isochorismate synthases catalyse the formation of isochorismate from chorismate and isochorismatases catalyse the cleavage of isochorismate into 2,3-dihydroxy-2,3-dihydrobenzoate and pyruvate. 2,3-dihydroxy-2,3-dihydrobenzoate could further be oxidized to 2,3-dihydroxybenzoate (DHB) by ORF8, a predicted 2,3-

dihydro-2,3-dehydroxybenzoate dehydrogenase. ORF6 is predicted to be a 2,3-dihydroxybenzoate-AMP ligase. 2,3-dihydroxybenzoate-AMP ligase activates the non-proteinogenic amino acid DHB with ATP and is involved in the biosynthesis of catechol-siderophores like enterobactin (WALSH et al. 1991). ORF6 therefore might activate DHB and transfer it onto ORF4 which has high homology to the DhbG protein in the griseobactin cluster, a predicted aryl carrier for DHB.

Table 4.14: ORFs of the siderophore gene cluster (cluster V) highly homologous to ORFs of the griseobactin gene cluster.

ORFs in *Streptomyces* sp. DSM 11171 gene cluster	genes in the *Streptomyes* sp. ATCC 700974 gene cluster	identity
ORF4	*dhbG*	57/77 (74%)
ORF5	*dhbB*	169/210 (80%)
ORF6	*dhbE*	449/533 (84%)
ORF7	*dhbC*	311/403 (77%)
ORF8	*dhbA*	188/280 (67%)
ORF9	*griA*	615/785 (78%)
ORF10	*griB*	287/402 (71%)
ORF11	*griC*	364/423 (86%)
ORF12	*griD*	39/55 (71%)
ORF13	*griE*	1750/2484 (70%)
ORF14	*griF*	291/352 (83%)
ORF15	*griG*	243/304 (80%)
ORF16	*griH*	210/259 (81%)

ORF9 is predicted to be an iron-siderophore uptake transporter. ORF10 is a putative esterase and homologous to the GriB protein of the griseobactin gene cluster. Due to the strong binding of iron by the catecholate siderophores iron is mostly released by cleavage and therefore by destruction of the siderophore. This has been shown for enterobactin and the Fes peptidase (Raymond et al. 2003b). ORF10 thus, is possibly involved in cleavage of the siderophore. ORF11 is a predicted major facilitator superfamily transporter potentially involved in export of the siderophore and is over 80 % identical with the griseobactin exporter. ORF14 is predicted to belong to the M20 peptidase superfamily. ORF14 shares more than 80 % identity with the griseobactin protein GriF. GriF is expected to contribute to the release of iron from the siderophore together with the esterase GriB (Patzer, Braun 2010). A similar

function for ORF14 might therefore be expected. ORF15 and ORF16 code for a siderophore-binding lipoprotein and an iron-siderophore ABC transporter highly homologous to GriG and GriH proteins in the griseobactin gene cluster of *Streptomyces sp.* ATCC 700974.

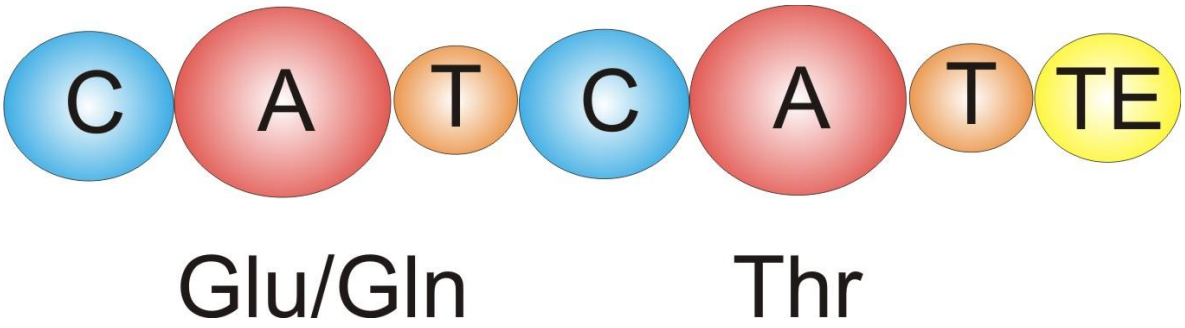

Figure 4.49: Modular organization of the NRPS gene and predicted amino acid specificities of the A-domains.

The NRPS gene in ORF13 shows over 70 % identity with the griseobactin NRPS gene (Patzer, Braun 2010) and 50 % identity with the bacillibactin NRPS gene from *Bacillus subtilis* responsible for the linking of 2,3-dihydroxybenzoate, glycine and threonine (May et al. 2001). The predicted amino acid usage is Glu or Gln for the first A-domain and Thr for the second A-domain (Figure 4.49). The homologous NRPS from *Streptomyces sp.* ATCC 700974 accepts arginine and threonine and forms a trimeric ester of 2,3-dihydroxybenzoyl-arginyl-threonine yielding griseobactin. The prediction of the A-domains of the griseobactin NRPS gene however wrongly resulted in a prediction of Gln and Thr which was explained by the low appearance of Arg in NRPS gene clusters. Due to the very high homology of the NRPS gene from *Streptomyces* sp. DSM 11171 with the one of *Streptomyces sp.* ATCC 700974 an identical amino acid usage of the A-domains might be expected and a likewise incorrect prediction of Glu/Gln instead of Arg. ORF12 codes for a putative MbtH-like protein. MbtH-like proteins have been found to facilitate amino acid activation in NRPS (Felnagle et al. 2010; Zhang et al. 2010).

Table 4.15: ORFs that were identified in the region of the small siderophore gene cluster (cluster V).

ORF		best match		
ORF	size (aa)	source	entry	proposed function
1	414	*Streptomyces venezuelae* ATCC 10712	CCA56420	NADH:flavin oxidoreductase/NADH oxidase
2	244	*Streptomyces cattleya*	CAD18969	putative oxidoreductase
3	302	*Stackebrandtia nassauensis* DSM 44728	YP_003511648	LysR family transcriptional regulator
4	77	*Streptomyces griseus subsp. griseus* NBRC 13350	YP_001828242	acyl carrier for DHBA
5	210	*Streptomyces* sp. ATCC 700974	CBA63658	isochorismatase
6	563	*Streptomyces cf. griseus* XylebKG-1	ZP_08240460	2,3-dihydroxybenzoate-AMP ligase
7	402	*Streptomyces* sp. ACTE	ZP_06271935	isochorismate synthase
8	276	*Streptomyces* sp. ACTE	ZP_06271936	2,3-dihydro-DHBA dehydrogenase
9	782	*Streptomyces* sp. ATCC 700974	CBA63668	siderophore uptake membrane transporter
10	403	*Streptomyces cf. griseus* XylebKG-1	ZP_08240464	esterase
11	531	*Streptomyces griseus subsp. griseus* NBRC 13350	YP_001828249	major facilitator superfamily permease
12	65	*Streptomyces cf. griseus* XylebKG-1	ZP_08240466	MbtH-like protein
13	2442	*Streptomyces* sp. ATCC 700974	CBA63680	NRPS
14	401	*Streptomyces griseus subsp. griseus* NBRC 13350	YP_001828252	M20/M25/M40 family peptidase
15	334	*Streptomyces* sp. ATCC 700974	CBA63680	putative siderophore-binding lipoprotein
16	284	*Streptomyces* sp. ATCC 700974	CBA63685	iron-siderophore uptake ABC transporter substrate-binding protein
17	219	*Streptomyces bingchenggensis* BCW-1	ADI07509	two-component system response regulator
18	302	*Streptomyces* sp. Mg1	ZP_04996507	ABC transporter ATP-binding protein

ORF	size (aa)	source	entry	proposed function
19	419	*Streptomyces bingchenggensis* BCW-1	ADI07508	two-component system sensor kinase
20	282	*Streptomyces* sp. Mg1	ZP_04996506	hypothetical protein
21	247	*Streptomyces griseoflavus* Tu4000	ZP_07315002	hypothetical protein
22	662	*Saccharopolyspora erythraea* NRRL 2338	YP_001107449	hypothetical protein
23	322	*Saccharopolyspora erythraea* NRRL 2338	ZP_06567748	membrane protein

The gene cluster may contain further genes involved in transport and regulation (Table 4.15). ORF18 codes for a putative ABC-multidrug transporter and ORF20 is a conserved hypothetical protein that is also predicted to contain a domain characteristic of ABC transporters.

ORF3 is a predicted LysR-type transcription regulator and ORF17 and ORF19 strongly resemble putative two-component system response regulators in different bacteria. These three ORF can therefore be expected to participate in regulation.

ORF21, ORF22 and ORF23 are conserved hypothetical proteins. A possible function of these ORFs in the gene cluster is arguable. ORF21 is a conserved hypothetical protein with nearly 50 % identity to a secreted serine protease from *Streptomyces fradia* (KITADOKORO et al. 1994) and a serine protease from *Streptomyces griseus* (Read et al. 1983). ORF21 might therefore function as a secreted protease. ORF23 possesses an exonuclease-endonuclease-phosphatase (EEP) domain. ORF1 and ORF2 are predicted to code for oxidoreductases. ORF1 is a putative NADH-FAD-dependent oxidoreductase and shows over 50 % identity to an oxidoreductase in antifungal garbonolides producing strain *Streptomyces galbus* (Karki et al. 2010) and nearly 49 % identity with a predicted morphinone reductase in *Pseudomonas aeruginosa* PA01 (Stover et al. 2000). Morphinone reductases are expected to be involved in the metabolism of morphine and codeine (French, Bruce 1995). ORF2 is a predicted 3-ketoacyl-ACP reductase and is to 40 % identical with the CetF1 gene from *Actinomyces* sp. Lu 9419 coding for a oxidoreductase involved in the biosynthesis of the antitumor agent cetoniacytone A (Wu et al. 2009). The role of the oxidoreductases in the siderophore gene cluster is doubtful.

The high homology to the griseobactin gene cluster not only in the gene sequence but also in the organization of the genes indicates a NRPS product very similar to griseobactin possibly even identical to griseobactin.

4.7.5 One-modular NRPS cluster (cluster VI)

The cluster termed as one-modular NRPS cluster (cluster VI) is expected to span over a region of about 35 kb and contains two SFPs and several transporters (Figure 4.50).

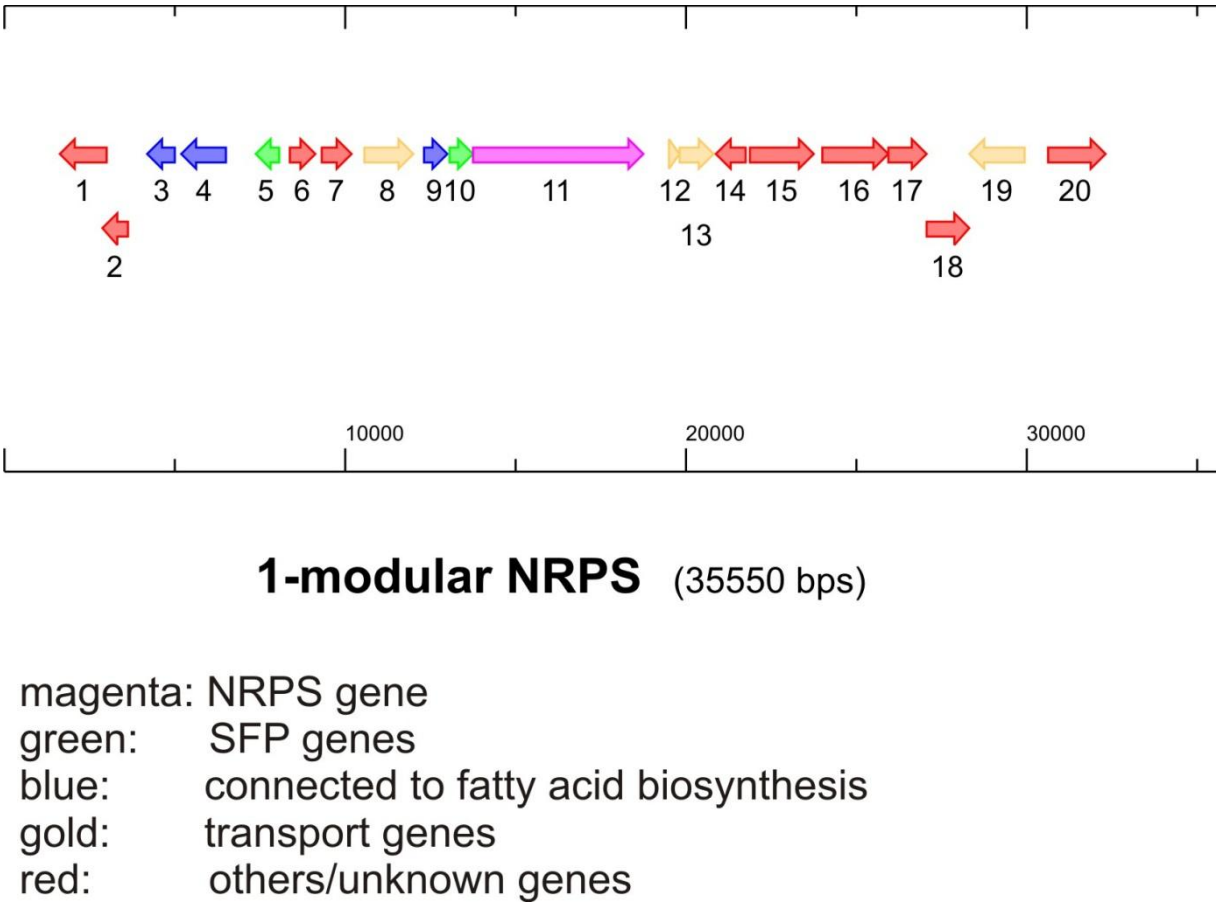

Figure 4.50: Organization of the one-modulare NRPS gene cluster (cluster VI).

Curiously, the cluster contains several genes that can be connected to fatty acid biosynthesis but no distinct PKS genes. ORF3 is a predicted enoyl-CoA hydratase. Enoyl-CoA hydratases play a role in the metabolism of fatty acids (Bahnson et al. 2002). ORF4 is predicted to be a putative PKS protein. A prediction with the online NRPS/PKS analysis tool of the University of Maryland (Bachmann, Ravel 2009a) however gave no characteristic PKS domains. ORF4 also possesses 30 % identity with a *β*-ketoacyl-ACP synthase connected to haemolytic activity of group B Streptococci (Pritzlaff et al. 2001). ORF9 is a predicted *β*-ketoacyl-ACP reductase

and is over 60 % identical to the chain A of a *β*-ketoacyl-ACP reductase from *Streptomyces coelicolor* A3(2) that is expected to be shared between PKS and fatty acid biosynthesis (Tang et al. 2006).

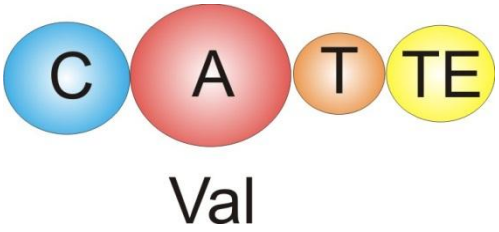

Figure 4.51: Organization of the NRPS gene (ORF11) and predicted amino acid specificity of the A-domain.

The NRPS gene in ORF11 contains only one module with a characteristic NRPS organization and is predicted to accept the amino acid Val (Figure 4.51). ORF5 and ORF10 are predicted SFP proteins. ORF5 shares nearly 50 % identity with a SFP in the tirandamycin gene cluster, an NRPS-PKS hybride antibiotic with a one-modular NRPS gene and three PKS genes (Carlson et al. 2010). SFP proteins are responsible for the activation of both NRPS and PKS.

ORF8, ORF12, ORF13 and ORF19 are putative multi drug efflux pumps and might help to confer host resistance (Table 4.16). ORF12 is very small and analysis with the NCBI blast tool indicates that ORF12 and ORF13 might form a single gene but were disrupted by default sequencing. ORF17 interestingly has a domain characteristic for a metallo-*β*-lactamase. *β*-Lactamases are responsible for antibiotic resistance to β-lactam antibiotics (Jacoby 2009).

ORF1 is a hypothetical protein with best homology to a predicted ATP-binding protein in *Streptomyces scabiei* 87.22 and also ORF6, ORF14 and ORF18 are conserved hypothetical proteins with unknown function. ORF2 is highly conserved predicted amidotransferase with nearly 80 % identity with a protein in the gene cluster of *Streptomyces fradiae* responsible for the biosynthesis of lipopeptide antibiotic A54145 (Miao et al. 2006). ORF7 is a predicted class II tRNA synthase with over 30 % identity with a seryl-tRNA-synthase (Bilokapic et al. 2006). ORF15 shows high homology to putative glycosyl hydrolases, ORF16 is a putative serine protease and ORF20 a putative dehydrogenase. The role these genes might play in the biosynthesis of the mysterious product however is also very mysterious.

Table 4.16: ORFs that were identified in the region of the one-modular NRPS gene cluster.

ORF		best match		
ORF	size (aa)	source	entry	proposed function
1	464	*Streptomyces scabiei* 87.22	YP_003488913	hypothetical protein
2	257	*Streptomyces* sp. C	ZP_07288290	amidinotransferase
3	265	*Rhodococcus equi* ATCC 33707	ZP_08156307	enoyl-CoA hydratase
4	441	*Candidatus Kuenenia stuttgartiensis*	CAJ74368	strongly similar to *β*-ketoacyl acyl carrier protein synthase II
5	229	*Saccharopolyspora erythraea* NRRL 2338	ZP_06564430	putative SFP type phosphopantetheinyl transferase
6	256	*Streptomyces flavogriseus* ATCC 33331	ADW01574	conserved hypothetical protein
7	291	*Bacillus cereus subsp. cytotoxis* NVH 391-98	YP_001373541	tRNA synthetase class II
8	495	*Verminephrobacter eiseniae* EF01-2	YP_995818	Na^+-driven multidrug efflux pump
9	234	*Streptomyces albus* J1074	ZP_04701280	3-oxacyl-(ACP) reductase
10	235	*Kitasatospora setae* KM-6054	BAJ28261	putative SFP type phosphopantetheinyl transferase
11	1658	*Verrucosispora maris* AB-18-03	YP_004406681	NRPS
12	84	*Streptomyces flavogriseus* ATCC 33331	ADW05458	multidrug resistance efflux protein
13	350	*Streptomyces* sp. ACTE	ZP_06274128	multidrug resistance efflux protein
14	293	*Streptomyces flavogriseus* ATCC 33331	ADW07485	conserved hypothetical protein
15	634	*Streptomyces viridochromogenes* DSM 40736	ZP_07303857	glycosyl hydrolase
16	654	*Streptomyces scabiei* 87.22	YP_003492078	protease
17	362	*Streptomyces scabiei* 87.22	YP_003492077	metallo-*β*-lactamase superfamily protein
18	418	*Streptomyces scabiei* 87.22	YP_003492076	conserved hypothetical protein
19	524	Streptomyces viridochromogenes DSM 40736	ZP_07302080	transmembrane efflux protein
20	729	*Streptomyces avermitilis* MA-4680	NP_822176	dehydrogenase

The untypical organization of the one-modular NRPS gene cluster makes it difficult to predict a possible target or foretell if this gene cluster can be activated. Striking is

perhaps the high number of ORF that possess strong homologues in the genome of *Streptomyces scabies* 87-22 however to homologues not annotated to specific gene clusters so far (Table 4.17). The gene locus of some of the homologues in *Streptomyces scabies* are also located in direct neighborhood as are the genes in the feglymycin gene cluster (e.g. ORF16, ORF17, ORF18) indicating that they belong to one gene cluster.

Table 4.17: ORFs in the one-modular NRPS gene cluster with highly homologous to ORFs in the genome of *Streptomyces scabies* 87-22.

ORF feglymycin gene cluster	gene locus of homologue genes in the *Streptomyces scabies* 87-22 genome	identity
ORF1	YP_003488913	90/287 (31%)
ORF2	YP_003486925	157/257 (61%)
ORF5	YP_003487252	107/199 (54%)
ORF7	YP_003485958	69/238 (29%)
ORF9	YP_003492663	145/239 (61%)
ORF14	YP_003486332	203/276 (74%)
ORF16	YP_003492078	412/620 (66%)
ORF17	YP_003492077	235/399 (59%)
ORF18	YP_003492076	305/410 (74%)
ORF19	YP_003493681	399/485 (82%)
ORF20	YP_003494105	400/533 (75%)

4.8 Further natural products isolated from the *Streptomyces* sp. DSM 11171 strain

4.8.1 Isolation of preparative amounts of nocardamine

As the *Streptomyces* sp. DSM 11171 strain was also expected to produce siderophores, the strain was additionally cultured in M9 minimal medium for different time periods (1-7 days), extracted with MeOH and the MeOH extract were check with LC-Exactive-Orbitrap-MS for production of interesting molecular masses.

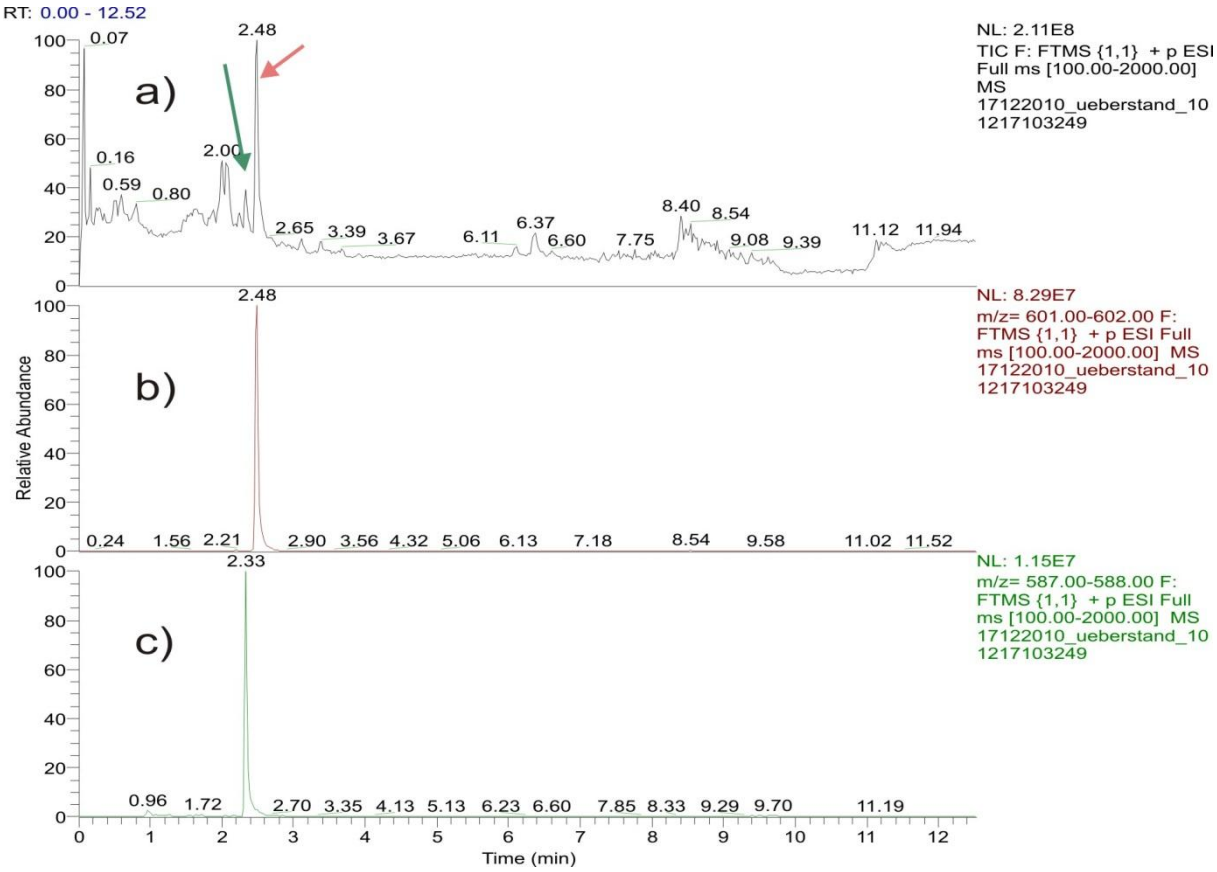

Figure 4.52: LC-Exactive-Orbitrap-MS measurements of a MeOH extract of *Streptomyces sp.* DSM 11171 cultured for 3 d in M9 medium in positive ionization mode. a) TIC, b) EIC 601 $[M+H]^+$ (R_t = 2.48 min) nocardamine, c) EIC 587 $[M+H]^+$ (R_t = 2.33 min) demethylenenocardamine.

In MeOH extracts of 3 d old cultures a very high yield of the molecular masses 601 $[M+H]^+$ and 587 [M+H] were detected in positive ionization mode (Figure 4.52). High resolving ESI-MS measurements detected an exact masses of 601.3593 $[M+H]^+$ and 587.3438 $[M+H]^+$ in positive mode. The addition of 10 mM $FeCl_2$ to the MeOH extracts led to the formation of iron complexes. In presence of iron the yield of the mass 601 decreased and a signal of 654 $[M+Fe]^+$ appeared, indicating a possible binding of iron accompanied by the loss of one proton (Figure 4.53).

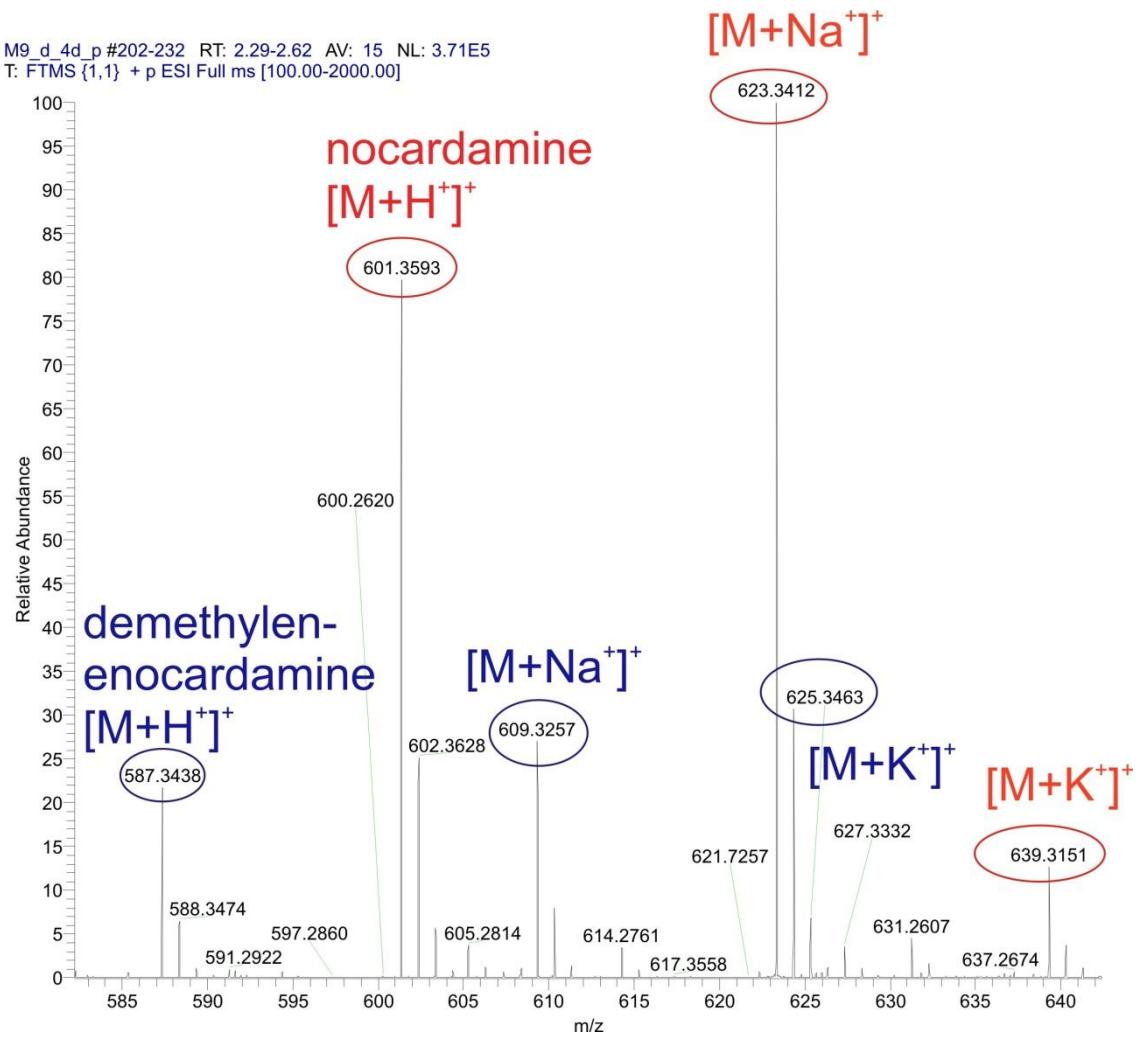

Figure 4.53: LC-Exactive-Orbitrap-MS measurements of a MeOH extract of *Streptomyces sp.* DSM 11171 cultured for 3 d in M9 medium in positive ionization mode. Mass spectrum integrated at a R_t range of 2.3-2.6 min.

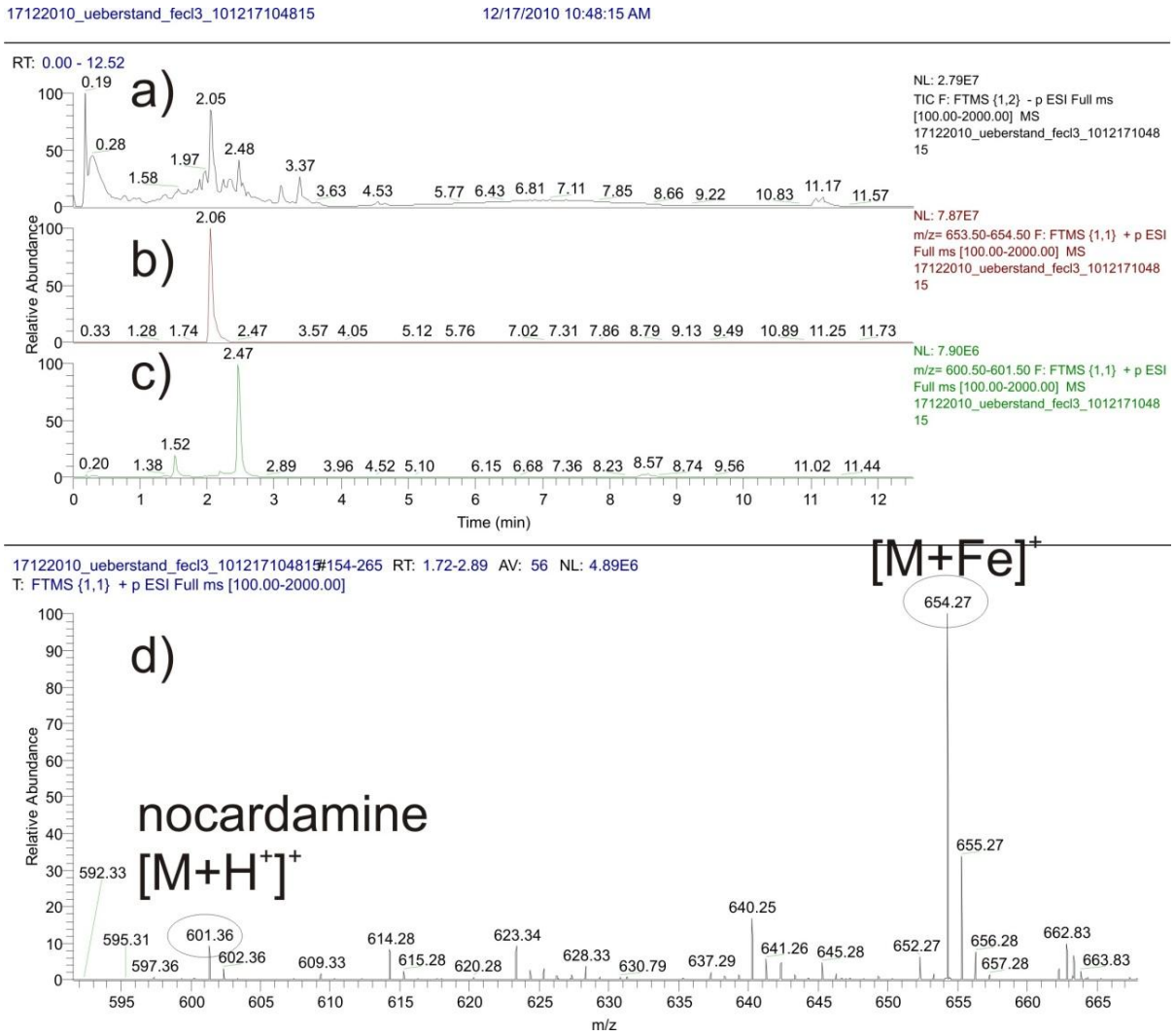

Figure 4.54: LC-Exactive-Orbitrap-MS measurements of a MeOH extract of *Streptomyces sp.* DSM 11171 cultured for 3 d in M9 medium in positive ionization mode upon incubation with of 10 mM $FeCl_2$. a) TIC, b) EIC 654 $[M+Fe]^+$ Fe-nocardamine, c) EIC 601 $[M+H]^+$ nocardamine, mass spectrum recorded at a R_t range of 2-2.5 min.

The molecular mass of 601.36 was calculated with the *Xcalibur* instrument software and found to correspond with a possible molecular formula of $C_{27}H_{49}O_9N_6$ and the molecular mass of 587.34 corresponds to a possible molecular formula of $C_{26}H_{47}O_9N_6$. The molecular formula of $C_{27}H_{49}O_9N_6$ was found in the Dictionary of Natural Products to correspond to the cyclic peptide siderophore nocardamine (also desferrioxamine E or proferrioxamine E) previously isolated from *Nocardia* sp. and different *Streptomyces* strains (Keller-Schierlein, Prelog 1961; Lee et al. 2005; Johnson et al. 2008). The molecular formula of $C_{26}H_{47}O_9N_6$.was found to correspond to the lower homologue of norcardamine, demethylenenocardamine previously isolated from a marine-derived *Streptomyces* sp. strain (Lee et al. 2005).

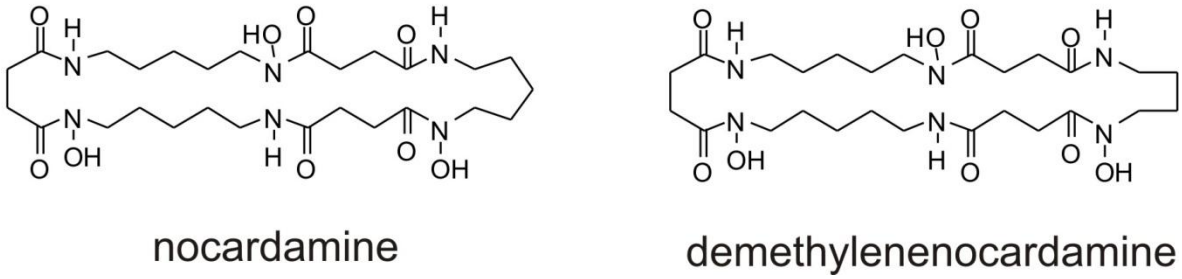

Figure 4.55: Structures of nocardamine and demethylenenocardamine.

Due to the high yield production both siderophores were isolated from the supernatant of bacterial culture after 2 d of cultivation in M9 medium. The supernatant was fractionated chromatographically with XAD-16 material. The nocardamine and demethylenenocardamine containing fraction was further fractionated by preparative RP-HPLC. From 1 L of bacterial culture about 11 mg of nocardamine and 2 mg demethylenenocardamine were isolated. Purity was verified by analytical HPLC and mass spectrometry. The isolated molecules were analyzed by Bahar Yanova (a PhD student in the group Prof. Roderich Süssmuth) with ^{1}H- and ^{13}C-NMR spectroscopy. The NMR spectra were found to be in perfect agreement with the NMR spectra predicted with the NMR software for nocardamine and demethylenenocardamine, which is very strong evidence that the isolated compounds are nocardamine and demethylenenocardamine (Figure 4.55).

4.8.2 Annotation of the nocardamine biosynthesis gene cluster

The nocardamine (desferoxamine E) biosynthesis was previously described to be coded by the *des* operon in *S. coelicolor* M145 (Barona-Gómez et al. 2004). The *des* operon contains the genes *desA*, *desB*, *desC* and *desD,* which are expected to be essential for the biosynthesis of desferoxamines. L-lysine is accordingly the starting material for desferrioxamine and converted by DesA, a decarboxylase, to cadaverine which is hydroxylized by DesB to *N*-hydroxycadaverine. DesC is expected to catalyze the acylation of *N*-hydroxycadaverine resulting in hydroxamic acid which is expected to be oligomerized to a trimer and cyclylized to desferrioxamine by DesD (Barona-Gómez et al. 2004) (Figure 4.56).

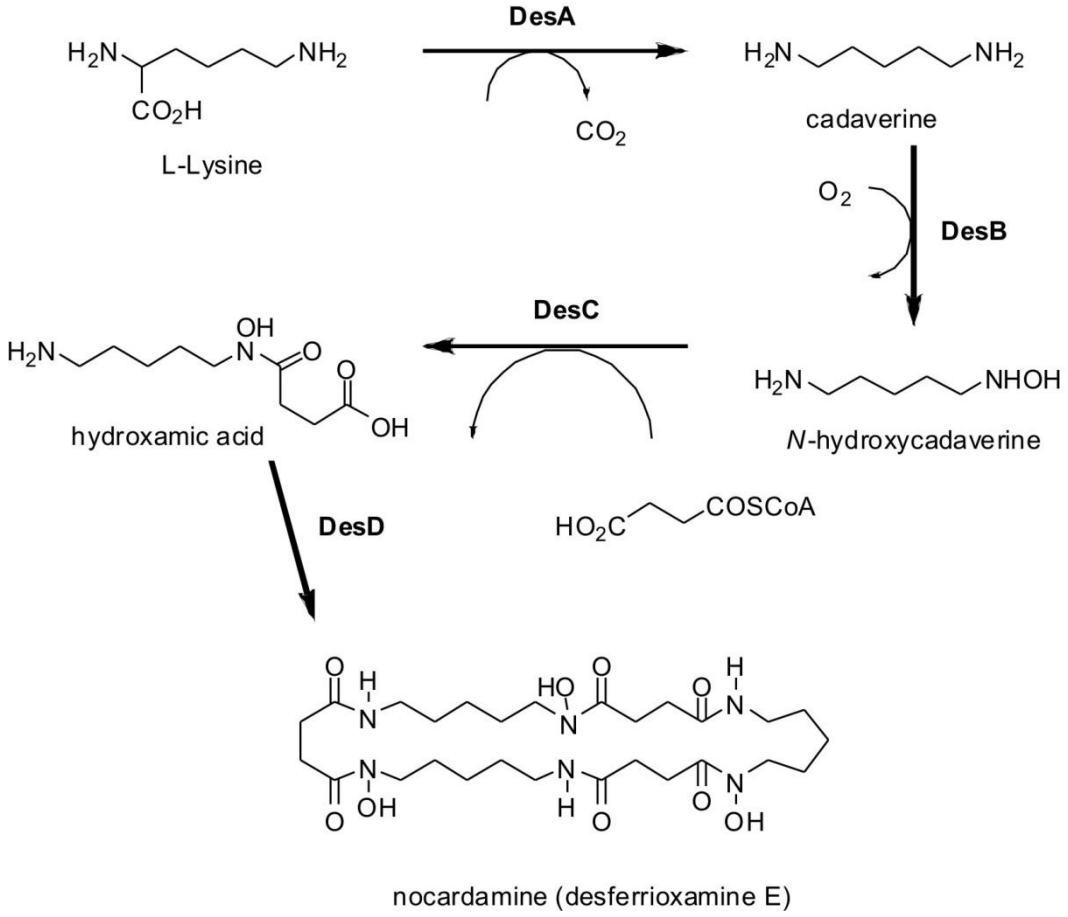

Figure 4.56: Scheme of the nocardamine biosynthesis (figure according to Barona-Gómez et al. 2004).

ORFs with homology to *desA*, *desB*, *desC* and *desD* were also found in the genome of *Streptomyces* sp. DSM 11171 arranged in line (ORF9-12) in a gene cluster denotated as nocardamine cluster (Figure 4.57). Several genes that were not described to be essential for nocardamine biosynthesis by Barona-Gomez et al.

(Barona-Gómez et al. 2004) but were found in close distance to the *des* operon are included here in the nocardamine gene cluster (ORF1-8, ORF13-14). These genes are listed for the sake of completeness, as a connection of these genes to nocardamine biosynthesis seems possible although is not certain.

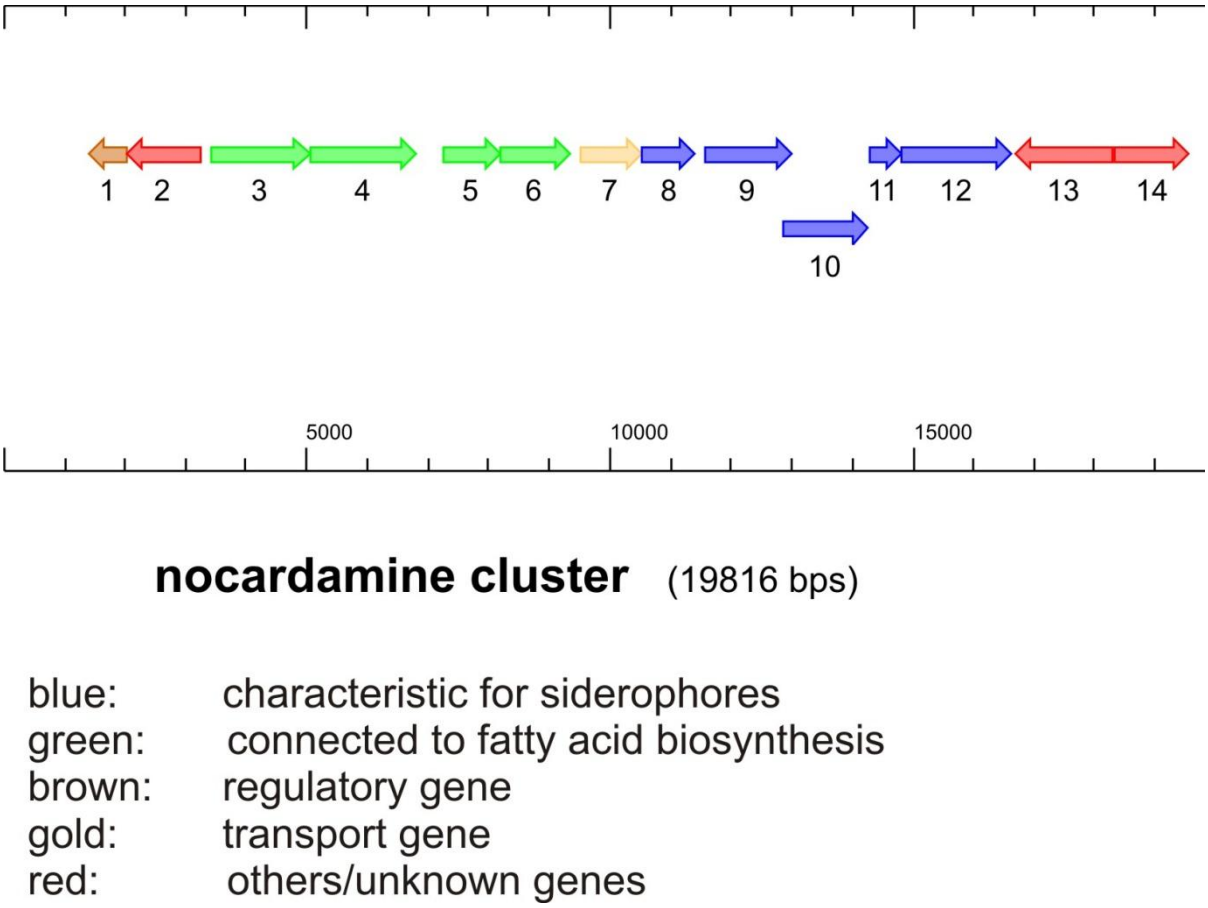

Figure 4.57: Organization of the nocardamine gene cluster.

Next to the *desD* gene a gene predicted to code for a *β*-*N*-acetylhexosaminidase was identified (ORF13) which is in concordance with an *N*-acetylhexosaminidase identified in the *des* gene cluster in *S. coelicolor* M145 in direct neighborhood of the *desD* gene (Barona-Gómez et al. 2004). *N*-Acetylhexosaminidases catalyze the hydrolysis of *N*-acetyl-*β*-hexosaminides. How this is connected to nocardamine biosynthesis is however unclear.

Table 4.18: ORFs that were identified in the region of the nocardamine gene cluster.

ORF		best match		
ORF	size (aa)	source	entry	proposed function
1	209	*Streptomyces pristinaespiralis* ATCC 25486	ZP_06911659	TetR-family transcriptional regulator
2	397	*Streptomyces clavuligerus* ATCC 27064	ZP_06769497	predicted membrane protein
3	538	*Streptomyces pristinaespiralis* ATCC 25486	ZP_06911658	putative acetyl/propionyl CoA carboxylase beta subunit
4	586	*Streptomyces pristinaespiralis* ATCC 25486	ZP_06911657	acetyl/propionyl CoA carboxylase alpha subunit
5	312	*Streptomyces* sp. C	ZP_07286861	hydroxymethylglutaryl-CoA lyase
6	386	*Streptomyces pristinaespiralis* ATCC 25486	ZP_06911655	Acyl-CoA dehydrogenase
7	341	*Streptomyces pristinaespiralis* ATCC 25486	ZP_06911653	ferrichrome ABC transporter
8	289	*Streptomyces venezuelae* ATCC 10712	CCA55855	siderophore-interacting protein associated with desferrioxamine E biosynthesis DesE
9	484	*Streptomyces ghanaensis* ATCC 14672	ZP_04688070	desferrioxamine E biosynthesis protein DesA
10	469	*Streptomyces pristinaespiralis* ATCC 25486	ZP_06911650	cadaverine *N*-monooxygenase DesB
11	175	*Streptomyces* sp. Mg1	ZP_05000049	acetyltransferase desferrioxamine E biosynthesis protein DesC
12	600	*Streptomyces griseus subsp. griseus* NBRC 13350	YP_001826259	desferrioxamine E biosynthesis protein DesD
13	536	*Streptomyces lividans* TK24	ZP_05526012	*β*-*N*-acetylhexosaminidase
14	401	*Streptomyces ghanaensis* ATCC 14672	ZP_04688066	conserved hypothetical protein

Several genes upstream of the *des* genes code for proteins that can be connected to fatty acid biosynthesis (Figure 4.57). ORF4 codes for the α-subunit and ORF3 for the β-subunit of a putative acetyl/propionyl CoA carboxylase. ORF5 codes for a possible hydroxymethylglutaryl-CoA lyase and ORF6 for an acyl-CoA dehydrogenase (Table 4.18).

Also the role of these enzymes in the biosynthesis of nocardamine is not totally clear. A connection might however be drawn from the fact that DesC is expected to use

acetyl-CoA as substrate for the acylation of *N*-hydroxycardaverine. DesC furthermore is expected to possess a relaxed substrate specificity and to accept also other CoA substrates like succinyl CoA (Barona-Gómez et al. 2004). ORF7 codes for an ABC transporter that might play a role in the transport of nocardamine and ORF8 a putative siderophore-interacting protein. ORF1 codes for a transcription regulator possibly involved in the regulation of the nocardamine gene cluster. ORF2 codes for a predicted membrane protein of unknown function and ORF14 for a conserved hypothetical protein. The function of these proteins in the nocardamine gene cluster is unknown.

The existence of a possible nocardamine gene cluster supports the prior described analytical experiments. *Streptomyces* sp. DSM 11171 therefore besides feglymycin, also produces the siderophores nocardamine and demethylenenocardamine.

5 Discussion

The peptidoglycan biosynthesis is a key step in the maturation of the bacterial cell wall. The Mur enzymes and the other enzymes involved in the peptidoglycan biosynthesis seem suitable as targets for development of antibacterials due to the fact that they are ubiquitous and essential (Kahne et al. 2005). Moreover these enzymes specifically occur in bacteria. The fact that at least the enzymes of late steps of this biosynthesis pathway are more easily accessible to drugs than other intracellular targets also favors the development of peptidoglycan biosynthesis inhibitors (Kahne et al. 2005). Additionally, the long history and experience of cell wall biosynthesis inhibitors makes the peptidoglycan biosynthesis pathway still a very popular and interesting research field. The ubiquitous spread of antibiotic resistant strains results in a strong need for development of new drug types and discovery of new antibiotic targets and inhibition modes for future drug development. As resistance against one member of a class of antibiotics due to a similar mode of action normally induces resistance against all members of the antibiotic class, new molecular targets and points of action need to be discovered.

There are a lot of different cell wall biosynthesis inhibitors belonging to very different molecular classes like the *β*-lactam antibiotics (Brakhage et al. 2005), the glycopeptide antibiotics (Kahne et al. 2005), the lantibiotics (Chatterjee et al. 2005) or phosphomycin. Some of the peptidoglycan biosynthesis inhibitors resulted in clinically or industrially used antibiotics like the *β*-lactam antibiotics (Brakhage et al. 2005), phosphomycin (Hendlin et al. 1969), nisin (Rogers, Whittier 1928) and vancomycin (McCormick et al. 1955-1956). Vancomycin e.g. is even used as last resort antibiotics to treat patients suffering from infections with multi-resistant bacteria when no other commonly applied antibiotics shows any effect anymore. The incident and spread of resistant strains also against vancomycin (Chang et al. 2003), however shows that vancomycin can not be the final answer toward multi-resistant bacterial strains.

Most of the known cell wall biosynthesis antibiotics target the late stages of peptidoglycan biosynthesis. Intensive research on the first step of peptidoglycan biosynthesis in the last years resulted in a detailed knowledge about the Mur enzymes and the biosynthetic mechanism (Schönbrunn et al. 1996; Benson et al. 1993; Jin et al. 1996; Bertrand et al. 1997; Gordon et al. 2001; Yan et al. 2000). Great efforts were made to find inhibitors targeting the Mur enzymes by screening

(Baum et al. 2001; Eschenburg et al. 2005) and target-specific design (Emanuele, JR. et al. 1996; Tanner et al. 1996; Marmor et al. 2001). The most successful of these efforts were perhaps the synthesis of a number of phosphinate inhibitors targeting the MurC enzyme (Marmor et al. 2001), dioxopyrazolidines as inhibitors for the MurB enzyme (Yang et al. 2006) and 5-sulfonoxy-anthranilic acid as inhibitor of the MurA enzyme (Eschenburg et al. 2005). From these synthetic inhibitors however none has entered clinical phases or has been followed up in more detailed pharmaceutical studies to become a pharmaceutically important antibiotic (El Zoeiby et al. 2003). Phosphomycin, a natural inhibitor of the MurA enzyme isolated in 1969 from *Streptomycetes* (Hendlin et al. 1969) is still the only pharmaceutically applied antibiotic targeting the first step of peptidoglycan biosynthesis.

Commonly, antibacterial effects of new compounds are first tested in agar diffusion assays *in vivo,* which give only a relative crude and incomplete picture on the activity of a compound. Nevertheless, such assays have been valuable for finding cell wall biosynthesis inhibitors in the past (Yang et al. 2006). By testing wild-type versus wall-less mutant bacterial strains, specific cell wall biosynthesis inhibitors can be screened (Trias, Yuan 1999). Also the induction of spheroplasts (Hendlin et al. 1969) and the accumulation of radio-labeled peptidoglycan precursors after feeding with radioactive amino acids (Allen et al. 1996) are indicators for the inhibition of cell wall biosynthesis. However, this still affords the exact determination of the molecular target. Additionally, whole cell assays fail to identify inhibitors that do not pass the cell wall or are actively effluxed. Also, in whole cell assays the susceptibility to the inhibitor depends mainly on the target concentration in the cell, which can strongly depend on the conditions applied. Cell-free assays (*in vitro*) might therefore be suited for independently finding new cell wall biosynthesis inhibitors (Trias, Yuan 1999) which might be later tailored for *in vivo* applications. However, one difficulty in studying particular enzymes of the peptidoglycan biosynthesis pathways *in vitro* is the availability of appropriate substrates. Except for the MurA enzyme, the substrates are not commercially available and need to be prepared enzymatically (Reddy et al. 1999) or synthetically (Michio Kurosu et al. 2007). A way out is the *in vitro* reconstruction of the complete pathway toward the synthesis of Park's Nucleotide, thus advantageously avoiding the isolation or synthesis of single substrates. Previously, cell-free high-throughput pathway screenings for the enzymes catalyzing the cytoplasmic steps of peptidoglycan biosynthesis have been developed using

radio-labeled amino acids for detection (Winn et al. 2010) or LC-ESI-MS for detection (El Zoeiby et al. 2001).

In this work, these assays were further optimized in a way that allowed dereplication and study of every single enzyme of the pathway separately instead of testing the integrity of the whole pathway. LC-MS was found to be very suitable for detection of both substrates and products of the Mur enzymes and gave highly reproducible results. Thus, feglymycin was found to target the early steps of the peptidoglycan biosynthesis and assigned to its specific target proteins.

Feglymycin is to our knowledge the first natural compound inhibitor of the MurC enzyme and shows an inhibitory effect in the low µM to upper nM range. Feglymycin additionally showed inhibitory effects toward the MurA enzyme, but no effect on any other of the Mur enzymes even in high concentrations. By testing MurA and MurC from *E. coli* but also from *S. aureus* it has been shown that these enzymes of gram-negative and gram-positive bacteria are principally inhibited by feglymycin. This underlines that the inhibitory effect of feglymycin to the MurA and the MurC enzyme is rather specific.

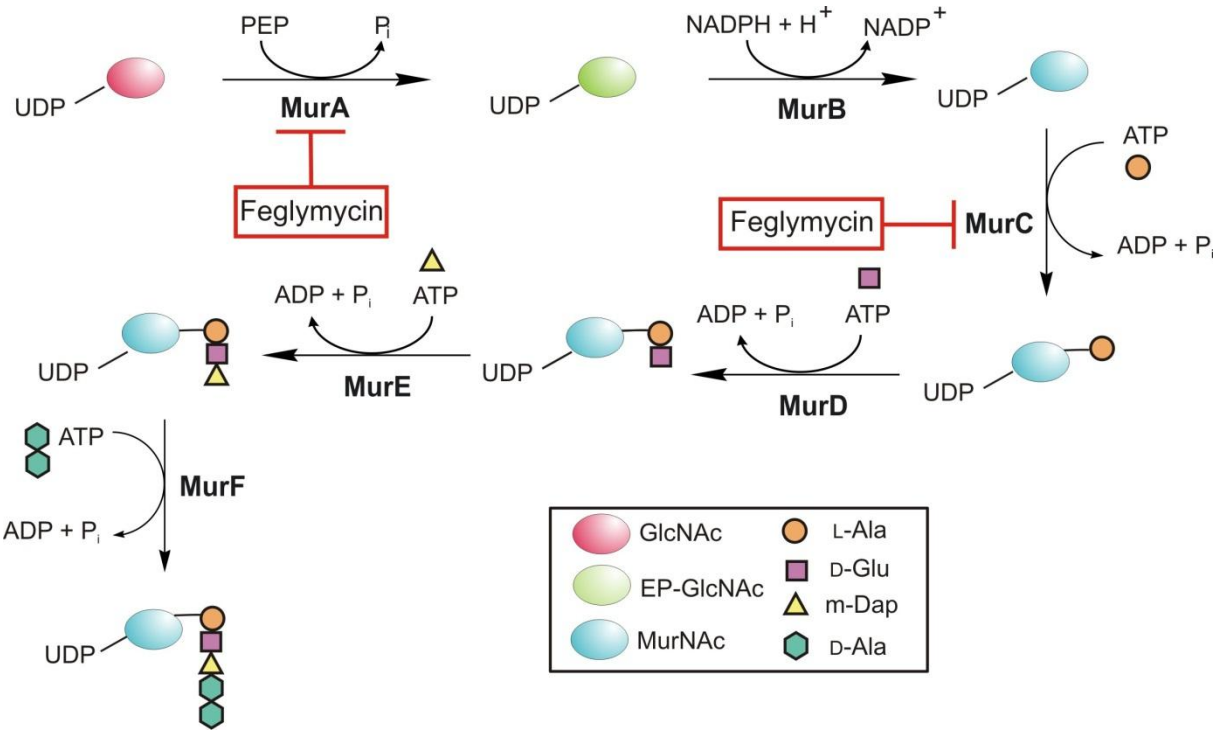

Figure 5.1: Scheme of the first stage of peptidoglycan biosynthesis and identified targets of feglymycin.

Studies with enzymes of the late steps of the peptidoglycan biosynthesis performed by Dr. Tanja Schneider (member of the group of Prof. Hans-Georg Sahl at the

university of Bonn, unpublished data) showed that feglymycin has no effect on the second and third step of the pathway. Feglymycin is also the first inhibitor known so far specifically inhibiting two enzymes in a linear sequence of the early peptidoglycan biosynthesis, while showing no effect on the activity of the other Mur enzymes.

To get a better idea of the inhibition mode of feglymycin *in vitro* spectroscopic assays with the isolated MurA and MurC enzymes both from *E. coli* and *S. aureus* were established. Spectroscopic assays have the advantage compared to the LC-MS assay that the product formation/substrate disappearance can be measured continuously over time without interfering into the reaction. LC-MS assays in contrast have to be performed as discontinuous assay or end-point assay. Before detection of the product formation/substrate disappearance the assay has to be stopped and the products/substrate needs to be extracted from the reaction mixture. This can be done at different time points or at a set end-point. The continuous detection of the enzyme reaction obviously allows a better monitoring and additionally allows generating more data points. A spectroscopic assay therefore seems better suitable for a more detailed kinetic study of the enzyme reactions and effect of the inhibitor. Spectroscopic assay of course also have a main drawback compared to LC-MS assays. In the LC-MS assay the substrate and products can be directly and unambiguously identified by their mass-to-charge ratio. A spectroscopic assay, in contrast, relies on the spectrophotometric properties of the substrates or products of the reaction which are less specific. If both substrates and products of a reaction do not undergo a change in the spectroscopic signal the reaction has to be coupled with a spectrophotometrically detectable reaction. However, coupled enzyme assays are prone to misinterpretation. At each point of the reaction it has to be made sure that the rate of the reaction is determined by the enzymes of interest and not by the coupling enzymes. Additionally of course, it has to be ruled out that the inhibitor has an inhibitory effect on the coupling enzymes.

The kinetic parameters obtained for the MurA and the MurC enzymes from *E. coli* and *S. aureus* in the spectroscopic assay however fit very well to values previous described in literature which attests that the assays have been optimized to reliably monitor the MurA and MurC enzyme reactions. The combinatory use of both LC-MS assays and spectrophotometric assays can provide both: A direct proof of the activity of the enzymes and the inhibitory effect of the inhibitor by specific detection of the substrates and products of the reaction by their mass-to-charge ratio and a direct

spectroscopic monitoring of the course of the enzyme reaction allowing a detailed kinetic interpretation. The determination of the IC_{50} values was performed with negative and positive controls to verify the functionality of the assay. The IC_{50} value for feglymycin was found to be lowest for the MurC enzyme from *E. coli* (0.3 µM). The IC_{50} values for the MurA enzymes are about 10 fold higher. This might indicate that MurC rather that MurA is the main target of feglymycin. The inhibition type was deduced from a Lineweaver-Burk plot. The values for the graphs were derived from non-linear regression of the untransformed data fitted to the Michaelis-Menten equation. Non-linear regression is less error-prone than linear regression due to the fact that in linear regression data obtained with different substrate concentrations are differently weighted. The use of non-linear regression makes the Lineweaver-Burk plot less error-prone but not faultless. The result still depends strongly on the substrate concentration range, inhibitor concentration range and reaction times used to obtain the data and on the reproducibility of the assay. The Lineweaver-Burk plot therefore still is only an approach to get an approximation of the inhibition type. It is however a very easy diagnostic tool and for this reason still widely used to obtain an estimation of the inhibition type (Copeland 2005). The Lineweaver-Burk plots obtained for both, for the MurA and MurC enzyme from *E. coli,* indicate a non-competitive inhibition by feglymycin towards all substrates. Non-competitive inhibitors show the same binding affinity towards the free enzyme and the substrate-enzyme complex. They therefore do not compete with substrates. As the inhibitor does not compete with the substrate it can be expected that inhibitor does not target the substrate binding pocket but another binding site. A non-competitive inhibition can be obtained if the binding of the inhibitor induces a conformational change of the enzyme that suppresses substrate conversion. The CD measurements performed with the MurC enzyme from *E. coli* in presence and absence of feglymycin, show that feglymycin has an alterative effect on the tertiary structure of the MurC enzyme. This supports the idea of a non-competitive inhibitor that induces conformational changes. In case of the MurA enzyme however the addition of feglymycin did not result in a conformational change detectable with CD spectroscopy. Possibly because the feglymycin concentration was too low to induce the conformational change or the conformational change was not severe enough to induce a visible change of the CD specta of MurA.

As a non-competitive inhibitor, possibly with an allosteric effect, is hypothesized for feglymycin the inhibitory effect and mode of action cannot be explained by substrate or transition state analogy. Likewise, structural analogies of feglymycin to one of the substrates or even a substrate transition state are not obvious. With regards to the fact that MurA uses PEP as a cosubstrate, whereas MurC uses ATP and L-alanine, no structural similarities or relationships can be found for these substrates. Hence, assuming inhibition of the ATP or L-alanine binding pocket, one would expect that subsequent reactions performed by MurD, MurE and MurF which are all ATP-dependant and using amino acid substrates like MurC are also inhibited by the MurC inhibitor feglymycin rather than MurA. More structural resemblance can be seen in the UDP-substrates of MurA and MurC as the product of the MurA reaction UDP-GlcNAc bears strong similarities with the substrate of the MurC reaction UDP-MurNAc. Remarkably, UDP-MurNAc has been described before to possess regulatory function by feed-back inhibition and thus exerts an inhibitory effect on the MurA enzyme (Winterhalter 2000). However, assuming inhibition of the UDP-substrate binding pocket, an inhibition of other Mur enzymes would have to be expected, since the UDP-motif is unifying all substrates of the MurA-MurF enzyme cascade. Also according to the present data no substrate dependency to any substrate was found. Instead an allosteric inhibition seems possible. Sequence alignments of MurA and MurC do not indicate a stronger relationship between the two proteins compared to the other Mur enzymes. In contrast, MurC shows strong structural similarities with the other ATP-dependent Mur ligases MurD-MurF (Bertrand et al. 1997; Gordon et al. 2001; Yan et al. 2000). However, it is interesting that both MurA and MurC have a two-domain structure while the other Mur enzymes show a tree-domain structure (El Zoeiby et al. 2003). MurA consists of two very similar domains connected by a double-stranded linker (Schönbrunn et al. 1996) while MurC is known to form dimers (Jin et al. 1996; Spraggon et al. 2004).

For a non-competitive inhibitor also speaks the finding that the mirror-image peptide of feglymycin possesses nearly the same activity, both *in vivo* and *in vitro,* as feglymycin (Dr. Anne Hänchen, unpublished data, see Appendix 6.7 and 6.8). A mirror image peptide of feglymycin with the same amino acids but in inverse order was synthesized by Dr. Anne Hänchen (a former PhD student in the group of Prof. Süssmuth) and tested both *in vivo* against MRSA strains (in cooperation with sanofi-aventis) and *in vitro* against die MurA and MurC enzymes from *E. coli*. Interestingly

the mirror image showed the same inhibitory effect on MurA and MurC as feglymycin and also nearly the same effect as feglymycin in the *in vivo* testing. In case of competitive inhibition the orientation of the inhibitor in the binding pocket is normally very important, wherefore mirror images of inhibitor often lack activity. That the orientation of feglymycin has no influence on the activity therefore might also hint to a non-competitive inhibitor.

Non-competitive inhibitors are not commonly clinically used (Copeland 2005). Some non-competitive inhibitors however are in clinical use in treatment of AIDS and cancer e.g. the non-nucleoside reverse transcriptase inhibitor nevirapine (Peschel, Sahl 2006) and the MAP kinase inhibitors (Bogoyevitch, Fairlie 2007) like PD0325901 (Haura et al. 2010). Non-competitive inhibition is also not described for most of the cell wall biosynthesis inhibitors. An exception constitute the 5-sulfonoxy-anthranilic acid inhibitors of MurA identified by Eschenburg et al. which were shown by co-crystallisation with the MurA enzyme from *E. coli* not to bind at the active center but to prevent conformational changes of the MurA enzyme (Eschenburg et al. 2005). Even though the resemblance of the 5-sulfonoxy-anthranilic acid inhibitors (T6361R/T6362R) to feglymycin is not very strong a similar mechanism of feglymycin could be imagined. Further conclusions on the specific mode of action of feglymycin are expected from structural data obtained from crystals of protein-inhibitor complexes.

With K_i values in the low µM and high nM range feglymycin shows no extremely high affinity. The inhibitory effect is however within the range of K_i values of other natural product cell wall biosynthesis inhibitors like phosphomycin (K_i 8.6 µM, *E. coli* MurA Baum et al. 2001), tunicamycin (K_i: 0.55 *µ*M, *E. coli* MraY Brandish et al. 1996b) and vancomycin (K_D 1,6 *µ*M D-Ala-D-Ala derivatives Rao et al. 1998). Even most of the synthetic inhibitors of the Mur enzymes did not show significantly lower K_i or IC_{50} values (e.g. MurA inhibitors by Baum et al. IC_{50} 0.2-0.9 µM, MurA *E. coli* Baum et al. 2001, MurB inhibitors by Yang et al. K_D 260 nM, MurB *E. coli* Yang et al. 2006). Time-dependency and reversibility experiments showed that the inhibition occurs fast and is also fast reversible.

In vivo experiments previously performed with feglymycin prove that feglymycin not only inhibits the peptidoglycan biosynthesis *in vitro,* but also shows inhibitory effects on MRSA strains *in vivo* in the low µM range (Dettner et al. 2009). No effect on gram-negative bacteria like *E. coli* has been found *in vivo* (Dettner et al. 2009), although

the *E. coli* enzymes were found to be sensitive to feglymycin in our *in vitro* assay. Therefore, we assume that feglymycin does not pass the outer membrane of gram-negative bacteria possibly accompanied by a lack of suitable transport/uptake systems as they exist for other antibacterials like for phosphomycin, which uses the L-α-glycerophosphate transport system (Hendlin et al. 1969). Because *S. aureus* was found to be sensitive to feglymycin, it can be assumed that feglymycin is able to unspecifically pass the inner cell membrane or that *S. aureus* possesses transport/uptake systems utilized by feglymycin. The inhibition of intracellular bacterial targets by molecules with masses >300 Da is also discussed for the lipoglycopeptide ramoplanin. Ramoplanin inhibits the transpeptidation reaction in the last extracellular stage of peptidoglycan biosynthesis but additionally targets the intracellular MurG enzyme *in vitro*. If the activity against MurG also plays a role for the *in vivo* activity is however not clear (McCafferty et al. 2002).

In this context, the *β*-helical dimer structure of feglymycin which has some analogies to gramicidin A could accounts for a membrane crossing of feglymycin (Bunkóczi et al. 2005). The specific structure of gramicidin A enables the molecule to form channels in phospholipid membranes (Wallace 1986). Bunkóczi however did not expect feglymycin to form channels. He expected the feglymycin dimer to be too short to span the membrane and predicted that a possible channel would be additionally blocked by phenylalanine side chains (Bunkóczi et al. 2005). Also this type of membrane crossing would not explain the lack of activity in *E. coli*. Some unpublished experiments were performed focusing of the membrane penetration by feglymycin by Prof. Dr.Ulrich Koert and Dr. Philipp Reiß (Philipps-university Marburg, (a detailed description of the experiments and the results can be found in the appendix chapter 6.9). Due to similarities in structure between feglymycin and gramicidin A, ion channel experiments were carried out with a so called black lipid membrane (BLM) (Derossi et al. 1998). In these experiments two chambers with an electrolyte solution were separated by a lipid bilayer and a potential was applied. These experiments indicated a possible membrane activity of feglymycin as an electrical current flow could be detected hinting to an at least partial destruction of the membrane. An electrical current flow however was only detected for relatively high potentials (180 mV-200 mV) and increased in disproportional steps what is in dissent with the formation of stable pores in the membrane. Beside the formation of stable and consistent pores like in case of gramicidin A, a more unspecific membrane

activity of feglymycin might be possible resulting in membrane crossing but a less consistent weakening of the bacterial membrane.

A membrane damaging activity as described for CAMPs (cationic antimicrobial peptides) (Bogoyevitch, Fairlie 2007; Magzoub et al. 2001) seems unlikely due to the negative character of the peptide. A model could be instead the cell penetrating peptides and trojan peptides as described by Derossi (Derossi et al. 1998) and Magzoub (Deshayes et al. 2004). For these small amphipathic peptides it was found that they cannot only penetrate cells but are even able to transport polypeptides, oligonucleotides or even full length proteins through cell membranes (Herbig et al. 2005). Most reknown of these peptides is perhaps penetratin (pAntp) a 16 amino acid α-helical part of Antennapedia homeodomain protein of *Drosophila* (Deshayes et al. 2004). The penetratin peptides were found to induce the formation of reverse micelles which allows the crossing of the membrane in an aqueous environment (Derossi et al. 1998) and can function also as carrier for other molecules (Lundberg, Langel 2003). This model might perhaps better fit to the ion channel results obtained for feglymycin. Bunkóczi expected from the three-dimensional structure of feglymycin a function as ion carrier (Bunkóczi et al. 2005). The mechanism of translocation of the cell penetrating peptides is however still a matter of discussion beside the formation of reverse micelles also endocytosis is debated (Yang et al. 2010, Yang et al. 2010). Additionally also for the cell penetrating peptides likewise as for the CAMPs a cationic charge is thought to be important.

An alternative explanation could be that feglymycin in not able to pass the cell membrane but instead has an additional extracellular target responsible for its *in vivo* activity. This target however cannot belong to the second or third stage of peptidoglycan biosynthesis where feglymycin was found to show no effect. Further studies will aid in elucidation the mechanism of membrane penetration by feglymycin or will help to indentify alternative extracellular targets of feglymycin.

The optimization of the feglymycin production by *Streptomyces* sp. DSM 11171 allowed the characterization of different *Streptomyces* sp. DSM 11171 mutant stains and therefore the unequivocal identification of the feglymycin biosynthesis gene cluster. The gene inactivation single cross-over mutants of four ORFs of the feglymycin gene cluster (ORF 7, ORF13 (DpgA), ORF26 and ORF27) failed to produce feglymycin in comparison to the wild type strain. As all four ORFs were

found to be essential for feglymycin production; the experiments give no answer on the questions for the precise borders of the feglymycin gene cluster. To answer these questions further single cross-over mutants of ORFs further up- and down-stream of the so far tested ORFs would be required. However the experiments prove that the identified gene cluster is indeed responsible for feglymycin production. They also show that all four ORFs are very important for feglymycin production. The information obtained from annotation of the feglymycin biosynthesis gene cluster confirms the theory that feglymycin is a non-ribosomally synthesized peptide. Despite the differences in structure and mode of action feglymycin seems to be closely related to the glycopeptides of the vancomycin group of antibiotics and the glycodepsipeptide antibiotic enduracidin. Especially the genes coding for the biosynthesis of the non-proteinogenic amino acids hydroxyphenylglycine (Hpg) and dihydroxyphenylglycine (Dpg) show a strong similarity to the genes in the gene cluster of the vancomycin group of antibiotics particularly to the genes of the A47934 gene cluster of *Streptomyces toyocaensis* (Pootoolal et al. 2002). Homologies were also found in some of the regulator genes (ORF7, ORF11, ORF19) and a gene predicted to code for an ABC transporter (ORF21). Due to the differences in structure however the NRPS genes and its modular organization show only little homology to the related gene clusters. Beyond that, the feglymycin gene cluster contains a lot of genes that have not been identified so far in any related cluster. Their function and their connection to the feglymycin biosynthesis remain speculative because of the lack of homologies in related gene clusters but they might reflect the different mechanism of action of feglymycin. Emphasized might be here the existence of a mysterious peptidoglycan binding protein (ORF26) in the feglymycin gene cluster and the high number of peptidases (ORF1, ORF29-32). The sequenced feglymycin cluster allows exploring these differences in more detail and will help to better understand the mechanism of feglymycin transport and host resistance und by that also the unique mode of action. Maybe it also contains an answer to the question how feglymycin is able to penetrate the cell membrane. By shedding light on the genes responsible for self-resistance, gene regulation and export of feglymycin also a better understanding of similarities and differences of feglymycin to other peptide antibiotics resulting in the very different mode of action could be gained.

Additionally to the feglymycin biosynthesis gene cluster five further NRPS and PKS gene clusters were identified in the feglymycin genome and also a cluster expected to be responsible for nocardamine production. The five NRPS and PKS clusters were found when searching the genome for particularly large ORFs. The nocardamine gene cluster in contrast was identified after detection of nocardamine production by *Streptomyces* sp. DSM 11171 and specific search for a possible nocardamine gene cluster. These findings support the theory that also long-known antibiotic producers can contain new unknown gene clusters (Bentley et al. 2002). As the whole *Streptomyces* sp. DSM 11171 genome has not been annotated so far it can be expected that the genomes contains further gene clusters responsible for the production of natural products, especially non-NRPS and non-PKS clusters (like the nocardamine gene cluster) that do not stick out due to the peculiar gene size of the NRPS or PKS genes. The finding of nocardamine production shows that the *Streptomyces* sp. DSM 11171 strain is able to produce further natural products beside feglymycin if facing different culture conditions. A prediction, if the additional NRPS and PKS gene clusters can be activated as well as a forecast of the structures of the possible NRPS and PKS products only from the annotation of the gene clusters is venturous. Only in case of the siderophore gene cluster (cluster V) a relatively safe prediction can be made due to the strong homology to the griseobactin gene cluster in *Streptomyces sp.* ATCC 700974 (Patzer, Braun 2010). An intensive and sensitive chemical screening approach with the *Streptomyces* sp. DSM 11171 strain under a lot of different culture conditions however might help to identify some of these predicted new natural products.

The work with the feglymycin and the feglymycin producer shows that natural products are still a very interesting and challenging topic to work on. Natural compounds like feglymycin outstrip most synthetic compounds in their wide range of efficacy and mechanistic complexity and bacterial strains like *Streptomyces* sp. DSM 11171 still contain a lot of secrets that wait to be discovered. The findings for the antibacterial activity and the feglymycin gene cluster open the door for a lot of new theories but still keep many questions unanswered. Thus the saying is true “every answer simply leads to another question”.

6 Appendix

6.1 Vector map pDrive cloning vector (Quiagen)

pDrive Cloning Vector

Positions of various elements

Vector size (bp)	3851
Multiple cloning site	266–393
LacZ α-peptide	216–593
T7 RNA polymerase promoter	239–258
T7 transcription start	256
SP6 RNA polymerase promoter	398–417
SP6 transcription start	400
Ampicillin resistance gene	1175–2032
Kanamycin resistance gene	2181–2993
pUC origin	3668
Phage f1 origin	588–1043
Primer binding sites:*	
M13 forward (–20)	431–447
M13 forward (–40)	451–467
M13 reverse	209–224
T7 promoter primer	239–258
SP6 promoter primer	400–418

** Primer sequences are provided below*

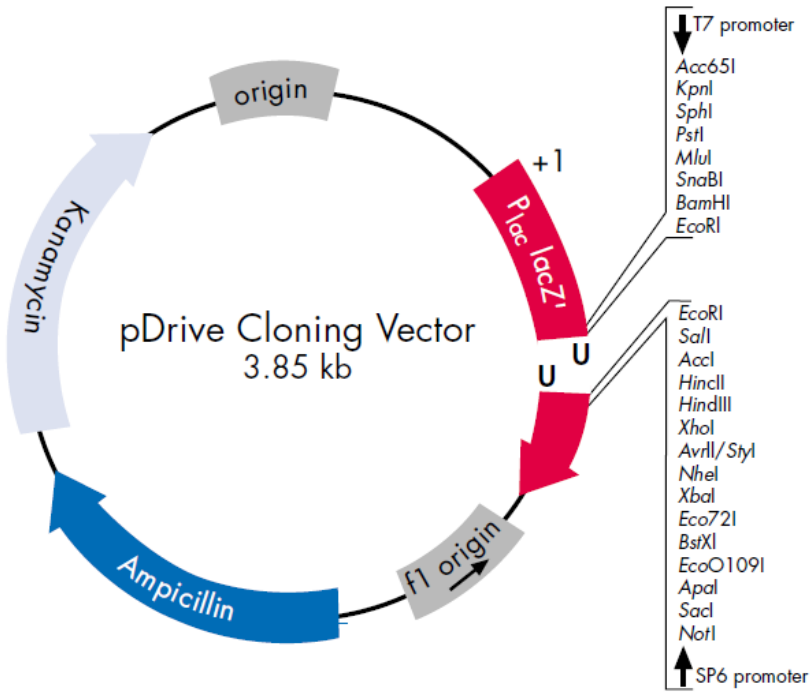

6.2 Vector map pET-24a(+) protein expression vector (Novagen)

pET-24a(+) sequence landmarks	
T7 promoter	311-327
T7 transcription start	310
T7•Tag coding sequence	207-239
Multiple cloning sites	
(*Bam*H I - *Xho* I)	158-203
His•Tag coding sequence	140-157
T7 terminator	26-72
lacI coding sequence	714-1793
pBR322 origin	3227
Kan coding sequence	3936-4748
f1 origin	4844-5299

The maps for pET-24b(+), pET-24c(+) and pET-24d(+) are the same as pET-24a(+) (shown) with the following exceptions: pET-24b(+) is a 5309bp plasmid; subtract 1bp from each site beyond *Bam*H I at 198. pET-24c(+) is a 5308bp plasmid; subtract 2bp from each site beyond *Bam*H I at 198. pET-24d(+) is a 5307bp plasmid; the *Bam*H I site is in the same reading frame as in pET-24c(+). An *Nco* I site is substituted for the *Nde* I site with a net 1bp deletion at position 238 of pET-24c(+). As a result, *Nco* I cuts pET24d(+) at 234, and *Nhe* I cuts at 229. For the rest of the sites, subtract 3bp from each site beyond position 239 in pET-24a(+). *Nde* I does not cut pET-24d(+). Note also that *Sty* I is not unique in pET-24d(+).

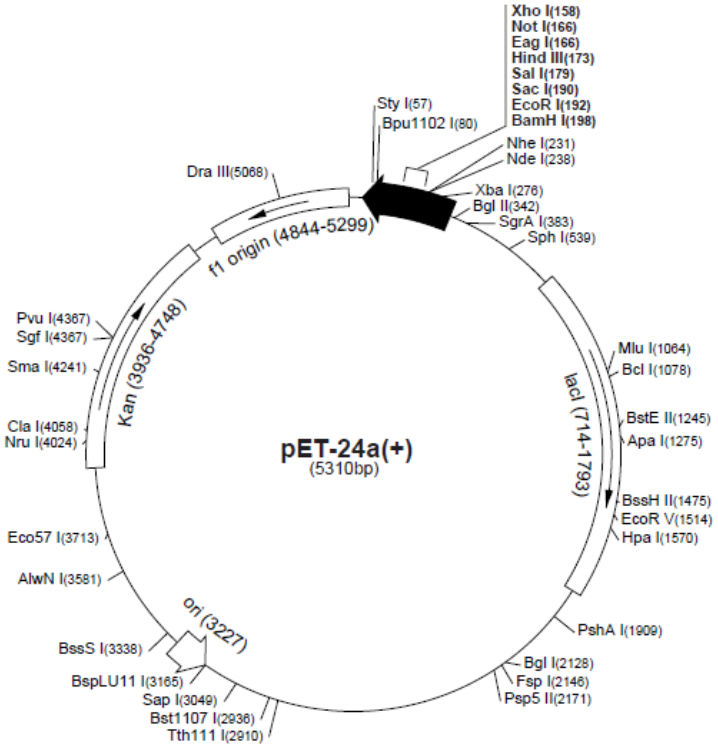

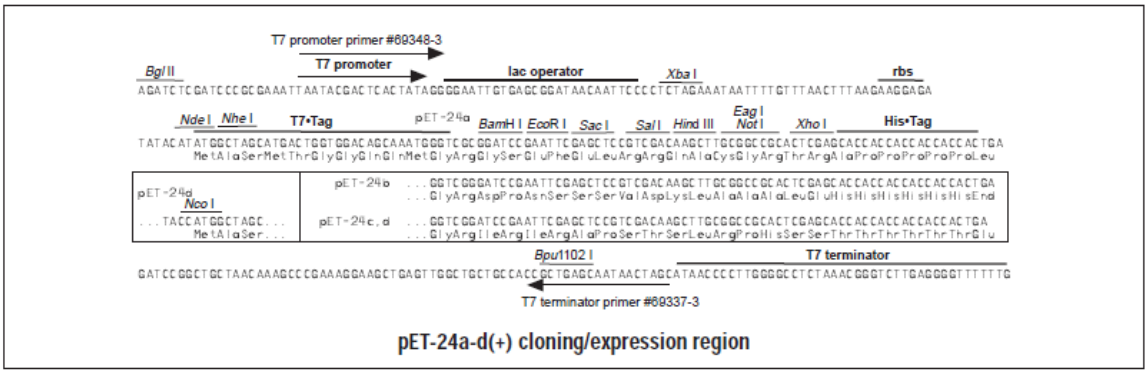

pET-24a-d(+) cloning/expression region

6.3 Vector map pET-28a(+) protein expression vector (Novagen)

pET-28a(+) sequence landmarks	
T7 promoter	370-386
T7 transcription start	369
His•Tag coding sequence	270-287
T7•Tag coding sequence	207-239
Multiple cloning sites	
(*Bam*H I - *Xho* I)	158-203
His•Tag coding sequence	140-157
T7 terminator	26-72
lacI coding sequence	773-1852
pBR322 origin	3286
Kan coding sequence	3995-4807
f1 origin	4903-5358

The maps for pET-28b(+) and pET-28c(+) are the same as pET-28a(+) (shown) with the following exceptions: pET-28b(+) is a 5368bp plasmid; subtract 1bp from each site beyond *Bam*H I at 198. pET-28c(+) is a 5367bp plasmid; subtract 2bp from each site beyond *Bam*H I at 198.

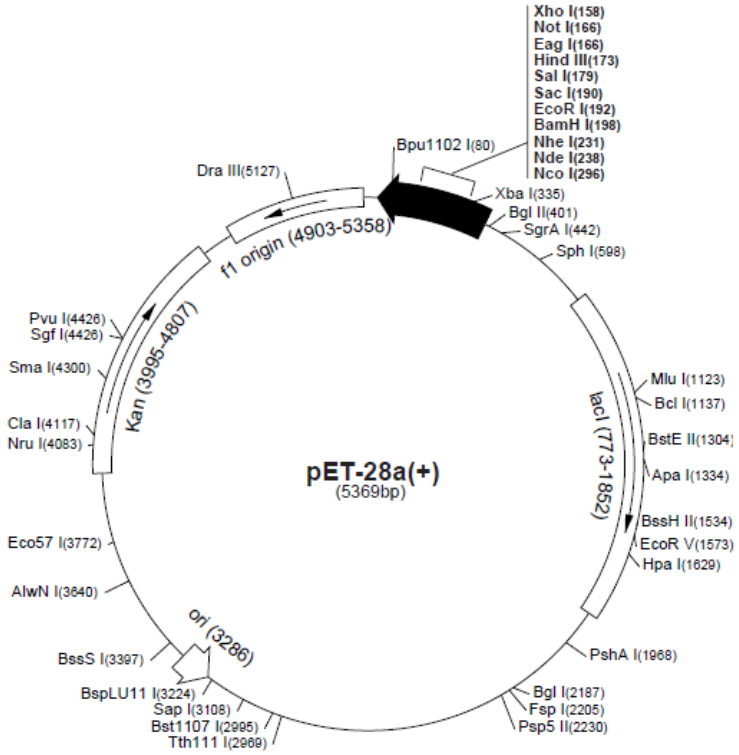

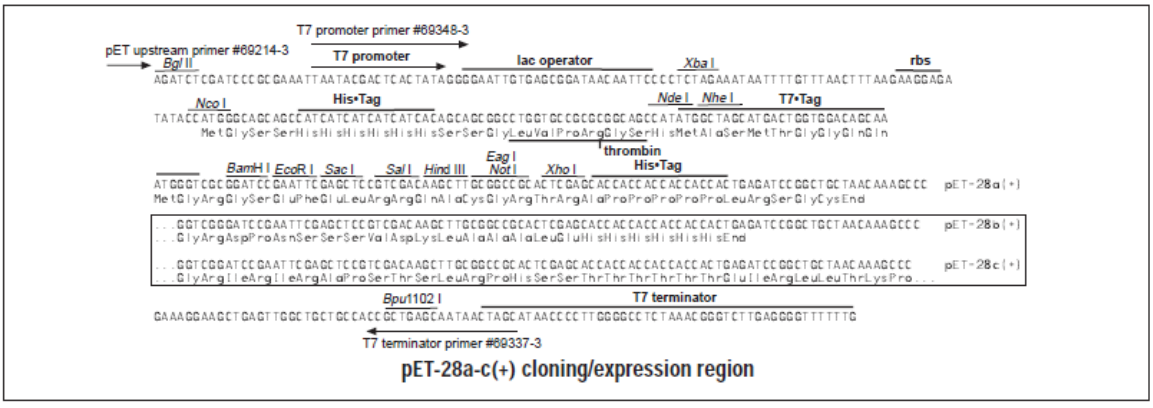

pET-28a-c(+) cloning/expression region

6.4 Vector map pET-21a(+) protein expression vector

pET-21a(+) sequence landmarks	
T7 promoter	311-327
T7 transcription start	310
T7•Tag coding sequence	207-239
Multiple cloning sites (*Bam*H I - *Xho* I)	158-203
His•Tag coding sequence	140-157
T7 terminator	26-72
lacI coding sequence	714-1793
pBR322 origin	3227
bla coding sequence	3988-4845
f1 origin	4977-5432

The maps for pET-21b(+), pET-21c(+) and pET-21d(+) are the same as pET-21a(+) (shown) with the following exceptions: pET-21b(+) is a 5442bp plasmid; subtract 1bp from each site beyond *Bam*H I at 198. pET-21c(+) is a 5441bp plasmid; subtract 2bp from each site beyond *Bam*H I at 198. pET-21d(+) is a 5440bp plasmid; the *Bam*H I site is in the same reading frame as in pET-21c(+). An *Nco* I site is substituted for the *Nde* I site with a net 1bp deletion at position 238 of pET-21c(+). As a result, *Nco* I cuts pET21d(+) at 234, and *Nhe* I cuts at 229. For the rest of the sites, subtract 3bp from each site beyond position 239 in pET-21a(+). *Nde* I does not cut pET-21d(+). Note also that *Sty* I is not unique in pET-21d(+).

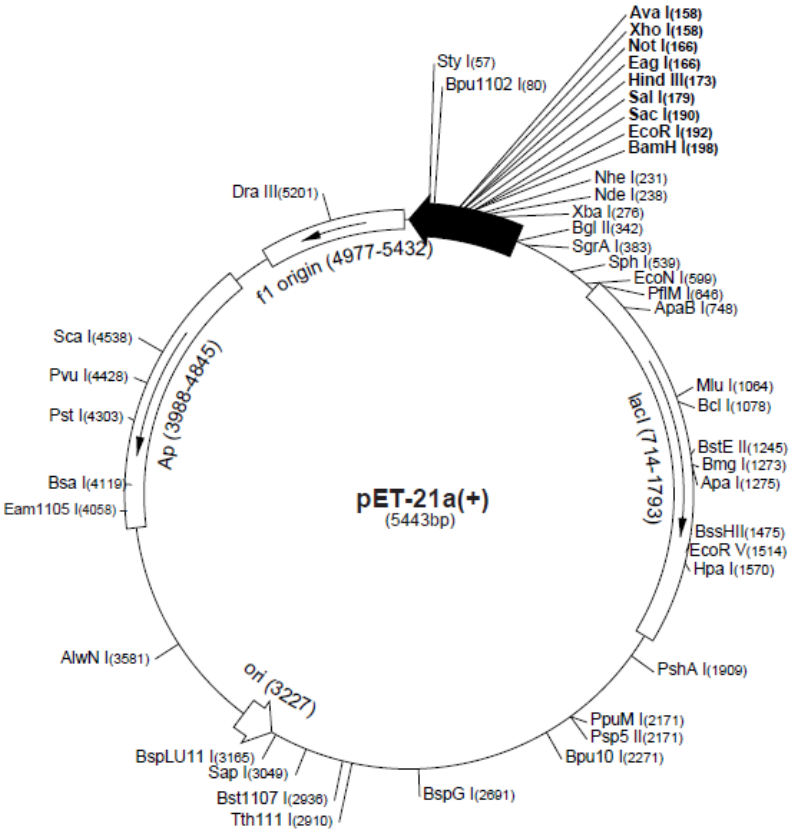

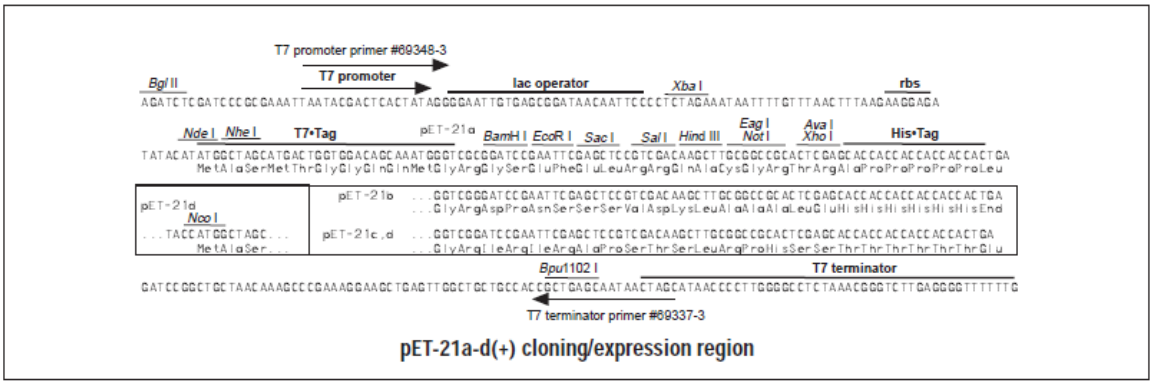

6.5 Vector map pK18mob

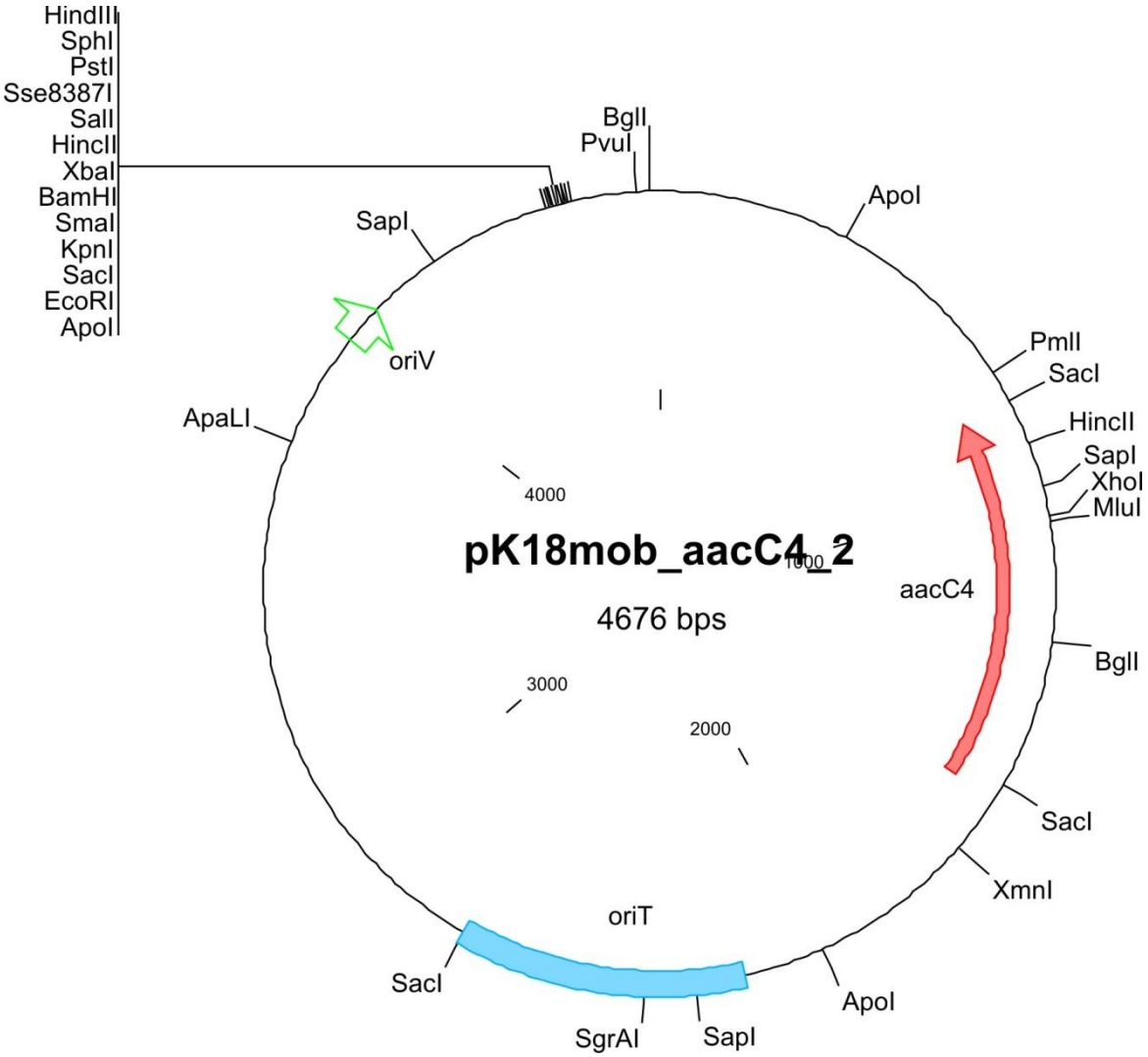

6.6 Thin layer chromatography (TLC) detection of the products of the MurA-F reactions (Dr. Tanja Schneider)

Method:

Conversion of UDP-*N*-glucosamine to UDP-*N*-acetylmuramyl pentapeptide by the sequential action of staphylococcal MurA to MurF enzymes and analysis of the reaction products by mass spectrometry and subsequent MraY-catalysed lipid I-synthesis. MurA-F were incubated in 50 mM Tris-Bis-propane; pH 8, 25 mM (NH4)SO4, 5 mM MgCl2, 5 mM, 5 mM KCl, 0.5 mM DTT, 2 mM ATP, 2 mM PEP, 2 mM NADPH, 1 mM of each amino acid (L-Lys, D-Glu, L-Ala, D-Ala-D-Ala, respectively), 10% DMSO, 100 nmol UDP-GlcNAc and 15 µg MurA-F protein in a total volume of 125 µl for 60 min at 30°C. MraY (2.5 µg), 2.5 nmol $C_{55}P$ and 0.3% (w/v) *N*-lauroylsarcosine were added to the reaction mixture (31.25 µl) and incubated for another 60 min at 30°C. Lipid I variants were extracted from the reaction mixture and separated by TLC.

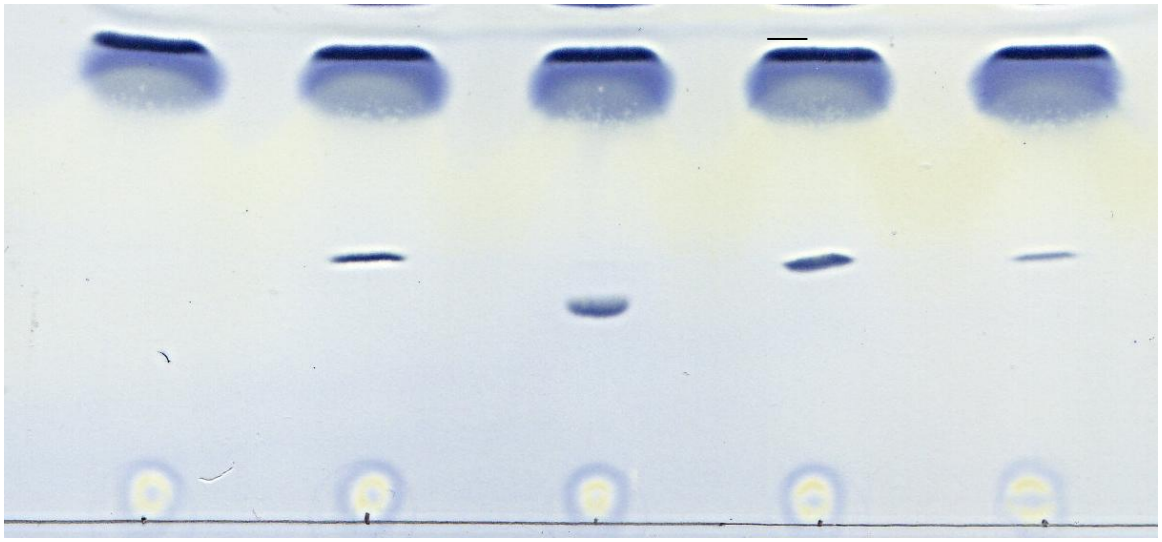

MurA-C **MurA-D** **MurA-E** **MurA-F** **MurA-F + Feglymycin**

Product MurA-D: C_{55}P-MurNAc-L-Ala-D-Glu

Product MurA-E: C_{55}P-MurNAc-L-Ala-D-Glu-L-Lys

Product Mur A-F: C_{55}P-MurNAc-L-Ala-D-Glu-L-Lys-D-Ala-D-Ala

Figure 6.1: TLC detection of the products of the MurA-F reactions**.**

In presence of feglymycin a visibly lower amount of the product of the MurA-F reaction can be detected.

6.7 Antimicrobial testing of feglymycin and the feglmycin mirror image against different *S. aureus* strains and other bacteria and yeast strains in cooperation with Sanofi-Aventis (Dr. Anne Hänchen, umpublished data)

Table 6.1: Antimicrobial testing of feglymycin and the feglymycin mirror image against different microbial strains.

	FH 6580 *S. aureus* ATCC29213	FH 6581 *S. aureus* ATCC33592	FH 6725 *S. aureus* ATCC13709	FH 6495 *E. coli* ATCC25922	FH 6585 *E. faecalis* ATCC2912	FH 6582 *S. pyogenes* ATCC12344	FH 2173 *C. albicans*	FH 6498 *M. smegmatis* ATCC607
		MRSA	MSSA					100 CFU / Well
Batch Ref.	**IC_{80} µg/mL**	**IC_{80} µg/mL**	**IC_{80} µg/mL**	**IC_{80} µg/mL**	**IC_{80} µg/mL**	**IC_{80} µg/mL**	**IC_{80} µg/mL**	**IC_{80} µg/mL**
Feglymycin	**0.31**	**0.65**	**0.54**	**>64**	**>64**	**>64**	**>64**	**>64**
Feglymycin-mirror image (M18)	**0.70**	**1.26**	**0.58**	**>64**	**>64**	**23.42**	**>64**	**>64**
Batch Ref.	**MIC µg/mL**	**MIC µg/mL**	**MIC µg/mL**	**MIC µg/mL**	**MIC µg/mL**	**MIC µg/mL**	**MIC µg/mL**	**MIC µg/mL**
Feglymycin	**0.5**	**1**	**1**	**>64**	**>64**	**>64**	**>64**	**>64**
Feglymycin-mirror image (M18)	**1**	**2**	**1**	**>64**	**>64**	**>64**	**>64**	**>64**

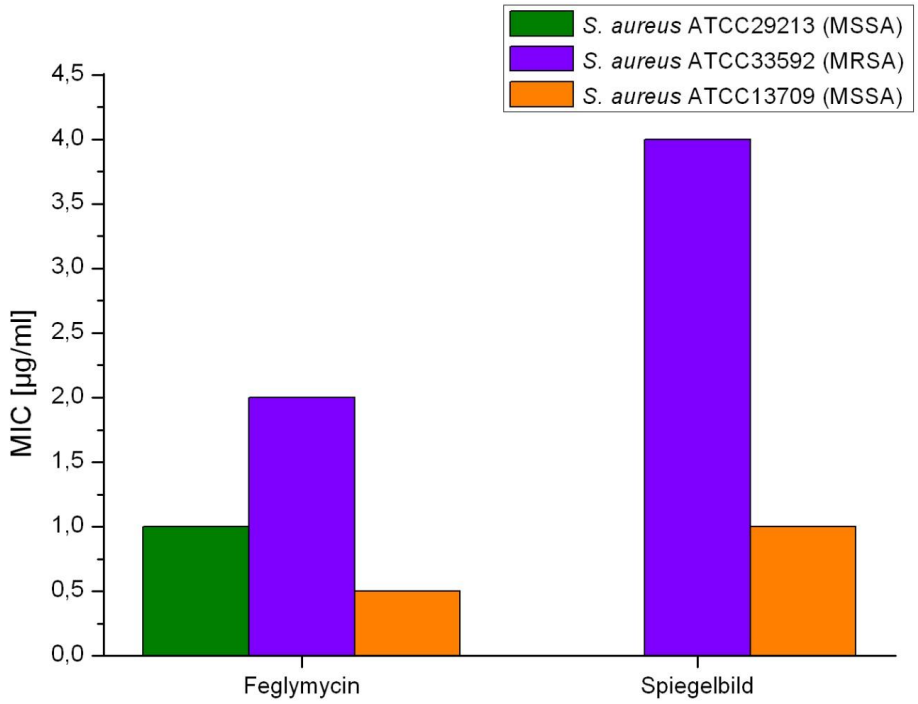

Figure 6.2: MIC values for feglymycin and the feglymycin mirror image (“Spiegelbild”) against different MRSA strains.

The mirror image of feglymycin shows a similar activity against different *S. aureus* strains a feglymycin.

6.8 Testing of feglymycin and the feglmycin mirror image against the MurC enzyme from *E. coli* (Dr. Anne Hänchen, umpublished data)

Table 6.2: IC50 values for feglymycin and the feglymycin mirror image (MurC *E. coli*).

MurC (*E. coli*)	**feglymycin**	**mirror image**
IC_{50}	**0.28**	**0.59**
standard deviation	**0.14**	**0.41**

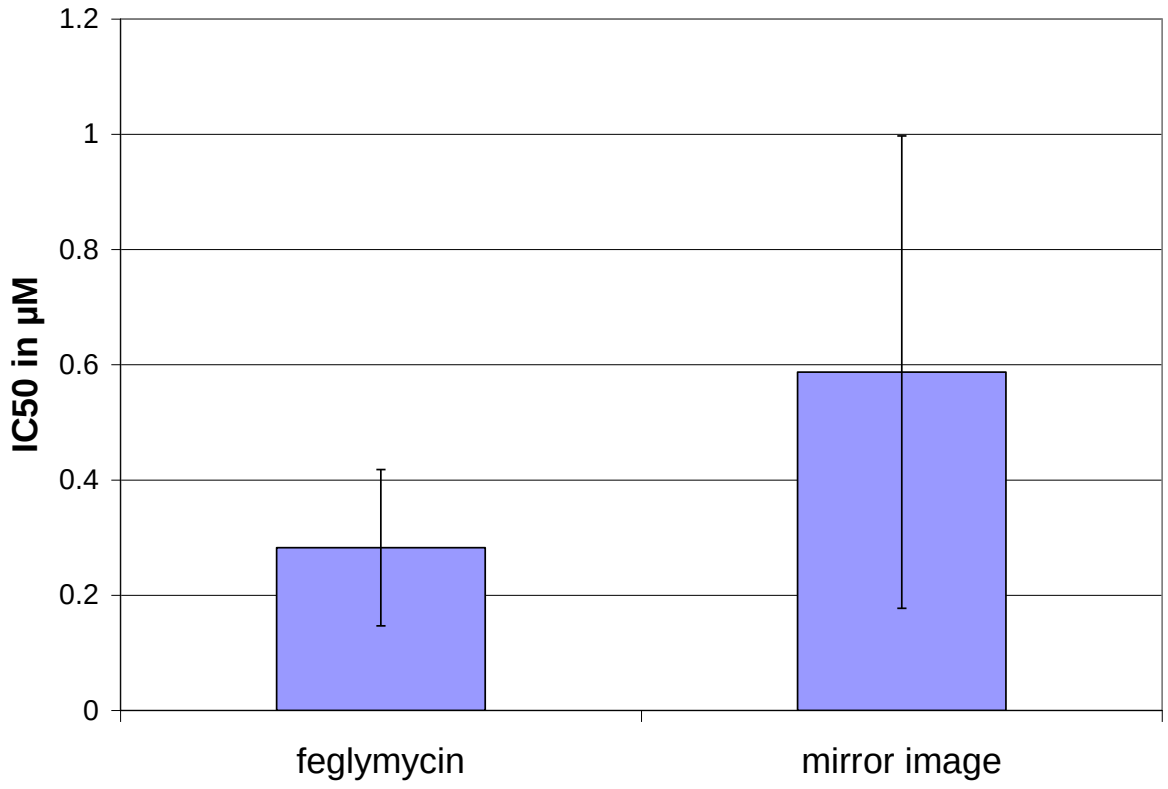

Figure 6.3: IC_{50} values of feglymycin and the feglymycin mirror image (MurC, *E. coli*).

The mirror image of feglymycin shows only a slightly lower activity against the MurC enzyme than felgmycin.

6.9 Ion channel experiments performed with feglymycin (cooperation with Prof. Dr.Ulrich Koert and Dr. Philipp Reiß Philipps-university Marburg)

Methods

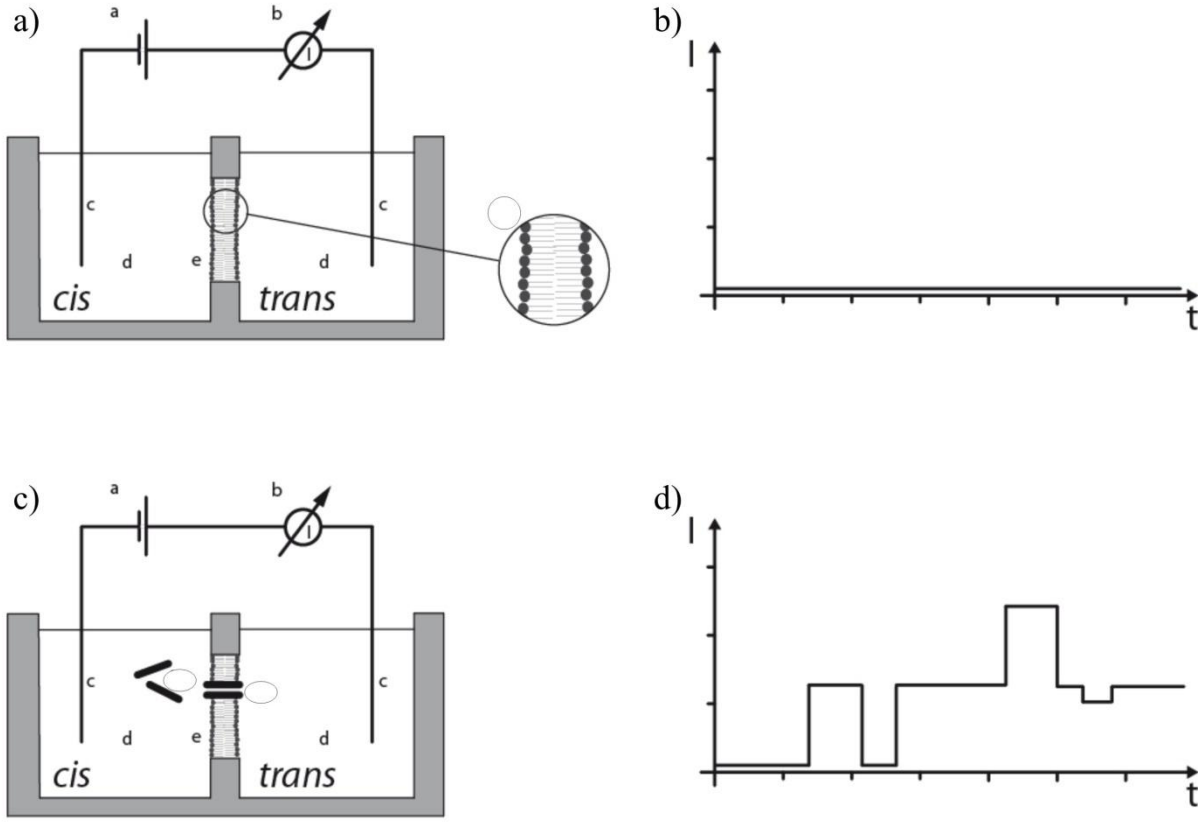

Figure 6.4: Scheme of the ion channel experiment (figure PhD thesis Dr. Anne Hänchen).

Feglymycin was dissolved in methanol to prepare a stock solution. Planar lipid membranes were prepared by painting a solution of DPhPC or Asolectine in n-decane (25mg / mL) over the aperture of a polystyrene cuvette with a diameter of 0.20 mm. Feglymycin, dissolved in methanol, was added to the trans-side of the cuvette (final concentration in the cuvette 2,5 10-10 mol/L). The membrane was destroyed, reconstituted at 0 V and the designated voltage was applied. Current detection and recording were performed with a patch-clamp amplifier Axopatch 200B, a Digidata A/D converter and pClamp 10 software (Axon Instruments, Foster City, CA, USA). The acquisition frequency was 5 kHz. The data were filtered with a digital filter at 50 Hz for further analysis, applying the pClamp 10 software.

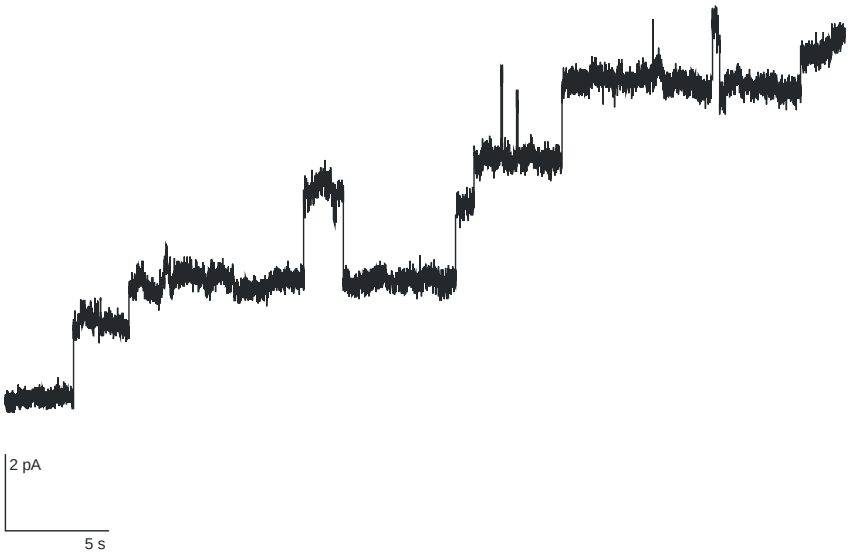

Figure 6.5: result of the ion channel experiment with feglymycin.

The ion channel characteristics were studied using the black lipid membrane (BLM) technique. Feglymycin increased the conductivity of the membrane. To observe individual openings and closings high voltage had to be applied (180 or 200 mV), as the conductibility proved to be quite small. Unlike other ion channel of similar size (e.g. gramicidin) Feglymycin does not show opening events of a well-defined size, but a wide distribution, ranging from the size of the noise to a few pA.

Eidesstattliche Erklärung:

Hiermit erkläre ich an Eides statt, dass ich die vorliegende Arbeit selbstständig verfasst und keine anderen als die angegebenen Quellen und Hilfsmittel benutzt habe. Alle Ausführungen die anderen veröffentlichten oder nicht veröffentlichten Schriften wörtlich oder sinngemäß entnommen wurden, habe ich kenntlich gemacht.

Unterschrift

_____

Declaration:

I hearby solemnly declare that I wrote the thesis in hand entirely by myself without outside help, that I clearly marked all the passages I adopted and that I did not use any source other than quoted.

Signature

_____

7 Literaturverzeichnis

Abraham, Edward P.; Chain, Ernst: An Enzyme from Bacteria able to Destroy Penicillin. In: Nature **1940,** *146, S.* 837-837.

Alanis, Alfonso J.: Resistance to Antibiotics: Are We in the Post-Antibiotic Era? In: Archives of Medical Research **2005,** *6, S.* 697–705.

Allen, Norris E.; Hobbs, Joe N., JR; Nicas, Thalia I.: Inhibition of peptidoglycan biosynthesis in vancomycin-susceptible and - resistant bacteria by a semisynthetic glycopeptide antibiotic. In: Antimicrob. Agents Chemother. **1996,** *10, S.* 2356–2362.

Allen, Norris E.; Nicas, Thalia I.: Mechanism of action of oritavancin and related glycopeptide antibiotics. In: FEMS Microbiology Reviews **2003,** *5, S.* 511–532.

Al-Nawas, Bilal; Shah, Pramod M.: Intracellular activity of vancomycin and Ly333328, a new semisynthetic glycopeptide, against methicillin-resistant Staphylococcus aureus. In: Infection **1998,** *3, S.* 165–167.

Andres, Charles J.; Bronson, Joanne J.; D'Andrea, Stanley V.; Deshpande, Milind S.; Falk, Paul J.; Grant-Young, Katharine A. et al.: 4-Thiazolidinones: novel inhibitors of the bacterial enzyme murB. In: Bioorganic & Medicinal Chemistry Letters **2000,** *8, S.* 715–717.

Auger, Geneviève; Crouvoisier, Muriel; Caroff, Martine; van Heijenoort, Jean; Blanot, Didier: Synthesis of an analogue of the lipoglycopeptide membrane intermediate I of peptidoglycan biosynthesis. In: Letters in Peptide Science **1997,** *4, S.* 371–376.

Auger, Geneviève; van Heijenoort, Jean; Mengin-Lecreux, Dominique; Blanot, Didier: A MurG assay which utilises a synthetic analogue of lipid I. In: FEMS Microbiology Letters **2003,** *1, S.* 115–119.

August, Paul R.; Tang, Li; Yoon, Yeo J.; Ning, Sandra; Müller, Rolf; Yu, Tin-Wein et al.: Biosynthesis of the ansamycin antibiotic rifamycin: deductions from the molecular analysis of the rif biosynthetic gene cluster of Amycolatopsis mediterranei S699. In: Chemistry & Biology **1998,** *2, S.* 69–79.

Babic, Andrej; Pecar, Slavko: Total synthesis of uridine diphosphate-N-acetylmuramoyl-l-alanine. In: Tetrahedron: Asymmetry **2008,** *19, S.* 2265–2271.

Bachmann, Brian O.; Ravel, Jacques **2009a:** Chapter 8 Methods for In Silico Prediction of Microbial Polyketide and Nonribosomal Peptide Biosynthetic Pathways from DNA Sequence Data. In: David A. Hopwood (Hg.): Methods in Enzymology : Complex Enzymes in Microbial Natural Product Biosynthesis, Part A: Overview Articles and Peptides: Academic Press, Volume 458, S. 181–217.

Bachmann, Brian O.; Ravel, Jacques: Methods for in silico prediction of microbial polyketide and nonribosomal peptide biosynthetic pathways from DNA sequence data. In: Methods Enzymol. **2009b,** *458, S.* 181–217.

Bahnson, Brian J.; Anderson, Vernon E.; Petsko, Gregory A.: Structural Mechanism of Enoyl-CoA Hydratase:Three Atoms from a Single Water Are Added in either an E1cb Stepwise or Concerted Fashion. In: Biochemistry **2002,** *8, S.* 2621–2629.

Baizman, Eugene R.; Branstrom, Arthur A.; Longley, Clifford B.; Allanson, Nigel; Sofia, Michael J.; Gange, David; Goldman, Robert C.: Antibacterial activity of

synthetic analogues based on the disaccharide structure of moenomycin, an inhibitor of bacterial transglycosylase. In: Microbiology **2000,** *12, S.* 3129–3140.

Balish, Edward; Shapiro, Stanley K.: Methionine biosynthesis in Escherichia coli: Induction and repression of methylmethionine(or adenosylmethionine):Homocysteine methyltransferase. In: Archives of Biochemistry and Biophysics **1967, S.** 62–68.

Banerjee, Dipak: Amphomycin: A tool to study protein N-glycosylation. In: Journal of Biosciences **1987,** *1, S.* 311–319.

Barbosa, Teresa M.; Levy, Stuart B.: The impact of antibiotic use on resistance development and persistence. In: Drug Resistance Updates **2000,** *5, S.* 303–311.

Baron, Samuel **1996:** Medical Microbiology. 4. ed. Baron, Samuel (Hg.). Galveston, Texas: University of Texas Medical Branch at Galveston.

Barona-Gómez, Francisco; Wong, Ursula; Giannakopulos, Anastassios E.; Derrick, Peter J.; Challis, Gregory L.: Identification of a Cluster of Genes that Directs Desferrioxamine Biosynthesis in Streptomyces coelicolor M145. In: Journal of the American Chemical Society **2004,** *50, S.* 16282–16283.

Baum, Ellen Z.; Montenegro, Deborah A.; Licata, Lisa; Turchi, Ignatius; Webb, Glenda C.; Foleno, Barbara D.; Bush, Karen: Identification and Characterization of New Inhibitors of the Escherichia coli MurA Enzyme. In: Antimicrob. Agents Chemother. **2001,** *11, S.* 3182–3188.

Benson, Timothy E.; Marquardt, John L.; Marquardt, Anne C.; Etzkorn, Felicia A.; Walsh, Christopher T.: Overexpression, purification, and mechanistic study of UDP-N-acetylenolpyruvylglucosamine reductase. In: Biochemistry **1993,** *8, S.* 2024–2030.

Bentley, S. D.; Chater, K. F.; Cerdeno-Tarraga, A. -M; Challis, G. L.; Thomson, N. R.; James, K. D. et al.: Complete genome sequence of the model actinomycete Streptomyces coelicolor A3(2). In: Nature **2002,** *6885, S.* 141–147.

Bernat, Bryan A.; Laughlin, L. Timothy; Armstrong, Richard N.: Fosfomycin Resistance Protein (FosA) Is a Manganese Metalloglutathione Transferase Related to Glyoxalase I and the Extradiol Dioxygenasesâ€ . In: Biochemistry **1997,** *11, S.* 3050–3055.

Bertrand, Jay A.; Auger, Geneviève; Fanchon, Eric; Martin, Lydie; Blanot, Didier; van Heijenoort, Jean; Dideberg, Otto: Crystal structure of UDP-N-acetylmuramoyl-L-alanine:D-glutamate ligase from Escherichia coli. In: EMBO J **1997,** *12, S.* 3416–3425.

Bilokapic, Silvija; Maier, Timm; Ahel, Dragana; Gruic-Sovulj, Ita; Soll, Dieter; Weygand-Durasevic, Ivana; Ban, Nenad: Structure of the unusual seryl-tRNA synthetase reveals a distinct zinc-dependent mode of substrate recognition. In: EMBO J **2006,** *11, S.* 2498–2509.

Bogatcheva, Elena; Dubuisson, Tia; Protopopova, Marina; Einck, Leo; Nacy, Carol A.; Reddy, Venkata M.: Chemical modification of capuramycins to enhance antibacterial activity. In: Journal of Antimicrobial Chemotherapy **2011,** *3, S.* 578–587.

Boggs, A. F.; Miller, G. H.: Antibacterial drug discovery: is small pharma the solution? In: Clinical Microbiology and Infection **2004, S.** 32–36.

Bogoyevitch, Marie A.; Fairlie, David P.: A new paradigm for protein kinase inhibition: blocking phosphorylation without directly targeting ATP binding. In: Drug Discovery Today **2007,** *15-16, S.* 622–633.

Borel, Jean F.; Feurer, Camille; Magnée, C.; Stähelin, Hartmann: Effects of the new anti-lymphocytic peptide cyclosporin A in animals. In: Immunology **1977,** *32, S.* 1017–1025.

Bouhss, Ahmed; Mengin-Lecreux, Dominique; Le Beller, Dominique; van Heijenoort, Jean: Topological analysis of the MraY protein catalysing the first membrane step of peptidoglycan synthesis. In: Molecular Microbiology **1999,** *3, S.* 576–585.

Brady, Sean F.; Chao, Carol J.; Handelsman, Jo; Clardy, Jon: Cloning and Heterologous Expression of a Natural Product Biosynthetic Gene Cluster from eDNA. In: Organic Letters **2001,** *13, S.* 1981–1984.

Brakhage, Axel A.; Al-Abdallah, Qusai; Tüncher, André; Spröte, Petra: Evolution of [beta]-lactam biosynthesis genes and recruitment of trans-acting factors. In: Phytochemistry **2005,** *11, S.* 1200–1210.

Brandish, Philip E.; Burnham, Martin K.; Lonsdale, John T.; Southgate, Robert; Inukai, Masatoshi; Bugg, Timothy D. H.: Slow Binding Inhibition of Phospho-N-acetylmuramyl-pentapeptide-translocase (Escherichia coli) by Mureidomycin A. In: Journal of Biological Chemistry **1996a,** *13, S.* 7609–7614.

Brandish, Philip E.; Kimura, Ken-ichi; Inukai, Masatoshi; Southgate, Robert; Lonsdale, John T.; Bugg, Timothy D. H.: Modes of action of tunicamycin, liposidomycin B, and mureidomycin A: inhibition of phospho-N-acetylmuramyl-pentapeptide translocase from Escherichia coli. In: Antimicrob. Agents Chemother. **1996b,** *7, S.* 1640–1644.

Breukink, Eefjan; Kruijff, Ben de: Lipid II as a target for antibiotics. In: Nat Rev Drug Discov **2006,** *4, S.* 321–323.

Briers, Yves; Volckaert, Guido; Cornelissen, Anneleen; Lagaert, Stijn; Michiels, Chris W.; Hertveldt, Kirsten; Lavigne, Rob: Muralytic activity and modular structure of the endolysins of Pseudomonas aeruginosa bacteriophages φKZ and EL. In: Molecular Microbiology **2007,** *5, S.* 1334–1344.

Brötz, Heike; Bierbaum, Gabriele; Leopold, Klaus; Reynolds, Peter E.; Sahl, Hans-Georg: The Lantibiotic Mersacidin Inhibits Peptidoglycan Synthesis by Targeting Lipid II. In: Antimicrob. Agents Chemother. **1998,** *1, S.* 154–160.

Brötz, Heike; Sahl, Hans-Georg: New insights into the mechanism of action of lantibiotics - diverse biological effects by binding to the same molecular target. In: Journal of Antimicrobial Chemotherapy **2000,** *1, S.* 1–6.

Brown, Eric D.; Marquardt, John L.; Lee, Jonathan P.; Walsh, Christopher T.; Anderson, Karen S.: Detection and Characterization of a Phospholactoyl-Enzyme Adduct in the Reaction Catalyzed by UDP-N-acetylglucosamine Enolpyruvoyl Transferase, MurZ. In: Biochemistry **1994,** *35, S.* 10638–10645.

Brown, W. E.; Seinerova, V.; Chan, W. M.; Laskin, Allen I.; Linnett, Paul; Strominger, Jack L.: INHIBITION OF CELL WALL SYNTHESIS BY THE ANTIBIOTICS DIUMYCIN AND JANIEMYCIN. In: Annals of the New York Academy of Sciences **1974,** *1, S.* 399–405.

Brumfitt, William; Salton, Milton R. J.; Hamilton-Miller, Jeremy M. T.: Nisin, alone and combined with peptidoglycan-modulating antibiotics: activity against methicillin-resistant Staphylococcus aureus and vancomycin-resistant enterococci. In: Journal of Antimicrobial Chemotherapy **2002,** *5, S.* 731–734.

Bulet, Philippe; Stöcklin, Reto; Menin, Laure: Anti-microbial peptides: from invertebrates to vertebrates. In: Immunological Reviews **2004,** *1, S.* 168–184.

Bunkóczi, Gábor; Vértesy, László; Sheldrick, George M.: The Antiviral Antibiotic Feglymycin: First Direct-Methods Solution of a 1000+ Equal-Atom Structure. In: Angewandte Chemie **2005,** *9, S.* 1364–1366.

Butaye, Patrick; Devriese, Luc A.; Haesebrouck, Freddy: Antimicrobial Growth Promoters Used in Animal Feed: Effects of Less Well Known Antibiotics on Gram-Positive Bacteria. In: Clin. Microbiol. Rev. **2003,** *2, S.* 175–188.

Cain, Brian D.; Norton, Peter J.; Eubanks, Willis; Nick, Harry S.; Allen, Charles M.: Amplification of the bacA gene confers bacitracin resistance to Escherichia coli. In: J. Bacteriol. **1993,** *12, S.* 3784–3789.

Calva, Juan J.; Sifuentes-Osornio, Jóse; Céron, Cecilia: Antimicrobial resistance in fecal flora: longitudinal community-based surveillance of children from urban Mexico. In: Antimicrob. Agents Chemother. **1996,** *7, S.* 1699–1702.

Campagne, Jean-Marc: Totalsynthesen von Lysobactin (Katanosin B). In: Angewandte Chemie **2007,** *45, S.* 8700–8704.

Capozzi, Francesco; Casadei, Federica; Luchinat, Claudio: EF-hand protein dynamics and evolution of calcium signal transduction: an NMR view. In: Journal of Biological Inorganic Chemistry **2006,** *8, S.* 949–962.

Carlson, Jacob C.; Fortman, J. L.; Anzai, Yojiro; Li, Shengying; Burr, Douglas A.; Sherman, David H.: Identification of the Tirandamycin Biosynthetic Gene Cluster from Streptomyces sp. 307-9. In: ChemBioChem **2010,** *4, S.* 564–572.

Cetinkaya, Yesim; Falk, Pamela; Mayhall, C. Glen: Vancomycin-Resistant Enterococci. In: Clin. Microbiol. Rev. **2000,** *4, S.* 686–707.

Chang, H. M.; Chen M. Y.; Shieh, Y. T.; Bibb, M. J.; Chen, Chia-Wei: The cutRS signal transduction system of Streptomyces lividans represses the biosynthesis of the polyketide antibiotic actinorhodin. In: Molecular Microbiology **1996,** *21, S.* 1075–1085.

Chang, Soju; Sievert, Dawn M.; Hageman, Jeffrey C.; Boulton, Matthew L.; Tenover, Fred C.; Downes, Frances Pouch et al.: Infection with Vancomycin-Resistant Staphylococcus aureus Containing the vanA Resistance Gene. In: New England Journal of Medicine **2003,** *14, S.* 1342–1347.

Chatterjee, Champak; Paul, Moushumi; Xie, Lili; van der Donk, Wilfred A.: Biosynthesis and Mode of Action of Lantibiotics. In: Chemical Reviews **2005,** *2, S.* 633–684.

Chatterjee, Sugata; Nadkarni, S. R.; Vijayakumar, E. K. S.; Patel, M. V.; Gangul, B. N.; Fehlhaber, H. -W; Vértesy, László: NAPSAMYCINS, NEW Pseudomonas ACTIVE ANTIBIOTICS OF THE MUREIDOMYCIN FAMILY FROM Streptomyces sp. HIL Y-82, 11372. In: J Antibiot **1994,** *5, S.* 595–598.

Chen, Huawei; Tseng, Claire C.; Hubbard, Brian K.; Walsh, Christopher T.: Glycopeptide antibiotic biosynthesis: Enzymatic assembly of the dedicated amino acid monomer (S)-3,5-dihydroxyphenylglycine. In: Proceedings of the National Academy of Sciences **2001,** *26, S.* 14901–14906.

Cheng, Ting-Jen Rachel; Sung, Ming-Ta; Liao, Hsin-Yu; Chang, Yi-Fan; Chen, Chia-Wei; Huang, Chia-Ying et al.: Domain requirement of moenomycin binding to

bifunctional transglycosylases and development of high-throughput discovery of antibiotics. In: Proceedings of the National Academy of Sciences **2008,** *2, S.* 431–436.

Chiu, Hsien-Tai; Hubbard, Brian K.; Shah, Aseema N.; Eide, Jonathan; Fredenburg, Ross A.; Walsh, Christopher T.; Khosla, Chaitan: Molecular cloning and sequence analysis of the complestatin biosynthetic gene cluster. In: Proceedings of the National Academy of Sciences **2001,** *15, S.* 8548–8553.

Choroba, Oliver W.; Williams, Dudley H.; Spencer, Jonathan B.: Biosynthesis of the Vancomycin Group of Antibiotics: Involvement of an Unusual Dioxygenase in the Pathway to (S)-4-Hydroxyphenylglycine. In: Journal of the American Chemical Society **2000,** *22, S.* 5389–5390.

Ciabatti, Romeo; Maffioli, Sonia I.; Panzone, Gianbattista; Canavesi, Augusto; Michelucci, Elena; Tiseni, Paolo S. et al.: Synthesis and Preliminary Biological Characterization of New Semisynthetic Derivatives of Ramoplanin. In: Journal of Medicinal Chemistry **2007,** *13, S.* 3077–3085.

Clarke, Tom: Drug companies snub antibiotics as pipeline threatens to run dry. In: Nature **2003,** *6955, S.* 225-225.

Colby, Gary D.; Chen, Jiann Shin: Purification and properties of 3-hydroxybutyryl-coenzyme A dehydrogenase from Clostridium beijerinckii ("Clostridium butylicum") NRRL B593. In: Appl. Environ. Microbiol. **1992,** *10, S.* 3297–3302.

Conti, Elena; Stachelhaus, Torsten; Marahiel, Mohamed A.; Brick, Peter: Structural basis for the activation of phenylalanine in the non-ribosomal biosynthesis of gramicidin S. In: EMBO J **1997,** *14, S.* 4174–4183.

Copeland, Robert A. **2000:** Enzymes-A practical introduction to structure, mechanism, and data analysis. pp. 285-287. Weinheim: WILEY-VCH.

Copeland, Robert A. **2005:** Evaluation of enzyme inhibitors in drug discovery. pp. 125-129. Weinheim: WILEY-VCH.

Cudic, Predrag; Kranz, James K.; Behenna, Douglas C.; Kruger, Ryan G.; Tadesse, Hellina; Wand, A. Joshua et al.: Complexation of peptidoglycan intermediates by the lipoglycodepsipeptide antibiotic ramoplanin: Minimal structural requirements for intermolecular complexation and fibril formation. In: Proceedings of the National Academy of Sciences **2002,** *11, S.* 7384–7389.

Dai, H. Jian; Parker, Christian N.; Bao, James J.: Characterization and inhibition study of MurA enzyme by capillary electrophoresis. In: Journal of Chromatography B: Analytical Technologies in the Biomedical and Life Sciences **2002,** *1, S.* 123–132.

Daniel, Rolf: The soil metagenome - a rich resource for the discovery of novel natural products. In: Current Opinion in Biotechnology **2004,** *3, S.* 199–204.

Davis, Michael; Myers, Karyn M.; Ressler, Kerry J.; Rothbaum, Barbara O.: Facilitation of Extinction of Conditioned Fear by D-Cycloserine: Implications for Psychotherapy. In: Current Directions in Psychological Science **2005,** *14, S.* 214–219.

Derossi, Daniele; Chassaing, Gerard; Prochiantz, Alain: Trojan peptides: the penetratin system for intracellular delivery. In: Trends in Cell Biology **1998,** *2, S.* 84–87.

Deshayes, Sébastien; Heitz, Annie; Morris, May C.; Charnet, Pierre; Divita, Gilles; Heitz, Frédéric: Insight into the Mechanism of Internalization of the Cell-Penetrating Carrier Peptide Pep-1 through Conformational Analysis†. In: Biochemistry **2004,** *6, S.* 1449–1457.

Dettner, Frank; Hänchen, Anne; Schols, Dominique; Toti, Luigi; Nußer, Antje; Süssmuth, Roderich D.: hTotalsynthese des antiviralen Peptidantibiotikums Feglymycin. In: Angewandte Chemie **2009,** *10, S.* 1888–1893.

DeVito, Joseph A.; Mills, Jonathan A.; Liu, Veronica G.; Agarwal, Anjana; Sizemore, Christine F.; Yao, Zhongjie et al.: An array of target-specific screening strains for antibacterial discovery. In: Nat Biotech **2002,** *5, S.* 478–483.

Dhalla, Adil M.; Yanchunas, Joseph; Ho, Hsu-Tso; Falk, Paul J.; Villafranca, Joseph J.; Robertson, James G.: Steady-State Kinetic Mechanism of Escherichia coli UDP-N-Acetylenolpyruvylglucosamine Reductase. In: Biochemistry **1995,** *16, S.* 5390–5402.

Dittmann, Joachim; Wenger, Roland M.; Kleinkauf, Horst; Lawen, Alfons: Mechanism of cyclosporin A biosynthesis. Evidence for synthesis via a single linear undecapeptide precursor. In: Journal of Biological Chemistry **1994,** *4, S.* 2841–2846.

Donadio, Stefano; Maffioli, Sonia I.; Monciardini, Paolo; Sosio, Margherita; Jabes, Daniela: Antibiotic discovery in the twenty-first century: current trends and future perspectives. ff. In: J Antibiot **2010,** *8, S.* 423–430.

Du, Wensheng; Brown, James R.; Sylvester, Daniel R.; Huang, Jianzhong; Chalker, Alison F.; So, Chi Y. et al.: Two Active Forms of UDP-N-Acetylglucosamine Enolpyruvyl Transferase in Gram-Positive Bacteria. In: J. Bacteriol. **2000,** *15, S.* 4146–4152.

Ducati, Rodrigo Gay; Ruffino-Netto, Antonio; Basso, Luiz Augusto; Santos, Diógenes Santiago: The resumption of consumption. A review on tuberculosis. In: Memórias do Instituto Oswaldo Cruz **2006, S.** 697–714.

El Zoeiby, Ahmed; Sanschagrin, François; Havugimana, Pierre C.; Garnier, Alain; Levesque, Roger C.: In vitro reconstruction of the biosynthetic pathway of peptidoglycan cytoplasmic precursor in Pseudomonas aeruginosa. In: FEMS Microbiology Letters **2001,** *2, S.* 229–235.

El Zoeiby, Ahmed; Sanschagrin, François; Levesque, Roger C.: Structure and function of the Mur enzymes: development of novel inhibitors. In: Molecular Microbiology **2003,** *1, S.* 1–12.

Emanuele, John J., JR.; Jin, Haiyong; Jacobson, Bruce L.; Chang, Chiehying Y.; Einspahr, Howard M.; Villafranca, Joseph J.: Kinetic and crystallographic studies of Escherichia coli UDP-N-acetylmuramate:L-alanine ligase. In: Protein Science **1996,** *12, S.* 2566–2574.

Emerson, Christopher R.; Marzella, Nino: Ramoplanin: A Promising Treatment Option for Clostridium difficile-Associated Diarrhea and Vancomycin-Resistant Enterococcus. In: P&T **2007,** *32, S.* 535–543.

Eschenburg, Susanne; Priestman, Melanie A.; Abdul-Latif, Farid A.; Delachaume, Carole; Fassy, Florence; Schönbrunn, Ernst: A Novel Inhibitor That Suspends the Induced Fit Mechanism of UDP-N-acetylglucosamine Enolpyruvyl Transferase (MurA). In: Journal of Biological Chemistry **2005,** *14, S.* 14070–14075.

Farmer, Bennett T.; Constantine, Keith L.; Goldfarb, Valentina; Friedrichs, Mark S.; Wittekind, Michael; Yanchunas, Joseph et al.: Localizing the NADP+ binding site on the MurB enzyme by NMR. In: Nat Struct Mol Biol **1996,** *12, S.* 995–997.

Felnagle, Elizabeth A.; Barkei, John J.; Park, Hyunjun; Podevels, Angela M.; McMahon, Matthew D.; Drott, Donald W.; Thomas, Michael G.: MbtH-Like Proteins as Integral Components of Bacterial Nonribosomal Peptide Synthetases. In: Biochemistry **2010,** *41, S.* 8815–8817.

Fernandes, Prabhavathi: Antibacterial discovery and development - the failure of success? In: Nat Biotech **2006,** *12, S.* 1497–1503.

Fleming, Alexander: On the antibacterial action of cultures of a penicillium, with special reference to their use in the isolation of B. influenzae. In: Br J Exp Pathol **1929,** *31, S.* 226–236.

French, C. E.; Bruce, N. C.: Bacterial morphinone reductase is related to Old Yellow Enzyme. In: Biochem. J. **1995,** *3, S.* 671–678.

Frère, Jean-Marie; Ghuysen, Jean-Marie; Reynolds, Peter E.; Moreno, Ramon: Binding of β-lactam antibiotics to the exocellular DD-carboxypeptidase–transpeptidase of Streptomyces R39. In: Biochem J. **1974,** *143, S.* 241–249.

Fronko, Richard M.; Lee, Julie C.; Gallazzo, J. G.; Chamberland, Simon; Malouin, Francois; Lee, May D.: New pacidamycins produced by Streptomyces coeruleorubidus, NRRL 18370. In: J Antibiot **2000,** *12, S.* 1405–1410.

Frumin, Jane; Gallagher, Jason C.: Allergic Cross-Sensitivity Between Penicillin, Carbapenem, and Monobactam Antibiotics: What Are the Chances? In: Ann Pharmacother **2009,** *2, S.* 304–315.

Gao, Qunjie; Thorson, Jon S.: The biosynthetic genes encoding for the production of the dynemicin enediyne core in Micromonospora chersina ATCC53710. In: FEMS Microbiology Letters **2008,** *1, S.* 105–114.

Giaever, Guri; Shoemaker, Daniel D.; Jones, Ted W.; Liang, Hong; Winzeler, Elizabeth A.; Astromoff, Anna; Davis, Ronald W.: Genomic profiling of drug sensitivities via induced haploinsufficiency. In: Nat Genet **1999,** *3, S.* 278–283.

Giardina, Anna; Alduina, Rosa; Gottardi, Elvira; Di Caro, Valentina; Sussmuth, Roderich; Puglia, Anna: Two heterologously expressed Planobispora rosea proteins cooperatively induce Streptomyces lividans thiostrepton uptake and storage from the extracellular medium. In: Microbial Cell Factories **2010,** *1, S.* 44.

Gillespie, Doreen E.; Brady, Sean F.; Bettermann, Alan D.; Cianciotto, Nicholas P.; Liles, Mark R.; Rondon, Michelle R. et al.: Isolation of Antibiotics Turbomycin A and B from a Metagenomic Library of Soil Microbial DNA. In: Appl. Environ. Microbiol. **2002,** *9, S.* 4301–4306.

Glinski, Mirko; Urbanke, Claus; Hornbogen, Till; Zocher, Rainer: Enniatin synthetase is a monomer with extended structure: evidence for an intramolecular reaction mechanism. In: Archives of Microbiology **2002,** *4, S.* 267–273.

Goldstein, Beth P.; Selva, Enrico; Gastaldo, Luciano; Berti, Marisa; Pallanza, Rosa; Ripamonti, Franca et al.: A40926, a new glycopeptide antibiotic with anti-Neisseria activity. In: Antimicrob. Agents Chemother. **1987,** *12, S.* 1961–1966.

Goldstein, Ellie J. C.; Citron, Diane M.; Merriam, C. Vreni; Warren, Yumi A.; Tyrrell, Kerin L.; Fernandez, Helen T.: In Vitro Activities of the New Semisynthetic

Glycopeptide Telavancin (TD-6424), Vancomycin, Daptomycin, Linezolid, and Four Comparator Agents against Anaerobic Gram-Positive Species and Corynebacterium spp. In: Antimicrob. Agents Chemother. **2004,** *6, S.* 2149–2152.

Gordon, Elspeth; Flouret, Bernard; Chantalat, Laurent; van Heijenoort, Jean; Mengin-Lecreux, Dominique; Dideberg, Otto: Crystal Structure of UDP-N-acetylmuramoyl-l-alanyl-d-glutamate:meso-Diaminopimelate Ligase from Escherichia Coli. In: Journal of Biological Chemistry **2001,** *14, S.* 10999–11006.

Gram, Christian: Über die isolierte Färbung der Schizomyceten in Schnitt- und Trockenpräparaten. In: Fortschritte der Medicin **1884,** *2, S.* 185–189.

Ha, Sha; Chang, Emmanuel; Lo, Mei-Chu; Men, Hongbin; Park, Peter; Ge, Min; Walker, Suzanne: The Kinetic Characterization of Escherichia coli MurG Using Synthetic Substrate Analogues. In: Journal of the American Chemical Society **1999,** *37, S.* 8415–8426.

Ha, Sha; Gross, Benjamin; Walker, Suzanne: E. Coli MurG: A Paradigm for a Superfamily of Glycosyltransferases. In: Current Drug Targets - Infectious Disorders **2001,** *1, S.* 201–213.

Hamburger, James B.; Hoertz, Amanda J.; Lee, Amy; Senturia, Rachel J.; McCafferty, Dewey G.; Loll, Patrick J.: A crystal structure of a dimer of the antibiotic ramoplanin illustrates membrane positioning and a potential Lipid II docking interface. In: Proceedings of the National Academy of Sciences **2009**.

Hanahan, Douglas: Studies on transformation of Escherichia coli with plasmids. In: Journal of Molecular Biology **1983,** *4, S.* 557–580.

Haura, Eric B.; Ricart, Alejandro D.; Larson, Timothy G.; Stella, Philip J.; Bazhenova, Lyudmila; Miller, Vincent A. et al.: A Phase II Study of PD-0325901, an Oral MEK Inhibitor, in Previously Treated Patients with Advanced Non–Small Cell Lung Cancer. In: Clinical Cancer Research **2010**.

Healy, Frank G.; Krasnoff, Stuart B.; Wach, Michael; Gibson, Donna M.; Loria, Rosemary: Involvement of a Cytochrome P450 Monooxygenase in Thaxtomin A Biosynthesis by Streptomyces acidiscabies. In: J. Bacteriol. **2002,** *7, S.* 2019–2029.

Heifetz, Aaron; Keenan, Roy W.; Elbein, Alan D.: Mechanism of action of tunicamycin on the UDP-GlcNAc:dolichyl-phosphate GlcNAc-1-phosphate transferase. In: Biochemistry **1979,** *11, S.* 2186–2192.

Heinzelmann, Eva; Berger, Susanne; Müller, Claudia; Härtner, Thomas; Poralla, Karl; Wohlleben, Wolfgang; Schwartz, Dirk: An acyl-CoA dehydrogenase is involved in the formation of the Δcis3 double bond in the acyl residue of the lipopeptide antibiotic friulimicin in Actinoplanes friuliensis. In: Microbiology **2005,** *6, S.* 1963–1974.

Hendlin, D.; Stapley, E. O.; Jackson, M.; Wallick, H.; Miller, A. K.; Wolf, F. J. et al.: Phosphomycin, a New Antibiotic Produced by Strains of Streptomyces. In: Science **1969,** *3901, S.* 122–123.

Herbig, Michael E.; Fromm, Ursina; Leuenberger, Jeannine; Krauss, Ulrike; Beck-Sickinger, Annette G.; Merkle, Hans P.: Bilayer interaction and localization of cell penetrating peptides with model membranes: A comparative study of a human calcitonin (hCT)-derived peptide with pVEC and pAntp(43-58). In: Biochimica et Biophysica Acta (BBA) - Biomembranes **2005,** *2, S.* 197–211.

Higgins, Luke J.; Yan, Feng; Liu, Pinghua; Liu, Hung-wen; Drennan, Catherine L.: Structural insight into antibiotic fosfomycin biosynthesis by a mononuclear iron enzyme. In: Nature **2005,** *7060, S.* 838–844.

Hirano, Shinpei; Ichikawa, Satoshi; Matsuda, Akira: Total synthesis of (+)-FR-900493 and establishment of its absolute stereochemistry. In: Tetrahedron **2007,** *13, S.* 2798–2804.

Hirano, Shinpei; Ichikawa, Satoshi; Matsuda, Akira: Synthesis of Caprazamycin Analogues and Their Structure-Activity Relationship for Antibacterial Activity. In: The Journal of Organic Chemistry **2008,** *2, S.* 569–577.

Hoffmann, Edmond de: Tandem mass spectrometry: A primer. In: J. Mass Spectrom. **1996,** *2, S.* 129–137.

Hoffmann, Edmond de; Stroobant, Vincent **2007:** Mass Spectrometry: Principles and Applications, 3rd Edition: John Wiley & Sons, Inc.

Holländer, Heike; Amrhein, Nikolaus: The Site of the Inhibition of the Shikimate Pathway by Glyphosate: I. INHIBITION BY GLYPHOSATE OF PHENYLPROPANOID SYNTHESIS IN BUCKWHEAT (FAGOPYRUM ESCULENTUM MOENCH). In: Plant Physiology **1980,** *5, S.* 823–829.

Hu, Qizhi; Noll, Robert J.; Li, Hongyan; Makarov, Alexander; Hardman, Mark; Graham Cooks, R.: The Orbitrap: a new mass spectrometer. In: J. Mass Spectrom. **2005,** *4, S.* 430–443.

Hu, Yanan; Helm, Jeremiah S.; Chen, Lan; Ginsberg, Cindy; Gross, Benjamin; Kraybill, Biran et al.: Identification of Selective Inhibitors for the Glycosyltransferase MurG via High-Throughput Screening. In: Chemistry & Biology **2004,** *5, S.* 703–711.

Huang, Jianqiang; Lih, Chih-Jian; Pan, Kuang-Hung; Cohen, Stanley N.: Global analysis of growth phase responsive gene expression and regulation of antibiotic biosynthetic pathways in Streptomyces coelicolor using DNA microarrays. In: Genes & Development **2001,** *23, S.* 3183–3192.

Hubbard, Brian K.; Thomas, Michael G.; Walsh, Christopher T: Biosynthesis of -p-hydroxyphenylglycine, a non-proteinogenic amino acid constituent of peptide antibiotics. In: Chemistry & Biology **2000,** *12, S.* 931–942.

Isono, Fujio; Inukai, Masatoshi; Takahashi, Shuji; Haneishi, Tatsuo; Kinoshita, Takeshi; Kuwano, Harumitsu: MUREIDOMYCINS A-D, NOVEL PEPTIDYLNUCLEOSIDE ANTIBIOTICS WITH SPEROPLAST FORMING ACTIVITY. In: J Antibiot **1989a,** *42, S.* 667–673.

Isono, Fujio; Katayama, Teruaki; Inukai, Masatoshi; Haneishi, Tatsuo: Mureindomycins A-D, novel peptidylnucleoside antibiotics with spheroplast forming activity. III. Biological properties. In: J Antibiot **1989b,** *5, S.* 674–679.

Isono, Kiyoshi; Uramoto, Masakazu; Kusakabe, Hiroo; Kimura, Ken-ichi; Izaki, Kazuo; Nelson, Chad C.; McCloskey, James A.: LIPOSIDOMYCINS: NOVEL NUCLEOSIDE ANTIBIOTICS WHICH INHIBIT BACTERIAL PEPTIDOGLYCAN SYNTHESIS. In: J Antibiot **1985,** *38, S.* 1617–1621.

Jacoby, George A.: AmpC {beta}-Lactamases. In: Clin. Microbiol. Rev. **2009,** *1, S.* 161–182.

Jin, Haiyong; Emanuele, John J., JR.; Fairman, Robert; Robertson, James G.; Hail, Mark E.; Ho, Hsu-Tso et al.: Structural Studies of Escherichia coli UDP-N-Acetylmuramate:l-Alanine Ligase. In: Biochemistry **1996,** *35, S.* 1423–1431.

Johnson, Balbina A.; Anker, Herbert; Meleney, Frank L.: BACITRACIN: A NEW ANTIBIOTIC PRODUCED BY A MEMBER OF THE B. SUBTILIS GROUP. In: Science **1945,** *12, S.* 376–377.

Johnson, Mark; Zaretskaya, Irena; Raytselis, Yan; Merezhuk, Yuri; McGinnis, Scott; Madden, Thomas L.: NCBI BLAST: a better web interface. In: Nucleic Acids Research **2008,** *suppl 2, S.* W5.

Kahne, Dan; Leimkuhler, Catherine; Lu, Wei; Walsh, Christopher T.: Glycopeptide and Lipoglycopeptide Antibiotics. In: Chem Rev. **2005,** *105, S.* 425–448.

Kallberg, Yvonne; Oppermann, Udo; Jörnvall, Hans; Persson, Bengt: Short-chain dehydrogenases/reductases (SDRs). In: European Journal of Biochemistry **2002,** *18, S.* 4409–4417.

Kaneko, Izumi; Fearon, Douglas T.; Austen, K. Frank: Inhibition of the alternative pathway of human complement in vitro by a natural microbial product, complestatin. In: The Journal of Immunology **1980,** *3, S.* 1194–1198.

Karki, Suman; Kwon, So-Yeon; Yoo, Hye-Gyeong; Suh, Joo-Won; Park, Si-Hyung; Kwon, Hyung-Jin: The methoxymalonyl-acyl carrier protein biosynthesis locus and the nearby gene with the β-ketoacyl synthase domain are involved in the biosynthesis of galbonolides in Streptomyces galbus, but these loci are separate from the modular polyketide synthase gene cluster. In: FEMS Microbiology Letters **2010,** *1, S.* 69–75.

Keller-Schierlein, W.; Prelog, V.: Stoffwechselprodukte von Actinomyceten. 29. Mitteilung. Die Konstitution des Ferrioxamins D1. In: HCA **1961,** *3, S.* 709–713.

Kessler, Nadine; Schuhmann, Holger; Morneweg, Sabrina; Linne, Uwe; Marahiel, Mohamed A.: The Linear Pentadecapeptide Gramicidin Is Assembled by Four Multimodular Nonribosomal Peptide Synthetases That Comprise 16 Modules with 56 Catalytic Domains. In: Journal of Biological Chemistry **2004,** *9, S.* 7413–7419.

Khan, Naveed Ahmed; Osman, Khadijo; Goldsworthy, Graham John: Lysates of Locusta migratoria brain exhibit potent broad-spectrum antibacterial activity. In: Journal of Antimicrobial Chemotherapy **2008,** *3, S.* 634–635.

Kim, Dennis H.; Lees, Watson J.; Kempsell, Karen E.; Lane, William S.; Duncan, Kenneth; Walsh, Christopher T.: Characterization of a Cys115 to Asp Substitution in the Escherichia coli Cell Wall Biosynthetic Enzyme UDP-GlcNAc Enolpyruvyl Transferase (MurA) That Confers Resistance to Inactivation by the Antibiotic Fosfomycinâ€ . In: Biochemistry **1996,** *15, S.* 4923–4928.

Kimura, Ken-ichi; Bugg, Timothy D. H.: Recent Advances in Antimicrobial Nucleoside Antibiotics Targeting Cell Wall Biosynthesis. In: ChemInform **2003,** *23, S.* no-no.

Kimura, Ken-ichi; Kanou, Fumiko; Yamashita, Yasushi; Yoshimoto, Tadashi; Yoshihama, Makoto: Prolyl Endopeptidase Inhibitors Derived from Actinomycetes. In: Bioscience, Biotechnology, and Biochemistry **1997,** *61, S.* 1754–1756.

Kitadokoro, Kengo; Tsuzuki, Hiroshige; nakamura, Etsuo; Sato, Tomohiro; TERAOKA, Hiroshi: Purification, characterization, primary structure, crystallization

and preliminary crystallographic study of a serine proteinase from Streptomyces fradiae ATCC 14544. In: European Journal of Biochemistry **1994,** *1, S.* 55–61.

Knecht, David A.; Dimond, Randall L.: Visualization of antigenic proteins on Western blots. In: Analytical Biochemistry **1984,** *1, S.* 180–184.

Knippers, Rolf **1985:** Molekulare Genetik. 4th Ed. Unter Mitarbeit von Klaus P. Schäfer und Ellen Fanning. Stuttgart: Georg Thieme Verlag.

Kobayashi, Seiji; Kuzuyama, Tomohisa; Seto, Haruo: Characterization of the fomA and fomB Gene Products from Streptomyces wedmorensis, Which Confer Fosfomycin Resistance on Escherichia coli. In: Antimicrob. Agents Chemother. **2000,** *3, S.* 647–650.

Kollef, Marin H.: Is Antibiotic Cycling the Answer to Preventing the Emergence of Bacterial Resistance in the Intensive Care Unit? In: Clinical Infectious Diseases **2006,** *Supplement 2, S.* S82-S88.

Kosowska-Shick, K.; McGhee, P. L.; Appelbaum, P. C.: Affinity of Ceftaroline and Other ß-Lactams for Penicillin-Binding Proteins from Staphylococcus aureus and Streptococcus pneumoniae. In: Antimicrob. Agents Chemother. **2010,** *5, S.* 1670–1677.

Kumarasamy, Karthikeyan K.; Toleman, Mark A.; Walsh, Timothy R.; Bagaria, Jay; Butt, Fafhana; Balakrishnan, Ravikumar et al.: Emergence of a new antibiotic resistance mechanism in India, Pakistan, and the UK: a molecular, biological, and epidemiological study. In: Lancet Infect. Dis. **2010,** *9, S.* 597–602.

Laemmli, Ulrich K.: Cleavage of Structural Proteins during the Assembly of the Head of Bacteriophage T4. In: Nature **1970,** *5259, S.* 680–685.

Lambalot, Ralph H.; Walsh, Christopher T.: Cloning, Overproduction, and Characterization of the Escherichia coli Holo-acyl Carrier Protein Synthase. In: Journal of Biological Chemistry **1995,** *42, S.* 24658–24661.

Lambert, Mary P.; Neuhaus, Francis C.: Mechanism of D-Cycloserine Action: Alanine Racemase from Escherichia coli W. In: J. Bacteriol. **1972,** *3, S.* 978–987.

Lee, Hyi-Seung; Shin, Hee Jae; Jang, Kyoung Hwa; Kim, Tae Sik; Oh, Ki-Bong; Shin, Jongheon: Cyclic Peptides of the Nocardamine Class from a Marine-Derived Bacterium of the Genus Streptomyces. In: Journal of Natural Products **2005,** *4, S.* 623–625.

Lee, Simon; Duce, Ian; Atkins, Helen; Khan, Naveed Ahmed: Cockroaches and locusts: physicians‘ answer to infectious diseases. In: International Journal of Antimicrobial Agents **2011,** *3, S.* 279–280.

Leman, Luke J.; Weinberger, Dana A.; Huang, Zheng-Zheng; Wilcoxen, Keith M.; Ghadiri, M. Reza: Functional and Mechanistic Analyses of Biomimetic Aminoacyl Transfer Reactions in de Novo Designed Coiled Coil Peptides via Rational Active Site Engineering. In: Journal of the American Chemical Society **2007,** *10, S.* 2959–2966.

Li, Tsung-Lin; Choroba, Oliver W.; Charles, Elizabeth H.; Sandercock, Alan M.; Williams, Dudley H.; Spencer, Jonathan B.: Characterisation of a hydroxymandelate oxidase involved in the biosynthesis of two unusual amino acids occurring in the vancomycin group of antibiotics. In: Chem. Commun. **2001,** *18, S.* 1752–1753.

Li, Tsung-Lin; Huang, Fanglu; Haydock, Stephen F.; Mironenko, Tatiana; Leadlay, Peter F.; Spencer, Jonathan B.: Biosynthetic Gene Cluster of the Glycopeptide

Antibiotic Teicoplanin: Characterization of Two Glycosyltransferases and the Key Acyltransferase. In: Chemistry & Biology **2004,** *1, S.* 107–119.

Liger, Dominique; Masson, Anne; Blanot, Didier; van Heijenoort, Jean; Parquet, Claudine: Over-production, Purification and Properties of the Uridine-diphosphate-N - Acetylmuramate: l-alanine Ligase from Escherichia coli. In: European Journal of Biochemistry **1995,** *1, S.* 80–87.

Lin, Yang-I; Li, Zhong; Francisco, Gerardo D.; McDonald, Leonard A.; Davis, Rachel A.; Singh, Guy et al.: Muraymycins, novel peptidoglycan biosynthesis inhibitors: semisynthesis and SAR of Their derivatives. In: Bioorganic & Medicinal Chemistry Letters **2002,** *17, S.* 2341–2344.

Lipsitch, Marc; Singer, Randall S.; Levin, Bruce R.: Antibiotics in agriculture: When is it time to close the barn door? In: Proceedings of the National Academy of Sciences **2002,** *9, S.* 5752–5754.

Liu, Haibin; Reynolds, Kevin A.: Precursor Supply for Polyketide Biosynthesis: The Role of Crotonyl-CoA Reductase. In: Metabolic Engineering **2001,** *1, S.* 40–48.

Lloyd, Adrian J.; Brandish, Philip E.; Gilbey, Andrea M.; Bugg, Timothy D. H.: Phospho-N-Acetyl-Muramyl-Pentapeptide Translocase from Escherichia coli: Catalytic Role of Conserved Aspartic Acid Residues. In: J. Bacteriol. **2004,** *6, S.* 1747–1757.

Lombó, Felipe; Braña, Alfredo F.; Salas, José A.; Méndez, Carmen: Genetic Organization of the Biosynthetic Gene Cluster for the Antitumor Angucycline Oviedomycin in Streptomyces antibioticus ATCC 11891. In: ChemBioChem **2004,** *9, S.* 1181–1187.

Lovering, Andrew L.; Castro, Liza H. de; Lim, Daniel; Strynadka, Natalie C. J.: Structural Insight into the Transglycosylation Step of Bacterial Cell-Wall Biosynthesis. In: Science **2007,** *5817, S.* 1402–1405.

Lugtenberg, E. J. J.; Hellings, J. A.; van de Berg, G. J.: Inhibition of Peptidoglycan Synthesis by the Antibiotic Diumycin A. In: Antimicrob. Agents Chemother. **1972,** *6, S.* 485–491.

Lundberg, Pontus; Langel, Ülo: A brief introduction to cell-penetrating peptides. In: Journal of Molecular Recognition **2003,** *5, S.* 227–233.

Luo, Chuanyun; Roussel, Patrick; Dreier, Jürg; Page, Malcolm G. P.; Paetzel, Mark: Crystallographic Analysis of Bacterial Signal Peptidase in Ternary Complex with Arylomycin A2 and a ß-Sultam Inhibitor. In: Biochemistry **2009,** *38, S.* 8976–8984.

Magzoub, Mazin; Kilk, Kalle; Eriksson, L. E. Göran; Lo Langel, Ülo; Gräslund, Astrid: Interaction and structure induction of cell-penetrating peptides in the presence of phospholipid vesicles. In: Biochimica et Biophysica Acta (BBA) - Biomembranes **2001,** *1, S.* 77–89.

Makarov, Alexander: Electrostatic Axially Harmonic Orbital Trapping: A High-Performance Technique of Mass Analysis. In: Analytical Chemistry **2000,** *6, S.* 1156–1162.

Maki, Hideki; Miura, Kenji; Yamano, Yoshinori: Katanosin B and Plusbacin A3, Inhibitors of Peptidoglycan Synthesis in Methicillin-Resistant Staphylococcus aureus. In: Antimicrob. Agents Chemother. **2001,** *6, S.* 1823–1827.

Malabarba, Adriano; Nicas, Thalia I.; Thompson, Richard C.: Structural modifications of glycopeptide antibiotics. In: Med. Res. Rev. **1997,** *1, S.* 69–137.

Mansour, Tarek S.; Caufield, Craig E.; Rasmussen, Beth A.; Chopra, Rajiv; Krishnamurthy, Girija; Morris, Koi M. et al.: Naphthyl Tetronic Acids as Multi-Target Inhibitors of Bacterial Peptidoglycan Biosynthesis. In: ChemMedChem **2007,** *10, S.* 1414–1417.

Mao, Yingqing; Varoglu, Mustafa; Sherman, David H.: Molecular characterization and analysis of the biosynthetic gene cluster for the antitumor antibiotic mitomycin C from Streptomyces lavendulae NRRL 2564. In: Chemistry & Biology **1999,** *4, S.* 251–263.

Marmor, Stephen; Petersen, Christian P.; Reck, Folkert; Yang, Wei; Gao, Ning; Fisher, Stewart L.: Biochemical Characterization of a Phosphinate Inhibitor of Escherichia coli MurC. In: Biochemistry **2001,** *40, S.* 12207–12214.

Marquardt, John L.; Brown, Eric D.; Lane, William S.; Haley, Terry M.; Ichikawa, Yoshitaka; Wong, Chi-Huey; Walsh, Christopher T.: Kinetics, Stoichiometry, and Identification of the Reactive Thiolate in the Inactivation of UDP-GlcNAc Enolpyruvoyl Transferase by the Antibiotic Fosfomycin. In: Biochemistry **1994,** *35, S.* 10646–10651.

Martin, Judith M.; Green, Michael; Barbadora, Karen A.; Wald, Ellen R.: Erythromycin-Resistant Group A Streptococci in Schoolchildren in Pittsburgh. In: New England Journal of Medicine **2002,** *16, S.* 1200–1206.

Mast, Yvonne; Weber, Tilmann; Gölz, Melanie; Ort-Winklbauer, Regina; Gondran, Anne; Wohlleben, Wolfgang; Schinko, Eva: Characterization of the 'pristinamycin supercluster' of Streptomyces pristinaespiralis. In: Microbial Biotechnology **2011,** *2, S.* 192–206.

May, Jürgen J.; Wendrich, Thomas M.; Marahiel, Mohamed A.: The dhb Operon of Bacillus subtilis Encodes the Biosynthetic Template for the Catecholic Siderophore 2,3-Dihydroxybenzoate-Glycine-Threonine Trimeric Ester Bacillibactin. In: Journal of Biological Chemistry **2001,** *10, S.* 7209–7217.

McCafferty, Dewey G.; Cudic, Predrag; Frankel, Brenda A.; Barkallah, Salim; Kruger, Ryan G.; Li, Wenkai: Chemistry and biology of the ramoplanin family of peptide antibiotics. In: Biopolymers **2002,** *4, S.* 261–284.

McCormick, Mack H.; McGuire, J. M.; Pittenger, G. E.; Pittenger, R. C.; Stark, W. M.: Vancomycin, a new antibiotic. I. Chemical and biologic properties. In: Antibiot. Annu. **1955-1956,** *3, S.* 606–611.

McDonald, Leonard A.; Barbieri, Laurel R.; Carter, Guy T.; Lenoy, Eileen; Lotvin, Jason; Petersen, Peter J. et al.: Structures of the Muraymycins, Novel Peptidoglycan Biosynthesis Inhibitors. In: Journal of the American Chemical Society **2002,** *35, S.* 10260–10261.

McGowan, John E.: Minimizing Antimicrobial Resistance: The Key Role of the Infectious Diseases Physician. In: Clinical Infectious Diseases **2004,** *7, S.* 939–942.

Meroueh, Samy O.; Bencze, Krisztina Z.; Hesek, Dusan; Lee, Mijoon; Fisher, Jed F.; Stemmler, Timothy L.; Mobashery, Shahriar: Three-dimensional structure of the bacterial cell wall peptidoglycan. In: Proceedings of the National Academy of Sciences of the United States of America **2006,** *12, S.* 4404–4409.

Miao, Vivian; Brost, Renee; Chapple, Joanne; She, Kevin; Gal, Marie-François; Baltz, Richard: The lipopeptide antibiotic A54145 biosynthetic gene cluster from Streptomyces fradiae. In: Journal of Industrial Microbiology & Biotechnology **2006,** *2, S.* 129–140.

Michio Kurosu; Sebabrata Mahapatra; Prabagaran Narayanasamy; Dean C. Crick: Chemoenzymatic synthesis of Park's nucleotide: toward the development of high-throughput screening for MraY inhibitors. In: Tetrahedron Letters **2007,** *5, S.* 799–803.

Miller, David J.; Hammond, Stephen M.; Anderluzzi, Daniela; Bugg, Timothy D. H.: Aminoalkylphosphinate Inhibitors of D-Ala-D-Ala Adding Enzyme. In: J. Chem. Soc., Perkin Trans. 1 **1998,** *1, S.* 131–142.

Mitchell, Douglas A.; Lee, Shaun W.; Pence, Morgan A.; Markley, Andrew L.; Limm, Joyce D.; Nizet, Victor; Dixon, Jack E.: Structural and Functional Dissection of the Heterocyclic Peptide Cytotoxin Streptolysin S. In: Journal of Biological Chemistry **2009,** *19, S.* 13004–13012.

Mitra, R.; Satpathy, M.; Srinivas, S. P.: Tunicamycin Induced Unfolded Protein Response (UPR) In Cultured Bovine Trabecular Meshwork (TM) Cells. In: Invest. Ophthalmol. Vis. Sci. **2002,** *12, S.* 4086.

Mizyed, Shehadeh; Oddone, Anna; Byczynski, Bartosz; Hughes, Donald W.; Berti, Paul J.: UDP-N-acetylmuramic Acid (UDP-MurNAc) Is a Potent Inhibitor of MurA (Enolpyruvyl-UDP-GlcNAc Synthase)†. In: Biochemistry **2005,** *10, S.* 4011–4017.

Montoya-Peleaz, Pedro J.; Riley, John G.; Szarek, Walter A.; Valvano, Miguel A.; Schutzbach, John S.; Brockhausen, Inka: Identification of a UDP-Gal: GlcNAc-R galactosyltransferase activity in Escherichia coli VW187. In: Bioorganic & Medicinal Chemistry Letters **2005,** *4, S.* 1205–1211.

Myers, Jeffrey K.; Nick Pace, C.; Martin Scholtz, J.: Trifluoroethanol effects on helix propensity and electrostatic interactions in the helical peptide from ribonuclease T1. In: Protein Science **1998,** *2, S.* 383–388.

Newman, David J.: Natural Products as Leads to Potential Drugs: An Old Process or the New Hope for Drug Discovery? In: Journal of Medicinal Chemistry **2008,** *9, S.* 2589–2599.

Nicas, Thalia I.; Mullen, D. L.; Flokowitsch, J. E.; Preston, D. A.; Snyder, N. J.; Stratford, R. E.; Cooper, R. D.: Activities of the semisynthetic glycopeptide LY191145 against vancomycin-resistant enterococci and other gram-positive bacteria. In: Antimicrob. Agents Chemother. **1995,** *11, S.* 2585–2587.

Nussbaum, Franz von; Anlauf, Sonja; Benet-Buchholz, Jordi; Häbich, Dieter; Köbberling, Johannes; Musza, Lászlo et al.: Structure and Total Synthesis of Lysobactin (Katanosin B). In: Angewandte Chemie **2007,** *12, S.* 2085–2088.

Nussbaum, Franz von; Anlauf, Sonja; Köbberling, Johannes; Telser, Joachim; Häbich, Dieter **04/13/2007:** PROCESS FOR THE MANUFACTURE OF LYSOBACTIN DERIVATIVES. EP20070724251.

O'Daniel, Peter I.; Zajicek, Jaroslav; Zhang, Weilie; Shi, Qicun; Fisher, Jed F.; Mobashery, Shahriar: Elucidation of the Structure of the Membrane Anchor of Penicillin-Binding Protein 5 of Escherichia coli. In: Journal of the American Chemical Society **2010,** *12, S.* 4110–4118.

Okada, Kazunori; Suzuki, Kengo; Kamiya, Yasuhiro; Zhu, XuFen; Fujisaki, Shingo; Nishimura, Yukinobu et al.: Polyprenyl diphosphate synthase essentially defines the length of the side chain of ubiquinone. In: Biochimica et Biophysica Acta (BBA) - Lipids and Lipid Metabolism **1996,** *3, S.* 217–223.

Oliphant, Cathrine M.; Green, Gary M.: Quinolones: A Comprehensive Review. In: Am Fam Physician. **2002,** *65, S.* 455–464.

Oliynyk, Markiyan; Samborskyy, Markiyan; Lester, John B.; Mironenko, Tatiana; Scott, Nataliya; Dickens, Shilo et al.: Complete genome sequence of the erythromycin-producing bacterium Saccharopolyspora erythraea NRRL23338. In: Nat Biotech **2007,** *4, S.* 447–453.

Ostash, Bohdan; Walker, Suzanne: Moenomycin family antibiotics: chemical synthesis, biosynthesis, and biological activity. In: Nat. Prod. Rep. **2010,** *27, S.* 1594–1617.

Otto, Michael; Peschel, Andreas; Götz, Friedrich: Producer self-protection against the lantibiotic epidermin by the ABC transporter EpiFEG of Staphylococcus epidermidis Tü3298. In: FEMS Microbiology Letters **1998,** *2, S.* 203–211.

Pallanza, Rosa; Scotti, R.; Beretta, G.; Cavalleri, B.; Arioli, Vittorio: In vitro activity of A-16686, a potential antiplaque agent. In: Antimicrob. Agents Chemother. **1984,** *4, S.* 462–465.

Papp-Wallace, Krisztina M.; Bethel, Christopher R.; Distler, Anne M.; Kasuboski, Courtney; Taracila, Magdalena; Bonomo, Robert A.: Inhibitor Resistance in the KPC-2 beta-Lactamase, a Preeminent Property of This Class A beta-Lactamase. In: Antimicrob. Agents Chemother. **2010,** *2, S.* 890–897.

Paradis-Bleau, Catherine; Lloyd, Adrian J.; Sanschagrin, François; Clarke, Tom; Blewett, Ann; Bugg, Timothy D. H.; Levesque, Roger: Phage display-derived inhibitor of the essential cell wall biosynthesis enzyme MurF. In: BMC Biochemistry **2008,** *1, S.* 33.

Patzer, Silke I.; Braun, Volkmar: Gene Cluster Involved in the Biosynthesis of Griseobactin, a Catechol-Peptide Siderophore of Streptomyces sp. ATCC 700974. In: J. Bacteriol. **2010,** *2, S.* 426–435.

Pegler, Scott; Healy, Brendan: In patients allergic to penicillin, consider second and third generation cephalosporins for life threatening infections. In: BMJ **2007,** *7627, S.* 991-991.

Peláez, Fernando: The historical delivery of antibiotics from microbial natural products - Can history repeat? In: Biochemical Pharmacology **2006,** *7, S.* 981–990.

Pelzer, Stefan; Süssmuth, Roderich D.; Heckmann, D.; Recktenwald, Jurgen; Huber, P.; Jung, G.; Wohlleben, Wolfgang: Identification and Analysis of the Balhimycin Biosynthetic Gene Cluster and Its Use for Manipulating Glycopeptide Biosynthesis in Amycolatopsis mediterranei DSM5908. In: Antimicrob. Agents Chemother. **1999,** *7, S.* 1565–1573.

Perkins, Herold R.; Nieto, Manuel: The preparation of iodinated vancomycin and its distribution in bacteria treated with the antibiotic. In: Biochem J. **1970,** *116, S.* 83–92.

Peschel, Andreas; Sahl, Hans-Georg: The co-evolution of host cationic antimicrobial peptides and microbial resistance. In: Nat Rev Micro **2006,** *7, S.* 529–536.

Peschel, Andreas; Vuong, Cuong; Otto, Michael; Götz, Friedrich: The D-Alanine Residues of Staphylococcus aureus Teichoic Acids Alter the Susceptibility to Vancomycin and the Activity of Autolytic Enzymes. In: Antimicrob. Agents Chemother. **2000,** *10, S.* 2845–2847.

Pfeffer, Sabine; Höhne, Wolfgang; Branner, Sven; Wilson, Keith; Betzel, Christian: X-Ray structure of the antibiotic bacitracin A. In: FEBS Letters **1991,** *1, S.* 115–119.

Pfeifer, Blaine A.; Wang, Clay C. C.; Walsh, Christopher T.; Khosla, Chaitan: Biosynthesis of Yersiniabactin, a Complex Polyketide-Nonribosomal Peptide, Using Escherichia coli as a Heterologous Host. In: Appl. Environ. Microbiol. **2003,** *11, S.* 6698–6702.

Pfeifer, Volker; Nicholson, Graeme J.; Ries, Johannes; Recktenwald, JÃ¼rgen; Schefer, Alexandre B.; Shawky, Riham M. et al.: A Polyketide Synthase in Glycopeptide Biosynthesis. In: Journal of Biological Chemistry **2001,** *42, S.* 38370–38377.

Pittet, Didier: Hand hygiene: improved standards and practice for hospital care. In: Current Opinion in Infectious Diseases **2003,** *4*.

Pootoolal, Jeff; Thomas, Michael G.; Marshall, C. Gary; Neu, John M.; Hubbard, Brian K.; Walsh, Christopher T.; Wright, Gerard D.: Assembling the glycopeptide antibiotic scaffold: The biosynthesis of from Streptomyces toyocaensis NRRL15009. In: Proceedings of the National Academy of Sciences **2002,** *13, S.* 8962–8967.

Pritzlaff, Craig A.; Chang, Jennifer C. W.; Kuo, Shrin P.; Tamura, Glen S.; Rubens, Craig E.; Nizet, Victor: Genetic basis for the β-haemolytic/cytolytic activity of group B Streptococcus. In: Molecular Microbiology **2001,** *2, S.* 236–248.

Raetz, Christian R. H.; Whitfield, Chris: LIPOPOLYSACCHARIDE ENDOTOXINS. Annual Review of Biochemistry. In: Annu. Rev. Biochem. **2002,** *1, S.* 635–700.

Rao, Jianghong; Lahiri, Joydeep; Isaacs, Lyle; Weis, Robert M.; Whitesides, George M.: A Trivalent System from VancomycinÂ·d-Ala-d-Ala with Higher Affinity Than AvidinÂ·Biotin. In: Science **1998,** *5364, S.* 708–711.

Ravanel, Stephane; Block, Maryse A.; Rippert, Pascal; Jabrin, Samuel; Curien, Gilles; Rebeille, Fabrice; Douce, Roland: Methionine Metabolism in Plants. In: Journal of Biological Chemistry **2004,** *21, S.* 22548–22557.

Raymond, Kenneth N.; Dertz, Emily A.; Kim, Sanggoo S.: Enterobactin: An archetype for microbial iron transport. In: Proceedings of the National Academy of Sciences **2003a,** *7, S.* 3584–3588.

Raymond, Kenneth N.; Dertz, Emily A.; Kim, Sanggoo S.: Enterobactin: An archetype for microbial iron transport. In: Proceedings of the National Academy of Sciences **2003b,** *7, S.* 3584–3588.

Read, Randy J.; Fujinaga, Masao; Sielecki, Anita R.; James, Michael N. G.: Structure of the complex of Streptomyces griseus protease B and the third domain of the turkey ovomucoid inhibitor at 1.8-.ANG. resolution. In: Biochemistry **1983,** *19, S.* 4420–4433.

Recktenwald, Jürgen; Shawky, Riham; Puk, Oliver; Pfennig, Frank; Keller, Ulrich; Wohlleben, Wolfgang; Pelzer, Stefan: Nonribosomal biosynthesis of vancomycin-type antibiotics: a heptapeptide backbone and eight peptide synthetase modules. In: Microbiology **2002,** *4, S.* 1105–1118.

Reddy, Sreelatha G.; Waddell, Sherman T.; Kuo, David W.; Wong, Kenny K.; Pompliano, David L.: Preparative Enzymatic Synthesis and Characterization of the Cytoplasmic Intermediates of Murein Biosynthesis. In: Journal of the American Chemical Society **1999,** *6, S.* 1175–1178.

Reynolds, Peter E.: Structure, biochemistry and mechanism of action of glycopeptide antibiotics. In: European Journal of Clinical Microbiology & Infectious Diseases **1989,** *11, S.* 943–950.

Rogers, L. A.; Whittier, E. O.: LIMITING FACTORS IN THE LACTIC FERMENTATION. In: J. Bacteriol. **1928,** *4, S.* 211–229.

Rolston, K. V.; Nguyen, H.; Messer, M.: In vitro activity of LY264826, a new glycopeptide antibiotic, against gram-positive bacteria isolated from patients with cancer. In: Antimicrob Agents Chemother **1990,** *11, S.* 2137–2141.

Rougraff, P. M.; Paxton, R.; Kuntz, M. J.; Crabb, D. W.; Harris, R. A.: Purification and characterization of 3-hydroxyisobutyrate dehydrogenase from rabbit liver. In: Journal of Biological Chemistry **1988,** *1, S.* 327–331.

Rutherford, Kim; Parkhill, Julian; Crook, James; Horsnell, Terry; Rice, Peter; Rajandream, Marie-Adele; Barrell, Bart: Artemis: sequence visualization and annotation. In: Bioinformatics **2000,** *10, S.* 944–945.

Ruzin, Alexey; Singh, Guy; Severin, Anatoly; Yang, Youjun; Dushin, Russell G.; Sutherland, Alan G. et al.: Mechanism of Action of the Mannopeptimycins, a Novel Class of Glycopeptide Antibiotics Active against Vancomycin-Resistant Gram-Positive Bacteria. In: Antimicrob. Agents Chemother. **2004,** *3, S.* 728–738.

Sakon, Joshua; Liao, Hans H.; Kanikula, Agnes M.; Benning, Matthew M.; Rayment, Ivan; Holden, Hazel M.: Molecular structure of kanamycin nucleotidyltransferase determined to 3.0-.ANG. resolution. In: Biochemistry **1993,** *45, S.* 11977–11984.

Saudagar, Parag S.; Survase, Shrikant A.; Singhal, Rekha S.: Clavulanic acid: A review. In: Biotechnology Advances **2008,** *4, S.* 335–351.

Sauvage, Eric; Kerff, Frédéric; Terrak, Mohammed; Ayala, Juan A.; Charlier, Paulette: The penicillin-binding proteins: structure and role in peptidoglycan biosynthesis. In: FEMS Microbiology Reviews **2008,** *2, S.* 234–258.

Schacht, U.; Huber, G.: MOENOMYCIN. VIII ISOLATION AND PROPERTIES OF FURTHER COMPONENTS OF THE ANTIBIOTIC MONENOMYCIN. In: J Antibiot **1969,** *12, S.* 597–602.

Schönbrunn, Ernst; Sack, Stefan; Eschenburg, Susanne; Perrakis, Anastassis; Krekel, Florian; Amrhein, Nikolaus; Mandelkow, Eckhard: Crystal structure of UDP-N-acetylglucosamine enolpyruvyltransferase, the target of the antibiotic fosfomycin. In: Structure **1996,** *9, S.* 1065–1075.

Schwartz, Dirk; Berger, Susanne; Heinzelmann, Eva; Muschko, Konstanze; Welzel, Kathrin; Wohlleben, Wolfgang: Biosynthetic Gene Cluster of the Herbicide Phosphinothricin Tripeptide from Streptomyces viridochromogenes Tu494. In: Appl. Environ. Microbiol. **2004,** *12, S.* 7093–7102.

Schwarzer, Dirk; Finking, Robert; Marahiel, Mohamed A.: Nonribosomal Peptides: From Genes to Products. In: ChemInform **2003,** *38, S.* no-no.

Seedorf, Henning; Fricke, W. Florian; Veith, Birgit; Bräggemann, Holger; Liesegang, Heiko; Strittmatter, Axel et al.: The genome of Clostridium kluyveri, a strict anaerobe

with unique metabolic features. In: Proceedings of the National Academy of Sciences **2008,** *6, S.* 2128–2133.

Sheldrick, George M.; Jones, Peter G.; Kennard, Olga; Williams, Dudley H.; Smith, Gerald A.: Structure of vancomycin and its complex with acetyl-D-alanyl-D-alanine. In: Nature **1978,** *5642, S.* 223–225.

Shoji, Jun'ichi; Hinoo, Hiroshi; Katayama, Teruaki; Matsumoto, Koichi; Tanimoto, Tatsuo; Hattori, Teruo et al.: ISOLATION AND CHARACTERIZATION OF NEW PEPTIDE ANTIBIOTICS, PLUSBACINS A1-A4 AND B1-B4. In: J Antibiot **1992,** *6, S.* 817–823.

Shoji, Jun'ichi; Hinoo, Hiroshi; Matsumoto, Koichi; Hattori, Teruo; Yoshida, Tadashi; Matsuura, Shinzo; Kondo, Eiji: ISOLATION AND CHARACTERIZATION OF KATANOSINS A AND B. In: J Antibiot **1988,** *6, S.* 713–718.

Singer, S. J.; Nicolson, Garth L.: The Fluid Mosaic Model of the Structure of Cell Membranes. In: Science **1972,** *4023, S.* 720–731.

Singh, M. P.; Petersen, Peter J.; Weiss, W. J.; Janso, J. E.; Luckman, S. W.; Lenoy, E. B. et al.: Mannopeptimycins, New Cyclic Glycopeptide Antibiotics Produced by Streptomyces hygroscopicus LL-AC98: Antibacterial and Mechanistic Activities. In: Antimicrob. Agents Chemother. **2003,** *1, S.* 62–69.

Sosio, Margherita; Kloosterman, Harm; Bianchi, Alessandra; Vreugd, Peter de; Dijkhuizen, Lubbert; Donadio, Stefano: Organization of the teicoplanin gene cluster in Actinoplanes teichomyceticus. In: Microbiology **2004,** *1, S.* 95–102.

Sosio, Margherita; Stinchi, Sofia; Beltrametti, Fabrizio; Lazzarini, Ameriga; Donadio, Stefano: The Gene Cluster for the Biosynthesis of the Glycopeptide Antibiotic A40926 by Nonomuraea Species. In: Chemistry & Biology **2003,** *6, S.* 541–549.

Spraggon, G.; Schwarzenbacher, R.; Kreusch, A.; Lee, C. C.; Abdubek, P.; Ambing, E. et al.: Crystal structure of an Udp-n-acetylmuramate-alanine ligase MurC (TM0231) from Thermotoga maritima at 2.3 A resolution. In: Proteins **2004,** *4, S.* 1078–1081.

Spratt, Brian G.: Properties of the Penicillin-Binding Proteins of Escherichia coli K12. In: European Journal of Biochemistry **1977,** *2, S.* 341–352.

Staunton, James; Weissman, Kira J.: Polyketide biosynthesis: a millennium review. In: Nat. Prod. Rep. **2001,** *4, S.* 380–416.

Stone, K. John; Strominger, Jack L.: Mechanism of Action of Bacitracin: Complexation with Metal Ion and C55-Isoprenyl Pyrophosphate. In: Proceedings of the National Academy of Sciences **1971,** *12, S.* 3223–3227.

Stover, C. K.; Pham, X. Q.; Erwin, A. L.; Mizoguchi, S. D.; Warrener, P.; Hickey, M. J. et al.: Complete genome sequence of Pseudomonas aeruginosa PAO1, an opportunistic pathogen. In: Nature **2000,** *6799, S.* 959–964.

Sun, Zhizeng; Zhong, Jin; Liang, Xiaobo; Liu, Jiale; Chen, Xiuzhu; Huan, Liandong: Novel Mechanism for Nisin Resistance via Proteolytic Degradation of Nisin by the Nisin Resistance Protein NSR. In: Antimicrob. Agents Chemother. **2009,** *5, S.* 1964–1973.

Takaku, Hironao; Sato, Junhei; Ishida, Hide-ki; Inazu, Toshiyuki; Ishida, Hideharu; Kiso, Makoto: A chemical synthesis of UDP-LacNAc and its regioisomer for finding ‘oligosaccharide transferases’. In: Glycoconjugate Journal **2006,** *7, S.* 565–573.

Takatsuki, Akira; Arima, Kei; Tamura, Gakuzo: TUNICAMYCIN, A NEW ANTIBIOTIC. I. ISOLATION AND CHARACTERIZATION OF TUNICAMYCIN. In: J Antibiot **1971,** *24, S.* 215–223.

Tanaka, Haruo; Oiwa, Ruiko; Matusukura, Shigekazu; Omura, Satoshi: Amphomycin inhibits phospho-N-acetylmuramyl-pentapeptide translocase in peptidoglycan synthesis of. In: Biochemical and Biophysical Research Communications **1979,** *3, S.* 902–908.

Tang, Yinyan; Lee, Ho Young; Tang, Yi; Kim, Chu-Young; Mathews, Irimpan; Khosla, Chaitan: Structural and Functional Studies on SCO1815:A β-Ketoacyl-Acyl Carrier Protein Reductase from Streptomyces coelicolor A3(2). In: Biochemistry **2006,** *47, S.* 14085–14093.

Tanner, Martin E.; Vaganay, Sabine; van Heijenoort, Jean; Blanot, Didier: Phosphinate Inhibitors of the d-Glutamic Acid-Adding Enzyme of Peptidoglycan Biosynthesis. In: The Journal of Organic Chemistry **1996,** *5, S.* 1756–1760.

Theuretzbacher, Ursula: Beta-Lactamasen und Beta-Lactamase-Inhibitoren. In: Chemotherapie Journal **1998,** *4, S.* 136–142.

Timothy E Benson; Walsh, Christopher T; James M Hogle: The structure of the substrate-free form of MurB, an essential enzyme for the synthesis of bacterial cell walls. In: Structure **1996,** *1, S.* 47–54.

Tomašić, Tihomir; Zidar, Nace; Kovač, Andreja; Turk, Samo; Simčič, Mihael; Blanot, Didier et al.: 5-Benzylidenethiazolidin-4-ones as Multitarget Inhibitors of Bacterial Mur Ligases. In: ChemMedChem **2010,** *2, S.* 286–295.

Trias, Joaquim; Yuan, Zhengyu: Mining bacterial cell wall biosynthesis with new tools: multitarget screens. In: Drug Resistance Updates **1999,** *6, S.* 358–362.

Trunkfield, Amy E.; Gurcha, Sudagar S.; Besra, Gurdyal S.; Bugg, Timothy D. H.: Inhibition of Escherichia coli glycosyltransferase MurG and Mycobacterium tuberculosis Gal transferase by uridine-linked transition state mimics. In: Bioorganic & Medicinal Chemistry **2010,** *7, S.* 2651–2663.

Tseng, H. -C; Chen, C. W.: A cloned ompR-like gene of Streptomyces lividans 66 suppresses defective melC1, a putative copper-transfer gene. In: Molecular Microbiology **1991,** *5, S.* 1187–1196.

Tsuchiya, Kanji; Kondo, Masahiro; Oishi, Tokiko; Yamazaki, Toshiyuki: ENDURACIDIN, A NEW ANTIBIOTIC. III IN VITRO AND IN VIVO ANTIMICROBIAL ACTVITY. In: J Antibiot **1968,** *2, S.* 147–153.

Twentyman, Peter R.: Bleomycin--mode of action with particular reference to the cell cycle. In: Pharmacology & Therapeutics **1983,** *3, S.* 417–441.

van Lanen, Steven G.; Shen, Ben: Microbial genomics for the improvement of natural product discovery. In: Current Opinion in Microbiology **2006,** *3, S.* 252–260.

van Wageningen, André M. A.; Kirkpatrick, Peter N.; Williams, Dudley H.; Harris, Barbara R.; Kershaw, Jo K.; Lennard, Nicola J. et al.: Sequencing and analysis of genes involved in the biosynthesis of a vancomycin group antibiotic. In: Chemistry & Biology **1998,** *3, S.* 155–162.

Vartoukian, Sonia R.; Palmer, Richard M.; Wade, William G.: Strategies for culture of ‘unculturable’ bacteria. In: FEMS Microbiology Letters **2010,** *1, S.* 1–7.

Vértesy, László; Aretz, Werner; Knauf, Martin; Markus, Astrid; Vogel, Martin; Wink, Joachim: Feglymycin, a Novel Inhibitor of the Replication of the Human Immunodeficiency Virus. In: J Antibiot **1999,** *4, S.* 374–382.

Wallace, B. A.: Structure of gramicidin A. In: Biophysical Journal **1986,** *1, S.* 295–306.

Wallhausser, K. H.; Nesemann, G.; Prave, P.; Steigler, A.: Moenomycin, a new antibiotic. I. Fermentation and isolation. In: Antimicrob. Agents Chemother. **1965, S.** 734–736.

WALSH, C. T.; LIU, J.; RUSNAK, F.; SAKAITANI, M.: ChemInform Abstract: Molecular Studies on Enzymes in Chorismate Metabolism and the Enterobactin Biosynthetic Pathway. In: ChemInform **1991,** *7, S.* no-no.

Walsh, Christopher T.; Fisher, Stewart L.; Park, I. -S; Prahalad, M.; Wu, Z.: Bacterial resistance to vancomycin: five genes and one missing hydrogen bond tell the story. In: Chemistry & Biology **1996,** *1, S.* 21–28.

Wandtner, Reinhard (2010): Tödliches Superbakterium. Im Wettlauf mit resistenten Erregern. In: Frankfurter Allgemeine Zeitung, 2010, 16.09.2010.

Watve, Milind; Tickoo, Rashmi; Jog, Maithili; Bhole, Bhalachandra: How many antibiotics are produced by the genus Streptomyces? In: Archives of Microbiology **2001,** *5, S.* 386–390.

Wiley, W. C.; McLaren, I. H.: Time-of-Flight Mass Spectrometer with Improved Resolution. In: Rev. Sci. Instrum. **1955,** *26, S.* 1150–1158.

Wilkinson, Barrie; Micklefield, Jason: Mining and engineering natural-product biosynthetic pathways. In: Nat Chem Biol **2007,** *7, S.* 379–386.

Williams, Keith J.; Bax, Richard P.: Challenges in developing new antibacterial drugs. In: Current Opinion in Investigational Drugs **2009,** *2, S.* 157–163.

Winn, Michael; Goss, Rebecca J. M.; Kimura, Ken-ichi; Bugg, Timothy D. H.: Antimicrobial nucleoside antibiotics targeting cell wall assembly: Recent advances in structure-function studies and nucleoside biosynthesis. In: Nat. Prod. Rep. **2010, S.** 279–304.

Winterhalter, Mathias: Black lipid membranes. In: Current Opinion in Colloid & Interface Science **2000,** *3-4, S.* 250–255.

Wu, Xiumei; Flatt, Patricia M.; Xu, Hui; Mahmud, Taifo: Biosynthetic Gene Cluster of Cetoniacytone A, an Unusual Aminocyclitol from the Endosymbiotic Bacterium Actinomyces sp. Lu 9419. In: ChemBioChem **2009,** *2, S.* 304–314.

Yamaguchi, Hiroshi; Sato, Shingo; Yoshida, Shiro; Takada, Kinji; Itoh, Masayoshi; Seto, Haruo; Otake, Noboru: CAPURAMYCIN, A NEW NUCLEOSIDE ANTIBOTIC. In: J Antibiot **1986,** *39, S.* 1047–1053.

Yan, Youwei; Munshi, Sanjeev; Leiting, Barbara; Anderson, Matt S.; Chrzas, John; Chen, Zhongguo: Crystal structure of Escherichia coli UDPMurNAc-tripeptide d-alanyl-d-alanine-adding enzyme (MurF) at 2.3 Å resolution. In: Journal of Molecular Biology **2000,** *3, S.* 435–445.

Yang, Sung-Tae; Zaitseva, Elena; Chernomordik, Leonid V.; Melikov, Kamran: Cell-Penetrating Peptide Induces Leaky Fusion of Liposomes Containing Late Endosome-Specific Anionic Lipid. In: Biophysical journal **2010,** *8, S.* 2525–2533.

Yang, Youjun; Severin, Anatoly; Chopra, Rajiv; Krishnamurthy, Girija; Singh, Guy; Hu, William et al.: 3,5-Dioxopyrazolidines, Novel Inhibitors of UDP-N-Acetylenolpyruvylglucosamine Reductase (MurB) with Activity against Gram-Positive Bacteria. In: Antimicrob. Agents Chemother. **2006,** *2, S.* 556–564.

Yeats, Corin; Bentley, Stephen; Bateman, Alex: New Knowledge from Old: In silico discovery of novel protein domains in Streptomyces coelicolor. In: BMC Microbiology **2003,** *1, S.* 3.

Yin, Xihou; Zabriskie, T. Mark: The enduracidin biosynthetic gene cluster from Streptomyces fungicidicus. In: Microbiology **2006,** *10, S.* 2969–2983.

Yost, R. A.; Enke, C. G.: Selected ion fragmentation with a tandem quadrupole mass spectrometer. In: Journal of the American Chemical Society **1978,** *7, S.* 2274–2275.

Zeng, Binqi; Wong, Kenny K.; Pompliano, David L.; Reddy, Sreelatha G.; Tanner, Martin E.: A Phosphinate Inhibitor of the meso-Diaminopimelic Acid-Adding Enzyme (MurE) of Peptidoglycan Biosynthesis. In: The Journal of Organic Chemistry **1998,** *26, S.* 10081–10085.

Zhang, Lixin; An, Rong; Wang, Jinping; Sun, Nuo; Zhang, Si; Hu, Jiangchun; Kuai, Jun: Exploring novel bioactive compounds from marine microbes. In: Current Opinion in Microbiology **2005,** *3, S.* 276–281.

Zhang, Wenjun; Heemstra, John R.; Walsh, Christopher T.; Imker, Heidi J.: Activation of the Pacidamycin PacL Adenylation Domain by MbtH-like Proteins. In: Biochemistry **2010,** *46, S.* 9946–9947.

Zhu, Dongqing; Seo, Myung-Ji; Ikeda, Haruo; Cane, David E.: Genome Mining in Streptomyces. Discovery of an Unprecedented P450-Catalyzed Oxidative Rearrangement That Is the Final Step in the Biosynthesis of Pentalenolactone. In: Journal of the American Chemical Society **2011,** *7, S.* 2128–2131.